

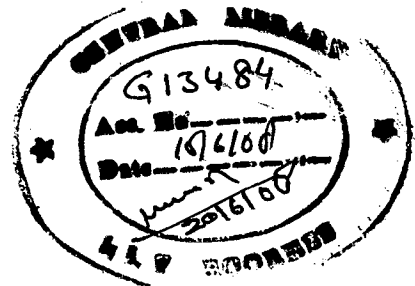
SOIL EROSION MODELLING IN LOKTAK LAKE CATCHMENT : AN INTEGRATED APPROACH

A THESIS

*Submitted in partial fulfilment of the
requirements for the award of the degree
of*
DOCTOR OF PHILOSOPHY
in
WATER RESOURCES DEVELOPMENT

By

KANGJAM SONAMANI SINGH



**DEPARTMENT OF WATER RESOURCES DEVELOPMENT & MANAGEMENT
INDIAN INSTITUTE OF TECHNOLOGY ROORKEE
ROORKEE-247 667 (INDIA)**

JULY, 2007

**© INDIAN INSTITUTE OF TECHNOLOGY ROORKEE, ROORKEE, 2007
ALL RIGHTS RESERVED**




INDIAN INSTITUTE OF TECHNOLOGY ROORKEE ROORKEE

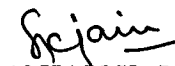
CANDIDATE'S DECLARATION

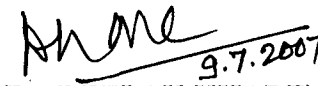
I hereby certify that the work which is being presented in the thesis entitled **SOIL EROSION MODELLING IN LOKTAK LAKE CATCHMENT : AN INTEGRATED APPROACH** in partial fulfilment of the requirements for the award of the degree of DOCTOR of PHILOSOPHY and submitted in the Department of Water Resources Development and Management of the Indian Institute of Technology Roorkee, Roorkee, is an authentic record of my own work carried out during the period from January 2004 to July 2007 under the supervision of Dr. Deepak Khare, Associate Professor, Department of Water Resources Development and Management, Indian Institute of Technology Roorkee, Roorkee, Dr. Sanjay K. Jain, Scientist E1 and Dr. Bhishm Kumar, Scientist F, National Institute of Hydrology, Roorkee. The matter presented in this thesis has not been submitted by me for the award of any other degree of this or any other Institute.


(KANGJAM SONAMANI SINGH)

This is to certify that the above statement made by the candidate is correct to the best of our knowledge.


(Dr. BHISHM KUMAR)
Scientist F
National Institute of
Hydrology, Roorkee


(Dr. SANJAY K. JAIN)
Scientist E1
National Institute of
Hydrology, Roorkee


(Dr. DEEPAK KHARE)
Associate Professor
Department of WRD & M
I.I.T. Roorkee

Date: July 9, 2007

The Ph.D. Viva-Voce Examination of Mr. **Kangjam Sonamani Singh**, Research Scholar, has been held on 28.9.2007


Signature of Supervisors 28/9/07


Signature of External Examiner 28/9/07

ACKNOWLEDGEMENT

At the outset I wish to express my immense sense of gratitude to my supervisors Dr. Deepak Khare, Associate Professor, Department of Water Resources Development and Management, Dr. Sanjay K. Jain, Scientist E1, National Institute of Hydrology and Dr. Bhishm Kumar, Scientist F, National Institute of Hydrology for their invaluable guidance, thought provoking discussions and untiring efforts throughout the tenure of this work. Their timely help, constructive criticism and painstaking efforts made it possible to present the work contained in this thesis in its present form.

It is a pleasure to acknowledge the support extended by all my fellow research scholars in general and Ajanta Goswami, Er. Pravinchandra Gaikwad, Er. Mahesh Jat, Er. Bhaskar R. Nikam, Mr. Biswas, Tejwant Singh Brar and Nitin Mishra in particular.

I also acknowledge my heartiest appreciation to all my friends for their moral support and everlasting encouragement given to me during my stay at Roorkee.

I can not close these prefatory remarks without expressing my deep sense of gratitude and reverence to my parents for their blessings and endeavour to keep my moral high throughout the period of my work.

Last but not the least I would like to express my sincere thanks to all those who directly or indirectly helped me at various stages of this work.


(KANGJAM SONAMANI SINGH)

ABSTRACT

Land degradation due to soil erosion by water is a widely recognized problem. It is a serious environmental problem affecting areas of different landscapes and land use. Assessment of soil erosion from catchment area is required for effective watershed planning, management and soil-water conservation. The process of soil erosion is influenced by spatial and temporal characteristics of input, i.e. rainfall and by the controls exerted by land surface. Such control include elevation, slope, soil cover and vegetal cover. The knowledge of spatial and temporal variations of inputs used in distributed modelling can enhance the capabilities to model these processes. The integration of a distributed soil erosion model with the spatial data handling capabilities of a Geographic Information System (GIS) provides desired distributed information about the soil erosion. In addition the use of remote sensing data provides a viable alternative for collection and interpretation of terrain data at a regular interval.

The present work deals with the western catchment of the endangered and ecologically fragile Loktak Lake in the Manipur state of India. The lake, considered as the lifeline for the state, has been facing a series of problems in the recent few years, one of the main reasons of which have been identified as extensive soil erosion in the upper catchment. It has been proposed to suggest a suitable soil erosion model for the region, which incorporates the local conditions and would efficiently estimate the erosion rate from the catchment.

Several models with a variety of structures and data requirements are available in literature to simulate soil erosion rate from catchment. A few soil erosion models viz, ANSWERS, WEPP, SWAT etc. have also been modified and combined with GIS software

during the past decade to take advantage of this new technology and provide more accurate value of soil erosion rate. But these models either require a vast exhaustive input-data or are event/location-specific.

The revised Morgan Morgan Finney (MMF) model has been used by several researchers in the past and was found to work very well with a minimum set of input data. As this model is suitable for hilly watersheds, therefore, this model has been chosen for the estimation of erosion rates in the two watersheds of Loktak Lake catchment namely Awang Khujairok and Waikhulok. The required input layers such as rainfall interception, effective rainfall and land use classes have been generated using the ILWIS 3.3, a raster based GIS software package. The image processing of satellite data has been carried out in ERDAS IMAGINE software. The soil erosion results estimated by the model ranges from 2.12 kg/m²/y in barren land to 0.21 kg/m²/y in the dense forest in the Awang Khujairok watershed. In the Waikhulok watershed the lowest soil erosion has been estimated in dense forest (0.19 kg/m²/y) and the maximum in barren land (2.18 kg/m²/y).

Besides this, as the observed data was very limited, another technique namely nuclear technique (²¹⁰Pb dating technique) has been used to estimate soil erosion rates to compare with the MMF results. For this, twelve soil cores were collected from the two watersheds which represented the existing land use classes and the ²¹⁰Pb content has been estimated on the basis of a theoretical mass balance model. In the Awang Khujairok watershed, the soil erosion rate ranges from 0.01 kg/m²/y (dense forest) to 1.87 kg/m²/y (built up land), whereas in the Waikhulok watershed, the lowest soil erosion rate has been found in dense forest (0.18 kg/m²/y) and the maximum in barren land (3.21 kg/m²/y) by using nuclear technique.

It has been found that the results of MMF model are in good agreement with the results of nuclear technique.

On the basis of soil erosion estimated by the MMF model in different land use classes in the two watersheds, the soil erosion in other watersheds on the basis of prevailing land use classes have been estimated.

Empirical relationships have been derived correlating effective rainfall and soil erosion for each land use class, e.g. the relationship for paddy field is $y = 0.0113x - 1.277$ ($x \geq 1.3$) and for dense forest is $y = 0.0013x - 0.206$, ($x \geq 0.21$); where y represents soil loss due to erosion ($\text{kg/m}^2/\text{y}$) and x is the effective rainfall (mm). Using the empirical relationship, the soil loss has been estimated for an independent year and a good correlation is found between the computed and observed soil loss.

Depending upon the soil erosion rate obtained, the prioritization of the watersheds has been done for effective watershed management. The watersheds are grouped into four categories-very high priority ($>12 \times 10^6 \text{ kg/km}^2$), high priority ($8-11 \times 10^6 \text{ kg/km}^2$), moderate priority ($4-7 \times 10^6 \text{ kg/km}^2$) and low priority ($1-4 \times 10^6 \text{ kg/km}^2$). The watersheds namely Khonga, Singda, Haibirok, Songtum and Thongjaorok, extending over an area of 39.6 km^2 fall under very high priority category. The high priority category covers 5 watersheds (Wangtha, Kharamkom, Phayeng, Nungshai and Kangchup) extending over an area of 38 km^2 . The moderate erosive category covers an area of 50.3 km^2 that comprises of 11 watersheds namely Ningthoukhong, Kongdun, Charoikhui, Wangjing, Sajirok, Awang Khujairok, Keinou, Thingin, Irum, Waikhulok and Lenghanbi. Six watersheds namely Ishinglok, Aigejang, Moirang Turel, Turelu, Laijamaril, Mashem (Kwakta) with an area of 11 km^2 have been identified under low erosive category.

The integrated approach of using revised MMF model and the nuclear technique for estimation of soil erosion in the present study reveals that the MMF model is suitable to be used in the catchment.

CONTENTS

Chapter	Descriptions	Page
	CANDIDATE'S DECLARATION	i
	ACKNOWLEDGEMENT	ii
	ABSTRACT	iii
	CONTENTS	vi
	LIST OF FIGURES	xiii
	LIST OF PLATES	xvii
	LIST OF TABLES	xviii
	NOMENCLATURES	xx
	ABBREVIATIONS	xxii
1.	INTRODUCTION	1-16
	1.1 GENERAL	1
	1.2 MECHANICS OF SOIL EROSION	2
	1.3 SOIL EROSION HAZARDS	4
	1.4 THE STATE OF MANIPUR	7
	1.5 THE LOKTAK LAKE	9
	1.5.1 Flora and Fauna	9
	1.5.2 Social and Cultural Values	10
	1.6 PROBLEM IDENTIFICATION	10
	1.7 OBJECTIVES	14
	1.8 ORGANIZATION OF THE THESIS	14
2.	LITERATURE REVIEW	17-70
	2.1 EROSION AND LAND DEGRADATION	17

	PROCESSES	
2.1.1	Estimation of Soil Erosion	21
	2.1.1.1 Rainsplash erosion	23
	2.1.1.2 Sheet erosion	24
	2.1.1.3 Rill erosion	25
	2.1.1.4 Gully erosion	26
	2.1.1.5 Streambank erosion	28
	2.1.1.6 Wind erosion	29
	2.1.1.7 Tunnel erosion	30
2.2	EFFECTS OF LANDSCAPE PATTERN ON	31
	SOIL EROSION	
2.2.1	Effects of Land Use Type on Soil	31
	Erosion	
2.2.2	Effects of Land Use Structure on Soil	32
	Erosion	
2.2.3	Effects of Landscape Pattern on Soil	33
	Erosion	
2.3	USE OF SATELLITE REMOTE SENSING AN	35
	GIS IN SOIL EROSION MODELING	
2.3.1	Modelling Soil Erosion	36
	2.3.1.1 Empirical models and semi-	37
	empirical models	
	2.3.1.2 Physical process-based models	38
2.4	SEDIMENT YIELD STUDIES FOR	43
	HIMALAYAN BASINS	

2.5	WATERSHED PRIORITIZATION	47
2.6	NUCLEAR TECHNIQUES (RADIOMETRIC DATING TECHNIQUES)	51
2.6.1	Beryllium-7 (⁷ Be) Dating Technique	52
2.6.2	Caesium-137 (¹³⁷ Cs) Dating Technique	55
2.6.3	Lead-210 (²¹⁰ Pb) Dating Technique	60
3.	STUDY AREA	71-97
3.1	CATCHMENT OF LOKTAK LAKE	71
3.1.1	Drainage Pattern	73
3.1.2	Land Use	77
3.1.3	Land Capability	79
3.1.4	Loktak Lake	80
3.1.5	Catchment Degradation and its Impacts	82
3.2	WATERSHEDS	84
3.3	THE AWANG KHUJAIROK & WAIKHULOK MICRO WATERSHEDS	86
3.3.1	Geomorphology	88
3.3.2	Soil Characteristics	89
3.3.3	Geological Characteristics of the Watersheds	90
3.3.4	Vegetation	91
3.3.5	Landuse and Socio-economic Conditions	91
3.3.6	Erosion Characteristics	91
4.	SOIL EROSION ASSESSMENT	98-132
4.1	EXISTING MODELS FOR SOIL EROSION	98

ASSESSMENT

4.1.1	LISEM Model	99
4.1.2	WEPP Model	100
4.1.3	TOPMODEL	101
4.1.4	ANSWERS Model	102
4.1.5	KINEROS Model	103
4.1.6	EPIC Model	104
4.1.7	AGNPS Model	105
4.1.8	SWMHMS Model	106
4.1.9	SWAT Model	107
4.2	THE UNIVERSAL SOIL LOSS EQUATION (USLE)	109
4.3	THE MORGAN MORGAN FINNEY MODEL	112
4.3.1	Water Phase	113
	4.3.1.1 Estimation of rainfall energy	113
	4.3.1.2 Estimation of runoff	114
4.3.2	Sediment Phase	115
	4.3.2.1 Soil particle detachment by raindrop impact	115
	4.3.2.2 Soil particle detachment by runoff	116
	4.3.2.3 Transport capacity of runoff	117
4.4	NUCLEAR TECHNIQUES	118
4.4.1	The ¹³⁷ Cs Dating Technique	120
4.4.2	The ⁷ Be Dating Technique	121

4.4.3	The ²¹⁰ Pb Dating Technique	121
4.4.4	Measurement of ²¹⁰ Pb Concentration in Sediment Samples	125
4.4.5	Lead-210 Separation from Sediment Samples	126
4.4.6	Lead-210 Measurement as ²¹⁰ Bi Using Liquid Scintillation Counter	130
4.4.7	Lead-210 Measurement by Gamma Spectrometry	131
4.4.8	Lead-210 Measurement by Alpha Spectrometry	132
5.	METHODOLOGY	133-189
5.1	GIS DATABASE PREPARATION	133
5.1.1	Digital Elevation Model	137
5.1.2	Analysis of Remote Sensing Data	140
	5.1.2.1 Import and visualization	140
	5.1.2.2 Geometric registration	140
	5.1.2.3 Multispectral classification	145
	5.1.2.4 Supervised classification	145
	5.1.2.5 Unsupervised classification	146
	5.1.2.6 Accuracy assessment and report	148
	5.1.2.7 Soil map	152
5.2	THE MORGAN, MORGAN AND FINNEY (MMF) MODEL	152
5.2.1	Collection of Input Data	154

	5.2.2	Field Survey	165
	5.2.3	Application of MMF Model	165
5.3		SOIL EROSION ASSESSMENT USING ^{210}Pb	178
		DATING TECHNIQUE OF SEDIMENT	
	5.3.1	Field Visit	178
	5.3.2	Sample Processing	180
	5.3.3	Lead-210 Measurement by Alpha	181
		Spectrometry	
6.		RESULTS AND DISCUSSION	190-232
	6.1	PREAMBLE	190
	6.2	SOIL EROSION USING USLE	190
	6.3	SOIL EROSION BY THE MMF MODEL	193
	6.3.1	Soil Erosion in Awang Khujairok	193
		watershed	
	6.3.2	Soil Erosion in Waikhulok watershed	198
	6.4	SOIL EROSION BY ^{210}Pb DATING	199
		TECHNIQUE	
	6.5	COMPARISION OF RESULTS	206
	6.5.1	Error	208
	6.6	ESTIMATION OF EROSION RATES IN OTHER	211
		WATERSHEDS	
	6.6.1	Analysis of Effect of Change of Slope on	212
		Soil Erosion	
	6.7	DEVELOPMENT OF EMPIRICAL MODEL FOR	216
		SOIL EROSION	

6.8	WATERSHED PRIORITIZATION	228
6.9	CONCLUDING REMARK	231
7.	CONCLUSIONS	234-237
7.1	CONCLUSIONS	234
7.2	SCOPE FOR FURTHER STUDIES	237
	REFERENCES	238-271

LIST OF FIGURES

Figure	Descriptions	Page
3.1	The location map of the study area	72
3.2	The stream channel network in the Manipur river basin	74
3.3	The drainage map of the study area	76
3.4	Land use classes in the Loktak Lake catchment	78
3.5	Watersheds in the study area	87
4.1	Flow chart for the revised MMF method of predicting soil loss	119
4.2	A) Total ^{210}Pb and ^{226}Ra activities in linear scale. B) Semi-log plot of variation of total and unsupported ^{210}Pb activities with depth	124
4.3	Use of unsupported ^{210}Pb measurements to estimate soil erosion and deposition rates	126
4.4	Sketch of the ion exchange column for extracting lead from the sediment sample	128
5.1	Location map of the two watersheds	134
5.2	Digital elevation model of the study area	139
5.3	False Colour Composite of 10 April 2000	141
5.4	False Colour Composite of 19 April 2005	142
5.5	False Colour Composite of 21 November 2000	143
5.6	False Colour Composite of 06 February 2005	144
5.7	Landuse map of the study area (10 April 2000)	149
5.8	Landuse map of the study area (19 April 2005)	150
5.9	Rainfall Interception (A) in Awang Khujairok watershed	169
5.10	Effective rainfall (mm) in Awang Khujairok watershed	169

5.11	Rainfall Interception, A, in Waikhulok watershed	170
5.12	Effective rainfall (mm) in Waikhulok watershed	170
5.13	Landuse map of Awang Khujairok watershed	176
5.14	Landuse map of Waikhulok watershed	176
5.15	Pathways through which ^{210}Pb reaches lake sediments	179
6.1	Soil detachment by raindrop impact (F) (kg/m^2) in Awang Khujairok watershed	195
6.2	Soil detachment by runoff, H (kg/m^2) in Awang Khujairok watershed	195
6.3	Total annual detachment, F+H (kg/m^2) in Awang Khujairok watershed	196
6.4	Transport capacity, TC, (kg/m^2) in Awang Khujairok watershed	196
6.5	Total Kinetic Energy (J/m^2) in Awang Khujairok watershed	197
6.6	Erosion map of Awang Khujairok watershed	197
6.7	Soil detachment by raindrop impact, F (kg/m^2) in Waikhulok watershed	200
6.8	Soil detachment by runoff, H (kg/m^2) in Waikhulok watershed	200
6.9	Total annual detachment, F+H (kg/m^2) in Waikhulok watershed	201
6.10	Transport capacity, TC, (kg/m^2) in Waikhulok watershed	201
6.11	Total kinetic energy (J/m^2) in Waikhulok watershed	202
6.12	Erosion map of Waikhulok watershed	202
6.13	Landuse wise ^{210}Pb activity plot in the Awang Khujairok watershed	203
6.14	Landuse wise ^{210}Pb activity plot in the Waikhulok watershed	205
6.15	Comparison of observed and estimated (MMF) soil erosion for Awang Khujairok watershed	209
6.16	Comparison of soil erosion estimated by MMF model and ^{210}Pb dating technique for Awang Khujairok watershed	209
6.17	Comparison of observed and estimated (MMF) soil erosion for	210

	Waikhulok watershed	
6.18	Comparison of soil erosion estimated by MMF model and ^{210}Pb dating technique for Waikhulok watershed	210
6.19	Effect of change of slope on soil erosion for the Awang Khujairok watershed	217
6.20	Effect of change of slope on soil erosion for the Waikhulok watershed.	218
6.21	Plot of effective rainfall (mm) & erosion ($\text{kg}/\text{m}^2/\text{y}$) for the paddy field land in the Awang Khujairok watershed	220
6.22	Plot of effective rainfall (mm) & erosion ($\text{kg}/\text{m}^2/\text{y}$) for the medium forest in the Awang Khujairok watershed	220
6.23	Plot of effective rainfall (mm) & erosion ($\text{kg}/\text{m}^2/\text{y}$) for the built-up land in the Awang Khujairok watershed	221
6.24	Plot of effective rainfall (mm) & erosion ($\text{kg}/\text{m}^2/\text{y}$) for the barren land in the Awang Khujairok watershed	221
6.25	Plot of effective rainfall (mm) & erosion ($\text{kg}/\text{m}^2/\text{y}$) for the dense forest in the Awang Khujairok watershed	222
6.26	Plot of effective rainfall (mm) & erosion ($\text{kg}/\text{m}^2/\text{y}$) for the paddy field in the Waikhulok watershed	222
6.27	Plot of effective rainfall (mm) & erosion ($\text{kg}/\text{m}^2/\text{y}$) for the medium forest in the Waikhulok watershed	223
6.28	Plot of effective rainfall (mm) & erosion ($\text{kg}/\text{m}^2/\text{y}$) for the built-up land in the Waikhulok watershed	223
6.29	Plot of effective rainfall (mm) & erosion ($\text{kg}/\text{m}^2/\text{y}$) for the barren land in the Waikhulok watershed	224
6.30	Plot of effective rainfall (mm) & erosion ($\text{kg}/\text{m}^2/\text{y}$) for the dense forest in the Waikhulok watershed	224
6.31	Combined plot of the Awang Khujairok and the Waikhulok watersheds for the paddy field	225

6.32	Combined plot of the Awang Khujairok and the Waikhulok watersheds for medium forest	225
6.33	Combined plot of the Awang Khujairok and the Waikhulok watersheds for the built-up land	226
6.34	Combined plot of the Awang Khujairok and the Waikhulok watersheds for the barren land	226
6.35	Combined plot of the Awang Khujairok and the Waikhulok watersheds for the dense forest	227
6.36	Prioritization of the watersheds in the catchment	233

LIST OF PLATES

Plate	Descriptions	Page
3.1	Panoramic view of the Loktak Lake	81
3.2	Fishermen in the Loktak Lake	81
5.1	Collection of meteorological reading in the study area	157
5.2	The meteorological station at the Awang Khujairok watershed	157
5.3	Medium forest land use in the study area	166
5.4	Paddy field land use in the study area	166
5.5	Dense forest land use in the Waikhulok watershed	167
5.6	Barren land use in the Awang Khujairok watershed	167
5.7	Bottle containing the sample being kept at the oven	184
5.8	Washing of the copper disks with Type 1 water	184
5.9	Observation of ^{210}Po counts by the Alpha-spectrometer	186
5.10	Spectrum of region of interest (ROI) depicting ^{209}Po and ^{210}Po peaks	186

LIST OF TABLES

Table	Descriptions	Page
1.1	Landuse of Manipur state	8
2.1	Average sediment yields in the Chenab basin at different locations along with their composition during the monsoon period	45
2.2	Correlation of mean basin monsoon rainfall with sediment yields (t/km ²)	46
3.1	The watersheds in the Loktak Lake catchment	88
3.2	The particulars of the two watersheds- Awang Khujairok and Waikhulok	94
3.3	Rainfall record for the Awang Khujairok watershed (mm).	97
3.4	Rainfall record for the Waikhulok watershed (mm).	97
4.1	Relationships between kinetic energy and rainfall intensity	114
4.2	Recommended values for Effective Hydrological Depth (EHD)	116
4.3	Guide values for soil parameters	117
4.4	The basic radionuclide decay data of isotopes of general interest	125
5.1	Classification accuracy assessment report for the FCC of 10 th April 2000	153
5.2	Classification accuracy assessment report for the FCC of 19 th April 2005	153
5.3	Input parameters for the revised MMF model adapted from Morgan, 2001	155
5.4	Effective rainfall (ER) of various land use patterns in Awang Khujairok watershed	158
5.5	Land use cover input values in the two watersheds	164
5.6	Slope in Awang Khujairok and Waikhulok watersheds	164

5.7	Calculation of the model parameters	173
5.8	Input values for the MMF model for the Awang Khujairok watershed	174
5.9	Input values for the MMF model for the Waikhulok watershed	175
5.10	Land use patterns in the different watersheds of the catchment	177
6.1	Soil loss estimation by the USLE	191
6.2	Soil particle detachment (both F and H), transport capacity (TC) and soil loss in the Awang Khujairok watershed	194
6.3	Soil particle detachment (both F and H), transport capacity (TC) and soil loss in the Waikhulok watershed	199
6.4	Landuse-wise soil loss in the Awang Khujairok watershed	206
6.5	Landuse-wise soil loss in the Waikhulok watershed	207
6.6	Comparison of the RMSE of results obtained from the two techniques.	211
6.7	Erosion rates in the different landuse patterns in the watersheds of the catchment	213
6.8	Effect of change of slope on soil erosion in the Awang Khujairok watershed	214
6.9	Effect of change of slope on soil erosion in the Waikhulok watershed	215
6.9	Estimation of total soil loss due to erosion in different watersheds of the catchment	230

NOMENCLATURES

Symbol	Descriptions
BD	Bulk density
C	Crop management factor
CC	Canopy cover
cm/h	Centimeter per hour
ER	Effective rainfall
ET	Evapotranspiration
GC	Ground cover
h	hour
ha	hectare
I	Rainfall intensity
J	Joule
km	Kilometer
K	Soil detachability index
kPa	Kilo pascal
mBq	milli Becquerel
mm	millimetre
m ³ /s	Cubic metre per second
MS	Moisture content
msl	Mean sea level
MW	Mega watt
Q	Runoff

U-238	Uranium-238
W_w	wet weight of the sample
W_d	dry weight of the sample
ρ_b	Bulk density
ν	kinematic viscosity of the liquid
λ	Decay constant
^{210}Pb	Lead-210
$^{210}\text{Pb}_{\text{ex}}$	Excess Lead-210
^{137}Cs	Caesium-137
^{222}Rn	Radon-222
^{226}Ra	Radium-226
^7Be	Beryllium-7
Z	Resistance of the soil

ABBREVIATIONS

Abbreviations	Descriptions
A	Rainfall interception
AGNPS	Agricultural Non-Point Source
AMC	Antecedent moisture content
ANSWERS	Areal Nonpoint Source Watershed Environment Response Simulation
COD	Chemical oxygen demand
COH	Cohesion of soil surface
CREAM	Chemicals, Runoff and Erosion from Agricultural Management Systems
DEM	Digital elevation model
DNs	Digital numbers
DTM	Digital terrain model
EHD	Effective hydrological depth
EPIC	Erosion Productivity Impact Calculator
ERDAS	Earth Resources Data Analysis System
F	Soil particle detachability by raindrop
F + H	Total annual detachment rate
H	Soil particle detachability by runoff
GCP	ground control points
GIS	Geographic Information System
GRASS	The Geographic Resources Analysis Support System,
HUMUS	Hydrological Unit Model of the United States
ILWIS	Integrated Land and Water Information System

IRS	Indian Remote Sensing
KE	Kinetic energy
KINEROS	KINematic EROsion Simulation
LD	Leaf drainage
LISEM	LImburg Soil Erosion Model
LISS	Linear Imaging Self Scanning
NASA	National Aeronautics and Space Administration
NGA	National Geospatial-Intelligence Agency
NIMA	U.S. National Imagery and Mapping Agency
PH	Plant height
RUSLE	Revised Universal Soil Loss equation
SIR-C	C-band Spaceborne Imaging RADAR
SRTM	Shuttle Radar Topography Mission
SWAT	Soil and Water Assessment Tool
SWMHMS	small watershed monthly hydrologic modelling system
TC	Transport capacity
TIF	Tag Image File
USDA	United States Department of Agriculture
USLE	Universal Soil Loss Equation
X-SAR	X-band Synthetic Aperture RADAR
MMF	Morgan Morgan Finney model
WAPCOS	Water and Power Consultancy Services
WEPP	Watershed Erosion Prediction Process

1.1 GENERAL

Soil and water are the most important natural resources within the ecosystem. They form the basis of sustenance of all forms of life. Yet, the exploitation of these precious resources without checks and balances and much thought for the future has led to their rapid degradation. Plants and trees will not grow and men and animals will have no food if there is no soil or if it is not good enough. Yet, loss of the soil continues to occur at an alarming rate due to the action of wind and flowing water. This process which is known as soil erosion increases tremendously due to human activities such as deforestation, uncontrolled grazing etc. The erosion of soil and corresponding degradation of land resources results in severe consequences. Farmlands get destroyed due to loss of topsoil and small rills get quickly transformed into wide gullies and unreclaimable ravines. In addition, erosion of soil has a direct bearing on the quality and quantity of water. Soil eroded from the upland areas of the catchment gets deposited in the river channels causing aggradation. Deposition of the eroded soil in reservoirs causes reduction in their storage capacity and hence their effective life span. The amount of eroded soil or more generally called; sediment-reaching the catchment outlet over a period of time is termed as sediment yield.

The importance of soil erosion modelling in surface water hydrology can hardly be over-emphasized. It has been a subject of considerable interest in the recent past and efforts are on, to develop new models and ways to understand these processes. The

process of soil erosion is a result of the complex interaction between several hydrological variables. Modelling of sediment yield from a catchment is required for river morphologic studies, soil-water conservation and for study of pollutant transport attached with the sediments. Spatial and temporal information about the runoff, soil erosion and sediment yield of a catchment can provide a useful perspective on the availability of water, rate of soil erosion and soil loss in the catchment. Spatial information about erosion may be utilized to plan effective conservation measures to check land degradation. The temporal variation of sediment yield from the catchments can be used as the upstream boundary condition in mathematical models used for river morphological studies. Also, temporal variation of the sediment yield is useful in designing efficient sediment control structures. In addition, temporal variation of sediment yield is needed for water quality and nutrient transport modelling (Onstad, 1984).

The dynamics of hydrological processes is influenced by spatial and temporal characteristics of inputs and by controls exerted by the land surface. These controls include elevation, soil, vegetation cover and underlying geology. The knowledge of spatial and temporal variation of inputs and controls and use of this undistributed modelling approach can enhance our understanding and capabilities to simulate complex hydrological processes.

1.2 MECHANICS OF SOIL EROSION

The generation of runoff from a catchment is the result of a complex interaction between factors related to meteorology and catchment characteristics. When rain falls over catchment, it interacts with land surface and some part of it, is utilized to meet the demands of interception, infiltration, evapotranspiration etc. Surface runoff is usually generated, when the rainfall intensity exceeds the demands of interception, infiltration and

surface storage. According to Woolhiser (1977) overland includes the sheet of flow over plane surface and also flow over rilled and irregular surfaces or flow in small channels. The overland flow is the main feature of flow in small catchments (Ponce, 1989). The boundary between overland flow and channel flow is not well defined. The components of rainfall-runoff process that largely affect the soil erosion are the overland flow and the channel flow.

Both the falling raindrops and the flowing water over the land surface are the driving mechanism of soil erosion in a catchment. The process of soil erosion involves detachment of soil from land surface, its transport and subsequent deposition (Meyer and Wischmeier, 1969). Soil particles are detached when the energy of the raindrop impact or shearing forces of flowing water either individually or in combination exceeds the soil resistive forces. Water from raindrop acts both as a wetting source and a source of energy that causes detachment of soil or sediment particles. The amount of detached sediment particles due to the raindrop impact varies with the degree of wetness of land surface, soil erodibility, depth of water on soil surface, presence of vegetation and other surface cover etc., Sediment is transported downslope primarily by flowing water, although there is a small amount of downslope transport by raindrop splash (Walling, 1988). Deposition of sediment can occur anywhere downslope of the point of erosion, when the transport capacity of the flow is less than the quantity of sediment available for transport. Since transport capacity is a function of flow velocity, the factors that reduce flow velocity in a flow segment also cause deposition of the eroded sediment.

The present thesis mainly intended to study the process of soil erosion within relatively small-sized catchments, the streams of which receive relatively insignificant contributions of groundwater flow. The main forces considered are detachment by runoff, detachment by raindrop impact and the transport by flow.

1.3 SOIL EROSION HAZARDS

Soil erosion is a natural process caused by movement of water, wind and ice and it has affected the earth's surface since its inception. Soil erosion and its off-site downstream damages are the major concerns around the world (Lal, 1994) causing losses in soil productivity and degradation of landscape (Walling, 1983). Many of men's activities results in accelerated soil erosion (Sombrock, 1995). Oldeman (1994) estimated that human-induced soil degradation affected 15 per cent of the world's arable land surface. Estimates of global soil erosion rates range from 0.088 mm/y (Walling, 1987) to 0.30 mm/y (Fournier, 1960) from the land surface that is carried downstream to lakes, reservoirs and estuaries leading to reduction in their storage capacities (Hotchkiss and Huang, 1995) and affecting water quality, navigation and biological productivity. On the land surface, soil erosion decreases organic matter, fine grained soil particles, water holding capacity and rooting depth resulting in the loss of soil fertility and quality.

Estimates of total suspended sediment yield for most of the major rivers in the world have been reviewed by Hadley *et al.*, (1985). A comparison of the estimated annual soil erosion presented by El-Swaify *et al.*, (1976) also indicated that the catchment areas in India and South America have extremely high values of soil erosion. In India, 144.3 million hectares of land have been degraded by soil erosion (Abrol, 1990). The most serious soil erosion problem in India is primarily attributed to sheet and rill erosion (Dhruva Narayana and Babu, 1983). Due to serious land degradation in catchment areas of reservoirs in India, the annual sediment inflow into many of the reservoirs varies from 0.6 to 122.7 ha m/100 km² (0.8-172 tonnes/ha) of the catchment (Dos *et al.*, 1969) and except for a few well-protected catchments, others are producing yields much higher than the 5.7-6.9 ha-m indicated by Garde and Kothyari (1987).

Ever-increasing pressure is being exerted on limited land resources and the available agricultural land is decreasing rapidly due to land degradation. Farmers in the mountains have to cultivate lands intensively and/or clear more land on steep slopes, resulting in further depletion and degradation of land resources. Soil erosion is an important contributing factor to land degradation and poverty in the mountainous north-eastern region of India.

North Eastern India is a vast landmass of 2,62,179 km² with 98% of its boundaries as international and only 2% as national. The region consists of eastern part of great Himalayan arc comprising the whole of Arunachal Pradesh and the eastern hill ranges comprising of the Patkai-Manipur-Mizoram-Arakan-Chittagaon hill tracts and the Shillong-Mikir plateau.

The unique geo-environmental setting of the region vis-à-vis the eastern Himalayas, heavy rainfall, weak geological formation, active seismicity, accelerated rates of erosion, rapid channel congestion, massive deforestation, intense land use pressure and high population growth especially in the flood plain belt and temporary palliative measures for flood control are some of the dominant factors that cause and intensify floods. Due to unplanned exploitation of resources, coupled with the above-mentioned factors, the region is crippled with problems such as food deficiency, energy shortage, inadequate surface communication, flood drainage congestion and declining productivity. The fragile hills are subjected to high rainfall and seismic activities, which trigger soil erosion and landslides. The average soil erosion in the region is about 28 tonnes/ha/year (www.necouncil.nic.in).

Although detailed data regarding soil erosion overall in the region are lacking, limited measurements of sediment show that values for the eastern Himalayan region exceed the world average by almost twice the magnitude (Alford, 1992). The direct and

primary effect of soil erosion is soil loss and nutrient leaching, resulting in reduction of land productivity. In a study carried out in Ningnan County, China, the nitrogen and organic matter in eroded soils were 2.7 and 4.2 times higher respectively than that of the topsoil of cultivated land. A study in middle Nepal indicates a soil loss of 20 tonnes/ha/yr from rainfed marginal land, indicating a nutrient loss of 300 kg of organic matter, 15 kg of nitrogen, 20 kg of phosphorus, and 40 kg of potassium (Carson, 1992). Soil loss from sloping farmlands under farmers' practices in the eastern Himalayas of India, the uplands of north-eastern Myanmar, and the uplands of south China is even higher at 54 to 57 tonnes/ha/year (Partap & Watson, 1994). From these data it becomes clear that soil erosion is a key cause of decline in soil fertility. These soil changes resulting from soil erosion will, in time, reduce crop yields and thereby farm income and household nutrition. Uncontrolled and continuous soil erosion will greatly reduce the soil depth and soil nutrient content, leading to abandonment of farming lands. The off-site effects of soil loss often have broader economic and environmental implications. Soil loss increases sediment and nutrient loads in streams. Eroded soils deposit reservoirs and rivers and often cause flooding in the lowlands. Deforestation and serious soil erosion in the Chinese Himalayan region were identified as the main causes for the disastrous floods in the Yangtze River.

Eroded soils also lead to siltation of dams and irrigation channels in the basin area of the catchment. Such examples of siltation of dams are not unusual in the mountainous region. The lifespan of the Kulekhani Reservoir in central Nepal has been reduced to half of the targetted design and one quarter of the expected lifespan due to serious soil erosion. The unusual rainfall in 1993 alone resulted in sedimentation of 5.12 M m^3 , which is 6% of the designed storage capacity of the reservoir and is about 60 times higher than the expected annual sedimentation (Sthapit, 1995; Galay *et al.*, 1995). The above facts clearly

indicate that conservation of water and soil is important for the harmonious development of population, resources and environments.

Soils of the warm perhumid Siwalik hill ecosystem, with a 'hyperthermic' temperature regime, are also Entisols and Inceptisols with a high to moderate acidic condition. The dominant soils of the northeastern Purvachal hill ecosystem, with 'hyperthermic' and 'thermic' temperature regimes, are Ultisols and Inceptisols. Inceptisols and Entisols are the dominant soils in the hot and humid plain ecosystem. The sloping landform and high rainfall are mainly responsible for a high erosion hazard in the region of the country (Maji *et al.*, 2001).

1.4 THE STATE OF MANIPUR

Manipur has a geographic area of 2.23 M-ha. It lies between latitude 23°50' and 25°42' N and longitude 92°59' and 94°46' E. The terrain in the state is predominantly hilly, except a broad central valley extending to about 1800 km². The average altitude of valley is 850 m while the maximum altitude of the hilly region is upto 3,000 m. The Imphal and the Barak rivers flowing in southern direction form the main drainage system. Mean temperature in the state varies from 15°C to 38°C and average annual rainfall ranges from 1,250 mm to 2,700 mm. Climate in the western part of the state is tropical whereas the rest of the state observes sub tropical climate with distinct summer, winter and rainy seasons. The land use of the state is given in Table 1.1.

Table 1.1: Land use of Manipur state

Land use	Area in '000 ha	Percentage
Total geographical area	2,233	
Forest	602	27.23
Not available for cultivation	1,445	65.36
Permanent pasture and grazing land	n	0
Land under misc. tree, crops & groves	24	1.09
Culturable wasteland	n	0
Fallow land other than current fallow	0	0
Current fallow	0	0
Net area sown	140	6.32

n-Included under the head 'Area put to non agricultural uses'

Source: www.necouncil.nic.in

Shifting cultivation is a prevalent land use in the state. In a study undertaken by the Forest Survey of India in 1999, it is estimated that an area of about 0.36 M-ha has been affected by this practice during 1987-97. At one point of time about 0.06 M-ha is under shifting cultivation. The recorded forest area of the state is 1.5 M-ha which constitutes 67.87% of the geographic area of the state. According to legal classification, the reserved forest constitutes 10% whereas the protected forest and unclassed forest 27% and 63% respectively.

Major forest types of the state are tropical semi-evergreen, subtropical pine, and montane wet temperate forests.

The forest area of the state falls under four distinct zones, viz; (a) Burma border forests (b) Ukhrul pine forests (c) Forest overlooking the valley and (d) Barak drainage forests. The forest cover based on the satellite data of December, 1998 was 17,384 km²,

which is 77.86% of the geographic area of the state. Extents of dense forest and open forest have been assessed as 5,936 km² and 11,448 km² respectively.

1.5 THE LOKTAK LAKE

Loktak Lake is considered to be the lifeline of the State of Manipur due to its importance in the socio-economic and cultural life of the people. It is the largest natural freshwater lake in the north - eastern region of India and plays an important role in the ecological and economic security of the region.

The lake is an important source of water, fisheries and vegetation providing sustenance to a large population dependent upon it for their sustenance. The lake water is used for irrigation, domestic purposes and power generation.

The staple food of Manipur is directly linked to Loktak Lake. The lake is rich in biodiversity and was designated as a Wetland of International Importance under Ramsar Convention in 1990 (Trisal and Manihar, 2004).

1.5.1 Flora and Fauna

The lake is covered extensively by naturally - occurring *phumdis* (mass of floating vegetation) which are a specialized habitat for many biota, besides being useful to the local people in many ways (Trisal and Manihar, 2004).

The Keibul Lamjao National Park, in the southern part of the lake, is a unique floating wildlife reserve and the only home of the endangered Manipur brow - antlered deer or Sangai, with an estimated population of 106 (in 1991). It has been the breeding ground of a number of riverine migratory fishes from the Irrawady-Chindwin river system and continues to be vital as a fish habitat. It is of enormous socio-economic importance for the inhabitants of Manipur valley. The lake also supports a significant population of resident and migratory waterfowl.

The Loktak lake with its numerous floating lands covers a variety of habitats which sustains rich biological diversity. The aquatic macrophytes comprising 233 species belonging to emergent, submergent, free - floating and rooted floating leaf types have been reported in the lake.

A total of 425 species of animals (249 vertebrates and 176 invertebrates) have been recorded from the lake, which includes some rare animals such as Indian python, sambhar and barking deer. The lake provides refuge to thousands of birds which belong to at least 116 species. Of these, 21 species of waterfowl are migratory, most migrating from different parts of the northern hemisphere beyond the Himalayas. Keibul Lamjao National Park is the natural habitat of one of the most endangered deer, the brow - antlered deer (*Cervus eldi eldi*) which is represented by about hundred individuals and was once thought to be extinct.

1.5.2 Social & Cultural Values

Besides influencing the climate of the State, the socio - economic values of the lake include hydropower generation (Loktak Hydel National Project), irrigation of 24,000 ha of agricultural land, fisheries, control of floods, supply of drinking water, production of aquatic organisms of food and of commercial importance, and the many uses of *phumdi* and water transport. More than 100,000 people, on and around the lake, depend for their livelihood to a great extent on the lake fishery, which is now a mix of capture and culture systems. The lake yields about 1,500 tonnes of fish per year.

1.6 PROBLEM IDENTIFICATION

Like all other national and international wetlands, the Loktak Lake is facing many problems regarding degradation in the catchment area and its surroundings. The root-cause problems can be traced to loss of vegetal cover in the catchment area. The degradation of

the catchment area has led to the problems of siltation and increased flow of nutrients (Trisal and Manihar, 2004). This in turn of has led to:

- i) Changes in hydrological regimes thereby affecting ecological processes and functions of the wetland;
- ii) Inundation of agricultural lands and displacement of people from flooded lands and loss of fish population and diversity and;
- iii) Decrease in the thickness of *phumdis* (the characteristic floating biomass) in the Keibul Lamjao National Park thereby threatening the survival of Sangai deer.

The processes of soil erosion are nowadays, generally studied with the aid of efficient mathematical models. These models integrate existing knowledge into a logical framework of rules and relationships (Moore and Gallant, 1991) and can be used to (i) improve our understanding of the environmental systems, that is, as a tool for hypothesis testing, and (ii) provide predictive tools for management (Beven, 1989; Grayson *et al.*, 1992).

In recent years, computer based soil erosion models have become useful tools for water resources management, flood forecasting and control and environmental concerns. The influence and importance of the spatial scale on soil erosion modelling has long been emphasized by hydrologists. With the advances in remote sensing and Geographic Information System (GIS) techniques in mapping and handling of large spatial databases, increasingly the trend is changing from using catchment system, lumped input and output type hydrologic models to distributed type modelling. This change in modelling approach reflects a general desire to increase the accuracy and the capability to describe the hydrologic response of a catchment both in spatial and temporal domains.

Although in the past it was considered sufficient to model only catchment outflow, it is now often necessary to estimate distributed surface and sub surface characteristics as the driving mechanism for soil erosion, sedimentation, chemical and nutrient transport and other spatially distributed effects (Abott *et al.*, 1986). The soil erosion processes are strongly dependent upon the soil, vegetation and topographic characteristics of the catchment. These characteristics have been found to vary spatially in a catchment. Many hydrological models require spatially distributed inputs because solution to accelerated soil erosion, non-point source pollution and other pervasive environmental problems involve changes in land use and management at the hill slope and catchment scales (Moore *et al.*, 1993).

The remote sensing and GIS technologies are now well-established tools for generation and interpretation of spatially distributed information required for use in distributed hydrological models. The GIS offers new opportunities for the collection, storage, analysis and display of spatially distributed hydrological data. Use of remotely sensed data provides viable alternative for collection and interpretation of data at regular grid interval with repetitive coverage. The most common applications of remote sensing data in hydrology are related to, investigations of cloud cover, impervious surfaces, floods, land use, radiation, rainfall, snow cover, soil moisture, soil erosion and surface temperature etc. The GIS is also a tool for effective and efficient storage and analysis of remotely sensed information and other spatial and non-spatial information. Remotely sensed data, effectively integrated within a GIS, can be used to facilitate measurements, mapping, monitoring and modelling activities. Remotely sensed data coupled with conventional data (e.g. hydrological, climatological, topographical etc.) within a GIS give a digital representation of the temporal and spatial variations of the selected variables and can be provided useful input into distributed hydrological models.

The integration or linkage of a distributed hydrological model with the spatial data handling capabilities of a digital elevation model (DEM) and digital terrain model (DTM) can provide distributed information about hydrological processes (Orlandini *et al.*, 1996). The grid and cell approach is quite adaptive for collection of input data on a regular pattern with the use of remote sensing and GIS and it accounts for the variation in topographic characteristics over a catchment in detail. Some of the distributed hydrological models existing in the literature are those developed by Beasley *et al.*, (1980); Abott *et al.*, (1986); Young *et al.*, (1989); Grayson *et al.*, (1992); Vieux and Gaur (1994); Julian *et al.*, (1995); Wang and Hjelmfelt (1998) and Fortin *et al.*, (2001) etc. In most of these the grid based catchment discretization procedures have been followed for simulation of hydrological behaviour of a catchment.

As a consequence of geomorphological and ecological developments of human activities, availability of advanced and sophisticated instrumentation, a number of nuclear techniques have been developed for quantitative assessment of soil erosion and sedimentation rates. Among these, ^{137}Cs has been extensively used to estimate rates of soil erosion (Ritchie and Ritchie, 2005). This technique compares the ^{137}Cs areal activity density at an eroded site to a nearby undisturbed site to assess the extent of soil loss. Similar methods based on the measurement of ^{210}Pb excess ($^{210}\text{Pb}_{\text{ex}}$) over ^{226}Ra and ^7Be have more recently been established. Caesium-137, ^{210}Pb and ^7Be are all highly particle reactive (Matisoff *et al.*, 2002). Their deposition to earth labels the land surface with a unique and identifiable radiological fingerprint. Due to differences in their half-life and fallout history, these radionuclides are suitable for estimating erosion rates over different timescales. Fissionogenic ^{137}Cs (half-life, 30.2 years) can provide a retrospective estimate of land erosion rates over the past 30-40 years (Zapata, 2003), i.e. since the cessation of large-scale nuclear weapon tests in the atmosphere, lithogenic ^{210}Pb (half-life, 22.6 years)

offers a means of estimating erosion rates dating back 100 years (Walling and He, 1999; Walling *et al.*, 2003) and ^7Be (half-life, 53.3 days) can provide an estimate of soil loss associated with a single erosive event.

Due to the remoteness of the location and keeping in view the absence of proper observed data, the present study adopted an integrated approach of remote sensing and GIS with the ^{210}Pb dating technique for the estimation of soil erosion and prioritization of the lake catchment.

1.7 OBJECTIVES

Estimation of soil erosion from the Loktak lake catchment is the primary focus of this work. The present study aims at selecting a soil erosion model suitable for the study area using remote sensing and GIS and establishing a relationship for the soil erosion determination in the study area.

The following objectives are considered for the present work;

1. Selection of the most suitable soil erosion model amongst the existing models on the basis of observed soil erosion data and estimation of soil erosion rates.
2. Estimation of soil erosion rates using nuclear techniques.
3. Validation and testing of the selected soil erosion model.
4. Development of area-specific empirical relationship for estimating soil erosion rates.
5. Prioritization of the watersheds according to the estimated soil loss.

1.8 ORGANIZATION OF THE THESIS

The organization of the thesis describes the details of each chapter. There are seven chapters in all, in the thesis. The chapter wise details of the thesis are as follows:

Chapter 1 introduces the importance of Loktak Lake for Manipur state of India. Massive soil erosion is one of the major threats to the lake. Proper means to predict the soil erosion from the catchments need to be established for adopting proper conservation practices in and around the lake. The objectives of the study are presented in the chapter.

Chapter 2 provides literature review on general erosion and land degradation processes, the types and the factors affecting the processes. Thereafter, the role of remote sensing and GIS in soil erosion and a number of soil erosion models presently in vogue have been discussed. Previous work done on watershed prioritization especially on sediment yield studies for Himalayan Basins too has been described. A detailed description of the work done by various researchers using Nuclear techniques has been discussed.

Chapter 3 gives the description of the study area, its importance and the data used for the present work. The drainage pattern, the land use and the land capability have also been covered. The various watersheds in the Manipur basin have also been discussed. The various morphological features and other watershed parameters have been dealt with. The vegetation, land use and socio-economic conditions, erosion characteristics, physical characteristics of the watersheds, soils characteristics and geomorphology of the watersheds considered for the study have also been presented.

Chapter 4 presents brief details of several soil erosion models and also the basic outlook of the three methods used in the present study i.e. the Universal Soil Loss Equation (USLE), the revised Morgan Morgan Finney (MMF) model and the nuclear techniques (radiometric dating technique of sediment).

Chapter 5 describes the USLE, the Morgan Morgan Finney model and the ^{210}Pb dating technique in detail. The details of data collected, field and laboratory experimental work carried out and the databases generated have been presented in this chapter.

Chapter 6 covers the results of soil loss obtained from the three techniques and their comparison with the observed values. Besides the results of calibration and validation of the MMF model with the ^{210}Pb technique in the two watersheds, the application of the results on the remaining watersheds, development of an empirical model for estimating soil erosion and prioritization of the watersheds are also presented in this chapter.

Chapter 7 presents the conclusions drawn along with scope for further research.

Towards the end, list of references including internet reference have been included.

LITERATURE REVIEW

The main aim of this work is to estimate soil erosion rate in the Loktak Lake catchment. The concept of soil erosion, its different forms and the various factors affecting the process have been presented in this chapter.

The review of the work done by past researchers in the area of soil erosion and some popular soil erosion models being used by various investigators have been discussed. The role of remote sensing and GIS techniques in soil erosion studies and the need for prioritization of the watersheds have also been included in this chapter. A separate section has been devoted to the past work done in the field of soil erosion estimation using nuclear techniques.

2.1 EROSION AND LAND DEGRADATION PROCESSES

Soil erosion results from the integrated interaction amongst rainfall, runoff, land use, soil property, topography, and conservation management. The types of soil erosion caused by water can be divided into splash erosion, sheet (inter-rill) erosion, rill erosion at plot and slope scale and divided into gully erosion, stream and channel erosion, gravity erosion and cave erosion at watershed scale.

Erosion in all its forms involves the dislodgement of soil particles, their removal and eventual deposition away from the original position. This natural process is fundamental in landscape and soil development. Susceptibility to erosion and the rate at which it occurs depend on land use, geology, geomorphology, climate, soil texture, soil structure and the nature and density of vegetation in the area. Morgan (1979, 1986)

defined soil erosion as a two-phase process consisting of the detachment of individual particles from the soil mass and their transport by erosive agents such as running water and wind. When sufficient energy is no longer available to transport the particles a third phase, the deposition, occurs. The rainsplash is the most important detaching agent and continuous exposure to intense rainstorms considerably weakens the soil. Drops behave as little bombs when falling on exposed/bare soil, displacing soil particles and destroying soil structure. With continued rainfall, displaced particles reorient on the surface, filling in larger soil pores and so restricting water infiltration into the soil profile. The soil is also broken up by the weathering processes, both mechanically, by alternate wetting and drying, freezing and thawing and frost action, and biochemically. Soil is disturbed by tillage operations and by the trampling of people and livestock. Running water and wind are further contributors to the detachment of soil particles. All these processes loosen the soil so that it is easily removed by the agents of transport (Morgan, 1979, 1986). Soils are particularly susceptible to erosion under heavy summer rainfall, when vegetative cover is low. These erodible fine particles of organic material, silt and clay are the life essence of the soil.

In India, an area of about 1,750,000 km² out of the total land area of 3,280,000 km², i.e., 53% of total land area is prone to soil erosion (Dhruva Narayana and Babu, 1983). The accelerated soil erosion has irreversibly converted vast tracts of land into infertile surfaces over the country. Deposition of soil eroded from upland areas in the downstream reaches of rivers has caused aggradation. This has resulted in an increase in the flood plain area of the rivers, reduction of the clearance below bridges and culverts and sedimentation of the reservoirs.

The rivers emerging out from the Himalayan region transport the sediment at a very high rate. The other regions of India with most spectacular erosion is the severely

eroded gullied lands along the banks of Yamuna, Chambal, Mahi and other west flowing rivers in Gujarat and the southern rivers, namely, the Cauvery and the Godavari river systems. As a result, agricultural production is greatly affected on the red soils, which cover an area of 720,000 km² in the basins of the Chambal and Godavari (Verma *et al.*, 1968). The depth of these soils is limited to 200 mm, in most of these areas. The lateritic soils which are associated with rolling and undulating topography have been found to lose about 4000 tonne km⁻² of valuable top soil annually due to erosion in Peninsular India (Babu *et al.*, 1978). The black soils, occupying nearly 640,000 km², are usually utilized for crop production under rainfed conditions. Surprisingly, these lands are normally cultivated and kept fallow during the intense rainy season, making them susceptible to serious erosion.

The entire Himalayan region is afflicted with a serious problem of soil erosion and rivers flowing through Himalayan region transport a heavy load of sediment. Himalayan and Tibetan region cover only about 5 percent of the Earth's land surface, but supply about 25 percent of the dissolved load to the world oceans (Raymo and Ruddiman, 1992). A total of 1.8×10^9 tonne yr⁻¹ of suspended sediment (about 9% of the total annual load carried from the continents to the oceans world-wide) is transported in three major river systems; the Brahmaputra, Ganga and Indus; with a combined runoff of 1.19×10^3 km³ (Meybeck, 1976). About 75% of the runoff in these three major rivers occur between June and September, in response to the monsoon precipitation, snow and glacier melt (Collins and Hasnain, 1994). Current estimates of sediment yield of the Ganga and the Brahmaputra rivers together is about 1.0×10^9 tonnes year⁻¹ compared with the global annual sediment flux of about 15×10^9 tonnes year⁻¹ (Milliman and Meade, 1993).

In the Himalayan mountains, as a consequence of loss of forest cover coupled with the influence of the monsoon pattern of rainfall, the fragile catchments have become prone

to low water retention and high soil loss associated with runoff (Valdiya, 1985; Rawat and Rawat, 1994; Joshi and Negi, 1995). Large-scale deforestation, which occurred in the lower range, known as Siwalik range of Himalayas during the 1960s, caused the soil on the land surfaces to be directly exposed to the rains. This unprotected soil was readily removed from the land surface in the fragile Siwalik by the combined action of rain and resulting flow (Kothyari, 1996). Most parts of the Himalayas, particularly the Siwalik, which represent the foothills of the Himalayas in the northern and eastern Indian states, are comprised of sandstone, grits and conglomerates with the characteristics of fluvial deposits and with deep soils. These formations are geologically weak, unstable and hence highly prone to erosion. Accelerated erosion has occurred in this region due to intensive deforestation, large-scale road construction, mining and cultivation on steep slopes. Approximately 30,000 km² have been severely eroded in the north-eastern Himalayas due to shifting cultivation (Dhruva Narayana and Babu, 1983). Increased runoff during the summer monsoon rain has been transferring sediments into the streams and causing floods (Ives and Messerli, 1989). Availability of typical rocks in the particular regions also adds substantially to sediment load. For example, presence of clay-rich rocks, such as the Spiti shales and schist and the widespread existence of limestone deposits, lacustrine mud, and tills contribute to sediment supply to the Spiti River in greater Himalayan range. The combined effects of natural and anthropogenic instability can be visualised in widespread surface erosion processes and local mass movements. Similar erosional features have also been reported by Fort (1987) for dry continental Mustang Himalaya of Nepal.

Deforestation and associated soil erosion has caused desertification of land in the Siwalik Hills in the Hoshiyarpur district of the Punjab state. In 1852, the extent of barren land in this area was 194 km², which increased to 2000 km² in 1939, and then to 20,000

km² in 1981. Similarly, large tracts of cultivable land have been abandoned because of the erosion of topsoil in the Kotabagh area of the Nainital district in the state of Uttar Pradesh. In addition about 45% of the perennial hill springs in these areas go dry during the non monsoon season because of the reduction in groundwater storage resulting from the erosion of the pervious soil horizons (Valdiya, 1985).

2.1.1 Estimation of Soil Erosion

Soil erosion/sediment yield is estimated using sediment curve, erosion modelling and related procedures. The regression equations, which relate the sediment yield to basin and hydrometeorological conditions in that basin, are mostly used for prediction of sediment yield from ungauged catchment. The simulation models provide a physically based representation of the process occurring in small segments of the catchment and route the response of these segments to the catchment outlet.

Surveys for determination of soil erosion rates from catchments and deposition rates in reservoirs are frequently conducted by the various governmental agencies in India (ICAR, 1984). Measurements of sediment load are made in many rivers across the country by other governmental agencies (CSWCRTI, 1991; Shangle, 1991). Nevertheless, sediment loads remain ungauged for the majority of the streams, because of the limitation of funds. However, the other hydrological data, such as rainfall and runoff, are available for the majority of river basins. Estimation procedures can therefore be used to estimate erosion rates for such catchments. In India Joglekar (1965) and Varsheney (1975) have suggested a number of enveloping curves for the prediction of sediment yield for different catchment areas. Correlation studies conducted revealed that areas alone do not have any significant association with sediment production rate (SPR) and hence there is scope for multivariate analysis using climatic and physiographic parameters. Statistical models on a

spatially distributed basis have been developed by Mishra and Satyanarayan (1991) and Bundela *et al.*, (1995) for small watersheds in river Damodar in east India.

Several equations are also available to estimate soil erosion. The Universal Soil Loss Equation (USLE), developed by Wischmeier and Smith (1978), is one of the most useful and reflects considerable research data. The USLE, an empirical equation, estimates average annual mass of soil loss per unit area as a function of most of the major factors affecting sheet and rill erosion. This equation is written as

$$A = R.K.S.L.C.P \quad (2.1)$$

where A is soil loss per unit area, expressed in units selected for K and for the period selected for R; in practice, the units are usually selected so that A is computed in tons per acre per year, but other units can also be selected. R is the rainfall-runoff factor- the number of rainfall-erosion index units, plus a factor for runoff from snow melt or applied water where such runoff is significant. K is erodibility factor-the soil loss rate per erosion index unit for a specified soil as measured on a unit plot, L is slope length factor- the ratio of soil loss from the field slope length, S is the slope steepness factor, C is crop management factor and P is the support practice factor. The USLE gives estimate of total soil detached and displaced over short distances, but does not indicate the sediment delivered to the reservoir. Much deposition and reduction in sediment yield occurs between the sediment source and reservoirs. This reduction is estimated with a sediment delivery ratio. Sedimentation in reservoirs defined by trap efficiency depends on factors such as the ratio of runoff inflow to reservoir capacity, sediment size, shape and stage of the reservoir, outlet works, and methods of reservoir operation. In India, reservoir sedimentation is generally estimated from the suspended load of the stream feeding the reservoirs, and by periodic direct measurement of sediment deposition in reservoirs.

An isoerodent map of India has been prepared based on the erosion index values (Babu *et al.*, 1978), which shows the potential erosivity of rainfall. Methods have also been evolved for determination of the off site deposition of eroded soil and the sediment yield from large catchments (Garde and Kothyari, 1987; Kothyari *et al.*, 1994). However, a statistical study to date for estimation of sediment yield from large catchments was made by Garde and Kothyari (1987). An analysis of the data from 50 catchments with areas ranging from 43 km² to 83,880 km² produced the following equation for mean annual sediment yield in plain areas:

$$S_{am} = C P^{0.6} F_e^{1.7} S^{0.25} D_d^{0.10} (P_{max}/P)^{0.19} \quad (2.2)$$

where

$$F_e = (0.8 F_A + 0.6 F_G + 0.3 F_F + 0.1 F_W)/A \quad (2.3)$$

where S_{am} is the mean annual sediment yield in cm, C is a coefficient depending on the geographical location of the catchment, P is the average annual rainfall in cm, S is the land slope, D_d is the drainage density in km km⁻², P_{max} is the average maximum monthly rainfall in cm and A is the catchment area in km². F_e is defined as the erosion factor and F_A is the area of arable land in the catchment, F_G is the area occupied by grass and shrub while F_W is the area of wasteland and F_F is the forested area.

The transporting agents comprise those which act areally and contribute to the removal of a relatively uniform thickness of soil and those which concentrate their action in channels. The first group consists of rainsplash, overland flow (sheet flow) and wind. The second group covers water flow in small channels, known as rill or in the larger, more permanent features of gullies and rivers.

2.1.1.1 Rainsplash erosion

The action of raindrops falling on soil particles is understood by considering the momentum of a single raindrop falling on a sloping surface. The transference of

momentum to the soil particles has two effects. First, it provides a consolidating force, compacting the soil, and second, it imparts a velocity to some of the soil particles, launching them into the air. On landing, they transfer their own downslope momentum to others particles and the jumping process is repeated (Morgan, 1986).

2.1.1.2 Sheet erosion

Sheet and rill erosion are two of several forms of land degradation resulting from flowing water. These occur mainly on sloping land where there is insufficient ground cover to prevent soil erosion. Such types of erosion dominate on cultivated lands (SCS of NSW, 1989) and decline land productivity by removing the uppermost layers of the soil, which contain higher proportions of nutrients and organic matter.

There are various methods of studying sheet erosion, ranging from prediction to direct measurements (Bryan, 1990; Toy *et al.*, 2002). All methods involve certain characteristics and a series of biases.

Bodoque *et al.*, (2005) described the determination of sheet erosion rates by using dendrogeomorphological methods on exposed tree roots. Two sites on the northern slope of the Guadarrama Mountains, Central Spain, were studied: a popular trail in a Scots pine forest (Senda Schmidt, Valsaín) growing on granites and gneisses, and an open holm-oak forest on granitic slopes (Monterrubio). These sites were selected because they showed high denudation morphologies due to accelerated soil-erosion processes caused by human influence (trampling by continuous trekking and overgrazing), resulting in exposed roots. The method applied was based on the morphological pattern of roots, defined by the growth-ring series of the sampled roots. In order to confirm the validity of the criteria used and to make the estimations of erosion more accurate, several anatomical indicators of exposed and non-exposed *Pinus sylvestris* roots were characterized.

The study entailed a statistical analysis of exposure time and erosion depth. The influence of environmental factors affecting the variation in velocity of the erosion processes was also examined. With a significance level of 95%, the mean erosion rates were in the range of 1.7–2.6 mm/year (29–44 t/ha/year) on Senda Schmidt over the last 101 years, and 1.1–1.8 mm/year (19–31 t/ha/year) in Monterrubio over the last 42 years. Using a multifactor analysis of variance, we observed a change in the erosion rates as a function of position on the path along Senda Schmidt. In Monterrubio, however, they reached no significant conclusions, apart from an inverse relationship between erosion and slope gradient that was difficult to interpret.

2.1.1.3 Rill erosion

Rills are small channels which function as both sediment source areas and sediment transport vehicles on hill slopes. They are therefore critical components to the erosion system for upland segments where erosion rates are great and actively eroding rills are generally present (Ellison, 1947). If rainfall exceeds infiltration, a surface film of water forms (see sheet erosion). Rill erosion results from a concentration of this surface water into deeper, faster-flowing channels, which follow depressions or low points through fields. The shearing power of the water can detach, pick up and remove soil particles making these channels the preferred routes for sediment transport (SCS of NSW, 1989). Rill erosion often occurs with sheet erosion and is commonly seen in fields of recently cultivated soils following high-intensity rainfall. It is easily identified as a series of little channels or rills up to 30 cm deep. Rill erosion is often described as the intermediate stage between sheet and gully erosion.

Rill erosion (Foster, 1986; Bryan, 1987; Flanagan, 2002) consists on the development of numerous minute closely spaced channels resulting from the uneven

removal of surface soil by running water that is concentrated in streamlets of sufficient discharge and velocity to generate cutting power. It is an intermediate process between sheet erosion and gully erosion (Jackson, 1997). While the presence of rills is restricted to planar elements of watersheds, ephemeral gullies occur on valley bottoms, within swales. Ephemeral gullies and rills are common in cultivated soils in many areas around the world, and can cause large soil losses.

2.1.1.4 Gully erosion

The first point of view considers that once rills are large enough to restrict vehicular access they are referred to as gullies or gully erosion. Major concentrations of high-velocity runoff water in these larger rills remove vast amounts of soil. This results in deeply incised gullies occurring along depressions and drainage lines. Removal of topsoil and subsoil by fast-flowing surface water creates abrupt deep and wide gullies. Gullies may widen through lateral erosion, where water undercutting causes subsequent slumping of the sides. Gully sides may also be subject to splash, sheet or rill erosion (SCS, 1989). Another point of view based on studies in the gullies of the southwest United States revealed that their initiation is a more complex process. In the first stage small depressions form on a hillside as a result of localized weakening of the vegetation cover grazing or by fire. Water concentrates in these depressions and enlarges them until several depressions coalesce and an incipient channel is formed. Erosion is concentrated at the heads of the depressions where near-vertical scarps develop over which supercritical flow occurs. Some soil particles are detached from the scarp itself but most erosion is associated with scouring at the base of the scarp which results in deepening of the channel and undermining of the headwall, leading to collapse and retreat of the scarp upslope (Ologe, 1972). Another way in which gullies are initiated is where linear landslides leave deep, steep-sided scars which may be occupied by running water in subsequent storms. This

type of gully development has been described in Italy by Vittorini (1972). Whatever the way gully erosion occurred, it means the loss of large volumes of soil. Deep wide gullies, sometimes reaching 30m deep, severely limit the use of the land, while offsite deposition of soil causes water-quality decline in streams or rivers and sedimentation of dams and reservoirs. Large gullies disrupt normal farm operations, creating access problems for vehicles and stock. Gully erosion often occurs on lower slopes, but can form quite high in the landscape in particularly susceptible areas.

Mass movement

In mass movement of soil *i.e.* slides, slips, slumps, flows and landslides, gravity is the principal force acting to move surface materials such as soil and rock. When natural slope stability is disrupted, a range of complex sliding movements may occur. As a rule of thumb, rapid movements of soil or rock that behave separately from the underlying stationary material and involve one distinct sliding surface are termed landslides. Such movement is rarely the result of a single factor, but more often the final act in a series of processes involving slope, geology, soil type, vegetation type, water, external loads and lateral support. Generally mass movement occurs when the weight (shear stress) of the surface material on the slope exceeds the restraining (shear strength) ability of that material. Factors increasing shear stress include erosion or excavation undermining the foot of a slope, loads of buildings or embankments, and loss of stabilising roots through removal of vegetation. Vegetation removal and consequent lower water use may increase soil water levels, causing an increase in pore water pressure within the soil profile. Increased pore water pressure or greater water absorption may weaken inter-granular bonds, reducing internal friction and therefore lessening the cohesive strength of the soil and ultimately the stability of the slope. The quantity of sediment moved from the hillsides into rivers by mass movement is far in excess of that contributed by gullies, rills and

overland flow (Morgan, 1979, 1986). In rural areas mass movement inhibits farm production and land use by loss of accessibility, exposure of infertile sub soils and loss of stock and capital items.

2.1.1.5 Streambank erosion

Streambank erosion is the direct removal of banks and beds by flowing water. Typically, it occurs during periods of high stream flow. It is sometimes confused with gully erosion as this has similarities with seasonal or ephemeral streams. Erosion of stream or river banks through lateral (side) erosion and collapse often causes high sediment loads in creeks and rivers. The problem is often initiated by heavy falls of rain in catchments with poor vegetation cover, causing excess run-off. The resultant high volume and velocity runoff will concentrate in the lower drainage lines or streams within catchments. When the stress applied by these stream flows exceeds the resistance of the local soil material, streambank erosion occurs. As the sediment load increases, fast-flowing streams grind and excavate their banks lower in the landscape. Later, the stream becomes overloaded or velocity is reduced, and deposition of sediment takes place further downstream or finally in dams and reservoirs. Streambank erosion is exacerbated by the lack of riparian zone vegetation and by direct stock access to streams. Subsequent deposition of soil causes problems on productive land downstream and sedimentation in reservoirs. Other problems include reduction in water quality due to high sediment loads, loss of native aquatic habitats, damage to public utilities (roads, bridges and dams) and maintenance costs associated with trying to prevent or control erosion sites (SCS, 1989). Catchments with little vegetation cover and steep gradients will often have high rates of water run-off that result in high-velocity stream flows. Stream straightening, dredging or realignment to accommodate roads or rail lines leads to increased stream power and velocity, which in turn will increase the energy applied to stream banks.

The erosive impact of these high-velocity stream flows will depend on the stability of the bank material. For instance, sand will erode more easily than gravel and silt will erode more easily than sand.

2.1.1.6 Wind erosion

Wind erosion is the movement and deposition of soil particles by wind. Wind erosion occurs when soils bared of vegetation are exposed to high-velocity wind. Wind erosion is an internationally recognized land degradation issue that affects 28% of the global land area experiencing land degradation (Oldeman, 1994; Callot *et al.*, 2000; Prospero *et al.*, 2002).

Wind erosion is initiated under favourable conditions when energy brought to an erodible surface by wind exceeds the energy required to mobilize micropeds on the soil surface (Callot *et al.*, 2000). The susceptibility of a landscape to wind erosion is dependent on atmospheric conditions, and the threshold friction velocity, which is a factor of land surface characteristics such as vegetation (cover, distribution and height), soil moisture, pedology (grain size, aggregation, surface crusting) and land use.

In Australia, the most developed arid continent, attempts have been made at quantifying and mapping land surfaces threatened by wind erosion (Shao *et al.*, 1994; Butler *et al.*, 1996; Lu and Shao, 2001). These studies have approached wind erosion at either a broad-scale (greater than 800×800 km) or paddock-scale (less than 2 km²). Although studies have found likely dust source regions, there is yet to be a quantitative assessment of landscape erodibility at a national scale (Shao *et al.*, 1994; Prospero *et al.*, 2002).

2.1.1.7 Tunnel erosion

Tunnel/piping erosion has been increasingly recognized as a significant hillslope hydrological and geomorphologic process in a wide range of climatic regions (Gilman and Newson, 1980; Jones and Bryan, 1997; McCaig, 1983). However, most of the field programs were designed to monitor hydrological responses of pipeflow to natural rainstorms. The pipeflow erosion processes and their relationship to hydrological processes are still not fully understood. The relative significance of surface and sub-surface erosion in hillslope sediment delivery, and the overall contributions of sub-surface erosion to basin sediment yield are not firmly established in the different regions.

Zhu *et al.*, (2002) carried out a detailed study of monitoring the water and sediment delivery from major tunnel systems in a small semi-arid sub-basin, locally known as Yangdaogou, in the hilly loess region, North China. These deep-seated tunnels were located as much as 30 m below the slope surface, in deep Quaternary loess formations. In the Yangdaogou, these systems have large amphitheatre-like inlets, with mean diameter and depth of 4.8 and 4.99 m, respectively. These dimensions represented some of the largest tunnel inlets in the world. During 1989 and 1990, fifteen rainstorms were monitored at six tunnel outlets. Due to practical difficulties, only 35 sets of tunnel-storm data were obtained. Observed sediment concentration of tunnel flows ranged from 8.2 to 893.2 g/l. The peak sediment concentrations in tunnel flows were not distinctively higher than those in channel flows but considerably higher than those measured from untunneled sideslopes. No significant correlations between runoff and sediment yield could be found in most tunnels at both within-and between-storm levels. Such an erratic relationship was ascribed to the rapid shift of runoff and sediment source area, the occurrence of collapses within tunnels, and the initiation of new tunnel inlets. Based on the field monitored data, 57% of basin sediment

production was delivered by the tunnel systems, suggesting that tunnel erosion was a major erosion process in the hilly loess region

2.2 EFFECTS OF LANDSCAPE PATTERN ON SOIL EROSION

At a large scale, the effects of landscape pattern on soil erosion should include both the effects of landscape component change at slope and plot scale on soil erosion, and also the interception function of landscape component spatial arrangement on soil loss. Landscape pattern could also change the quantity of soil loss from watersheds through gully and cave erosion.

2.2.1 Effects of Land Use Type on Soil Erosion

The intensity of soil erosion varies sharply in different land use types. Soil cover is the most significant factor in controlling the erosion process. Vegetation of all kinds is nature's protective soil cover, protecting soil from the direct impact of raindrops. Basically, the protective function of vegetation cover and soil cover can: (1) protect the surface of the soil from the impact of falling precipitation, (2) maintain or enhance the soil's infiltration capacity, (3) hold the soil particles in place, and (4) retard the velocity of runoff (Liu *et al.*, 2001). Land use types could greatly affect soil erosion by altering the characteristics of underlying surfaces (Qiu *et al.*, 2002). A number of studies have shown that rainfall interception and absorption varied with the type of vegetation. Consequently, the ability to hold soil particles also varies with the type of vegetation (Zhu *et al.*, 2003). Land-use could result in the changes of soil's physical and chemical properties (Fu *et al.*, 2002a; Guo *et al.*, 1999), which may help to control soil erosion. A comparative study of soil erosion considering different types of vegetation (natural forest, horticultural crops in rotation, pasture, apple trees cultivated on bench terraces) was conducted in an ecological unit of the Venezuelan Andes. Soil losses were quantified by using erosion plots in areas

covered by four types of vegetation, including both natural and cultivated vegetation. The results of this research indicated that the erosion measured on the four vegetation systems showed significant differences (horticultural crops in rotation > apple trees cultivated on a bench terrace > pasture > natural forest) and the lowest and highest soil loss rate occurred with natural forest and with horticultural crops in rotation, respectively. Meanwhile, soil erosion under different horticultural crops showed significant variation (potato crop > carrot > arracacha) (Sa'nchez *et al.*, 2002). Therefore, land use is a dominant factor that affects the occurrence of the soil erosion processes. Soil conservation practices and management levels could have an impact on soil loss by changing micro-terrain and soil loss ratio. Fu *et al.*, (2002c, 2004) examined the effects of land use type on soil erosion in a hilly and gully area of the Loess Plateau of China. Results revealed that under the same slope angle, slope length, slope aspect, slope type, slope position and plot area, sediment yield and runoff showed significant differences with the change in land use, and conversion of farmland to forest or pasture could greatly reduce sediment yield and runoff. Remodelling the badland features by creating a longer slope at lower angles has altered the degree to which soil erosion processes operate in these areas, erosion and deposition were strongly localized with minimal sediment delivery to ephemeral or perennial channel systems (Clarke and Rendell, 2000). In addition, it was found that agricultural practice and cattle grazing could increase soil losses in pasture and the average soil loss for apple trees on bench terraces was significantly lower than that in a cultivated field with conservation practices (Sa'nchez *et al.*, 2002).

2.2.2 Effects of Land Use Structure on Soil Erosion

Changes in land use structure have a significant impact on soil loss. Sedimentation surveys of dams in a small sandstone drainage basin near Sydney, Australia, demonstrated that land use was the dominant factor determining sediment yields and soil loss rates.

Cultivated basins produced an average sediment yield of 7.1 ton/ha/year whereas grazed pasture and forest/woodland basins exported averages of only 3.3 and 3.1 ton/ha/year, respectively. Nevertheless, these yields were high by Australian standards. Sediment exported from grazed pasture and forest/woodland basins were similar because the forest/woodland basins are also grazed (Erskine *et al.*, 2002). Ni and Li (2001) used a characteristic index to reflect the comprehensive impacts of land use structure in loess area in China and results demonstrated that there was a significantly negative relationship between soil erosion rate at watershed scale and characteristic index of land use structure given that perennial precipitation was the same. At watershed or catchment scale, there was a certain correlation between land use types and sediment yields. In Hongtagou watershed, located in Shaanxi province of China, there was a negative exponential correlation between ratio of farmland and sediment yield and a positive exponential correlation between ratio of slop farmland and soil loss rate. Changes in land use structures from 1976 to 1986 played an important and positive role in controlling soil loss in this watershed (Yu, 1996). However, the relationship between land use types and sediment yield showed significant spatial variation characteristics in different regions due to the spatial variation of rainfall, terrain and soil properties.

2.2.3 Effects of Landscape Pattern on Soil Erosion

The spatial variability of landscape components, particularly the change of spatial distribution of land use on the environmental factors such as rainfall, topography and soil property, may change the hydrological structure and soil erosion systems (Ludwig *et al.*, 1995; Vandaele and Poesen, 1995). The spatial variation of land use could also change (increase or decrease) its interception ability in soil loss, which may further affect the final sediment load at watershed scale (Slattery and Burt, 1997; Takken *et al.*, 1999). In order to identify the relationship between land use pattern and soil erosion, some distributed soil

erosion models were applied to simulate soil erosion rate under different land use patterns. Fu *et al.*, (2002b) applied the LISEM model to study the impact of five land use patterns on soil loss in Danangou catchment in the Loess Plateau in China and results demonstrated that soil loss rate showed a declining trend with the conversion of land use pattern from their actual condition to planning scenarios. Oost *et al.*, (2000) applied the WATEM model, a spatially distributed water and tillage erosion model, to study the impact of land use pattern changes on water erosion in three small watersheds in the Belgian Loam Belt during the period from 1947 to 1990. Results suggested that the calculation of LS-value (slope length and slope steepness) has been affected by the average size of plots, which may have an impact on erosion risk from water erosion. It was also found that dynamics of water erosion rate were controlled by an integrated interaction of determinant factors including changes in land use types, plot area, and position of field boundary. At a watershed or catchment scale, the relationship between landscape pattern change and soil loss may be quantified based on a descriptive index of landscape pattern characteristics. Chen *et al.*, (2003) applied the source-sink ecological process theory to quantify the relationship between landscape pattern and non-point source pollution. Chen proposed a new landscape metric index, location-weighted landscape contrast index (LCI), which could be used to determine the impact of ecological processes as related to distance, relative elevation and slope degree and to quantify landscape spatial pattern by using point-based ecological measurements. Zhao *et al.*, (2004a, 2004b) applied Chen's theory to their research on a hilly catchment in the Loess Plateau and found that "distance to river" could be used to denote the "distance" and "relative elevation" of landscape units to the outlet of the catchment, assuming that the basic sediment discharge ratio was 1. Zhao also found that the characteristics of land use pattern could be denoted by the spatial distribution of C value (crop coverage factor value) on "slope gradient" and the

“distance to rivers”, and the dynamics of soil loss were analyzed by the relative ratio of rainfall and runoff, rainfall and sediment yield, rainfall erosivity and sediment discharge.

2.3 USE OF REMOTE SENSING AND GIS IN SOIL EROSION MODELLING

Remote sensing is very useful in assessing the land cover of an area at a particular time and monitoring the change over a given period (Lillisand and Kiefer, 1987). Furthermore, the land cover being spatial in nature, GIS can be employed as a powerful tool in monitoring and data processing. With the creation of digital terrain model, it is possible to make digital representation of the topography of the area. This information is very useful in estimating soil erosion, runoff and other analyses (Burrough, 1986; Arnof, 1991; Goyal, 2004; Chatterjee *et al.*, 2005 and Goswami *et al.*, 2007).

The soil and forest are the two main resources of the watershed. Their amount of change in specified period of time is the indication of the status changing speed. So by assessing the forest and soil loss change between a time period and contribution to the soil loss change, degradation speed index (DSI) can be calculated using the empirical formula given by Sah *et al.*, (1998).

An integrated approach of digital image processing of satellite data and visual interpretation of aerial photograph combined with GIS and USLE was carried out for land cover change and soil loss estimation. Matrix analysis between Degradation speed index and Sensitivity index was done. They were grouped into different classes, which were used for second matrix analysis with present condition of watershed for the prioritization.

Tripathi (2001) has worked for identification of watershed project formulation and implementation. Sediment yield index was used as prioritization parameter of River Valley Projects (RVP) and Flood Prone Rivers Project (FPRP). Other parameters were

introduced keeping in view of soil and water characteristics in a participatory watershed management programme. These included silt yield index, existing water resources, water quality, fertility of the soil, existing employment opportunity, availability of basic amenities viz; transport, school, hospital, post office, bank, cooperative societies, marketing, communication and adoption of the village by other agencies.

2.3.1 Modelling Soil Erosion

Field studies for prediction and assessment of soil erosion are expensive, time-consuming and data need to be collected over many years. Though providing detailed understanding of the erosion processes, field studies have limitations because of complexity of interactions and the difficulty of generalizing from the results. Soil erosion models can simulate erosion processes in the watershed and may be able to take into account many of the complex interactions that affect rates of erosion.

Soil erosion prediction and assessment has been a challenge to researchers since the 1930s' and several models have been developed (Lal, 2001). These models are categorized as empirical, semi-empirical and physical process-based models. Empirical models are primarily based on observation and are usually statistical in nature. Semi-empirical model lies somewhere between physically process-based models and empirical models and are based on spatially lumped forms of water and sediment continuity equations. Physical process-based models are intended to represent the essential mechanism controlling erosion. They represent the synthesis of the individual components which affect erosion, including the complex interactions between various factors and their spatial and temporal variabilities. Some of the widely used erosion models are discussed below:

2.3.1.1 Empirical models and semi-empirical models

Universal Soil Loss Equation (USLE)

USLE is the most widely used empirical overland flow or sheet-rill erosion equation. The equation was developed to predict soil erosion from cropland on a hillslope. The equation is given by –

$$A = R.K.L.S.C.P \quad (2.4)$$

where, A is the average annual soil loss (mass/area/year); R is the rainfall erosivity index; K is the soil erodibility factor (t/ha); L is the slope length factor; S is the slope gradient factor; C is the vegetation cover factor, and P is the conservation protection factor.

Revised Universal Soil Loss Equation (RUSLE)

The RUSLE updates the information on data required after the 1978 release, and incorporates several process-based erosion models (Renard *et al.*, 1997). RUSLE remains to be a regression equation –

$$A = R.K.L.S.C.P \quad (2.5)$$

A principal modification is in R factor which includes rainfall and runoff erosivity factor (run-off erosivity also includes snow melt where run-off is significant). There are also changes in C factor which is based on computation of sub-factor called soil loss ratios (SLR). The SLR depends on sub-factors: prior land use, canopy cover, surface cover, surface roughness and soil moisture (Renard *et al.*, 1997).

Modified Universal Soil Loss Equation (MUSLE)

Williams (1975) proposed a modified version of USLE that can be written as–

$$S_{ye} = X_e.K.L.S.C_e.P_e \quad (2.6)$$

Where, S_{ye} is the event sediment yield

$$X_e = \alpha \cdot (Q_e \cdot q_p)^{0.56} \quad (2.7)$$

Where, α is an empirical co-efficient; Q_e is the run-off amount and q_p is the peak run-off rate obtained during the erosion event and K, L, S, C_e and P_e are as defined for USLE.

2.3.1.2 Physical process-based models

Empirical models have constraints of applicability limited to ecological conditions similar to those from which data were used in their development. Further, USLE cannot deal with deposition; its applicability limits large areas and watersheds. Based on these considerations, several process-based models have been developed (e.g. WEPP, EUROSEM, LISEM (Lal, 2001)).

Water Erosion Prediction Project (WEPP) model

The WEPP is an example of widely used physically process-based erosion model (Renard *et al.*, 1996). It was developed as a system modelling approach for predicting and estimating soil loss and selecting catchment management practices for soil conservation. Basic erosion and deposition equations in WEPP are based on the mass balance formulation that uses rill and inter-rill concept of soil erosion, which is a steady-state sediment continuity equation. The WEPP model computes erosion by rill and inter-rill processes. The sediment delivery to rill from inter-rill is computed by following equation

$$D_i = K_i \cdot I_e^2 \cdot G_e \cdot C_e \cdot S_f \quad (2.8)$$

where, D_i is the delivery of sediment from inter-rill areas to rill ($\text{kg}/\text{m}^2/\text{sec}$); K_i is the inter-rill erodibility ($\text{kg}/\text{m}^4/\text{sec}$); I_e is the effective rainfall intensity (m/sec .); G_e is the ground cover adjustment factor and S_f is the slope adjustment factor calculated as per equation given below –

$$S_f = 1.05 - 0.85 \exp(-4 \sin \alpha) \quad (2.9)$$

where, α is the slope of the surface towards nearby rill. In comparison, rill erosion is the detachment and transport of soil particles by concentrated flowing water -

$$D_c = K_r \cdot (T - T_c) \quad (2.10)$$

Where, K_r is the rill erodibility (sec/m); T is the hydraulic shear of flowing water (Pa) and T_c is the critical hydraulic shear that must be exceeded before rill detachment can occur (Pa).

Wind Erosion model

Comparable to the USLE, a wind erosion model was proposed by Woodruff and Siddoway (1965) as shown in equation given below –

$$E = f(I, K, C, L, V) \quad (2.11)$$

where, E is the mean annual wind erosion; I is the soil erodibility index; C is the climatic factor (Wind energy); L is the unsheltered median travel distance of wind across a field; V is the equivalent vegetative cover. This equation has been widely adopted and used for estimating erosion hazard in dry lands.

The potential utility of remotely sensed data in the form of aerial photographs and satellite sensors data has been well recognized in mapping and assessing landscape attributes controlling soil erosion, such as physiography, soils, land use/land cover, relief, soil erosion pattern (e.g. Pande *et al.*, 1992). Remote sensing can facilitate studying the factors enhancing the process, such as soil type, slope gradient, drainage, geology and land cover. Multi-temporal satellite images provide valuable information related to seasonal land use dynamics. Satellite data can be used for studying erosional features, such as gullies, rainfall interception by vegetation and vegetation cover factor. DEM (Digital Elevation Model) one of the vital inputs required for soil erosion modelling can be created by analysis of stereoscopic optical and microwave (SAR) remote sensing data. Geographic Information System (GIS) has emerged as a powerful tool for handling spatial and non-spatial geo-referenced data for preparation and visualization of input and output, and for interaction with models. There is considerable potential for the use of GIS technology as

an aid to the soil erosion inventory with reference to soil erosion modelling and erosion risk assessment. Erosional soil loss is most frequently assessed by USLE. Spanner *et al.*, (1982) first demonstrated the potential of GIS for erosional soil loss assessment using USLE. Several studies have shown the potential utility of remote sensing and GIS techniques for quantitatively assessing erosional soil loss (Saha *et al.*, 1991; Saha and Pande, 1993; Mongkosawat *et al.*, 1994). Satellite data analyzed soil and land cover maps and DEM derived and ancillary soil and agro-climatic rainfall data are the basic inputs used in USLE for computation of soil loss. The availability of GIS tools and more powerful computing facilities makes it possible to overcome difficulties and limitations and to develop distributed continuous time models, based on available regional information. Recent development of deterministic models provides some spatially distributed tools, such as AGNPS (Young *et al.*, 1989); ANSWERS (Beasley *et al.*, 1980), and SWAT (Arnold *et al.*, 1993). The primary layers required for soil erosion modelling are terrain slope gradient and slope length which can be generated by GIS aided processing of DEM. Flanagan *et al.*, (2000) generated the necessary topographic inputs for soil erosion and model simulations by linking WEPP model and GIS and utilizing DEM.

Manju *et al.*, (2005) carried out a study to delineate the wetlands of east Champaran district of Bihar using IRS 1D LISS III data. The data for the pre and post monsoon seasons were analyzed and the wetlands have been qualitatively characterized based on the turbidity and aquatic vegetation status. The extent of water logging problem in the study area was inferred from the seasonal variation of the waterspread during both the seasons. The three categories of wetlands (ponds/lakes, water logged areas and oxbow lakes) were identified. From the analysis, it was concluded that the inland wetlands constitute 2.7% of the study area, of which 1.8% is subjected to water logging. Thus, this

study highlights the usefulness of remotely sensed data for wetland mapping, seasonal monitoring and characterization.

Morgan *et al.*, (1984) developed a model to predict annual soil loss which endeavors to retain the simplicity of USLE and encompasses some of the recent advances in understanding of erosion process into a water phase and sediment phase. Sediment phase considers soil erosion to result from the detachment of soil particles by overland flow. Thus, the sediment phase comprises two predictive equations, one for rate of splash detachment and the other for the transport capacity of overland flow. The model uses six operating equations for which 15 input parameters are required. The model compares predictions of detachment by rain splash and the transport capacity of the run-off and assesses the lower of the two values as the annual rate of soil loss, thereby denoting whether detachment or transport is the limiting factor.

Morgan (2001) presented a revised version of the Morgan–Morgan–Finney model for prediction of annual soil loss by water. Changes were made to the way soil particle detachment by raindrop impact is simulated, which now took account of plant canopy height and leaf drainage, and a component was added for soil particle detachment by flow. When tested against the same data set used to validate the original version at the erosion plot scale, predictions made with the revised model gave slopes of a reduced major-axis regression line closer to 1.0 when compared with measured values. The coefficient of efficiency, for sites with measured runoff and soil loss, increased from 0.54 to 0.65. When applied to a new data set for erosion plots in Denmark, Spain, Greece and Nepal, very high coefficients of efficiency of 0.94 for runoff and 0.84 for soil loss were obtained. The revised version was applied to two small catchments by dividing them into land elements and routing annual runoff and sediment production over the land surface from one element to another. The results indicate that, when used in this way, the model provides useful

information on the source areas of sediment, sediment delivery to streams and annual sediment yield.

Teklehaimanot (2003) carried out simple field tests in Lom Kao Area in Thailand to estimate the erodibility of different landforms. The findings of the research indicate that the soil erodibility differed between landscapes and within landscapes. In the Hilllands the erodibility was high (0.5). It varied from moderate to very high in the piedmonts (0.3 – 0.7). In the Low Mountains, it ranged from very low to moderate (0.05 to 0.30). In the High Mountains, it varied from low to moderate (0.10 – 0.30). The dry crumb test, manipulation test, rainfall acceptance test, pinhole test and shear van test were used to parameterise erodibility factor that was used in the revised MMF model. The soil erodibility estimated by the simple field test was compared with the given erodibility values (Guide value for soil parameters in revised MMF model). The statistical test showed that there is no significant difference between the two values. The revised MMF model was used to estimate the annual soil loss in the study area. In general the findings showed that the annual soil loss rate is low, which is less than 1.5 tones ha yr⁻¹. Relatively it was found to be higher in the hilllands i.e. 1.4 tones ha yr⁻¹ and lower in the Low Mountain and High Mountain i.e. almost 0. The aggregated soil loss per landforms or soil map units that ranged between 0.01 to 1.4 tones ha yr⁻¹ is within the soil loss tolerance determined for tropical soils.

Jain *et al.*, (2001) used two different soil erosion models, i.e. the Morgan model and Universal Soil Loss Equation (USLE) model, to estimate soil erosion from a Himalayan watershed. Parameters required for both the models were generated using remote sensing and ancillary data in GIS mode. The Morgan method gave fairly good results for areas located in hilly terrain.

2.4 SEDIMENT YIELD STUDIES FOR HIMALAYAN BASINS

For Himalayan basins some typical studies have been carried out. Rao *et al.*, (1997) has worked on sediment yield estimation for Chenab basin. In this study data of 9 sediment stations within Chenab basin varying from 17 to 27 years was utilised to develop a statistically significant spatial model to estimate sediment yield using geomorphological, climatic and land use, landcover parameters. The sediment yield was estimated for total and fine sediment for monsoon, winter, pre-monsoon and annual seasons. The study revealed the high rates of sedimentation in Chenab basin and its effect on capacity of existing Salal dam reservoir near Jammu.

The sediment yield response of snow and glacier dominated catchments in the Himalayas is different from rainfed catchments in the rest of India. Rao *et al.*, (1997) attempted to relate sediment yield with geomorphological, land use and climatic parameters for the Chenab basin having an area of 22,200-km², which is a large Himalayan basin. Sediment yield characteristics in the Chenab basin vary depending on the season. During the winter season (October-March) the sediment yield is minimal and is less than 5-10% of the annual yield. During pre-monsoon season (April-June) the seasonal snow cover melts in the intermediate and upper reaches and lower reaches receive rain. Thus, a significant sediment yield is observed from the catchment in the pre-monsoon season. During the monsoon season (July-Sept.) rainfall contribution to flows is very high in the lower reaches and gradually tapers at elevations of about 4,000 m (Singh *et al.*, 1995). Air temperatures are also at their maximum during the season resulting in snow and glacier melt from permanent snow covered zones. Consequently, a major part of the sediment yield is received during the monsoon season. Average sediment yields for annual and monsoon season periods in terms of coarse, medium and fine sediment are shown in Table 2.1.

The rates of suspended sediment transport in the Chenab river are high as compared with other river systems in India (with exception of Ganges) and in the world (Milliman and Meade, 1993). The precipitation and runoff characteristics in the Chenab basin influence sediment yield to a large extent. Snowmelt and glacier melt runoff contribution increase with elevation, while rainfall decreases with elevation in the upper reaches (Rao *et al.*, 1996). To verify, how far rain is responsible for sediment production in various subbasins of Chenab located at different elevations, mean weighted rainfall during the monsoon (Jul to Sep.) in each sub-basin was correlated (log-linearly) with sediment yield per unit area using 10 years of concurrent data, assuming that catchment characteristics remained unchanged during the period. The correlation coefficients, r , shown in Table 2.2, with exception of Kuriya sub-basin indicate less sediment yield on rainfall in the upper reaches as compared with the lower reaches of Chenab basin. In other words, rainfall may have little to do with the sediment yield in the upper reaches of Chenab catchment. The amounts of mean rainfall during the monsoon season (July-Sep.) and the winter season (Oct to Mar.) decreases with increase in elevation (Table 2.2). Consequently sediment response characteristics vary markedly between the upper and lower reaches of the catchment and hence the low coefficient of correlation is obtained for Kuriya stations in the transition zone. The transition zones also experience rain-on-snow phenomena. Beside rainfall, some of the reasons besides rainfall may also be attributed to the prevailing geologic and soil conditions and melts runoff from permanent

Table 2.1: Average sediment yields in the Chenab basin at different locations along with their composition during the monsoon period

Site	Annual average sediment yield (t/km ² /yr)	Monsoon Season (t/km ² /yr)			Total Sediment yield for monsoon Period (Jul - Sep.) (t/km ² /yr)
		Fine	Medium	Coarse	
Akhnoor	1029	455.9	180.8	85.9	722.7
Benzwar	1597	694.5	360.9	169.6	1225.0
Dhamkund	1900	533.5	386.4	314.3	1234.3
Ghousal	513	221.2	90.3	69.7	381.3
Kuriya	878	300.9	152.4	138.9	592.3
Premnagar	1363	222.9	112.9	102.9	438.7
Sirshi	939	221.4	186.6	146.7	554.8
Tandi	371	164.0	70.6	51.3	286.0
Tillar	373	92.4	62.2	40.7	195.4

Source: Rao *et al.*, 1997.

Table 2.2: Correlation of mean basin monsoon rainfall with sediment yields (t/km^2)

Sediment Station	Basin average winter rainfall up to respective gauging sites (mm)	Elevation of sediment gauging station (m)	Basin average monsoon rainfall up to respective gauging sites (mm)	Correlation coefficient between mean weighted rainfall and sediment yield
Akhnoor	588	305	740	0.61
Dhamkund	277	600	353	0.70
Premnagar	201	886	252	0.75
Kuriya	226	1,106	229	0.16
Benzwar	408	1,135	197	0.66
Sirshi	103	1,162	170	0.50
Tillar	71	2,066	153	0.50
Tandi	15	2,846	90	0.33
Ghousal	17	2,850	90	0.44

Source: Rao *et al.*, 1997

snow cover zones with presence of glaciers in the upper reaches, as compared with the lower reaches.

2.5 WATERSHED PRIORITIZATION

Watershed prioritization is the ranking of different sub watersheds of a watershed according to the order in which they have to be taken for treatment and soil conservation measures (Suresh *et al.*, 2004; Singh *et al.*, 2002). Catchments and watersheds have been identified as planning units for administrative purpose to conserve these precious resources (FAO, 1985). In most of the cases watershed projects have been predetermined and priorities have not been laid out properly. But looking to the massive investment in watershed development programs, it is not feasible to treat the complete watershed and prioritization has to be carried out so that most sensitive sub-watershed can be taken up. Hence prioritization will facilitate in addressing the problem areas to arrive at suitable solutions and protective measures can be better planned and implemented. Remote sensing and GIS are very useful techniques for extracting spatial, temporal and spectral data of any watershed. The GIS offers many new opportunities for hydrological modelling (Schumann *et al.*, 2000; Jurgen *et al.*, 2001). Remote sensing data of IRS-1C and IRS-1B have been used in the watershed characterization and prioritization to estimate soil losses based on the Universal Soil Loss equation (USLE) in Indian conditions (Chakraborty, 1993; Ravishanker, 1994; Saxena *et al.*, 2000). Various studies revealed that remotely sensed spatial database in conjunction with GIS could form the basis of appropriate and convenient hydrologic simulation and generate the essential quantitative information on soil erosion (Baban, 2001).

Adinarayana and Ramakrishna (1996) carried out a study on the integration of multi-seasonal remotely-sensed images for improved land use classification of hilly

watershed using GIS. The authors have described the methodology developed to compile agriculture land use map of a hilly watershed using GIS. For this study IRS LISS-II data had been used. The rasterised classified images and the relevant watershed resources were used as inputs and stored as separate layers in the GIS and then geometrically co-registered to a regular 30 m grid. Finally, the improved and the agricultural land use pattern map was classified into thick forest, sparse forest, degraded pastures, open (with/without scrub) areas, cropped (kharif + rabi) and fallow (kharif + rabi) lands. The areal extent of improved/final land use map classes compared favourably with the natural conditions of the agro-climatic region of the watershed.

Watershed prioritization for soil conservation planning with Mos-1 Messr Data, GIS applications and socio- economic information through a case study of Tinau watershed, Nepal was done by Shrestha *et al.*, 1997. They introduced a term called soil erosion status (SES). The sub watershed can be divided into one of the three categories low erosion area (LEA), medium erosion area (MEA), and high erosion area (HEA). In this approach parameters for prioritization of watershed were taken as aspect, slope gradient, drainage density, soil type, land use cover. After drawing thematic maps and classifying the study area into LEA, MEA and HEA for each parameter, a final map of soil erosion status was developed showing the erosion status of different sub watershed within the study area. The study concluded that it is possible to study watershed erosion status by using simple methods. Remote Sensing and GIS, with the integration of socio economic data is very useful for watershed planning and management.

Prasad *et al.*, (1997) has worked on sub watershed prioritization using remote sensing and GIS. The study was carried out in Trijuga sub watersheds of Nepal. These sub-watersheds were prioritized by considering their degradation condition and land sensitivity. Land Sensitivity was defined as locational relationship between forest loss and

soil loss. Universal Soil Loss Equation (USLE) in conjunction with remote sensing and GIS has been used for estimating soil loss and land cover change. Degradation speed index, sensitivity analysis -sensitivity index and present condition (PC) were considered as indicators of prioritization.

Anonymous (2001) has worked in the Cooks Creek Watershed, Pennsylvania for development of an index to prioritize watershed restoration. The objective of the study was to evaluate riparian corridor integrity, identify land parcel with degraded riparian buffers, prioritize degraded riparian land parcels, and engage priority land owners in conservation and restoration efforts. Parameters for prioritization of riparian buffer in watershed were taken as stream order (determined by visual inspection of USGS 7.5 minutes quadrangle maps), land use ranking based on total phosphorous loading rates of different land uses, drainage area and buffer width. Drainage area was determined by delineating the drainage areas from a USGS topographic map in Arc View. Buffer width is a critical factor in determining the need for restoration at each parcel due to the pollutant removal potential.. Wider buffers provide more sediment and nutrient removal capability than narrow buffers, but the marginal value of a buffer decreases with increasing buffer width. Prioritization was carried out using Riparian Restoration Prioritization Index (RRPI).

Khan *et al.*, (2001), studied watershed prioritization using remote sensing and GIS through a case study from Guhiya, India. The watersheds were ranked according to their tendency towards erosion using erosion intensity and delivery ratio to create sediment yield index. Erosion intensity (susceptibility towards erosion) and delivery ratio (indicating the transportability of sediment to the dam reservoir) were considered as the parameters of prioritization. Erosion intensity units were calculated with respect to soil depth and texture, land slope, present land use, vegetation and drainage density.

Pandey *et al.*, (2002) conducted a study for evolving a watershed prioritization scheme of predicted sediment yield for developing management plan for Banikdih agricultural watershed of Gowai river catchment using remote sensing and physically based continuous hydrological model SWAT2000. All the thematic layers including Digital Elevation Model, land use/land cover and digital soil map were integrated using AVSWAT interface that is a tight coupling between a hydrological model and GIS. The prioritization was done on the basis of the watershed having the highest sediment yielding.

Suresh *et al.*, (2004) used a logical approach in prioritization of watersheds on the basis of Sediment Production Rate (SPR). This technique was found to be time saving as compared to the usual Sediment Yield Index (SYI) and Universal Soil Loss Equation (USLE) methods which take a lot of time and require a precise judgment about giving weightages. Also the SPR method was found useful when land use/cover data and soil and slope information is not available.

Khare *et al.*, (2007) applied a logical approach for the prioritization of 25 sub-watersheds in Madhya Pradesh state of India. In the absence of many relevant data, the soil erosion status of these sub-watersheds was assessed by the soil erosion status (SES). For this, certain factors of the study area namely slope, drainage, aspect, forest, soil and water availability were considered and weightage of each of these parameters was assigned as per its importance.

2.6 NUCLEAR TECHNIQUES (RADIOMETRIC DATING TECHNIQUES)

The high energy and active morphodynamic environments associated with mountain areas introduce important technical constraints in the application of traditional classical techniques which possess many limitations in terms of operational problems, the

substantial resources required and their limited spatial and temporal coverage. In addition, it is difficult to use short-term, site-specific measurements in the interpretation of longer-term contemporary relief evolution. Little is currently known about the residence times of sediment particles moving through the fluvial system of drainage basins of different scales. The use of ^7Be , ^{210}Pb , and ^{137}Cs as a tracer therefore affords a valuable means of investigating the mobilization of sediment and its transfer through the fluvial system over timescales of several decades and over a range of spatial scales, and therefore overcomes many of the limitations of classical monitoring techniques.

2.6.1 Beryllium-7 (^7Be) Dating Technique

Quite a few researchers have carried out studies to exploit the potential of ^7Be for application in soil erosion studies (Brown *et al.*, 1981; Brown, 1987; Burch *et al.*, 1988; Monaghan *et al.*, 1985; Barg, 1992; Caillet *et al.*, 2001).

Due to the shallow penetration depth of the radionuclide ^7Be , it is particularly well-suited as a tracer to detect recent soil and erosion processes. In the case of homogeneous bare soil, ^7Be concentrations have been shown to increase exponentially with depth. Elsewhere, ^7Be concentration profiles commonly show constant or increasing concentration down to about 4 mm below which the concentrations decrease exponentially with depth, reaching detection limits at between 10 – 20 mm. In the latter case, low sorption capacity and rapid infiltration in coarser surface material probably account for low retention of ^7Be in the surface layers (Wallbrink and Murray, 1996).

The depth of penetration appears to be primarily controlled by physical properties such as vegetation cover, soil density and structure (Wallbrink and Murray, 1993; Wallbrink *et al.*, 1999).

Wallbrink and Murray (1996) reported that ^7Be and ^{10}Be were naturally occurring radionuclides of cosmogenic origin with a high affinity to clays and these elements had

large spatial variability because of interception by vegetation. The authors used ^7Be to develop quantitative models of soil erosion and describe soil redistribution properties. The measurements of ^7Be in soils were used to indicate movement of topsoil, and this study aimed to contribute to this technique by examining ^7Be in soils under a range of conditions. The penetration and areal concentration of ^7Be were measured in bare soil, grassland, and eucalypt forest and compared with total measured fallout. Inventories in the bare soil decreased progressively from 64 to 46% of total fallout over the sampling period, probably owing to a decrease in infiltration capacity. For grassed soil, average inventories were 96-142% of total fallout; for eucalypt litter plus soil, inventories were 73-95%. Natural variability of areal concentration of the nuclide was calculated to be about 20% (relative standard deviation), irrespective of soil type and/or surface cover. However, soil disturbance following logging operations increased variability to about 50%, even after more than 7 half-lives of ^7Be had elapsed. Penetration could be approximated by an exponential in bare soil and in eucalypt forest soil without litter, and average penetration half depths (P_h) in these soils were calculated to be 0.7 and 3.4 mm, respectively. Beryllium-7 concentration was found to increase as particle size decreased. The nuclide was not found below 20 mm depth in any soil or surface cover condition, thus confirming its utility in qualitative models that infer erosion processes by its use as a tracer of surface soil.

Blake *et al.*, (2002) attempted to explore the potential for using other shorter-lived radionuclides (besides ^{137}Cs and ^{210}Pb) to provide evidence of sediment mobilisation, transport and storage over shorter timescales and particularly for individual events. The authors reported the results of their study aimed at exploring the potential for using beryllium-7 (^7Be , $t_{1/2} = 53.3$ days) to meet this requirement. The study investigated the use of ^7Be as a sediment tracer in three key components of the sediment budget, namely, soil

erosion and sediment mobilisation from slopes, the transport, storage and remobilisation of fine sediment in river channels and overbank deposition on river floodplains. The results presented clearly demonstrate the potential for using ^7Be to obtain information on short-term and event-based sediment redistribution rates for use in catchment sediment budget investigations.

Wilson *et al.*, (2003) used an inventory balance for ^7Be to calculate sediment erosion in a 30.73 m^2 plot during a series of runoff-producing thunderstorms occurring over three days at the Deep Loess Research Station in Treynor, Iowa, USA. The inventory balance included determination of the pre- and post-storm, ^7Be inventories in the soil, the atmospheric influx of ^7Be during the event, and profiles of the ^7Be activity in the soil following the atmospheric deposition. The erosion calculated in the plot using the ^7Be inventory balance was 0.058 g cm^{-2} , which is 23 per cent of the annual average erosion determined using ^{137}Cs inventories. The calculated erosion from the mass balance is similar to the 0.059 g cm^{-2} of erosion estimated from the amount of sediment collected at the outlet of the 6 ha field during the study period and the delivery ratio (0.64). The inventory balance of ^7Be provides a new means for evaluating soil erosion over the time period most relevant to quantifying the prediction of erosion from runoff.

Schuller *et al.*, (2006) studied a few rapid and reliable methods for documenting soil erosion associated with forest harvest operations are needed to support the development of best management practices for soil and water conservation. To address this need, the potential for using ^7Be measurements to estimate patterns and amounts of soil redistribution associated with individual post-harvest events was explored. The ^7Be technique, which was originally developed for use on agricultural land, was employed to estimate soil redistribution associated with a period of heavy rainfall within a harvested forest area located in the Lake Region of Chile. The results provided by the ^7Be technique

were validated against direct measurements of soil gain or loss during the same period obtained using erosion pins. The information produced by the two approaches was similar. The results of this study demonstrate the potential for using ^7Be measurements to document event-based erosion in recently harvested forest areas.

2.6.2 Caesium-137 (^{137}Cs) Dating Technique

Ritchie *et al.*, (1974) constructed a coarse budget using ^{137}Cs for a forest, grass, and grass/crop watershed. Recent years have seen increasing interest in the potential for using caesium-137 as a tracer in soil erosion investigations. This man-made fallout radionuclide was released into the global environment as a result of the atmospheric testing of the thermonuclear weapons, which took place primarily from the mid-1950s to the mid 1970s. In most environments, radiocaesium reaching the soil surface as fallout was rapidly and strongly adsorbed by the surface soil horizons and its subsequent redistribution occurred in association with soil particles. It therefore affords an effective and valuable means of assessing medium-term rates and patterns of soil redistribution (Campbell *et al.*, 1986; Walling and Quine, 1991).

Since then the method has also been applied to a variety of other geomorphic locations (Walling *et al.*, 1986; Owens *et al.*, 1997; Walling and Quine, 1992).

Walling and Bradley (1990) have studied the use of ^{137}Cs for fingerprinting suspended sediment sources, secondly, investigating patterns of soil erosion and sediment delivery on cultivated hillslopes and thirdly elucidating rates and patterns of flood plain deposition. They investigated the use of possible applications involving the use of ^{137}Cs technique for firstly fingerprinting suspended sediment sources, investigating patterns of soil erosion and sediment delivery on cultivated hillslopes and elucidating rates and patterns of flood plain deposition.

In Australia, Loughran *et al.*, (1992) used the nuclide as the basis for developing a sediment budget within a small drainage basin, including actively cultivated vineyard slopes. It has also been used in other Mediterranean climates (Quine *et al.*, 1994).

Garcia-Ruiz *et al.*, (1995) found out that sheet erosion processes caused ^{137}Cs redistribution within the landscape. The crests had significantly higher ^{137}Cs activity than midslopes and lower concentration than the footslopes. There was no clear relationship between ^{137}Cs activity redistribution and local topographic variables in the study. Soils in a gentle midslope had lower ^{137}Cs activity than those in a steeper midslope. However, hill morphology explained ^{137}Cs redistribution within landscape that is high. ^{137}Cs activity was associated with sites at the base of hillslopes. Thus net soil erosion was found to be strongly influenced by hill morphology. Calculated erosion and deposition rates for the undisturbed watershed were $13.2 \text{ Mgha}^{-1}\text{yr}^{-1}$ and $4.9 \text{ Mg ha}^{-1}\text{yr}^{-1}$ respectively.

He and Walling (1997) opinionated that ^{137}Cs activity are very time consuming and may cause a considerable delay before the results are available. Therefore, empirical relationships between *in situ* measurements of ^{137}Cs activity and total ^{137}Cs inventories have been established for soils from a cultivated field and for floodplain sediments based in information on the vertical distribution of ^{137}Cs in the soils and in the sediments provided by the forward scattering ratio derived from the field measured spectra. These relationships have been used to estimate ^{137}Cs inventories from *in situ* measurements of ^{137}Cs technique activity at other locations.

Bouhlassa *et al.*, (2000) established long-term erosion rates on cultivated land in the Nakhla watershed located in the north of Morocco, using ^{137}Cs technique. Two sampling strategies were adopted. The first was aimed at establishing areal estimates of erosion, whereas the second, based on a transect approach, intended to determine point erosion. Twenty-one cultivated sites and seven undisturbed sites apparently not affected

by erosion or deposition were sampled to 35 cm depth. Nine cores were collected along the transect of 149 m length. The assessment of erosion rates with models varying in complexity from the simple Proportional Model to more complex Mass Balance Models included the processes controlling the redistribution of ^{137}Cs in soil and enabled to demonstrate the significance of soil erosion problem on cultivated land. Erosion rates were observed to rise up to $50 \text{ t ha}^{-1} \text{ y}^{-1}$. The ^{137}Cs derived erosion rates provided a reliable representation of water erosion pattern in the area and indicated the importance of tillage process on the redistribution of ^{137}Cs in soil.

Golosov *et al.*, (2000) used the ^{137}Cs technique to assess the soil redistribution within different cultivated watersheds in area with Chernobyl contamination. It was found that soil erosion rates computed by the ^{137}Cs technique fit very good with gross erosion rates obtained using modified version of USLE and SGI model.

The ^{137}Cs tracer budgets have been used in southeastern Australian forested catchments to assess the impacts of erosion after forest harvesting (Wallbrink *et al.*, 2002, and Wallbrink and Croke 2002).

Krause *et al.*, (2003) used the fallout radionuclide ^{137}Cs to estimate the net surface and minor rill soil erosion rates for hillslopes. A transect-based soil sampling technique was applied to one woodland and five grazed pasture hillslopes in the Williams River water-supply catchment in the Hunter Valley, New South Wales. An Australian regression model (SOILOSS) relating net soil loss from runoff-erosion plots to ^{137}Cs deficit in soils was used to calculate a weighted net surface and minor rill erosion rate for the six hillslopes. The net median surface erosion rates ranged between 0.00 and $0.64 \text{ t ha}^{-1} \text{ y}^{-1}$ with the average median soil erosion rate of $0.19 \text{ t ha}^{-1} \text{ y}^{-1}$ (std. dev. = 0.23), indicating that these hillslopes were unlikely to be major sources of sediment to the catchment's waterways. Net soil loss rates were also shown to be low in comparison to Australia-wide

data and comparable to hillslope data obtained elsewhere in the same region. Minimum and maximum error bounds were provided with each erosion rate to account for radionuclide detector count error. For one hillslope the estimated error due to detection was $1.34 \text{ t ha}^{-1}\text{y}^{-1}$, while the remaining five hillslopes exhibited error of up to $0.41 \text{ t ha}^{-1}\text{y}^{-1}$. Correlation analyses between the net soil loss rates and physical hillslope characteristics were non-significant.

Loughran *et al.*, (2004) sampled two hundred and six sites (100 within rotational cropping and horticultural use, 52 within uncultivated permanent pasture and forest and 54 in rangelands) in Australia using the fallout radioisotope caesium-137 as an indicator of topsoil redistribution. Average net soil losses were approximately equal for cultivated cropping lands and rangelands (*ca.* $5.5 \text{ t ha}^{-1} \text{ y}^{-1}$) and just over $1 \text{ t ha}^{-1} \text{ y}^{-1}$ for pasture and forest. The Mann Whitney U Test revealed that losses under cropping and rangeland conditions were significantly higher ($p < 0.05$) than under uncultivated pasture and forest. Soil loss was negatively correlated with mean annual rainfall and slope gradient and positively correlated with slope length (Spearman's rank correlation). There was no correlation between rates of soil loss and a rainfall erosivity index. An assessment of erosional events was provided by landholders for 104 sites, with their ranking being weakly but significantly correlated with soil loss estimates ($r = +0.35$). Sixty percent of sites had net soil losses greater than $1 \text{ t ha}^{-1} \text{ y}^{-1}$, and 74% of sites had losses of more than $0.5 \text{ t ha}^{-1} \text{ y}^{-1}$. This latter rate was regarded as a limit for a tolerable level of soil loss. These high rates of soil loss have occurred since the mid-1950s despite there being significant landholder awareness of the soil erosion hazard.

Haciyakupoglu *et al.*, (2005) estimated the results of rates of soil loss from uncultivated areas within the catchment in western Istanbul, Turkey. The soil erosion rate

estimated using the profile distribution conversion model was in the order of 16.11 t/ha/year.

Quine *et al.*, (1994) examined the potential for using caesium-137 to identify the patterns and rates of soil erosion and redistribution within the semiarid regions of Spain, including the central part of the Ebro River basin. Samples for the determination of caesium-137 were collected from uncultivated slopes and cultivated valley floor sites near the head and outlet of a small representative basin in the Las Bardenas area. The measured patterns of caesium-137 mobilization, redistribution and export provided a semiquantitative indication of the variation in erosion within the study site. Calibration of the caesium-137 measurements, taking account of the differing behaviour of radiocaesium on cultivated and uncultivated land, allowed estimation of the actual rates of erosion and deposition involved. The results showed that the erosion rates on the cultivated land (1.6-2.5 kg m⁻² y⁻¹) were typically more than five times those seen on the uncultivated land (0.2-0.4 kg m⁻² y⁻¹) and the erosion on the uncultivated land was significantly less severe at the head of the basin than at the outlet. Study of the vegetation cover suggested that lower growing shrubs and grasses might be more effective in reducing erosion in this environment than trees.

Despite the success of the ¹³⁷Cs techniques used to determine the soil erosion and redistribution rates, one important limitation hampering the application of the ¹³⁷Cs approach in some parts of the world, relates to the low ¹³⁷Cs inventories found in equatorial areas. This problem will be further compounded in the future by the progressive reduction in ¹³⁷Cs activity caused by radioactive decay, and it may become impossible to apply the ¹³⁷Cs approach in such areas in the foreseeable future.

Due to the limitations on the use of ^{137}Cs to investigate soil erosion in some areas of the world, an alternative technique involving environmental radionuclides including lead-210 (^{210}Pb) was developed.

2.6.3 Lead-210 (^{210}Pb) Dating Technique

Lead-210, a naturally occurring radionuclide (half-life 22.6 years), is a product of ^{238}U decay series, derived via a series of other short-lived radionuclides from the decay of gaseous radon-222 (^{222}Rn) (half-life 3.8 days), the daughter of radium-226 (^{226}Ra) (half-life 1622 years). The ^{210}Pb content of soils and rocks produced by the natural in situ decay of ^{226}Ra is termed “supported” ^{210}Pb because it is in equilibrium with its parent. However, upward diffusion of a small proportion of the of the ^{222}Rn produced naturally in soils and rocks releases ^{222}Rn to the atmosphere, and the subsequent fallout of ^{210}Pb provides an input to surface soils and sediments which is not in equilibrium with ^{226}Ra . Such fallout ^{210}Pb is commonly termed ‘excess’ or ‘unsupported’ ^{210}Pb (Robbins, 1978). Because of its natural origin, the deposition of the fallout ^{210}Pb has, unlike that of ^{137}Cs , been essentially constant through time.

The similar behaviour of fallout ^{210}Pb in soils offered potential for its use as an alternative to ^{137}Cs , in areas where ^{137}Cs inventories are low or are complicated by additional fallout from the Chernobyl accident (Porto *et al.*, 2007). Comparison of the estimates of water-induced soil erosion in three small forest/rangeland catchments located in Calabria, southern Italy, for which measurements derived from ^{210}Pb measurements with the measured sediment output, confirmed the validity of the ^{210}Pb approach. The soil redistribution rates estimated using ^{210}Pb measurements were also consistent with equivalent estimates obtained for the same study catchments using ^{137}Cs measurements.

Relatively little is currently known about the global distribution of fallout ^{210}Pb , although in a review of existing data on ^{210}Pb deposition fluxes for different areas of the

world, Appleby and Oldfield (1992) indicate that such fluxes are greater over the land than over the ocean and lower over the western margins of continental land masses, due to the pre-dominant west to east trajectory of air mass movement. The same authors reported an average deposition flux for the world of $118 \text{ Bq m}^{-2} \text{ year}^{-1}$, with values generally lying in the range $50\text{-}150 \text{ Bq m}^{-2} \text{ year}^{-1}$.

Due to its strong affinity for soil and sediment particles (Van Hoof and Andren, 1989; He and Walling, 1996), fallout ^{210}Pb reaching the soil surface is readily adsorbed and its subsequent vertical and lateral redistribution are primarily controlled by erosion, transport and deposition processes. Consequently, unsupported ^{210}Pb , like ^{137}Cs , offers the potential for use as a tracer in estimating rates of soil redistribution.

To date, there have been few attempts to exploit this potential (Das *et al.*, 1994; Huh *et al.*, 1996; Kumar *et al.*, 1999; Brenner *et al.*, 2001; Froehlich and Walling, 2002; Lu and Matsumoto 2005; Mizugaki *et al.*, 2006; Kumar *et al.*, 2007), although Walling and He (1999) reported the successful use of unsupported ^{210}Pb measurements to estimate soil erosion rates within a cultivated field in Devon, UK.

Lead-210 analysis is a classic dating technique for young (<200 years) sediments (Krishnaswamy *et al.*, 1971; Chillrud *et al.*, 1999). The basic methodology of ^{210}Pb dating was established in a seminal paper by Golberg (1963). Initially the technique was applied to measure accumulation rates in ice sheets (Golberg, 1963; Crozaz *et al.*, 1964; Crozaz and Langway, 1966) and glaciers (Picciotto *et al.*, 1967). Many researchers in various parts of the world have carried out studies in soil erosion incorporating this method (Krishnaswamy *et al.*, 1971; He and Owens, 1995; Walling and Woodward, 1992; Wallbrink and Murray, 1993; Wallbrink and Murray, 1993, 1996).

Farmer (1978) measured lead concentrations in soil cores from four sites distributed among the three major sedimentary basins-Niagara, Mississauga and

Rochester-of Lake Ontario for which sedimentation rates had been previously determined by ^{210}Pb dating. Around 90% of the total lead present in fine-grained surface sediments was removed by $\text{CH}_3\text{CO}_2\text{H}/\text{NH}_2\text{OH}$. HCl leaching, concentrations ranging from 137 $\mu\text{g/g}$ in surface sections to a constant background of 12-13 $\mu\text{g/g}$ at unpolluted depths. Lead-210 dating indicated that increases in lead concentrations commenced ca. 1850-1875 with 5, 10, 35 and 50% of the total "excess" lead inventory in the sediment column being assigned to the pre-1900 period and successive 25-year intervals during the 20th Century, respectively. Anthropogenic inputs of lead from such sources as the combustion of leaded gasoline and coal were responsible for these increases. About 10 $\mu\text{g/g}$ lead remained in the sediment residue after leaching. The total natural lead flux to the sediments ranged from 0.4-1.3 $\mu\text{g}/\text{cm}^2/\text{yr}$ while "excess" lead of anthropogenic origin varied from 1.2--6.7 $\mu\text{g}/\text{cm}^2/\text{yr}$ and totalled 0.5-1.5 g/m^2 at the four sites.

Bloesch and Evans (1982) have discussed the methods to provide accurate accumulation rates for lake models. Cores were taken in 1979 in two basins of Lake Lucerne, Switzerland and accumulation rates were calculated by using Pb-210 dating and by a natural landslide marker of 1795 in one basin (Weggis). In the other basin (Horw Bay) the sediment accumulation rates based on the lead method were compared with yearly sedimentation rates measured by sediment traps in 1969/70. At the Weggis station, the core dating yielded sediment accumulation rates of about 400 $\text{g dry wt. m}^{-2} \text{ y}^{-1}$ with the lead method, averaged over a sediment depth of 4-20 cm; accumulation was about 700 $\text{g dry wt. m}^{-2} \text{ y}^{-1}$ with the marker method, averaged over 0-33 cm. In Horw Bay, the trap method yielded about 1300 $\text{g dry wt. m}^{-2} \text{ y}^{-1}$ compared with 400-1000 $\text{g dry wt. m}^{-2} \text{ y}^{-1}$ obtained with the lead method and related to various depth intervals. The characteristic sources of error of the three methods as well as several hypotheses for these discrepancies were discussed.

Irlweck and Danielopol (1985) determined the mean annual sedimentation rates in the pre-alpine Mondsee (Upper Austria) over the last 20–30 years using Cs-137 and Pb (Po)-210 profiles for sediment core dating and two natural sediment markers. Lower sedimentation rates of about 2–3 mm yr⁻¹ were observed in the central part of the lake near the shore at 18–20 m and in the southern part at 30 m depth. Higher sedimentation rates of 4–7 mm yr⁻¹ were found in the central part of the lake at 47 and 65 m and in the northern bay at 18 and 41 m depth. At both these sites the Pb-210 profiles were strongly disturbed in the upper zone of the sediment cores, whereas the Cs-137 pattern remained intact. The higher annual sediment accumulation rates could be explained only partly by deposition of allochthonous material discharged by the streams, enhanced eutrophication in these parts of the lake, erosion and sediment focusing by turbidity currents being also probable.

Joshi (1987) described a method for the non-destructive determination of ²¹⁰Pb and ²²⁶Ra in sediments. The procedure was based on the direct counting of the 46.5-keV γ -ray of ²¹⁰Pb and the 351.9-keV γ -emission of ²¹⁴Pb. The self-absorption of the 46.5-KeV γ -ray was corrected using a technique involving direct gamma transmission measurements on sample and efficiency calibration standard. Several reference materials when assayed by the described method yielded results in general agreement with the certified values. The application of the method was illustrated through the analysis of the excess ²¹⁰Pb profile of a Lake Ontario sediment core.

El-Daoushy *et al.*, (1991) summarized that various laboratory techniques have been utilized worldwide for measuring lead-210 in sub-recent deposits through its grand-daughter product polonium-210. Isotope dilution alpha spectrometry proved a suitable tool for absolute determination of lead-210 for the dating of aquatic deposits. Moreover, isotope dilution alpha spectrometry along with speciation experiments could be used to resolve depositional anomalies arising from supported lead-210/Ra-226 disequilibrium

levels and unsupported lead-210 mobile fractions. Isotope dilution alpha spectrometry of sub-recent sediment and peat deposits were critically evaluated for more than ten years. They concluded that type, size and composition of deposits analyzed as well as radiochemical procedures used, together with alpha counting techniques, were important factors influencing lead-210 determinations and tailing corrections using its granddaughter product polonium-210. Optimization of these parameters was of prime importance to achieve economic and accurate analyses, especially at low lead-210 concentrations and small sample sizes.

Joshi *et al.*, (1991) studied the partitioning of ^{210}Pb between dissolved and the suspended sediment phases of the Ottawa River waters. The results indicated high affinity of the radionuclide for particulates (K_d , $1.9 \times 10^5 \text{ mL g}^{-1}$). Companion studies on the precursor ^{226}Ra gave an average (K_d value of $7.8 \times 10^3 \text{ mL g}^{-1}$). Nearly 77% of the total ^{210}Pb (i.e., dissolved plus particulate) and 99% of the total ^{226}Ra were transported through the system in the dissolved form. The suggestion was made that the low availability of particulates in the system promotes the export of ^{210}Pb in the dissolved form. The conventional approach gave a mean residence time of about 2000 yr for the atmospherically-derived ^{210}Pb in the watershed. However, if the flux of this ^{210}Pb falling directly on the river's surface was taken into account, a mean residence time of about 6200 yr was inferred for this radionuclide in the area soils. This aspect of the study was largely applicable to metals with geochemical behavior similar to that of ^{210}Pb since the radionuclide itself has a mean life of only 22.6 years.

Moser (1993) compared three different methods for the ^{210}Pb determination: ^{210}Pb β -counting with a low level proportional counter, ^{210}Pb γ -spectroscopy and ^{210}Po α -spectroscopy. Agreement within analytical errors was found for the three methods in two sediment cores from Lake Zurich, Switzerland and in IAEA SD-A-1 deep sea reference

material. For ^{210}Po α -spectroscopy, the detection and determination limit was an order of magnitude lower than these for the other methods.

Porto *et al.*, (2006) reported an attempt to explore the use of fallout ^{210}Pb to estimate rates of water-induced soil erosion on uncultivated land. It focused on three small forest/rangeland catchments located in Calabria, southern Italy, for which measurements of sediment output were available. Comparison of the estimates of net soil loss from the catchments derived from ^{210}Pb measurements with the measured sediment output, confirmed the validity of the ^{210}Pb approach. The soil redistribution rates estimated using ^{210}Pb measurements were also consistent with equivalent estimates obtained for the same study catchments using ^{137}Cs measurements.

Narayana *et al.*, (2006) studied the distribution and behavior of ^{210}Po and ^{210}Pb in beach sand and surface soil samples from the Quilon district of Kerala. Beach sand and soil samples were collected and analyzed for ^{210}Po and ^{210}Pb radionuclides using standard radiochemical analytical techniques. Mean activities of ^{210}Po and ^{210}Pb were found to be maximum in the samples collected at 20 m away from waterline. The depth profile study indicated the mean activity of ^{210}Po to decrease with depth for samples collected 20 m away from waterline whereas the activity slightly increases with depth 40 m away from sea. The activity concentration of ^{210}Po and ^{210}Pb in surface beach sand showed good correlation, with a correlation coefficient of 0.81.

Lead-210 has been used as the basis of shorter-term soil redistribution in a forest that had been harvested in NSW, Australia (Wallbrink *et al.*, 2002).

Recent applications of $^{210}\text{Pb}_{\text{ex}}$ as a tracer include the combination of ^{137}Cs and $^{210}\text{Pb}_{\text{ex}}$ to assess sources and redistribution patterns of sediments in Western Port Bay, Victoria, Australia (Wallbrink *et al.*, 2003), and to trace pollutant sources in the Wingecarribee Catchment, Sydney (Olley and Deere, 2003).

Smith *et al.*, (1997) measured the inventories and vertical profiles of fall-out ^{210}Pb , ^{137}Cs (both weapons test and Chernobyl) and ^{241}Am (a decay product of ^{241}Pu) in the soils of three catchments in Cumbria, UK. Soil types varied from mineral soils to highly organic peat bog. The ^{210}Pb inventories in different cores from the same catchment were relatively uniform, the standard deviation of measurements being around 30%. Mean annual fluxes of ^{210}Pb calculated from the soil inventories were $63 \text{ Bq m}^{-2} \text{ year}^{-1}$ (Brotherswater and Blelham Tarn catchments), and $97 \text{ Bq m}^{-2} \text{ year}^{-1}$ (Devoke Water catchment) per metre of rainfall. From these and earlier data published in the literature, the mean ^{210}Pb flux is estimated to be $77 \pm 14 \text{ Bq m}^{-2} \text{ year}^{-1}$ per metre of rainfall. Inventories of ^{137}Cs (weapons test and Chernobyl) were found more variable, but mean values for each of the catchments were in agreement with independent studies. The mean weapons test deposition (decay corrected to 1986) was 2790 Bq m^{-2} per metre of rainfall, compared to a UK average of 3160 Bq m^{-2} derived from extensive national surveys. Although ^{241}Am levels in Brotherswater soils were comparable with those expected from weapons test fall-out, significantly higher values were recorded at Blelham Tarn and Devoke Water. Well-resolved peaks in ^{241}Am activity some distance below the present surface suggest that this radionuclide is relatively immobile within the soil column. The depth of penetration of 75% of the inventory into the soil column was similar for ^{210}Pb , ^{137}Cs (weapons) and ^{241}Am , all being significantly greater than Chernobyl ^{137}Cs . The vertical profiles of ^{137}Cs (weapons) suggest that there has been little mobility during the decade.

Zapata and Agudo (1998) reported that in Chile and New Zealand, besides empirical models based on the correlation between average rainfall and ^{137}Cs soil inventory values, unsupported ^{210}Pb , has also been recently included in soil erosion studies, either alone or in combination with ^{137}Cs . The results were very promising. And

one of the components of these CRPs, the IAEA carried out an intercomparison exercise among the participating laboratories, for the analysis of ^{137}Cs and ^{210}Pb in a soil sample from China. Twenty-one laboratories provided data for ^{137}Cs but only nine conducted analysis in unsupported ^{210}Pb . Both radionuclides were measured by gamma spectrometry, using a wide range of detectors and geometries. The results for ^{137}Cs were excellent. After discarding 6 outliers, a CV of only 9.3% was obtained for the remaining 34 reported values. Five of the six outliers were due to the use of a more than 30 years old standard solution for efficiency calculation.

Three soil cores collected from China and UK showed very similar depth distribution of ^{210}Pb and ^{137}Cs on uncultivated and cultivated land (Xinbao *et al.*, 2003). However nuclides concentrations were higher in the top horizon and decreased exponentially with depth in uncultivated land while the concentrations were almost uniform throughout the plough layer as a result of mixing associated due to cultivation in case of cultivated land. In contrast, distribution of natural fallout of $^{210}\text{Pb}_{\text{ex}}$ was in a steady state under constant conditions of land environment and erosion processes for a long term, e.g. > 100 years. Therefore mass balances in soil were different. According to the continuous fallout of ^{210}Pb from the atmosphere, its natural decay and loss with soil losses, ^{210}Pb steady state mass balance models were developed for cultivated as well as uncultivated land to estimate the soil erosion rates. Besides, the proportion of freshly deposited $^{210}\text{Pb}_{\text{ex}}$ fallout removed by erosion on cultivated land could also be calculated from the $^{210}\text{Pb}_{\text{ex}}$ depth distribution at a reference site of uneroded permanent grassland.

Golosov *et al.*, (2005) carried out an evaluation of the net soil losses from cultivated slopes for assessing sediment redistribution in river basins. Different methods were used to determine the spatial pattern of soil loss/deposition within cultivated areas. These included the soil-morphological method, direct measurement of rills and deposition

zones and radionuclide techniques. The soil-morphological method provided information on soil losses for the entire period of cultivation. Soil losses for single erosion events were assessed using direct measurements of rills. The caesium-137 (^{137}Cs) and excess lead-210 ($^{210}\text{Pb}_{\text{ex}}$) techniques provided information on sediment redistribution over approximately the past 50 and 100 years respectively. Available data concerning net soil losses from slopes of different topographic configurations, obtained using these different methods, were collected from studies undertaken in various landscape zones around the world. The relationship between erosion and deposition was shown to be very similar for slopes or slope catchments of similar configuration, despite differences in the temporal scales, the methods employed and the landscape characteristics (soil, precipitation, etc.). Hence, the morphological characteristics exerted a key influence on sediment redistribution on hillslopes. Establishment of buffering capacity coefficients for different slope types permitted the sediment output from cultivated areas to be predicted based on a classification of slope morphology and using information from topographic maps or the Digital Elevation Model (DEM).

Fukuyama *et al.*, (2006) simulated the sediment transport capacities of both overland flow, expressed as a function of the upslope contributing area and local slope gradient, rainsplash, expressed as a function of the local slope gradient and the kinetic energy of the rainfall, for 45 sampling points in the cypress plantations of Japan. They then compared the simulated soil loss results with the erosion rates estimated using Cesium-137 (^{137}Cs) and unsupported Lead-210 ($^{210}\text{Pb}_{\text{ex}}$) measurements undertaken at each sampling point. The results indicated a close correspondence between the simulated local transport capacity of overland flow and the local erosion rates estimated using the radionuclide measurements. In contrast, there was no significant correlation between the simulated rainsplash transport and the local erosion rates estimated from the radionuclide

measurements. Furthermore, radiometric and physical properties of eroded sediment varied depending on both the magnitude of the storm event and the spatial scale of monitoring. These results demonstrated the potential for using ^{137}Cs and $^{210}\text{Pb}_{\text{ex}}$ measurements to produce independent information on long-term soil erosion rates, which can be used for investigating erosion processes and validating erosion models. To determine the potential variability of erosion rates, O'Farrell *et al.*, (2007) applied three independent, field-based methods to a well-studied catchment in the Marin Headlands of northern California and presented short-term, basin-wide erosion rates determined by measuring pond sediment volume (40 years) and measured activities of the fallout nuclides ^{137}Cs and ^{210}Pb (40-50 years) for comparison with long-term (>10 ka) rates previously determined from *in situ*-produced cosmogenic ^{10}Be and ^{26}Al analyses. In addition to determining basin-averaged rates, ^{137}Cs and ^{210}Pb enabled to calculate point-specific erosion rates and use these rates to infer dominant erosion processes across the landscape. When examined in the context of established geomorphic transport laws, the correlations between point rates of soil loss from ^{137}Cs and ^{210}Pb inventories and landscape morphometry (i.e. topographic curvature and upslope drainage area) demonstrated that slope-driven processes dominate on convex areas while overland flow processes dominate in concave hollows and channels. The study showed a good agreement in erosion rates determined by three independent methods: equivalent denudation rates of $143 \pm 41 \text{ m Ma}^{-1}$ from pond sediment volume, $136 \pm 36 \text{ m Ma}^{-1}$ from the combination of ^{137}Cs and ^{210}Pb , and $102 \pm 25 \text{ m Ma}^{-1}$ from ^{10}Be and ^{26}Al . Such agreement suggested that erosion of this landscape is not dominated by extreme events; rather, the rates and processes observed at present are indicative of those operating for at least the past 10,000 years.

CONCLUDING REMARKS

The review of literature has provided useful information about the status of research in the area of soil erosion studies with emphasis on modelling. The status of limited data availability in remote far-flung areas has resulted in very few attempts for systematic modelling of the erosion process.

Also though ^{137}Cs has been widely in use for estimating erosion rate and sedimentation, ^{210}Pb is still a new technique to be harnessed yet. Though, a few researchers in the recent past have used the Remote Sensing and GIS methods to conduct study on lakes and its catchments, not much work has ever been performed using the combination of the Remote Sensing and GIS methods with the nuclear techniques.

Chapter 3

STUDY AREA

For the present research, the western part of the Loktak Lake catchment has been chosen as the study area. The Loktak Lake is located at the centre of the state of Manipur, India. The location of the study area is shown in Fig. 3.1. Loktak (*Lok* = stream + *Tak* = the end) is the journey end of several streams and rivers, with over 25 small & medium-sized streams draining into it. The pulsating lake is the largest fresh water lake in the northeastern region of India. In the present chapter, description of the lake catchment and its characteristics are presented.

3.1 CATCHMENT OF LOKTAK LAKE

The Loktak Lake catchment comprises of direct and indirect catchment area. The direct catchment area in the western hills covers 96 villages, extending over an area of 1046 km² and varying in altitude from 780 m at the foothills adjoining the central valley to 2068 m above MSL at the peak of the hills. The western part of catchment which, directly drains into the lake, has been focused since it is more erosion-prone and has been referred to as the Loktak Lake catchment henceforth. The bulk of the indirect catchment comes under the built-up category which mostly falls under the urban belt. The Lake catchment is under pressure mainly due to practice of *jhum* cultivation by local tribal population, deforestation, landslides and land slips (Cairns, 1998). These factors have mainly contributed to rapid siltation of the lake consequently reducing its water holding growth of floating weedmats locally called as *phumdis*.

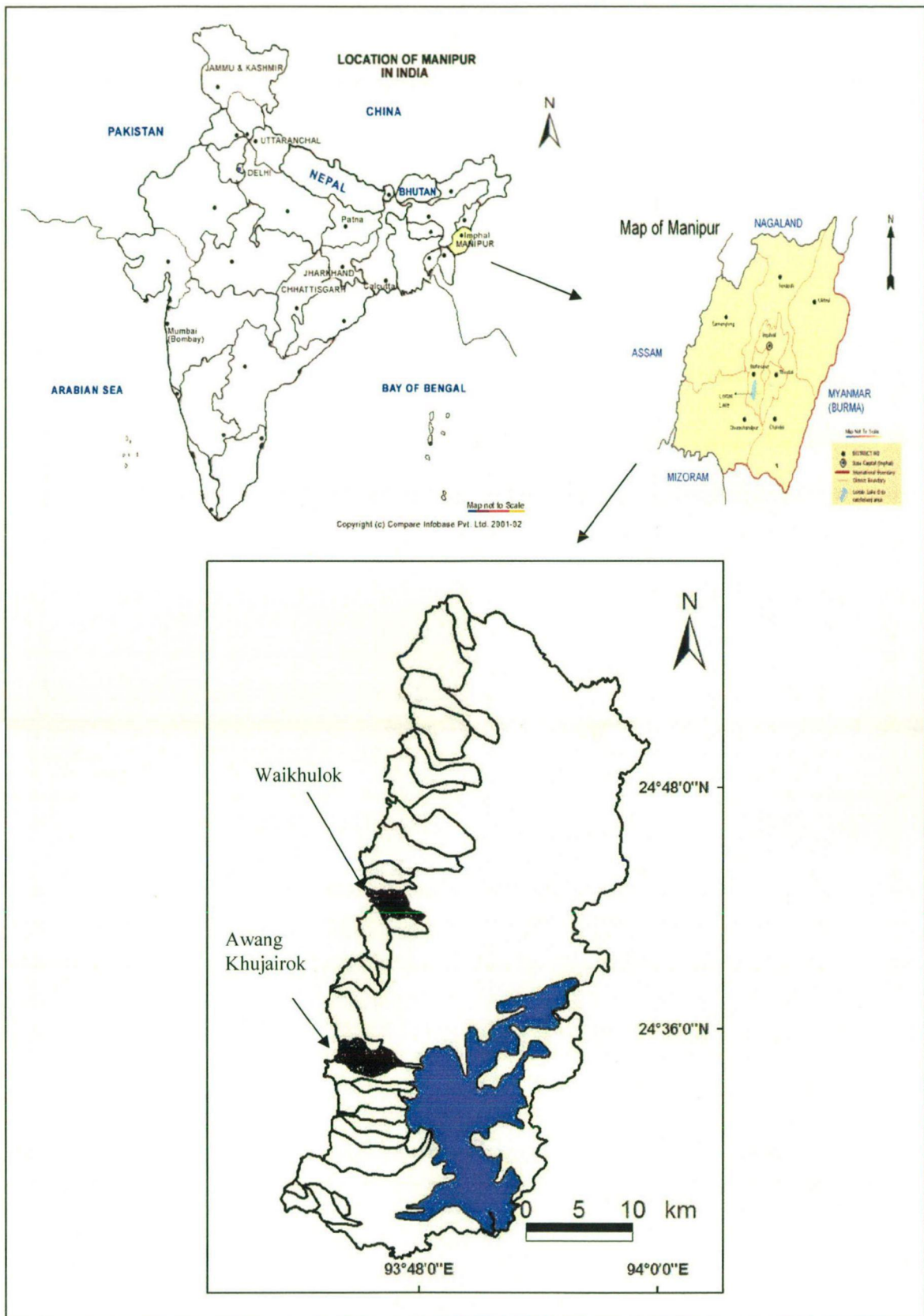


Fig. 3.1: The location map of the study area

and overall carrying capacity. The problem has further been aggravated due to prolific Developmental activities and increasing human population have led to changes in hydrological regimes and loss of vegetal cover thereby enhancing lake siltation and reducing overall benefits accrued from the wetlands through their natural processes.

3.1.1 Drainage Pattern

The hilly areas of Manipur constituting catchment of Loktak and associated wetlands fall within Manipur river basin covering an area of 6,872 km², which represents 31% of the total geographical area of the state. Geologically, the hills of the state comprise of rocks of tertiary age belonging to Disang and Barail formation. They are predominantly argillaceous comprising of shales with bands of siltstone, sandstone and mudstone giving rise to clayey soils in the valley. The shales are well bedded, highly cleaved, jointed and intensely folded and faulted. Hill soils are red in colour and vary in depth from deep to shallow. The base of the hills surrounding Manipur valley is highly weathered and oxidised. Valley soils are deep with texture ranging from silt loam to clay. They are slightly permeable, grey to brown in colour and acidic in reaction.

Figure 3.2 shows the stream channel network in the Manipur river basin. Manipur river arises in the north at Karong and flows southwards of Imphal city where it is known as Imphal river. Iril river joins Imphal river on its left bank about 10 km south of Imphal. Further downstream, Thoubal river also joins it on the left bank at *Irong Ichil*. After another 10 km it is joined by Sekmai river near village Sekmajin and thereafter, it is known as Manipur river. Further downstream, Khuga river joins the Manipur river on its right bank. Later, the Manipur river flows south through a narrow gorge and undulating terrain of about 26 km where it meets the north flowing Chakpi river near village *Sugnu*. It continues flowing south to Myanmar where it joins the Chindwin river, a tributary of the

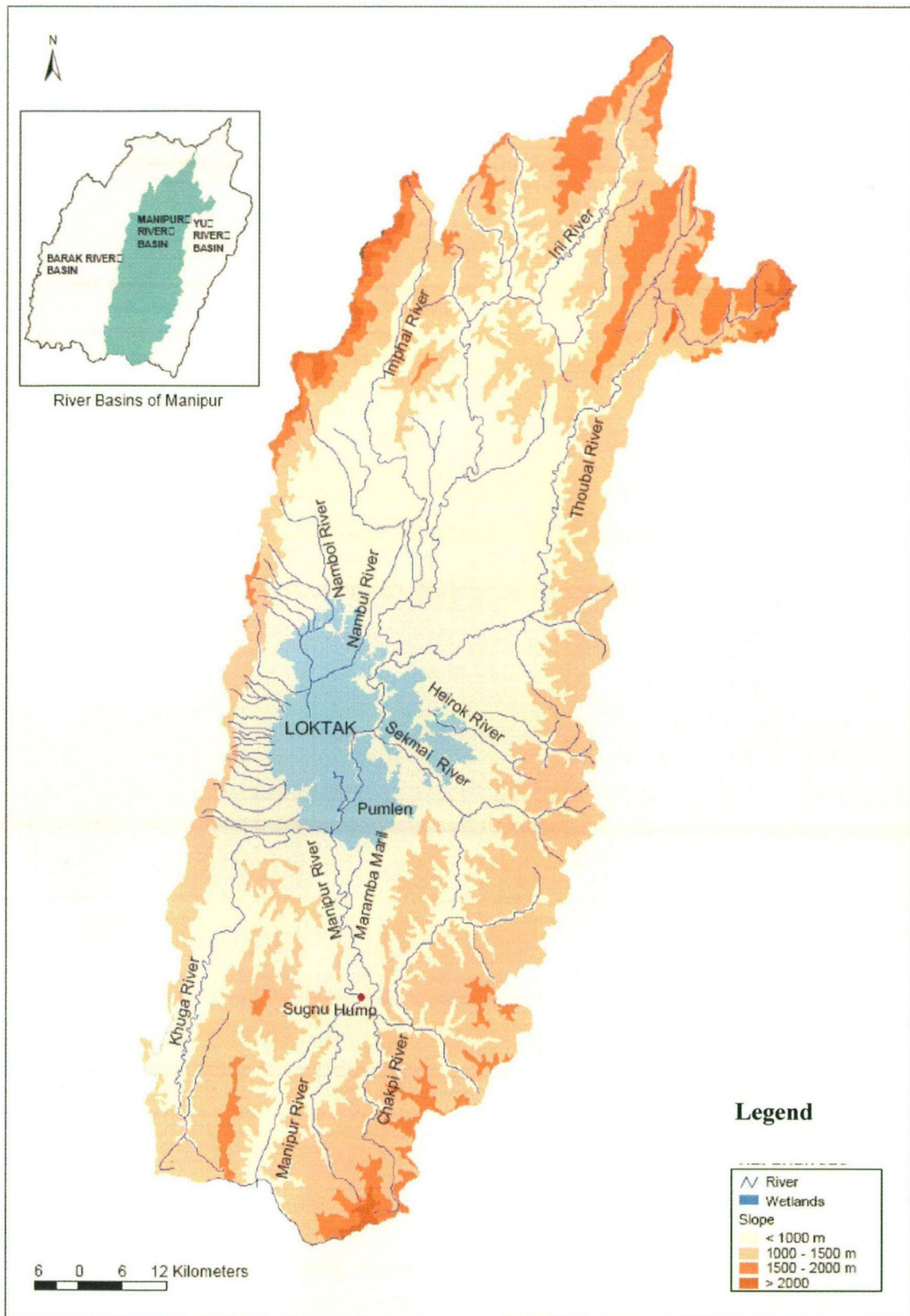


Fig. 3.2: The stream channel network in the Manipur river basin

Irrawaddy river. Along its course through the valley downstream of Imphal, the riverbed slopes very gently. The bed level is 773 m at Imphal and 768.6 m at Lilong (near its confluence with Iril river) and 762.2 m at Ithai, downstream of the confluence of the Manipur and Khuga rivers located 65 km. south of Imphal. As shown in Fig. 3.3, the drainage pattern of the sub basin is sub-dendritic to subparallel.

The important feature of the Manipur river from the hydrological point of view is the natural blockage of flow in its lower reaches. About 27 km downstream of Ithai barrage, after sloping down to 756.7 m, the river bed suddenly rises by 8 m within a distance of 800 m and remains above 762.5 m for about 2.5 km. This rocky barrier to the flow is known as '*Sugnu* hump', named after *Sugnu* village. It reduces the capacity of Manipur river to discharge its flow. Chakpi river drains a large part of the southern hills and meets the Manipur river at a right angle in its full capacity during the rainy season. During such times it acts as a barrier to the flow of the Manipur river. On the other hand sometimes the Chakpi river discharges into Manipur river earlier in the season filling the section between Ithai barrage and the *Sugnu* hump thereby creating an obstruction to its flow. The excessive flow of both Chakpi and Manipur rivers spreads backwards flooding large areas of the southern parts of the valley. Besides, this barrier also causes siltation in the river during receding floods. The Imphal river has a total discharge of 6550 m³/s which is partly utilised at the Imphal Barrage for irrigation purposes through left and right bank canals with a maximum expected discharge of 30 and 70 m³/s respectively and an irrigation potential of 6400 ha. Even though this river does not flow directly into the lake, it is connected to the Loktak Lake through Khordak and Ungamel channels.

In years of low flood whenever the water level in the lake is lower, water from the river enters the lake and vice-versa. The two way flow of water to some extent has been modified by creation of the Ithai barrage. In years of high flood, the Loktak Lake, Pumlun

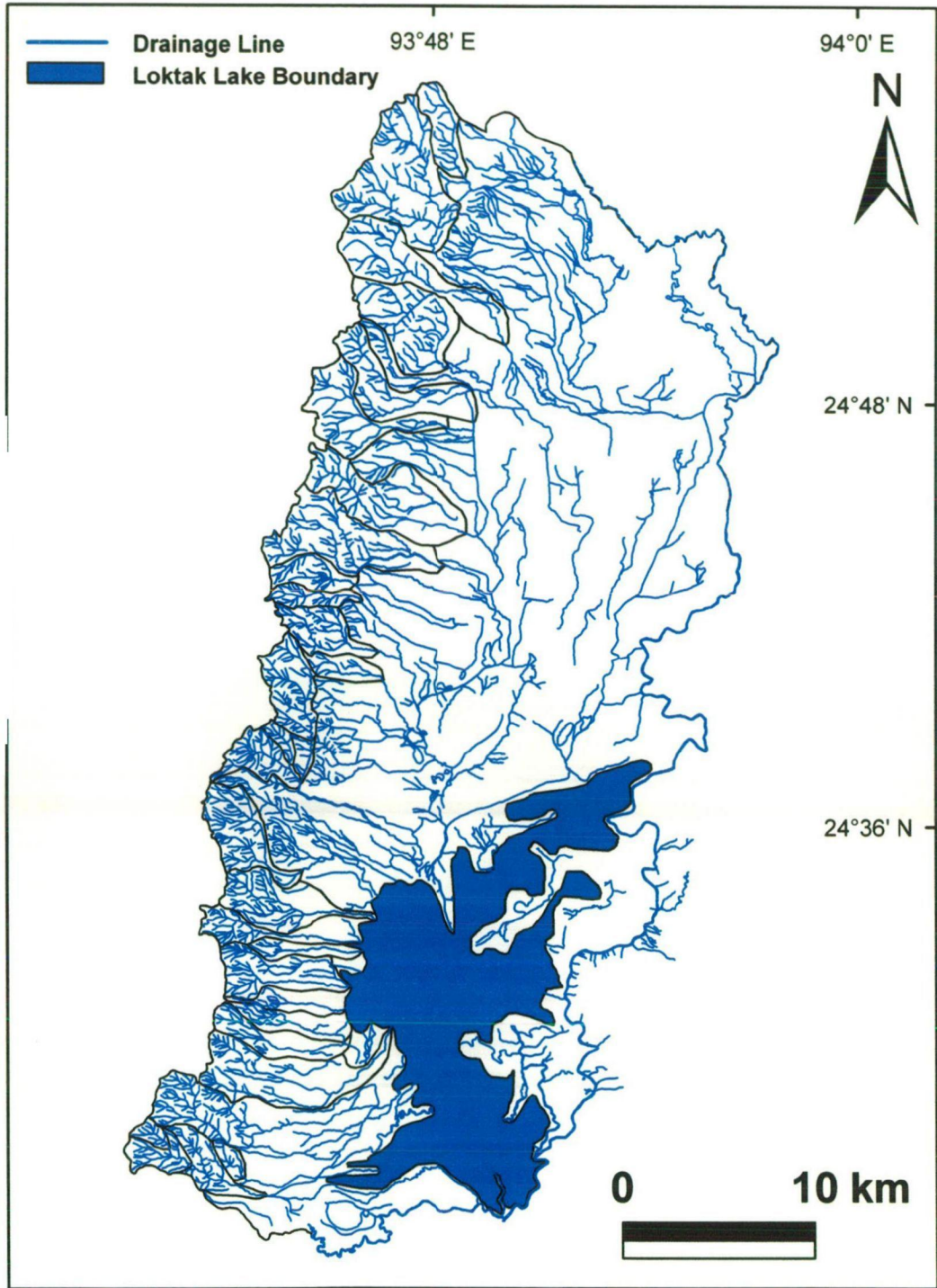


Fig.3.3: Drainage map of the study area

Lake on the left bank of Imphal river and Khuga and Manipur rivers merge together to become one sheet of water just upstream of Ithai barrage site. The Manipur river during this period functions as a discharge channel only. Thoubal river with an annual discharge of 12,900 m³/s has an ongoing multipurpose project with an irrigation potential of 33,400 ha. Sekmai barrage on the Sekmai river, another tributary of Imphal river, is used to irrigate 8094 ha culturable command area (CCA).

3.1.2 Land Use

The land use of the basin broadly comprises of forests, agricultural land and settlements. Forests constitute 73.6 % of the total land area of the basin. The degraded forests constitute 42% of the total forest area of the basin, followed by dense forest (38%) and moderate forest (20%) in decreasing order (Fig. 3.4). Major forest types occurring in the basin are tropical semi evergreen, subtropical pine, and montane wet temperate forest. A large part of forests is barren and denuded, primarily due to large scale shifting cultivation practiced in the hilly regions of the basin. Rapid deforestation has led to severe erosion problems as well as reduction in flood cycle and drying of streams. There has also been reduction in the availability of timber and non timber forest products.

Agricultural land occupies 15.1% of the basin area. There are two broad farming systems practiced in the basin. Shifting cultivation is the characteristic feature of agriculture in the hilly regions whereas a more settled form of agriculture is practised in the valley. The valley region contributing to 65% of the overall paddy production of the state is also known as rice bowl of Manipur. Overall 54% of the valley area is under paddy cultivation. Pulses, tobacco, potato, chilies and vegetables etc. are other important crops grown in the valley area. The major crops grown in the hills are paddy, maize, foxtail, finger millets, beans, cassava, yam, banana, sweet potato, chillies, sesame etc. Citrus fruits

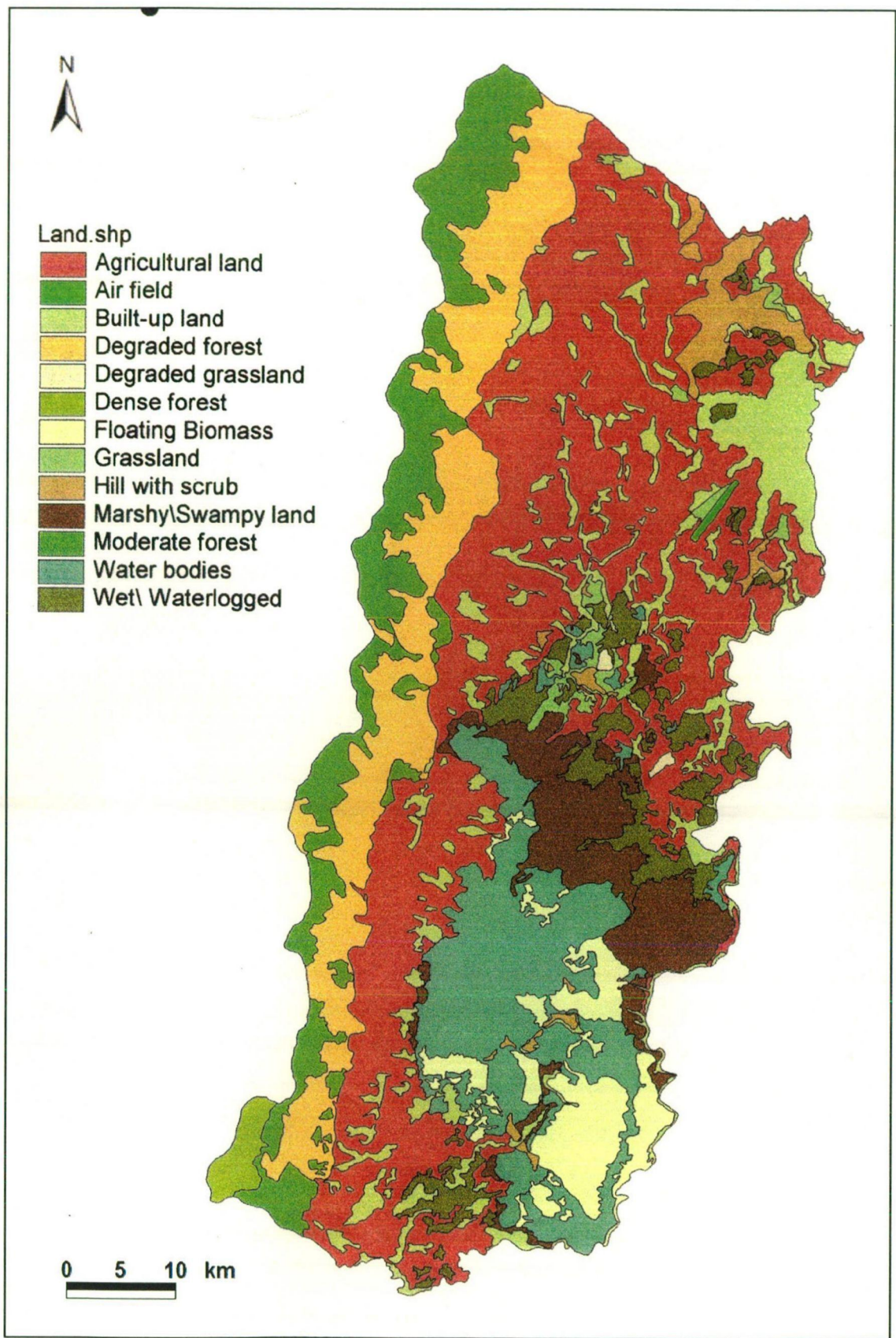


Fig. 3.4: Land use classes in the Loktak Lake catchment

and sugarcane are important cash crops of the hill and valley regions respectively. Rapid increase in population has induced severe pressures on agriculture. The area sown more than once in the valley region has increased at an annual rate of 6.23% during 1990-2000. Similarly, the intensity of fertilizer usage has also increased tremendously. The area of paddy under shifting cultivation has also expanded at an annual rate of 5.9% during 1995-2000. Manipur river basin with 1429 villages and 30 towns accounts for 66% of total settlements of the state as per 1991 census. The hills are sparsely populated and are inhabited by 29% of overall population. The valley region with 455 villages and 29 towns are inhabited by 71% of the total basin population and is one of the most densely populated regions of the country. Most of the settlements in the valley region are concentrated near water bodies, out of which 14% is located in and around Loktak Lake alone. Rapid growth of population in the valley region, especially in its 29 urban areas has led to tremendous pressure on civic amenities and high amount of wastes being dumped into water bodies.

3.1.3 Land Capability

The Loktak watershed has montane subtropical forests; Group 8 subtropical broadleaf hill forests according to the Champion's Classification of forest type. The common species found in the forests are *Quercus serrata*, *Castanopsis spp.*, *Schima wallichii*, *Alnus nepalensis*, *Litsea* etc. The *jhum* fallows have large blanks of *Imperata* mixed with *Azzeratum*, *Eupatorium*, *Odoratum* and *Artimisia* etc. The swamps are infested with association of aquatic plants like *Cymbopogon spp.*, *Eichhornia crassipes*, *Nymphaea spp.*, *Euryale ferox*, *Cynodon spp.*, *Phragmites*, *Typha*, *Scirpus*, *Carex*, *Eleocharis*, *Friglochlin*, *Azolla*, *Pistia*, *Salvinia*, *Hydrilla*, *Nelumbo*, *Zizania* etc. The slightly elevated tracts of the alluvial plain have tree vegetation of different types. Bamboo is the common species occurring throughout the region. Assessment of current pressures

on Loktak catchment has been carried out for identification of specific problems and developing strategies for regulating flow regimes and control of soil erosion. A detailed land use study was undertaken to assess the current status of the watershed. The study indicated that western catchment area directly draining into the lake has 342 km² under agriculture, 133 km² under habitation, 262 km² under forests, 22 km² under waterlogged and 287 km² being the lake area itself. Land capability studies of catchment area of Loktak Lake undertaken to assess the status of the catchment area using slope gradient and soil and vegetation characteristics highlight its erosion status and land capability. The Loktak watershed can be broadly divided into four physiographic units viz; high hills (elevation ranging from 900 to 1940 MSL), medium hills (elevation ranging between 760 to 900 MSL), plains (very gentle slope) and marshy lands (shallow water with presence of thick growth of floating and submerged plants). The study highlights that the soils developed on the higher slopes of both high and medium hills are deep to very deep, well drained, fine loamy to fine in texture with coarse fragments in place, and are moderately to excessively eroded. The soils in the higher slopes of both high and medium hills are prone to excessive erosion. About 5.9% of the Loktak watershed falls under the very severe erosion class, 14.6% under severe and 7.2 % under moderately severe (Trisal and Manihar, 2004).

3.1.4 Loktak Lake

Loktak Lake (shown in Plate 3.1) is considered as the lifeline of the people of Manipur due to its importance in their socio-economic and cultural life. Loktak Lake has been traditionally used for agriculture and fisheries (as shown in Plate 3.2). Local people sustainably managed its rich biodiversity and derived benefits through its natural functioning. However, onslaught of unsustainable developmental activities without understanding the nature of the wetland ecosystem has led to its degradation and loss of benefits accrued from the ecosystem. The denudation of lake catchments due to *jhum*



Plate 3.1: Panoramic view of the Loktak Lake



Plate 3.2: Fishermen in the Loktak Lake

farming, deforestation and increasing demands for fodder, fuel and other forest products contributed to enhanced siltation and reduction of water holding capacity of the lake.

The Loktak Lake which is located between $93^{\circ} 46'$ and $93^{\circ} 55'$ E and from $24^{\circ} 25'$ to $24^{\circ} 42'$ N is a floodplain wetland of Manipur river and is flooded by its lateral flows as well as back flow of water from *Sugnu* hump. Further, confluence of several rivers, particularly the river Chakpi, is responsible for inundation of large areas. The lake earlier used to experience large fluctuations in the water level during a year and several minor wetlands (*pats*) with the Loktak were distinct during the low water phase and merged into one sheet of water during high floods. The commissioning of Ithai barrage in 1983 has brought drastic changes in the character of the wetland from fluctuating water levels to more or less constant water level. The lake is oval shaped with maximum length and width of 32 km and 13 km respectively. The depth of the lake varies between 0.5 and 4.6 m with average recorded at 2.7 m. The lake covers an area of 287 km² which is mainly dictated by maintenance of water level at Ithai at 768.5 m above msl. There are 14 hills located in the

3.1.5 Catchment Degradation and its Impacts

The major causes for degradation of the lake are increasing human population and unsustainable developmental activities within the catchment area. The following are the impacts of various developmental activities on Loktak catchment and ultimately on lake ecosystem.

Enhanced unsustainable agriculture activities, particularly shifting cultivation, has led to overall land degradation in hill areas leading to increased soil erosion and lake sedimentation. Area under paddy cultivation in the hill villages has increased at 2.3% per annum, thereby creating pressure on the forest resources. The shifting cultivation cycle, which until a few decades was more than 20 years has currently been reduced to five years or less due to increasing population and declining land productivity. The silt is deposited

in the lake, which is responsible for declining water holding capacity and loss of wetland processes and functions. Lake varying in size and elevations appear as islands in the southern part of the lake. The most prominent among these are Sendra, Ithing and Thanga islands. Loktak Lake is very important in terms of its socio economic, environmental, cultural and ecological value. The first international concern of this lake was aroused in the year 1990 in which “The Convention on Wetlands of International Importance” drafted at the Iranian City of ‘Ramsar’ (1971) gave recognition to the Loktak Lake for its peculiar characteristics. This Convention popularly known as “Ramsar Convention” thereby brought the Loktak Lake into international status for its uniqueness and put into limelight for its conservation and management. Out of the 23,88,634 (as per 2001 census) populations of Manipur more than 1.2 millions people are directly or indirectly benefited from this lake. Since time immemorial people have depended on this lake for food, agriculture, irrigation, pisci-culture, energy, aesthetic and recreational purposes.

Nearly 29 to 30 rivers and streams feed Loktak Lake. Figure 3.3 shows the drainage map of the catchment showing the main rivers and streams draining into the lake. ‘*Ungamel Channel*’ (Ithai Barrage) is the only outlet for this lake. The perennial rivers and streams, which flow into Loktak Lake, bring sediments every day in their course to the lake. Continuous soil erosion in the hilly terrain due to deforestation further enhances the process. The sediments deposited at the mouth of the rivers contribute to shallowing of the lake bottom. As most of the rivers flow through the heart or center of the cities and towns, the urban sewage dumped into these rivers ultimately reach the lake, thereby deteriorating the delicate ecosystem of the lake. Highly toxic substances such as insecticides, pesticides, oils, polythene bags, other non-biodegradable waste and municipal wastes further create a disastrous situation to the lake environment. Nambul river the most polluted river in Manipur ends up in this lake after depositing whatever possible pollutant it brings in its

course. “*Thongjaorok*” or Bishnupur river on the other hand brings its entire sediment load, caused due to massive deforestation in the upper part of the hilly region of this river.

3.2 WATERSHEDS

Manipur river basin has been delineated into nine mega watersheds based on land use and drainage features. The salient features of watersheds are briefly outlined here.

Khuga watershed

The Khuga watershed covers an area of 504.76 km² and is drained by Khuga river. This watershed is further delineated into 6 subwatersheds. Barren forests constitute 70% of its geographical area, comprising mainly of open (28%) and scrub forests (42%). *Jhum* cultivation is the main contributory factor for degradation of this watershed. Abandoned *jhum* occupies 16% of the total geographical area of the watershed. Khuga multipurpose project with an irrigation potential of 4,000 ha, besides supply of 4 MGD water for domestic use and power generation of 1.75 MW is operational in this watershed.

Heirok watershed

The Heirok watershed, drained by the Heirok and Sekmai rivers, extends to an area of 860.82 km² and comprises of 11 subwatersheds. Forest cover in this watershed is low and the vegetation is mostly degraded. Seventeen percent of this watershed is under shifting cultivation. Pumlun and Ikop wetlands/lakes are located within this watershed. A medium irrigation project is operational in this watershed on Sekmai river.

Thoubal watershed

The Thoubal watershed extends to a total area of 911.61 km² and is drained by the Thoubal river. The watershed consists of 10 subwatersheds and has two third of its area under forest cover. The watershed has the highest intensity of shifting cultivation among

all 9 watersheds of the basin and one fifth of its area is under present or abandoned *jhum* cultivation. The Thoubal multipurpose project with an irrigation potential of 29,400 ha, water supply of 10 MGD and power generation capacity of 7.50 MW is operational on Thoubal river.

Imphal watershed

The Imphal watershed with an area of 474.8 km² is the smallest watershed of the basin and consists of 7 subwatersheds. The watershed has 66% of its area under forests and only 2% under shifting cultivation.

Upper and lower *Iril* watersheds

The Iril river drains two watersheds, viz., the *Iril* upper watershed with an area of 758.09 km² and *Iril* lower watershed with an area of 633.28 km². The upper watershed consists of 10 subwatersheds and has 81.49% of its area under forests cover. The lower watershed has relatively lower area under forests (51.16%) with absence of dense forest cover. The two watersheds have a high intensity of shifting cultivation, with 12.74% of their area under present or abandoned *jhum*. The *Doloithabi* medium irrigation project with an irrigation capacity of 7,545 ha is operational in the lower watershed. The Chakpi and Manipur river watersheds below Ithai barrage cover a total area of 1,681.27 km² and are drained by Chakpi and Manipur rivers.

Watersheds after Ithai Barrage

Two watersheds of Chakpi and Manipur rivers after Ithai barrage do not drain directly into Loktak Lake. However they contribute significantly to the back flow of water due to Sugnu hump near Sugnu village.

Loktak watershed

Loktak watershed is the largest watershed of the Manipur river basin and it is also known as the catchment of the Loktak Lake. The watershed has the lowest forest cover (21%) among all watersheds of the basin. In this watershed, an area of 516 km² is classified as reserve forests. Loktak Lake forms 27% of the total geographical area of the watershed.

There are 27 watersheds in the catchment of the Loktak Lake. These two watersheds are a part of the twenty-seven watersheds located in the western catchment of the Loktak Lake as shown in Fig. 3.5. The watersheds have been enlisted in Table 3.1. In view of the limited data availability, two watersheds namely Awang Khujairok and Waikhulok have been chosen in the present study for modelling of soil erosion. Therefore, in the catchment of the lake, the two watersheds of Awang Khujairok & Waikhulok have been selected for the present study where a very short duration observed data were available. The detailed hydrogeological and other characteristics of these watersheds have been discussed separately in the subsequent sections.

3.3 THE AWANG KHUJAIROK AND WAIKHULOK WATERSHEDS

The region experiences sub-humid climate and the main crops grown are rice, maize and pulses. Based on the results of these two watersheds, the soil erosion can be estimated for the entire catchment. The subsequent sections describe the characteristics of these watersheds.

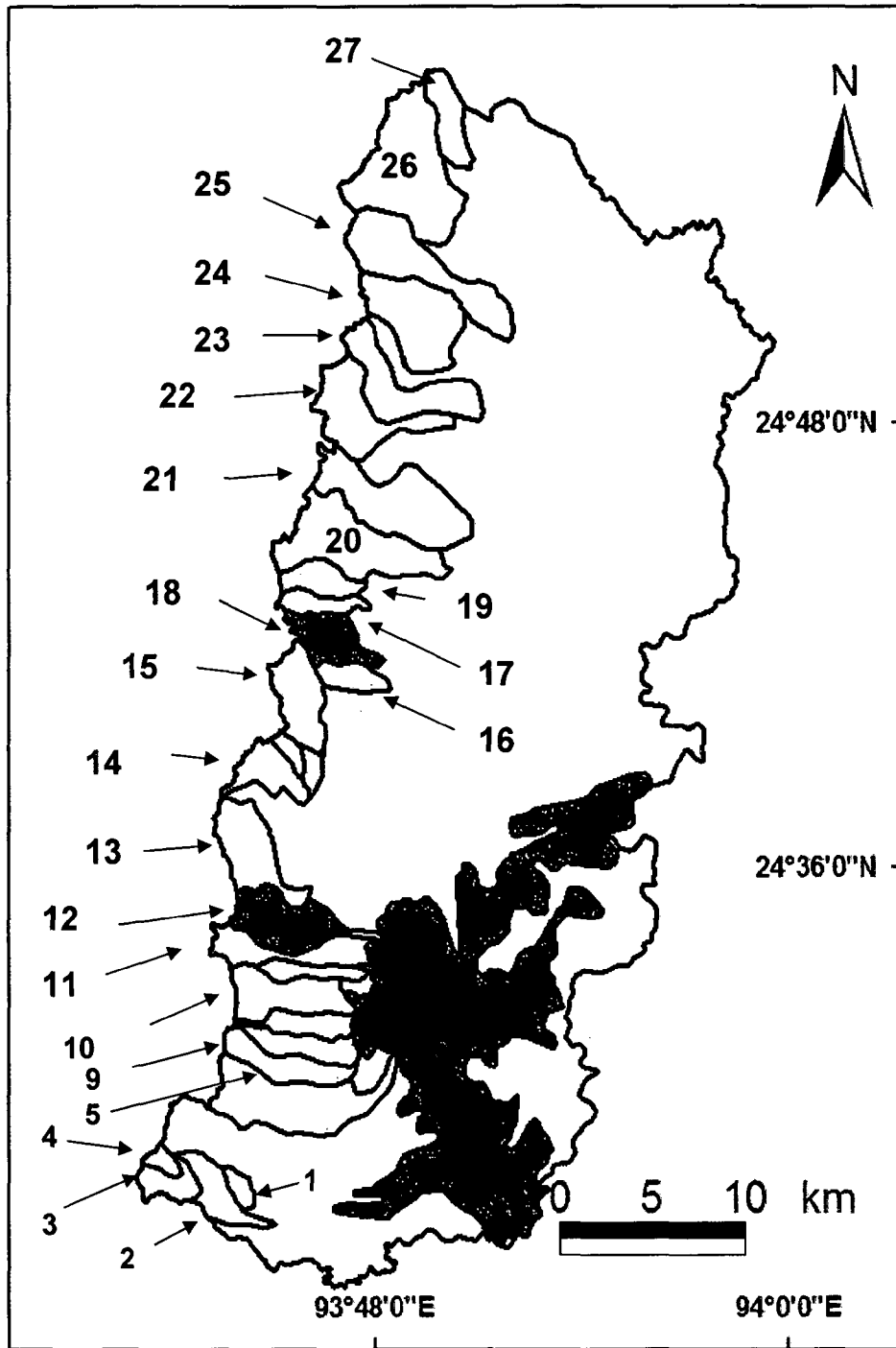


Fig. 3.5: Watersheds in the study area

Table 3.1: The watersheds in the Loktak Lake catchment

Sl. No.	Name
1	Turelu
2	Moirang Turel
3	Mashem (Kwakta)
4	Laijamaril
5	Wangtha
6	Thingin
7	Irum
8	Lenghanbi
9	Kongdun
10	Ningthoukhong
11	Charoikhui
12	Awang Khujairok
13	Nungshai
14	Keinou
15	Thongjaorok
16	Aigejang
17	Ishinglok
18	Waikhulok
19	Wakching
20	Sajirok
21	Haibirok
22	Khonga
23	Phayeng
24	Kangchup
25	Kharamkom
26	Singda
27	Songtum

3.3.1 Geomorphology

The drainage basins display interesting geomorphic situations. The watersheds are divided into three major divisions. The upper catchment is mainly with longitudinal spurs and break in slope areas beside other erosional landforms. The flat-topped hills indicate the denudation topography in watersheds. Denudation slopes on valley sides usually develop following dissection by fluvial erosion on an uplifted block. Stream erosion incises the valley flanks and denudation attacks the valley flanks and causes them to

retreat. The denudation rate at water divided also increases progressively during the slope steepening. The equilibrium includes the relationship between weathering rate and net denudation rate at each slope point, which corresponds to summit denudation rate. The moderate slopes are more prone to erosion where there is no vegetative cover. The foothills have moderate to gentle slopes, occupied by settlement and agriculture.

There are number of N-S to NNW–SSE trend lineaments along the river. The break in slope is the linear areas tending NW- SE, which indicates the evidences of neotectonic activities in the river basin. There are few slope facets in NE-SW direction, which is similar to regional tectonic trend. The river basin is in its youthful stage. The depositional landforms such as flood plain, piedmont zone are observed along the foothills. The flood plains are coalescing with the alluvial plains of Imphal valley.

3.3.2 Soil characteristics

The soils of catchments are derived from shale and sandstones and are found to occur mostly on hills of various slopes. Soils occurring on gently sloping foothills are deep to very deep and well drained but vulnerable to sheet and rill erosion. The soil is grayish brown to yellowish brown in colour. The upper reaches of the rills are in the forest cover of deciduous trees. Due to high acidity and soil erosion, the soils are not being used for agricultural purpose. There are many plantation sites in the watersheds on moderate slopes. The following categories of soil are identified in the watersheds:

- Mn 012** Deep excessively drained clayey soils on gentle to moderate sloping sides of hill having clayey surface with moderate to severe erosion hazards and slight stoniness.
- Mn 015** Deep poorly drained, fine silty soil on nearly level to gently sloping valleys having clayey surface with slight erosion hazards and ground water table is below two meters from the surface.

Mn 017 Associated with deep, well drained, clayey skeleton soil on steep slope of hills with less erosion hazard and slight stoniness.

3.3.3 Geological Characteristics of the Watersheds

Geologically a series of sedimentary rocks mainly shales and sandstones of Disang Group (Tertiary age) constitute the catchment. These sedimentary rocks are subjected to tectonic activity and resulted into the present day topography in the form of anticlinal hills and synclinal valleys. Geologically, Disang groups are of Eocene age and overlain by Barail group of Oligocene age. The Older Alluvium and Recent Alluvium (Pleistocene to Recent) is deposited along the river valleys.

The regional strike of all the rock formations is from N-S to NE- SW with dip ranging between 60° – 70° . The dip direction trends either towards east or west. The alteration of argillaceous and arenaceous rocks has a series of N-S to SW trending longitudinally symmetrical and plunging anticlines and synclines. The study of trend lines indicates two distinct phases of folding. The folds are asymmetrical, compressed tight in nature with axial planes vertical to sub-vertical. These folds are plunged towards NE to N in southern part and S-W to South in northern part. They are broad and open folds with axial plane trending E-W to ESE-WNW directions. The lineament analysis indicates mostly faulty and fracturing of rocks. Numerous well-defined lineaments trending N-S, NNW-SSE, ENE-WSW, NE-SE and NNE have been observed.

The watersheds display an interesting feature, the contact between Disang and Barail groups. There are number of local faults trending NNE-SSW to NE-SW ^{direction} _{fractures} indicating that the faulting is along the main regional strike of the hills. The structural and denudation hill predominantly delineate the Barail sandstone from the linear Disang shale in the watersheds. The deciduous forest cover is the characteristics land use of sandstone hills whereas the moderate to barren land use cover delineate the shale hills. Overall, the

area is highly deformed due to past tectonic activities. The Disang group of rocks are prone to more weathering than Barail group.

3.3.4 Vegetation

Medium to thick deciduous and evergreen forest occupies the upper reaches of the catchment. The ground is covered with thick undergrowth of bushes, shrubs, tall grasses and other types of vegetation. The variation of vegetation is marked by growth of specific species at particular altitudes. The flora found in the area contains a variety of orchids, pine, oak, teak, cane, flowering trees including the famous Himalayan magnolia (Tree lotus) *Engellei* and *Thaballei* (raitomatous plants) etc.

3.3.5 Land use and Socio-economic Condition:

Nearly 70% of the total geographical area is under forest. Cropping systems are largely dependent on the factors like landscape, climate, water resources, and economic value of the crops and hence systems are very much diversified. Agricultural practices are primarily of primitive nature in the major parts of the state. The *Jhum* cultivation is fairly common and practiced on slopes in the vicinity of habitation. A large area is under terrace cultivation. Some pockets are under permanent cultivation without any terracing. The gently sloping piedmonts are terraced for intensive and permanent cultivation. The hilly regions are under horticultural crops. Non-cereal crops are also grown. Widespread practice of shifting cultivation contributes to the problem of soil erosion and loss of soil fertility. All these factors together have become constraints with poor road communication in the way of agricultural development of the state.

3.3.6 Erosion Characteristics

Erosion is one of the most important agricultural problems in the region. Erosion is mainly caused by geological reasons and human activities. The small seasonal streams

along the hill slopes formed immediately after the torrential rain is the chief factor to accelerate the land water erosion. The types of water erosion prevalent are rill, gully and stream channel erosion, which is accelerated by shifting cultivation practices and construction activities.

The major variables, affecting the soil erosion are climate, soil, vegetation and topography. The climatic factors affecting the erosion are precipitation, temperature, humidity, wind and solar radiation. The relationship between precipitation characteristics, runoff and total soil loss is complex. It is inferred that the inter-rill erosion varies with the rainfall intensity. Rill erosion is a function of runoff rate, which depends both on rainfall intensity as well as soil infiltration rates.

The physical properties of soil affects the infiltration capacity and extent to which particle can be detached and transported. The soil detachability increases as the size of soil particle or aggregate increases and soil transportability increase with a decrease in particle or aggregate size.

The major effects of vegetation in reducing erosion phenomenon are interception of rainfall by absorbing the energy of raindrops and thus reducing surface sealing and runoff. These vegetative influences vary with the season, crop, and degree of maturity of vegetation, soil and climate and plant residues.

The Loktak Lake area is subjected to a complex set of environmental pressures and associated management problems. There are important gaps in the understanding of the hydrology of the lake and the consequences of change in land use that have taken place over time, particularly in relation to the impact of these changes on the lake ecosystem. Understanding these is vital for improving the water resource management in the catchment.

The present study focused primarily on the two micro watersheds-Awang

Khujairok and Waikhulok in the western catchment. The salient features of the two micro watersheds considered for study are given in Table 3.2. The rainfall record in the two micro watersheds is given in Table 3.3 and Table 3.4.

Table 3.2: The particulars of the two watersheds- Awang Khujairok and Waikhulok

Particulars	Awang Khujairok watershed	Waikhulok watershed
Geographic Location	Latitude: 24°69' N to 24° 72' N Longitude: 93°74' E to 93°77'E Senapati District	Latitude: 24°82' N to 24°84' N Longitude: 93°77' E to 93°79' E Senapati District
Geographical Area	6.49 km ²	3.86 km ² .
Climate	Subhumid, Moderate rainfall with annual average of 1330 mm.	Subhumid, Moderate rainfall with annual average of 1435 mm.
Physiography	Moderate relief, Moderately dissected topography. Elevation between 800 m to 1800 m.	Moderate relief, Moderately dissected topography. Elevation between 900 m to 1500 m.
Geology	Mainly shales with intercalation of sandstone (Disang group)	Mainly shales with intercalation of sandstone (Disang group)
Economic Activity	Agriculture, Horticulture and Animal husbandry	Agriculture, Horticulture and Animal husbandry
No. of villages	2	1
Villages	Tuikhang Aimol and Aigejang	Khongakhul
Population		
Human	142	175
Cattle	164	145
Land use/ Land cover	Area (km²)	Area (km²)
Decidious forest	1.255	
Pine forest	1.216	
Exposed soil	0.02528	
Mixed plantation	0.6106	
Plantation		0.066
Barren land	3.02	
Bamboo breaks	0.1786	
Settlement	0.1834	0.021
Thick vegetation		0.956
Medium vegetation		0.651
Scrub		2.164
Land Capability	Area (Ha)	Area (Ha)
Class IV	193.7	
Class VI	254.9	133.2

Table 3.2 (continued)

Land Capability	Area (Ha)	Area (Ha)
Class VII	169	252.5
Class VIII	68.38	
Major crops	Rice, Maize and pulses	Rice, Maize and pulses
Cash crops	Aroids, Sugarcane, Ginger and Pine apple	Pine apple, Banana, Pumpkin, Mustard and Parkia
Forest produce	Timber and fuel wood	Timber and fuel wood
Rainfall	(mm)	(mm)
Monsoon (May – September)	806	835
Non-monsoon (October - April)	524	600
Annual	1330	1435
Elevation	800 m -1800 m	900 m - 1500m
Air Temperature		
Daily Maximum (°C)	33	33
Daily Minimum (°C)	1	1
Rel. Humidity (%)		
Maximum (%)	98.8	98.8
Minimum (%)	35	32
Evaporation		
Daily Maximum (mm/day)	9.6	9.6
Daily Minimum (mm/day)	0.1	0.1
Total Dissolved Solid mg/l	75 to 95	105 to 170
Phosphate mg/l	0.005 to 0.026	0.013 to 0.030
Boron mg/l	0.000152 to 0.002	0.00045 to 0.0007
Ammonical -N ₂ mg/l	0.0112 to 0.410	0.000152 to 0.700
Conductivity µs/Cm	115 to 185	140 to 165
Colour Alpha Platinum Cobalt unit	65 to 80	105 to 125
Water Demand	(L.P.D.)	(L.P.D.)
Domestic	8520	10500
Cattle	6560	5800
Water Availability	(Monthly)	(Monthly)
Rainfall (mm)	22.5, 12.5, 109, 166, 213.5, 199, 93.5, 101.5, 198.5, 201.5, 13, 0	16.5, 18, 156, 74.5, 201.5, 218, 271.5, 168.5, 177, 132, 0, 0
Domestic	8520	10500
Cattle	6560	5800

Table 3.2 (continued)

Geomorphology	Awang Khujairok watershed	Waikhulok watershed
Stream Orders	1=6, 2=7, 3=2, 4=1	1=15, 2=5, 3=1
Stream Length (km)	1=14.43, 2=6.476, 3=3.946, 4=0.0846	1=8.220, 2=1.317, 3=2.731
Drainage Density (km/km ²)	3.84	3.18
Slope	10% - 50%	15% - 50%
Geology	Mainly shales with intercalation of sandstone (Disang group)	Mainly shales with intercalation of sandstone (Disang group)
Soil Texture	Predominantly gravely sandy loam	Predominantly gravely sandy loam
Streamflow	(cumec)	(cumec)
Maximum	4.9	2
Minimum	0	0
Water Quality		
D.O. mg/l	7 to 9	6 to 8
B.O.D. mg/l	1.5 to 2.5	0.5 to 1.5
Nitrogen mg/l	0.3 to 0.9	0.5 to 0.8
Total Coli. MPN/100	30 to 33	42 to 46
Chloride (mg/l)	9 to 18	12 to 20
Hardness as CaCO ₃ (mg/l)	45 to 85	50 to 75
Calcium as CaCO ₃ (mg/l)	20 to 50	25 to 40
Magnesium as CaCO ₃ (mg/l)	20 to 35	25 to 35
Alkalinity (mg/l)	40 to 65	45 to 95
Sulphate (mg/l)	5 to 13	1 to 16
Sodium (mg/l)	3 to 22	4 to 16
C.O.D. (mg/l)	10 to 13	13 to 30
Total Suspended Solid (mg/l)	95 to 330	110 to 315

Source: Project Report, NRDMS, 2001.

Table 3.3: Rainfall record for the Awang Khujairok watershed (mm)

Months	2000	2001	2002	2003	2004	2005	2006
Jan	6	0	25	1.16	9.38	0.00	0.00
Feb	6.5	0	2	0.71	8.70	0.00	0.00
Mar	49.5	44	19.5	0.99	77.57	17.84	32.21
Apr	58	44	98	2.02	98.91	97.16	165.21
May	89	11	141.5	9.98	101.47	145.21	158.84
June	128.5	99	144.5	27.27	333.32	228.27	121.24
Jul	137.5	99.5	249	87.27	78.35	278.99	258.98
Aug	115	86.5	251.5	169.32	78.56	131.87	187.21
Sept	106	384	83	285.54	167.40	124.68	110.92
Oct	50	162.5	104.5	158.67	21.20	23.87	107.54
Nov	0	220.5	54	8.00	3.00	38.01	9.47
Dec	0	0	12	0.00	0.00	0.00	21.22

Table 3.4: Rainfall record for the Waikhulok watershed (mm)

Months	2000	2001	2002	2003	2004	2005	2006
Jan	16.50	5.00	16.00	0.00	12.40	0.00	0.00
Feb	18.01	58.00	1.50	5.00	8.70	0.00	0.00
Mar	156.21	27.50	17.50	22.50	34.57	13.24	26.57
Apr	74.50	84.50	61.30	142.50	101.80	84.61	145.34
May	201.50	127.21	35.50	138.00	103.47	165.21	167.58
June	218.21	425.50	151.50	241.50	421.32	228.27	116.87
Jul	271.50	93.50	264.60	345.50	85.23	247.58	268.98
Aug	168.50	75.00	313.00	66.00	89.65	127.89	188.67
Sept	177.24	157.50	143.50	0.00	167.40	127.68	103.87
Oct	132.20	157.00	137.00	0.00	24.20	23.21	112.54
Nov	0.00	26.00	58.00	0.00	0.00	42.10	8.00
Dec	0.00	0.00	3.00	0.00	0.00	0.00	16.78

METHODS FOR SOIL EROSION ASSESSMENT

In the present chapter, methods for assessment of soil erosion are described. For the present study, two approaches, i.e. existing soil erosion model and nuclear techniques have been used for the assessment of soil erosion. In soil erosion modelling, remote sensing and GIS techniques have been applied, whereas in case of nuclear technique, experimental work has been carried out to determine the ^{210}Pb contents in the soil cores collected from the selected location in the study area. These two approaches have been described in the following section.

4.1 EXISTING MODELS FOR SOIL EROSION ASSESSMENT

Watershed management implies rational utilisation of land and water resources for optimum production. Land and water are two natural resources on which social and economical structure of any country depends. In an analysis of annual soil erosion rates in India (Dhruva Narayana and Babu, 1983), it was estimated that about 5334 m tonne (16.35 tonne/ha) of soil is detached annually due to agriculture and associated activities alone. The annual soil loss in India has been estimated as 5334 million tonnes (16.35 tonne/ha) due to agriculture and related activities. Thus the estimation of soil erosion, runoff and sediment yield is important and essential parameters for any watershed development planning.

A number of models are available for the assesment and prediction of soil erosion in different types of field conditions. Depending on local conditions, requirements, goals

and available information, a model can be selected for the estimation of soil loss and runoff in the study area. In this section, various watershed models like, AGNPS, SWMHMS, SWAT, MUSLE, KINEROS, WEPP, TOPMODEL, LISEM and EPIC have been described. The input, output and physical processes of the various watershed models have been compared and suitability of the model for the study area has been highlighted.

4.1.1 LISEM Model

Because of spatial and temporal variation in runoff and soil erosion processes, GIS has been a very useful tool to use in hydrological applications. The *Limburg Soil Erosion Model* (LISEM) is one of the first models to use GIS. LISEM is a physically based hydrological and soil erosion model developed by the Department of Physical Geography at Utrecht University and the Soil Physics Division of the Winard Staring Centre in Wageningen, The Netherlands. The LISEM is a powerful model that simulates hydrological and soil erosion processes during single rainfall events on a catchment scale (De Roo, 1996). The various hydrological and soil erosion processes which are simulated using LISEM models are rainfall, infiltration, soil water transport, storage, hydraulic conductivity, splash detachment, sediment bed load, etc.

The model, in the soil erosion part, accounts also for roads, wheel tracks and channels. LISEM, though one of the best known soil erosion models, requires a vast input data for its operation. To simulate a drainage basin of 45 hectares with a 10 x 10m pixel, 4500 values are needed for all 15 variables (De Roo, 1996). Saturated hydraulic conductivity of wheel tracks, number of wheel tracks, depth of wheel tracks, Manning's coefficient of wheeltracks, cohesion of wheel tracks, drainage directions of wheel tracks, K-h-theta relationships, wetness index etc are just some of the exhaustive range of input data required to run the model.

4.1.2 WEPP Model

The Watershed Erosion Prediction Process (WEPP) watershed model, a process-based and distributed parameter computer simulation model, was developed to predict erosion from different agricultural management practices and to accommodate spatial and temporal variability in topography, soil properties, and land use conditions within small agricultural watersheds of less than 260 ha (Ascough *et al.*, 1994; Jain and Dolezal, 2000). The erosion component of the WEPP model uses a steady-state sediment continuity equation as the basis for the erosion computations. The WEPP considers only Hortonian flow or flow that occurs when the rainfall rate exceeds the infiltration rate. The model uses two methods of computing the peak discharge: a semi-analytical solution of the kinematic wave model and an approximation of the kinematic wave model. The first method is used when WEPP is run in single event mode while the second is used when WEPP is run in continuous simulation mode (Ascough *et al.*, 1994; Flanagan and Livingston, 1995).

The erosion prediction from the WEPP model is meant to be applicable to "field-sized" areas or conservation treatment units. When applied to a single hillslope, the model simulates a representative profile, which may or may not approximate the entire field. For large broad zones in which there is a definite slope shape dominating an entire field, one profile representation may be sufficient to adequately model the site. However, for much dissected landscapes, in which several different, distinct slope shapes exist, several hillslopes will need to be simulated (either as separate runs within the Hillslope Interface, or as a single watershed simulation in the Watershed Interface). The maximum size "field" is about a section (259 ha) although an area as large as 809 ha is needed for some rangeland applications. The model should not be applied to areas having permanent channels such as classical gullies and perennial streams, since the processes occurring in these types of channels are not simulated in WEPP. Use of the watershed application of

WEPP is necessary to simulate flow, erosion, and deposition in ephemeral gullies, grassed waterways, terrace channels, other channels, and impoundments. Because of the greater complexity of watershed applications of the WEPP model and the interface, it is recommended that the user first be familiar and comfortable with hillslope applications and the hillslope interface.

4.1.3 TOPMODEL

The TOPMODEL (a topography-based hydrological model) is a set of conceptual tool which is used to simulate the hydrological behaviour of watershed in a distributed or in a semi-distributed way in a relatively simple way, particularly the dynamics of surface and subsurface contributing areas. It is a topography based watershed hydrology model that has been used to study a range of topics, including spatial scale effect on hydrological process, topographic effect on hydrological process, topographic effect on water quality, topographic effect on stream flow, climatic change effect on hydrological process, geomorphological evolution of basin and the identification of hydrological flow path etc. The simplicity of model comes from using the soil-topographic index as an index of hydrological similarity. It is premised upon the following basic assumptions:

- i) that the dynamics of the saturated zone can be approximated by successive steady state representations,
- ii) that the hydraulic gradient of the saturated zone can be approximated by the local surface topographic slope $\tan(\theta)$,
- iii) that the distribution of downslope transmissivity with depth is an exponential function of storage deficit or depth to the water table.

The inputs to the model are:

Digital Elevation Model (DEM), rainfall, evapotranspiration (ET), transmissivity, watershed characteristics data etc.

The outputs from the model are:

Runoff, extent of saturated area, ground water table simulation, runoff from each sub-area, effect of watershed manipulation on runoff etc. The various physical processes estimated are evaporation, recharge and channel routing.

4.1.4 ANSWERS Model

The Areal Nonpoint Source Watershed Environment Response Simulation (ANSWERS) was developed at the Agricultural Engineering Department of Purdue University (Beasley and Huggins, 1981). It is an event based, distributed parameter model capable of predicting the hydrologic and erosion response of agricultural watersheds. Application of ANSWERS requires that the watershed to be subdivided into a grid of square elements. Each element must be small enough so that all important parameter values within its boundaries are uniform. For a practical application element sizes range from one to four hectares. Within each element the model simulates the processes of interception, infiltration, surface storage, surface flow, subsurface drainage, and sediment drainage, and sediment detachment, transport, and deposition. The output from one element then becomes a source of input to an adjacent element. As the model is based on a modular program structure it allows easier modification of existing program code and/or addition of user supplied algorithms. Model parameter values are allowed to vary between elements, thus, any degree of spatial variability within the watershed is easily represented. Nutrients (nitrogen and phosphorus) are simulated using correlation relationships between chemical concentrations, sediment yield and runoff volume. A research version (Amin-Sichani, 1982) of the model uses clay enrichment information and a very descriptive phosphorus fate model to predict total, particulate, and soluble phosphorus yields. The

erosion process assumes that sediment can be detached by both rainfall and runoff but can only be transported by runoff. ANSWERS model divides a watershed into small, independent elements. Within each element the runoff and erosion processes are treated as independent functions of the hydrological and erosion parameters of that element.

The primary disadvantage of the ANSWERS approach is that the cost, for both data preparation and computer time, to use it increases somewhat proportionally to the area being simulated. The model is a storm event model and the input data file is quite complex to prepare. Snowmelt processes or pesticides cannot be simulated by the model. The water quality constituents modeled are limited to nitrogen and phosphorous. These constituents are represented by relationships between chemical concentrations with sediment yield and runoff volume. No transformation of nitrogen and phosphorus is accounted for in the model. And above all, the data requirement is event-based, which was not available for the present study area.

4.1.5 KINEROS Model

The KINematic EROsion Simulation model (Smith, 1981) is an event oriented, physically based model describing process of interception, infiltration, surface runoff and erosion from small agricultural and urban catchments. KINEROS is composed of elements of a network, such as planes, channels or conduits, and ponds or detention storages, connected to each other. It uses the Smith/Parlange infiltration model and the kinematic wave approximation to route overland flow. The catchment is represented by a cascade of planes and channels. It runs on event-based data. The sediment component of the model is based upon the one-dimensional unsteady state continuity equation. Erosion/deposition rate is the combination of raindrop splash erosion and hydraulic erosion/deposition rates. Splash erosion rate is given by an empirical equation in which the rate is proportional to the second power of the rainfall. Hydraulic (runoff) erosion rate is estimated to be

proportional to the transport capacity deficit, which is the difference between the current sediment concentration in the flow and steady state maximum concentration. Hydraulic erosion may be positive or negative depending upon the local transport capacity.

However, the greater complexity of KINEROS also entails greater data requirements. It has been developed and validated largely in arid and semi-arid setting with explicit treatment of channel losses. In addition, KINEROS has a specially developed space-time rainfall interpolator that allows it accurately treatment of highly variable thunderstorm rainfall. KINEROS infiltration and erosion parameters are primarily derived through soil characteristics with modifications made for surface cover conditions. For watersheds larger than 1000 ha, application of a detailed, process based model, such as KINEROS, may be difficult to justify in the absence of distributed rainfall data, given comparable results from a simpler model which does not entail the costs associated with detailed basin characterization required for KINEROS model inputs (So and Yatapanage, 2004; Semmens *et al.*, 2005).

4.1.6 EPIC Model

The Erosion Productivity Impact Calculator (EPIC) model (Williams *et al.*, 1984) was originally developed to assess the effects of the soil erosion productivity of the natural resource base. It is a continuously daily time step model designed to provide simulation output summaries on a daily, monthly, annual and/or multi-year basis. It is frequently used for 50 to 100 year simulations or even longer. The drainage area considered by EPIC is generally a field-sized area up to 100 ha. The major components and processes simulated by model are hydrology, erosion-sediment. In more recent years the model has evolved to also address issues of i) water quality with the addition on pesticide fate, better nitrification and volatilization submodels, ii) climate change assessment capabilities with addition of CO₂ sensitivity and vapour pressure deficit equations, iii) improved wind erosion submodel, iv)

improved estimation curves for peak runoff rates, v) better manure and organic carbon management and decomposition capabilities.

In EPIC model the runoff volume is determined by using a modification of the soil Conservation Service (SCS) Curve number technique. The erosion submodel estimates soil losses from six alternative equations designed to predict erosion using various methodologies like MUSLE (Modified Universal Soil Loss Equation), (Williams, 1975),

The inputs to the model are:

Rainfall intensity, soil parameters, transmissivity, climatic parameters like temperature, relative humidity, wind velocity, solar radiation, ET, effect of alternate practice on peak runoff, parameters related to the plant management etc.

The outputs from the model are:

Peak runoff, sediment yield, nutrient, nutrient cycling, plant growth, biomass, plant water use, aluminium toxicity/lime, soil temperature, tillage, economics, and plant environment control.

Nitrogen, Phosphorous, Pesticides, Plant Growth are the major nutrients and parameters which are simulated by the model. The EPIC model can be used on small plots upto 100 ha. The model provides better manure and organic carbon management and decomposition capabilities. Also one can explore the potential option and possible combination of the resources to be used.

4.1.7 AGNPS Model

The Agricultural Non-Point Source (AGNPS) is an event based non point source pollution model for evaluating agricultural watersheds of mild topography. The AGNPS can be used for watersheds upto 20,000 ha. in size with element size of 0.4 to 16 ha. Accuracy of result can be increased by reducing the cell size, but this increases the time and labour required to run the model. The model simulates runoff using SCS curve number method,

sediments using modified USLE equation (Wischmeier and Smith, 1978) and nutrients movement adapted from the CREAM model (Frere *et al.*, 1980) from agricultural watersheds. The AGNPS model consists of four components, basically hydrology, erosion, sediments and chemical transport with nitrogen and phosphorous as major surface water pollutants. The model also considers point source of sediments from gullies and input of water, sediment, nutrients, and chemical oxygen demand (COD) from animal feedlots, springs and other point source. The distributed parameter approach of this model preserves spatial characteristics and makes it appropriate to use a GIS for storage of those spatial characteristics.

A critical analysis of studies of Panuska and Moore (1991) and Srinivasan and Engel (1991) indicate that AGNPS model can be effectively and efficiently linked with GIS and terrain to develop a decision support system to assist in management of runoff and erosion from agricultural watersheds. The GIS output layers are intended to be used in to determine locations within a watershed that are critical in the contribution of the pollutants.

The model provides realistic estimation of nutrient concentration in runoff water from smaller runoff events and antecedent moisture condition and USLE 'C' factor is reported to be most sensitive parameters (Young *et al.*, 1989). The calibration run showed that 20x20 meters cell size provides best simulations of peak runoff rate and sediment yield (Mitchell *et al.*, 1993). Also the validation results indicate poor simulation of the real events.

4.1.8 SWMHMS Model

The small watershed monthly hydrologic modelling system (SWMHMS) is a continuous simulation conceptual modelling program which attempts to account for all watershed precipitation through hydrologic processes such as surface runoff, infiltration, and evapotranspiration from a small nonurban watershed (Allred and Haan, 1996). The model was developed with the purpose of providing a computational less complex computer

modelling program capable of accurately predicting monthly runoff while requiring a minimum of watershed data input.

The input needed to run the model simulation include daily precipitation, monthly data for evapotranspiration i.e. average temperature, crop consumptive coefficients, and present daylight hours and six watershed parameters. The output from the model is total daily watershed runoff.

Of the six watershed parameters, the most sensitive is the curve number, CN. The optimal curve number for the majority of the watershed was found to be closest to SCS III type value. In terms of monthly runoff prediction, SWMHMS works well where snowfall accumulation is low. It has been reported that this modelling programme can be significantly used for determining water management practices on small agricultural watersheds. The SWMHMS is less complex than any other computer model to calculate monthly runoff and it can be used as an educational tool for learning the principle hydrologic modelling.

In terms of application, the model is useful for establishing hydrologic management practices on small watersheds. Also, conceptually the simple nature of SWMHMS allows it to be productively utilized as a tool for teaching hydrologic modelling principles.

4.1.9 SWAT Model

The Soil and Water Assessment Tool (SWAT), (Arnold *et al.*, 1993) was originally developed by the US Department of Agriculture- Agriculture Research Service and modified for use in the Hydrological Unit Model of the United States (HUMUS) support project with the objective to predict the impact of management on water, sediment and agricultural chemicals on small and large ungauged basins. Like EPIC, the SWAT model simulate various processes like hydrology, weather sedimentation, soil temperature, crop growth, nutrients, pesticides, ground water, lateral flow and agricultural management. SWAT functions on daily time step and can simulate in excess of hundred total years. This model is

designed to predict stream flow using soil, land use, elevation and weather information. It is also sensitive to changing land use and environmental practices. The SWAT modelling is designed to simulate the nested lay out of the smaller drainage area with in larger basins, and thus support environmental analysis at virtually any level of basin activity so that the environmental effect of proposed policy alternatives can be assessed. The system is built around a GIS framework.

The various physical processes included in the model are surface water hydrology, percolation, lateral subsurface flow, evapo-transpiration, snowmelt, weather simulation capabilities and statistics which are obtained from the GIS map of the chosen subbasin. This technique greatly facilitates the exploration of alternative watershed management options.

The inputs to the model are:

Rainfall, soil parameters information, land use type, elevation, climatic information data.

The outputs to the model are:

Stream flow, sediment yield, irrigation scheduling, plant- growth, nutrients, pesticides, the effect of changing land use and environmental practices can be assessed helping in decision making policy etc.

An interface has been developed for SWAT (Srinivasan and Arnold, 1993) using the GRASS (Graphical Resources Analysis Support System) (US Army, 1988) as the GIS support system. Using the submodel developed to support watershed management, the interfaces will automatically subdivide a basin (either grids or sub watersheds) and then extract model input data from map layers and associated relational data based for each subbasin. Soil, land use, weather, management and topographic data are collected using spatial techniques and written to appropriate model input files. In similar manner, output

interfaces allow the user to display outputs like maps, graphs, hygrographs and other relevant information.

By using SWAT model, the impact of management of water, sediment and agricultural chemicals on small and large ungauged basin can be examined. Also the environmental effect of proposed policy alternatives can be assessed effectively and this model's capability can be enhanced greatly using GRASS GIS, exploring the alternative watershed management option and planning.

All these models though quite popular in modelling of soil erosion, are either event-based or require a vast set of exhaustive input, which was not available for the two watersheds considered for the study.

4.2 THE UNIVERSAL SOIL LOSS EQUATION (USLE)

The Universal Soil Loss Equation (USLE) is the most widely used empirical equation for estimation of annual soil loss from agricultural watershed. A number of studies have been carried out to investigate the erosion processes and governing physical factors. Based on these studies, numerous computer based models have been developed for the estimation of soil erosion. These models have also been extensively used for the simulation of sediment yield and nutrient transport from agricultural lands. In hydrological modelling spatial information is essential for model analysis, prediction and validation. While conventional methods yield point based information, Remote Sensing (RS) technique makes it possible to measure hydrologic parameters on spatial scales. Some studies have been carried out wherein Geographic Information System (GIS) has been used for the determination of soil erosion in different plot size areas.

As USLE is widely used for the estimation of soil erosion therefore, as a first choice this model has been considered for the present soil erosion analysis.

The USLE (Hudson, 1981) remains the most commonly used means of estimating erosion rates (Gray, 1995). The USLE is used to predict the long-term average soil loss in runoff due to the combined effects of sheet and rill erosion (Wischmeier and Smith, 1948). It does not take account of gully erosion, and does not attempt to predict sediment deposition or transport within a catchment. It is given as

$$A = R.K.L.S.C.P \quad (4.1)$$

where A = computed annual loss per unit area (t/ha/year),

R = rainfall factor as an erosion index EI , where EI = erosion index.

K = soil erodibility factor, measured using a standard plot 22.13 m long sloping at 9%,
= function (wet density, particle size distribution or texture and organic matter content),

L = slope length factor,

S = slope steepness factor generally lumped with L as the topographic factor LS ,

C = cover and management factor, and

P = conservation practice factor.

The United States Department of Agriculture Soil Conservation Service Curve Number Method (Boughton, 1989; Schroeder, 1994) has been traditionally used in Australia for estimating runoff from rainfall on small rural catchments, and has been applied to mine spoil (Schroeder, 1994).

Limitations of USLE

The USLE remains the most commonly used means of estimating erosion rates (Gray, 1995). However, the equation is based on United States data from agricultural slope angles in the range from 0 to 8.8% (0 to 5°; Barker, 1995). Bowen Basin spoil slopes are typically regarded to 15% (8.5°) or steeper, well outside this range. Also, the linear USLE

has been shown not to apply for tropical soils and climatic conditions (Odermerho, 1986). Further, the available plant hydrology data relates mainly to level ground (Calder *et al.*, 1992). The USLE is used to predict the long-term average soil loss in runoff due to the combined effects of sheet and rill erosion (Wischmeier and Smith, 1948). It does not take account of gully erosion, and does not attempt to predict sediment deposition or transport within a catchment.

Use of the USLE, without modification, at mine sites has several disadvantages. The calculation does not account for erosion from gullies, or stream channels, or take into account deposition. It was primarily designed to predict soil-loss from small fields and should not be used to predict sediment levels in rivers at the drainage basin level. For most applications at mine sites, the basic USLE described above would not provide useful estimates as most impact analyses require knowledge of deposition and actual sediment yield from watersheds or disturbed areas, and calculations of sediment transport in gullies and channels. Consequently, this method is not recommended, except for calculations of potential soil-loss from a small disturbed area to aid in the application of best management practices (BMPs) and the design of other area-specific controls (www.yosemite.epa.gov).

One problem with the USLE model is that there is no direct consideration of runoff although erosion depends on sediment being discharged with flow which varies with runoff and sediment concentration

Erosion is a hydrologically driven process and the failure of the USLE model to include direct consideration of runoff leads to systematic errors in the prediction of event erosion.

RUSLE incorporates data from rangeland and other research sites in the United States to significantly improve erosion estimates on untilled lands. RUSLE can be used to compute soil loss on areas where significant overland flow occurs, but is not designed for

lands where no overland flow occurs, such as undisturbed forest lands (Dissmeyer and Foster, 1980). Since a significant proportion of the study area is comprised of medium and dense forest lands, RUSLE was not considered.

4.3 THE MORGAN MORGAN FINNEY (MMF) MODEL

The MMF model uses the concepts proposed by Meyer and Wischmeier (1969) and Kirkby (1976) to provide a stronger physical base than the Universal Soil Loss Equation (Wischmeier and Smith, 1978) yet retain the advantages of an empirical approach regarding ease of understanding and availability of data (Morgan, 2001).

The MMF model was developed for predicting annual soil loss from small to medium-sized areas on hill slopes (Morgan *et al.*, 1984). The model tries to encompass some of the recent advances in understanding of erosion processes. The advantage of this model as opposed to empirical models and other process-based models include its simplicity, flexibility, has more physical base and need less data than most of the process-based erosion predictive models (Shrestha, 1997). The MMF model separates the soil erosion process into a water phase and a sediment phase. The water phase determines the energy of the rainfall available to detach soil particles from the soil mass and the volume of runoff. In the revised MMF model (Morgan, 2001), rates of soil particle detachment by rainfall and runoff are determined along with the transporting capacity of runoff. Using the procedure proposed by Meyer and Wischmeier (1969) predictions of total particle detachment and transport capacity is compared and erosion rate is equated to the lower of the two rates.

In the revised version of the MMF model, changes have been made as the soil particle detachment by raindrop impact is simulated, which now take into account the

plant canopy height and leaf drainage, and a component has been added for soil particle detachment by flow.

4.3.1 Water Phase

4.3.1.1 Estimation of rainfall energy

The procedure for calculating the energy of rainfall is revised from that in the original version of the MMF model. Rainfall is partitioned during interception and the energy of the leaf drainage is considered in the model. The model takes the annual rainfall (R: mm) and computes the proportion (between 0 and 1) that reaches the ground surface after allowing for rainfall interception (A) to arrive at the effective rainfall (ER):

$$ER=R*A \quad (4.2)$$

The effective rainfall (ER) is then split into two parts, one of which reaches the ground surface as direct through fall (DT) and the other part is intercepted by the plant canopy and reaches the ground as leaf drainage (LD). The split is a direct function of the percentage canopy cover (CC):

$$LD=ER*CC \quad (4.3)$$

$$DT=ER-LD \quad (4.4)$$

The estimation of the Kinetic energy of rainfall (KE) consists of direct through fall and that of leaf drainage. The kinetic energy of the direct through fall (KE (DT); J/m²) is determined as a function of the rainfall intensity (I; mm/hr), as follows:

$$KE (DT)=DT*(9.81+10.60\log_{10}(I)) \quad (4.5)$$

where the bracketed term is taken from Table 4.1 (Morgan 2001), which was developed by Onaga *et al.*, (1988) for Okinawa, Japan; use for eastern Asia.

The kinetic energy of the leaf drainage (KE (LD); J/m²) is dependent upon the height of the plant canopy (PH; m) as follows:

$$KE (LD) = (15.8*PH^{0.5})-5.87 \quad (4.6)$$

When the above equation yields a negative value, the energy of the leaf drainage is assumed to be zero.

The total energy of the effective rainfall (KE; J/m²) is obtained from:

$$KE=KE(DT)+KE(LD) \quad (4.7)$$

Table 4.1: Relationships between kinetic energy (KE; J m⁻² mm⁻¹) and rainfall intensity (I; mm/h)

Equation	Remarks
$KE=11.87 +8.73\log_{10} I$	Used as the basis for rating erosivity in the Universal Soil Loss Equation (Wischmeier and Smith, 1978); suitable for North America east of the Rocky Mountains
$KE= 8.95+8.44\log_{10} I$	Suitable for north-western Europe and similar climates
$KE= 9.81+11.25\log_{10} I$	Developed by Zanchi and Torri (1980) for central Italy; suitable for Mediterranean-type climates
$KE= 35.9(1-0.56e^{-0.034 I})$	Developed by Coutinho and Toma's (1995) in Portugal; suitable for western Mediterranean
$KE= 29.8-(127.5/I)$	Developed by Hudson (1965) in Zimbabwe; use for tropical climates
$KE= 9.81+10.60\log_{10} I$	Developed by Onaga <i>et al.</i> (1998) for Okinawa, Japan; use for eastern Asia
$KE= 29.0(1-0.6e^{-0.04 I})$	Developed by Rosewell (1986) for New South Wales, Australia; use for temperate southern hemisphere climates

where available, other locally derived equations may be used in preference to the above.

4.3.1.2 Estimation of runoff

The procedure for estimating the annual runoff (Q; mm) remains unchanged. It is based on the method proposed by Kirkby (1976) which assumes that runoff occurs when the daily rainfall exceeds the soil moisture storage capacity (R; mm) and that daily rainfall amounts approximate an exponential frequency distribution. The annual runoff is obtained from:

$$Q=R*\exp (-R_c/R_o) \quad (4.8)$$

where R_o = the mean rain per rain day (mm). It is calculated by using number of rainy days in a year. The soil moisture storage capacity is estimated from:

$$R_c=1000*MS*BD*EHD*(E_t/E_o) \quad (4.9)$$

where MS = the soil moisture content at field capacity (% w/w), BD = the bulk density of the soil (Mg/m^3), EHD = the effective hydrological depth of the soil (m) and E_t / E_o = the ratio of the actual to potential evapotranspiration. The term, EHD, replaces the rooting depth (RD) used in the original model and indicates the depth of soil within which the moisture storage capacity controls the generation of runoff. It is a function of the plant cover, which influences the depth and density of roots, and, in some instances, the effective soil depth, for example on soils shallower than 0.1m or where a surface seal or crust has formed. Table 4.2 gives some guide values for EHD for use with the revised MMF model. At present, the effect of different types of tillage practice on EHD has not been evaluated. It is recommended that tillage be accounted for by adjusting the C factor value in the equation for transport capacity.

4.3.2 Sediment Phase

4.3.2.1 Soil particle detachment by raindrop impact

In the revised MMF model, rainfall interception is allowed for in the estimation of rainfall energy. It is therefore removed from the equation used to describe soil particle

Table 4.2: Recommended values for Effective Hydrological Depth (EHD)

Condition	EHD (m)
Bare soil without surface crust; no impermeable barrier in top 0.2 m	0.09
Bare shallow soils on steep slopes; crusted soils	0.05
Row crops (e.g. wheat, barley, maize, beans, rice)	0.12
Row crops intercropped with legumes/grasses	0.15
Mature forest, dense secondary forest	0.20
Rubber, oil palm	0.15
Cocoa, coffee	0.12
Banana	0.18
Savanna/prairie grass	0.14
Cultivated grass	0.12
Cotton	0.10
Groundnut	0.12

where terracing is used, add 0.01 to EHD to take account of the resulting increase in water storage

Source: Morgan, 2001.

detachment by raindrop impact. In the sediment phase the soil particle detachment by raindrop impact and runoff is calculated. Table 4.3 gives the values to be adopted for the soil parameters. The transport capacity of runoff is also calculated. Soil particle detachment by raindrop impact (F ; kg/m^2), is calculated as follows:

$$F = K * KE * 10^{-3} \quad (4.10)$$

where K is the erodibility of the soil (g/J) and KE is total energy of the effective rainfall (KE ; J/m^2).

4.3.2.2 Soil particle detachment by runoff

The revised model includes a new component to estimate the detachment of soil particles by runoff. This is considered as a function of runoff (Q), slope steepness (S) and the resistance of the soil (Z). The detachment by runoff (H ; kg/m^2) is estimated from:

Table 4.3: Guide values for soil parameters

Soil type	Moisture content (MS) (%)	Bulk Density (BD) (Mg/m ³)	Soil detachability index (K) (g/J)	Cohesion of surface (COH) (kpa)
Sand	0.08	1.5	1.2	2
Loamy sand	–	–	0.3	2
Sandy loam	0.28	1.2	0.7	2
Loam	0.20	1.3	0.8	3
Silt	–	–	1.0	–
Silt loam	0.25	1.3	0.9	3
Sandy clay loam	–	–	0.1	3
Clay loam	0.40	1.3	0.7	10
Silty clay loam	–	–	0.8	9
Sandy clay	–	–	0.3	–
Silty clay	0.30	–	0.5	10
Clay	0.45	1.1	0.05	12

Source: Morgan, 2001.

$$H=Z*Q^{1.5}\sin S*(1-GC)*10^{-3} \quad (4.11)$$

where GC = percentage ground cover. The equation assumes that soil particle detachment by runoff occurs only where the soil is not protected by ground cover. As a first approximation, this seems reasonable since, where a vegetation cover is present, the shear velocity of the flow is imparted to the plants and not to the soil.

For loose, non-cohesive soils, Z = 1.0, which emphasized the cohesion of the soil (COH: kpa) as an important component of its resistance to erosion:

$$Z=1/(0.5*COH) \quad (4.12)$$

4.3.2.3 Transport capacity of runoff

The method for estimating transport capacity of the runoff (TC; kg/m²) remains unchanged from that used in the original version of the model and is calculated as follows:

$$TC=C*Q^2\sin S*10^{-3} \quad (4.13)$$

where C is the crop or plant cover factor, taken as equal to the product of the C and P factors in the Universal Soil Loss Equation, and S is the slope gradient in degrees. The C factor can be adjusted to take account of different tillage practices and levels of crop residue retention.

The complete flowchart of the methodology of the model is given in Fig 4.1.

4.4 THE NUCLEAR TECHNIQUES

The existing methods for soil erosion assessment can be grouped into two main categories: erosion modelling and prediction methods and erosion measurement methods. In all cases, there is a need for direct measurement of soil erosion, which can be done using erosion plots, and surveying methods. The choice of one or another method will basically depend on the objectives of the study and the availability of resources (Elliot *et al.*, 1991). Existing classical techniques such as erosion plots and surveying methods for monitoring soil erosion are capable of meeting some of these requirements but they possess a number of important limitations in terms of the representativeness of the data obtained, their spatial resolution and potential to provide information on long-term rates of soil erosion and associated spatial patterns over extended areas and the costs involved (Loughran, 1989).

In addition, advances in the use of distributed numerical models and the application of GIS and geostatistics to erosion modeling have highlighted the need for spatially distributed data representing the spatial variability of soil erosion and deposition rates within the landscape, in response to the local topography and land use/management (Walling, 2001).

Due to the problems associated with conventional approaches to soil erosion

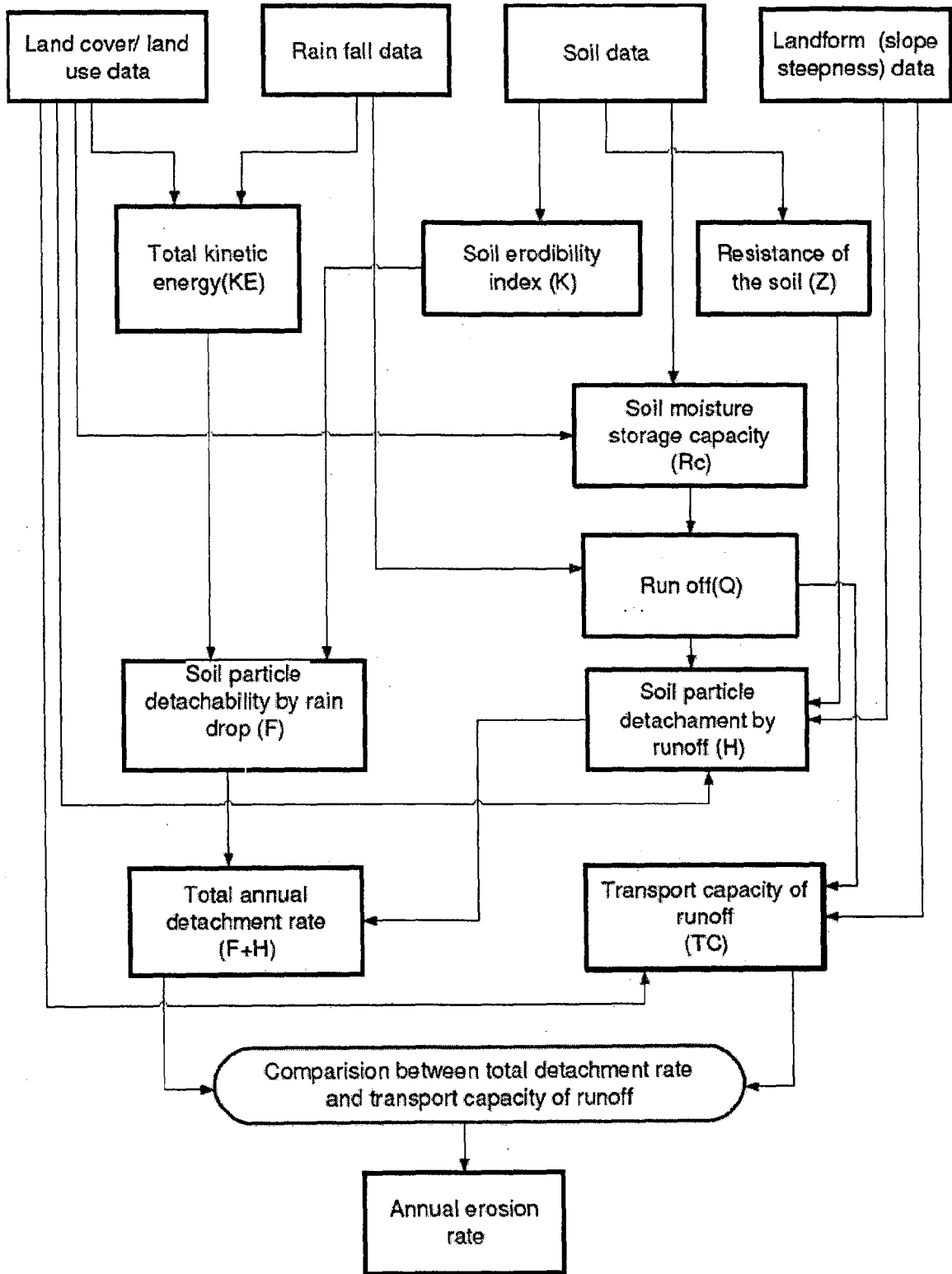


Fig 4.1: Flow chart for the revised MMF method of predicting soil loss

assessment and the uncertainties introduced by prediction equations and models in many areas of the world, there has been a quest for alternative techniques for soil erosion assessment to complement existing methods and to meet new requirements. This has directed attention to the use of radionuclides as tracers, as an alternative approach for documenting soil loss rates without the need for costly and time-consuming long-term monitoring programmes. (Walling and Quine, 1995). The fallout nuclides Caesium-137 (^{137}Cs), Beryllium-7 (^7Be) and Lead-210 and ($^{210}\text{Pbex}$) are used popularly for soil erosion studies.

4.4.1 The ^{137}Cs Dating Technique

The artificial radionuclide ^{137}Cs (half-life: 30.2 years) was introduced into the environment by the atmospheric testing of thermonuclear weapons during a period extending from the mid-1950s to the mid-1970s. The use of ^{137}Cs measurements to assess medium-term (~40 years) rates of soil erosion and redistribution in the study area involve

- (i) Reconnaissance soil sampling to confirm the viability of the approach.
- (ii) Sampling of reference locations to establish the reference inventory.
- (iii) Comprehensive soil sampling to document the spatial variation of soil redistribution processes within the study catchment.
- (iv) Estimation of erosion and sedimentation rates by comparing the ^{137}Cs inventories measured for individual sampling points with the reference inventory, using calibration models relating the percentage loss or gain in the inventories to rates of soil loss or deposition

This method is simpler compared to other radiodating techniques. However there are certain parts of the world where the low where the ^{137}Cs inventories are low. This

problem progresses due to the radioactive decay of the existing inventory, most of which was deposited as fallout ca. 40 years ago.

4.4.2 The ^7Be Dating Technique

Beryllium-7, with a half life period of 53 days, is a naturally occurring radionuclide, which is produced continuously in the upper atmosphere by cosmic ray spallation of nitrogen and oxygen and are attached to aerosols and associated with both wet and dry fallout. Accordingly, there is a strong correlation between rainfall and ^7Be delivery to the landscape, with the areal concentration of ^7Be (Bq m^{-2}) tending to increase with rainfall. Its penetration into soils tends to be shallow, declining exponentially with depth and generally contained within the top 20 mm of the profile. It reaches the surface mostly through thunderstorms that scub ^7Be from the stratosphere and is sorbed to particulates. The short-term erosion is generally measured with the ^7Be dating technique (Hawley *et al.*, 1986).

4.4.3 The ^{210}Pb Dating Technique

Lead-210 is a member of the U-238 decay series. Disintegration of the intermediate isotope ^{226}Ra (half-life 1622 years) yields the inert gas ^{226}Rn . This in turn decays (half-life 3.83 days) through a series of short-lived isotopes to ^{210}Pb . Radium-226 is supplied to the lake sediments as part of the particulate erosive input. The ^{210}Pb formed by the in situ decay of this radium is termed as the “supported ^{210}Pb ” and is normally assumed to be in radioactive equilibrium with the radium. In general, however, this equilibrium will be disturbed by the supply of ^{210}Pb from other sources. Lead-210 activity in excess of the supported activity is called the “excess” or “unsupported” ^{210}Pb . The principal source of unsupported ^{210}Pb is generally taken to be direct atmospheric fallout, although the importance of the other sources has not been extensively evaluated. Three

components or main pathways by which “excess ^{210}Pb ” or “unsupported ^{210}Pb ” reaches the sediments, have been identified, Oldfield and Appleby, 1984 as

1. Direct atmospheric fallout: A fraction of the radon atoms formed by ^{226}Ra decay in soils escape into the interstices and then diffuse through the soil into the atmosphere. The decay of radon in the atmosphere yields ^{210}Pb , which may be removed either by dry deposition or wet fallout. Lead-210 falling directly into the lakes is absorbed onto sediment particles and deposited on the bed of the lake.
2. Indirect atmospheric fallout: Atmospheric ^{210}Pb also reaches the lake indirectly via the lake catchment. Although the distinction may be less clear-cut in practice, it is convenient to separate a sub-component of this one, which is incorporated into the drainage network and flows quickly into the lake without being detained on solid terrestrial particles and another sub-component, which may have a long residence time in the catchment before being delivered to the lake in association with the erosive input of fine surface particulate to which it is attached.
3. Radon decay in the water column: Radon is delivered to the lake waters by diffusion from the underlying sediments, and by the decay of ^{226}Ra in the water column and inflowing streams. A part of the radon is lost by diffusion across the surface of the lake, and the remainder decays in the water column to ^{210}Pb .

Studies by Benninger *et al.*, (1975) on the fate of ^{210}Pb in the Susquehanna river system showed that dissolved ^{210}Pb in the river waters was quickly removed from solution by suspended particles. Further, stream borne particles carried away no more than 0.8% of the atmospheric flux of ^{210}Pb , which reached the catchment soils. Studies by Hammond and Fuller (1979) and Krishnaswamy and Lal (1978) about the production of ^{222}Rn and

^{210}Pb in the lake waters have indicated that this component too may be negligible, around second orders of magnitude lower than the atmospheric flux.

In dating by ^{210}Pb , it is the “unsupported” component only, which is used since once incorporated in the sediment, it decays exponentially with time in accordance with its half-life. The supported ^{210}Pb activity is estimated by assay of the ^{226}Ra . Although radon diffusion through the sediments may result in a small dis-equilibrium between the ^{226}Ra and supported ^{210}Pb near the sediment - water interface, provided that the total ^{210}Pb activity is well in excess of the ^{226}Ra activity, a correction for this will generally be negligible. Once the supported ^{210}Pb activity is known, the “unsupported ^{210}Pb ” can be determined by subtracting it from the total ^{210}Pb activity. (Fig 4.2). A typical plot of the beta spectrum with ^{210}Pb and ^{226}Ra peaks is given in Fig. 4.2 A. The plot of total of supported and unsupported ^{210}Pb is given in Fig. 4.2 B.

Ideally total ^{210}Pb and ^{226}Ra assays should be carried out on every sample. In practice, total ^{210}Pb determination may be scattered down a profile with intervening levels unanalyzed and the supported component is often estimated from only two or three ^{226}Ra determinations, from amalgamated samples, or simply from the total ^{210}Pb activity of sediments too old to give any significant disintegration from “unsupported ^{210}Pb ”.

In determining ^{210}Pb chronology, it is assumed that the “unsupported ^{210}Pb ”, once incorporated in a sediment layer, declines with time (age) in accordance with the ^{210}Pb radioactive decay law. The validity of the chronology will then rest on the accuracy with which the ^{210}Pb dating model represents the ^{210}Pb delivery mechanism outlined above. This assumes that the unsupported ^{210}Pb , once incorporated in the sediments, does not “migrate” or “diffuse” via the pore water of the sediment. Strong empirical evidence in support of this assumption is derived from the presence of sharply defined peaks and inflexions in some ^{210}Pb profiles, and from profiles considered here and elsewhere in

which the unsupported ^{210}Pb activity at independently dated depths is as expected from the operation of in situ radioactivity decay alone. There is evidence in some cases for redistribution of ^{210}Pb in association with sediment mixing or sediment re-suspension. Where this takes place, the decay law will operate only for sediment layers beneath the zone of mixing. There are different models that are used in different conditions. The details of these models are discussed in the subsequent sections. The procedure followed to use unsupported ^{210}Pb measurements for quantifying longer-term (~100 years) rates of

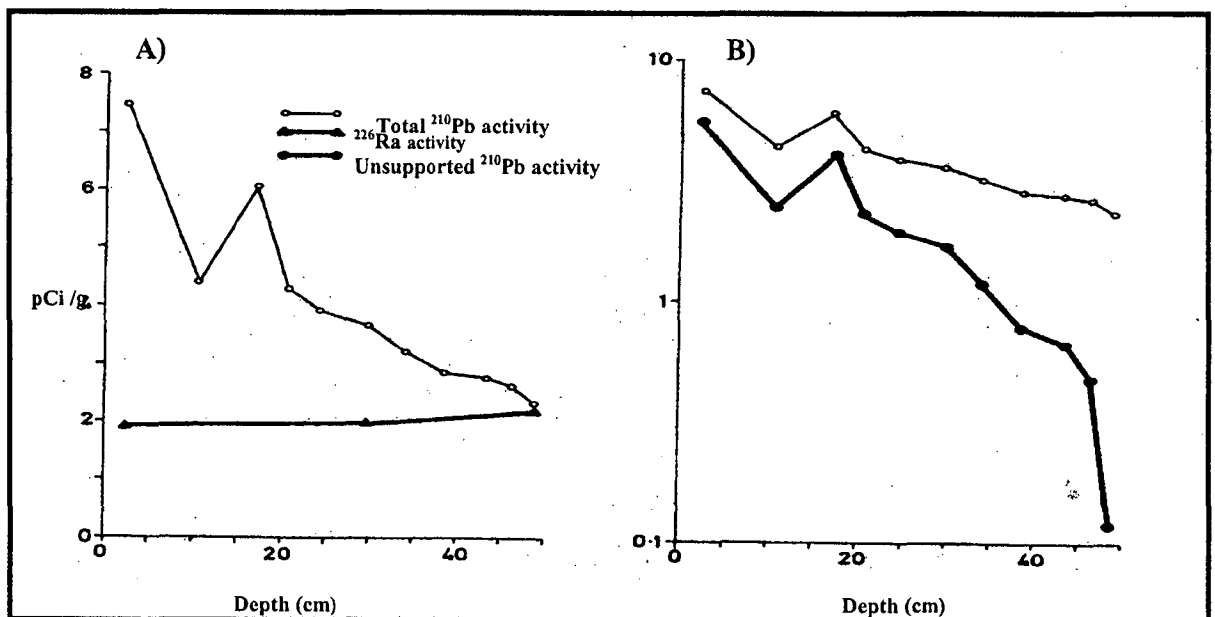


Fig 4.2. A) Total ^{210}Pb and ^{226}Ra activities in linear scale. B) Semi-log plot of variation of total and unsupported ^{210}Pb activities with depth. (After Oldfield and Appleby, 1984)

soil erosion redistribution associated with cultivated and uncultivated land within the study area involved the following elements:

- Reconnaissance soil coring to confirm the viability of the approach (i.e. unsupported ^{210}Pb activities and inventories of sufficient magnitude) and the

validity of the assumptions (e.g. surface adsorption confirmed by exponential depth distributions in undisturbed soils).

- Collection of soil cores from an undisturbed location with minimal slope and no evidence of erosion or deposition to establish the unsupported ^{210}Pb reference inventory.
- Collection of soil cores to document the spatial variation of unsupported ^{210}Pb inventories within cultivated and uncultivated land in the communal and commercial sectors.
- Derivation of estimates of erosion and deposition rates for the sampling points by comparing their measured unsupported ^{210}Pb inventories with the local reference inventory and using a theoretical conversion model to convert the values for the percentage decrease or increase in the inventory to equivalent estimates of the erosion or deposition rate. The elements are shown in Fig. 4.3.

4.4.4 Measurement of ^{210}Pb concentration in sediment samples

The basic radionuclide decay data pertaining to the isotopes of interest in Uranium series that are pertinent to the ^{210}Pb dating techniques are given in the Table 4.4.

Table 4.4: The basic radionuclide decay data of isotopes of general interest

Isotope	Half-life	Decay mode	Energy (MeV)	%
^{226}Ra	1600y	α	5.684	94.5
		α	5.442	5.5
^{222}Rn	3.823d	α	5.486	100
^{210}Pb	21y	β	0.061	19.0
		β	0.015	81.0
		γ	0.046	4.0
^{210}Bi	5.01d	β	1.160	99.0
^{210}Po	138.4d	α	5.035	100

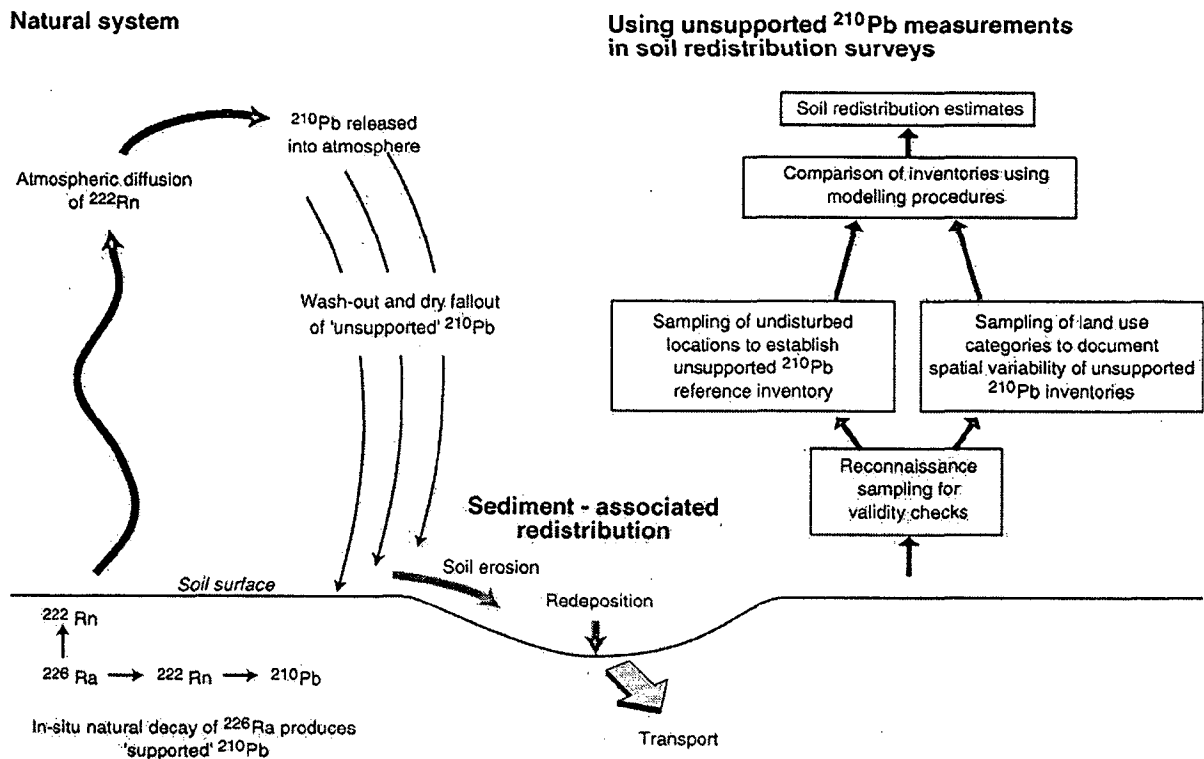


Fig 4.3: Use of unsupported ²¹⁰Pb measurements to estimate soil erosion and deposition rates (Walling *et al.*, 2003)

From the table it is seen that ²¹⁰Pb may be measured directly by gamma counting using a gamma counter or through its daughter product ²¹⁰Bi using a liquid scintillation counter or through its granddaughter product ²¹⁰Po using an alpha spectrometer. The most preferred method to measure ²¹⁰Pb activity through ²¹⁰Po by alpha spectrometry has been used for the present study. However other methods are also presented in brief.

4.4.5 Lead-210 separation from sediment samples

Lead-210 is a low energy beta emitter with a low transformation yield for the gamma transition (about 4%) at energy of 46.52 KeV. ²¹⁰Pb decays to a high energy beta emitter Bismuth-210 (half life 5.012 d) followed by an alpha emitter Po-210 (half-life 138.38 days). If Pb-210 is counted directly by gamma spectrometry, the time need for sample preparation is short but the required detection limit is too high for most environmental samples. Therefore, after radiochemical separation of ²¹⁰Pb fraction, the

beta radiation of Bi-210 is detected after a build-up of at least 30 days. The waiting time increases substantially if one is interested in using the more sensitive alpha spectrometry for Po-210.

The Quantulus Liquid Scintillation System: This system adopts the Bi-210 daughter isotope method. The detailed procedure is outlined below:

- i) Ash a small quantity (usually 1g) of dried sediment at 550°C in the muffle furnace (as described above).
- ii) Leach the ashed sample with 0.8M HBr. This is done by taking the sediment sample in a Teflon beaker and adding 10 ml of 0.8M HBr, cover with a Teflon lid. Leave it overnight. Dry down the sample solution completely by placing it in a hotplate at 110°C. Elute the sample with 1ml of 0.8M HBr and 1 ml carrier solution of lead (10ppm).
- iii) The above solution is subjected to anionic exchange to separate Pb and Bi. This is a time consuming and sensitive procedure. The steps to be followed in the anionic exchange column are given below:

Description of Anion Exchange Columns:

The column is a very simple one with a sintered disc fused near the bottom above the stop-valve (Fig 4.4). The column is filled with DOWEX resin up to 10cc volume. The following steps are involved in lead separation.

a. Equilibration of column (Column preparation)

- i) Pass 40ml Double distilled water through column three times.
- ii) Pass 40ml 1N HCl through column three times.
- iii) Pass 40ml Double distilled water through column.
- iv) Pass 40 ml 6.2N HCl through column three times.

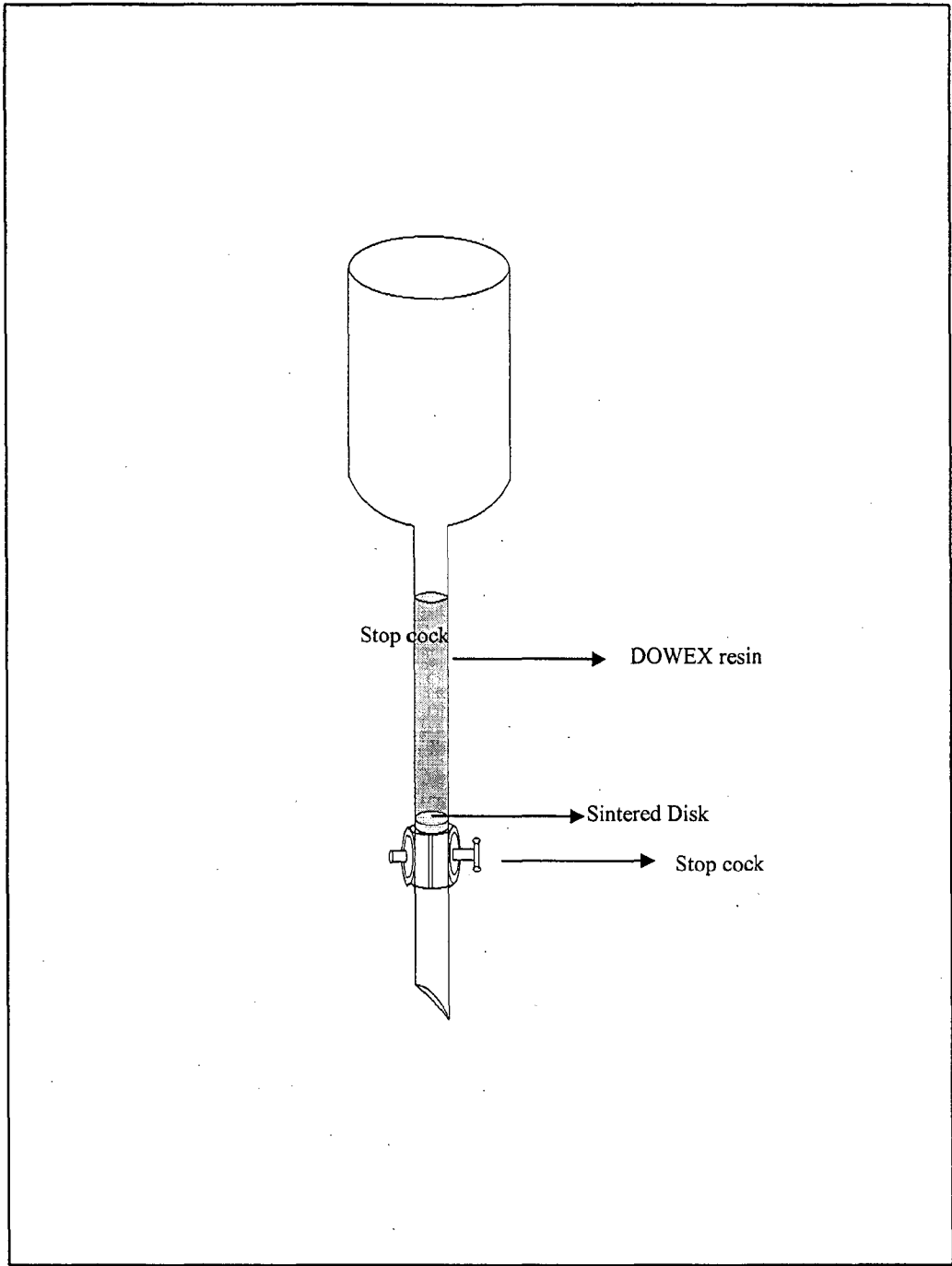


Fig 4.4: Sketch of the ion exchange column for extracting lead from the sediment sample

- v) Pass 40 ml Double distilled water through column.

Now the column is ready to be used for the lead separation.

b. First step of lead separation through the column

- i) Pass 40 ml 0.8M HBr through column.
- ii) Load the sample (in 1 ml 0.8M HBr and 1 ml Pb carrier solution).
- iii) Pass 40 ml 0.8M HBr through column two times.
- iv) Pass 10 ml 6.2N HCl through column five times
- v) Collect the solution in a clean Teflon beaker. Add few drops of H_3PO_4 in beaker.
Dry down the sample solution completely by placing it in a hotplate at 90°C .
- vi) Add 2 ml of 3N HCl.

c. Re-equilibration of the column.

- i) Pass 40ml double distilled water through column three times.
- ii) Pass 40ml 1N HCl through column three times.
- iii) Pass 40ml Double distilled water through column.
- iv) Pass 40 ml 6.2N HCl through column three times.
- v) Pass 40 ml double distilled water through column.

Second step of lead separation

- i) Pass 40 ml 3N HCl through column.
- ii) Load the final solution of Step I in the column.
- iii) Pass 10 ml 3N HCl through the column two times.
- iv) Pass 40 ml 6.2N HCl through the column.
- v) Collect the solution in a clean Teflon beaker,

- vi) Add few drops of H_3PO_4 .
- vii) Dry down the sample solution completely by using a hotplate at $90^\circ C$.
- viii) Add 7 ml 0.5N HCl in Teflon beaker and
- ix) Transfer the final solution in to clean plastic vials.

4.4.6 Lead-210 measurement as ^{210}Bi using Liquid Scintillation Counter

The final solution collected in plastic vials, as stated above, is subjected to β -counting in Ultra Low Level Liquid Scintillation Counter (Quantulus) after a waiting period of approximately 30 days. This waiting period is for establishment of radioactive equilibrium between ^{210}Pb and ^{210}Bi . Usually 6 half-lives are sufficient for this purpose (the half-life of ^{210}Bi is about 5 days). The sample is transferred into a scintillation grade vial of 20ml capacity. After this 10ml of a special cocktail called "UltimaGold AB" is added into the vial containing the sample. The UltimaGold AB cocktail is highly useful for alpha and beta decay event discrimination in samples. The vial is then placed in the Quantulus counting chamber.

A special counting protocol is used for the purpose. The MCA is set to the in-built α/β counting setup. Spectra 11 records the pure beta events and spectra 12 records the pure alpha events, spectra 21 records the guard anti-coincidence events and the spectra 22 records the guard coincident events. The Pulse Shape Analyser is set to 100%. The configuration is set in such a way that only spectra 11 and 12 are saved in the registry. The coincidence bias is set to low.

In a single batch of counting in Quantulus, at least two standard and two background samples are added in addition to the samples to be analysed. The standard that is used presently was purchased from IAEA, Vienna, Austria. The standard is known as IAEA-300 Baltic Sea sediment. The ^{210}Pb activity in the IAEA-300 standard is about 366mBq/g as on 01.01.1991. The standard is also subjected to the ashing and column

separation procedure, therefore, the overall efficiency in lead separation and counting procedures may be evaluated from the activity measured in the counter (CPM) and the known activity as reported in the Activity Information Report of the IAEA-300. Similar to the procedures followed in the low level tritium measurement in Quantulus, the procedure to be adopted for ^{210}Pb also makes use of the higher Figure of Merit technique to evaluate the appropriate windows setting.

The activity measured in CPM is then converted to mBq/g units using the overall efficiency and then corrected for density of the corresponding sediment sample. Once the ^{210}Pb activity in each sample of a sediment core is measured, the data is plotted against the depth of the sample, in a semi-logarithmic paper. The activity of ^{210}Bi is converted into ^{210}Pb using the equation $A_1\lambda_1=A_2\lambda_2$ where A_1 and A_2 are the activities of ^{210}Bi and ^{210}Pb , while λ_1 and λ_2 are the decay constants of ^{210}Bi and ^{210}Pb respectively. The slope of the exponential fitting will give the ratio of radioactive decay constant of ^{210}Pb to the rate of sedimentation. The minimum activity measured in the lower parts of sediment core is considered as that due to supported fraction of ^{210}Pb . This value is then deducted from the total ^{210}Pb activity to evaluate the unsupported portion of ^{210}Pb activity. The slope of the best-fit curve for the unsupported ^{210}Pb activity versus depth gives the ratio of rate of sedimentation to the radioactive decay constant of ^{210}Pb . This is achieved by dividing the slope with the decay constant of ^{210}Pb (~ 0.031) and the result is expressed in cm/y units.

4.4.7 Lead-210 measurement by Gamma Spectrometry

The activity of ^{210}Pb may be directly measured by using the weak (4%) gamma emitted by ^{210}Pb . This method is unlike the previously described methods in that this uses the direct measurement procedures rather than daughter or granddaughter products. Further, this does not require separation or deposition steps that require yield estimations. By this method, one directly places sufficient quantity of the sediment sample in the HPGe

detector and counts the gamma activity of 46.52 keV energy. With proper calibration and longer counting time reasonably accurate measurements are possible by this method. However, due to larger background as noise is generated in the lower energy part of the spectrum, it is often difficult to get sufficiently large net-counts. Because of this reason very few laboratories opt for this method.

4.4.8 Lead-210 measurement by Alpha Spectrometry

This method involves digestion of the sample, spontaneous deposition on a silver planchet/copper disc and counting in the Alpha Spectrometer (Silicon surface barrier detector coupled with Multi Channel analyzer). The method uses the granddaughter product viz. ^{210}Po and a secular equilibrium is presumed for the purpose of ^{210}Pb dating. The procedure involved is described in detail in Chapter 5.

In the previous chapter, the two techniques for the assessment of soil erosion have been discussed in detail. The methodology adopted for the present work is described in the following sections. The soil erosion assessment has been done for each land use in the western part of the Loktak Lake catchment and then the soil erosion loss has been estimated in other watersheds. The software used and GIS database prepared are also presented in this chapter.

5.1 GIS DATABASE PREPARATION

The base map of the study area on a scale of 1:250,000 have been prepared from the Survey of India toposheets. The catchment boundary has been taken from Survey of India toposheets at a scale of 1:250,000. The analog maps have been converted to digital form through scanning. These digital data are then edited and converted to vector form using R2V software. The drainage map and boundary maps are then imported to Integrated Land and Water Information System (ILWIS) GIS Software. The watershed delineation has been done and two watersheds chosen for the present study are shown in Fig. 5.1.

Software Used

In the present study, two image processing and GIS softwares ILWIS (Integrated Land and Water Information System) and ERDAS (Earth Resources Data Analysis System) have been used for the preparation of the required database and for analysis of the

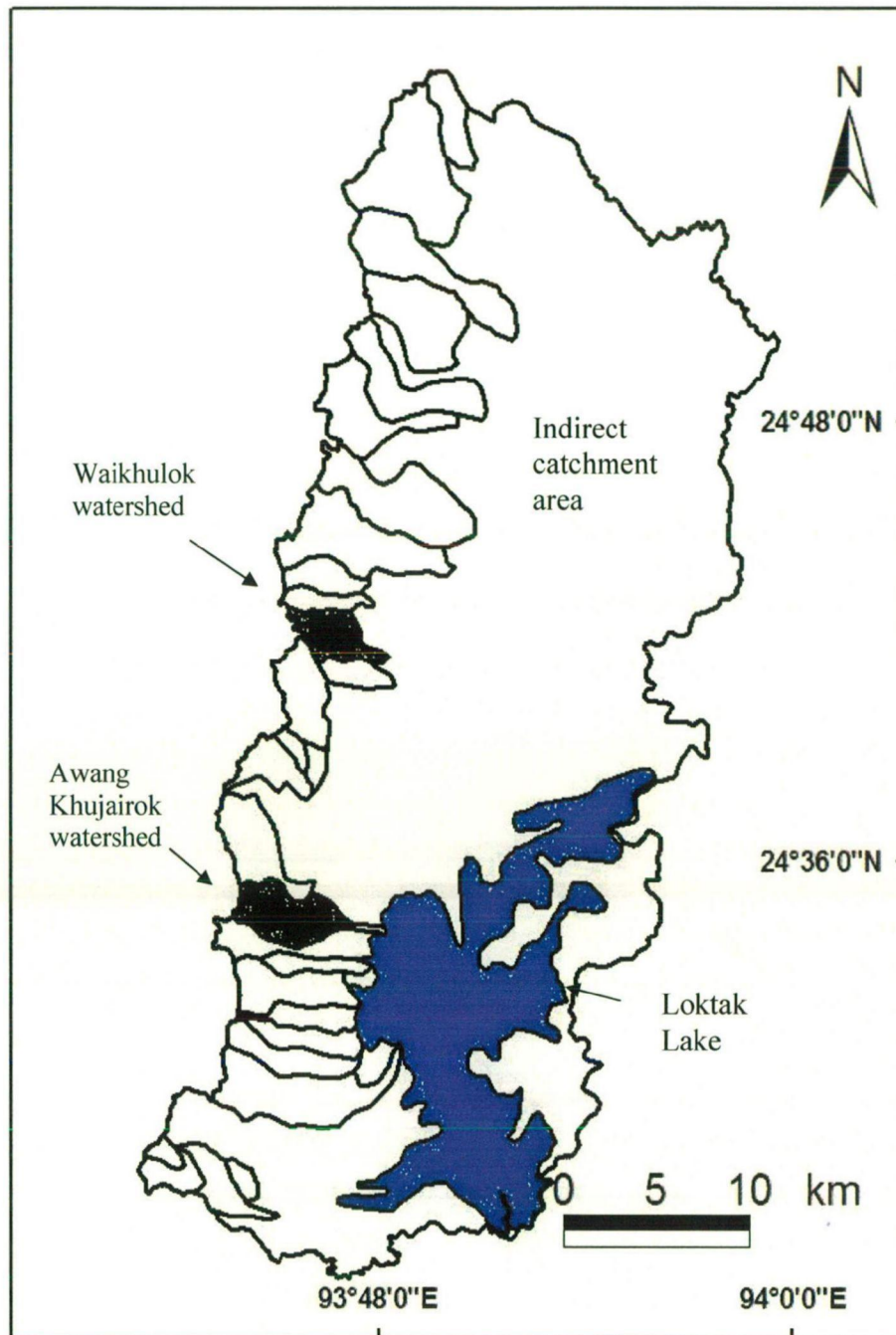


Fig. 5.1: Location map of the two watersheds

data. The ILWIS is a GIS package that integrates image processing and spatial analysis capabilities, tabular databases and conventional GIS characteristics. The ERDAS IMAGINE has been mainly used for image processing purpose.

ILWIS was developed at the Computer Center of International Institute of Aerospace Survey and Earth Sciences (ITC), Enschede, The Netherlands. ILWIS provides users with state of the art of data gathering, data input, data storage, data manipulation and analysis and data output capabilities, merging and integrating conventional GIS procedures with image processing capability and a relational database. The system is tailored for use with microcomputers and uses both vector and raster graphics data (Valenzuela, 1988). As a GIS and remote Sensing software package, ILWIS allows inputting, managing, analyzing and presenting geographical data. Information on spatial and temporal pattern and processes on earth surface can be generated from this data.

The methodology followed in this study includes preparation of base map involving map acquisition, conversion into digital form, polygonizing *segment* map and overlay operation. From the map prepared, modelling of soil loss in the watershed was done. In developing the model database, original source maps have been scanned and digitized by onscreen method, through a Raster to Vector Software package (R2V). First scanning of source map was done in Tag Image File (TIF) format and then digitized and saved as project file in '.shp' format.

Layers generated from this scanning procedure are boundary, land use, drainage and contour maps. At this stage, map referencing was done by putting control points. A digitizer records the location of spatial features by means of digitizer coordinates. To correctly register features in a map, the relationship between map and digitizer coordinates need to be established. A minimum of three control points and the corresponding map

coordinates should be specified by user in order to complete the transformation between digitizer and map coordinates.

Errors involved in digitization and editing the errors

The most important errors that may occur during digitization are

- dead end segment,
- segment being not connected to another segment,
- intersection without nodes,
- segment overlaying another segment without node,
- same segment being digitized twice,
- self overlap etc.

After the digitization of the segments, care was taken that they were error-free. The errors were checked and corrected by the facilities available in ILWIS under check segment vector-digitize module.

Polygonization

The specific polygons for any given polygon file were assigned with the identification name and color values. It is worth to note that polygon feature attribute labels are normally entered only after the topology of the digitized data has been checked and corrected if necessary. In GIS package used program facilities are also available for calculation of perimeter and area of each polygon through *histogram* function in ILWIS.

Coordinate System and Georeferences

A coordinate system defines the possible XY – coordinate or Lat-Long coordinates that should be used in maps and thus stores information on the kind of coordinates which are used in maps. A coordinate system may have information on the map's projection, ellipsoid and datum.

Georeferencing is needed for raster maps and uses a user specified coordinate system. A georeference is a service object, which stores the relation between the rows and columns in raster maps and ground coordinates. Description Coordinate System and Georeference of study is:

Coordinate System Projection "Cat"

Projection : Polyconic

Datum : Everest 1969

Ellipsoid : Everest 1969

Ellipsoid Parameter:

a = 6378160.000

1/f = 298.247.000.000

False Easting = 5 0000.000000

False Northing = 0.000000

Central Meridian : 93° 50' 0.12" E

Central Parallel : 24° 42' 6.22" N

Vector to Raster Conversion (Rasterization)

Since most of the analysis and overlay operations were easily and efficiently implemented in the raster model, all maps encoded in vector structure (both in polygon and segment) were converted into raster (Rasterization). Boundary and land use maps which were already in polygon form were rasterized through polygon to raster module.

5.1.1 Digital Elevation Model

In this study, digital elevation model of the study area was extracted from the global DEM. The Shuttle Radar Topography Mission (SRTM) obtains elevation data on a near-global scale to generate the most complete high-resolution digital topographic database of Earth. SRTM consisted of a specially modified radar system that flew on board the Space Shuttle Endeavour during an 11-day mission in February of 2000. SRTM

is an international project spearheaded by the National Geospatial-Intelligence Agency (NGA) and the National Aeronautics and Space Administration (NASA). The SRTM is a joint project of NASA and the U.S. National Imagery and Mapping Agency (NIMA). Using C-band Spaceborne Imaging RADAR (SIR-C) and X-band Synthetic Aperture RADAR (X-SAR), SRTM collected data during the shuttle flight in February 2000. The SIR-C/X-SAR is a multifrequency, multipolarization imaging RADAR system, complemented by additional antennas located at the end of a 60 m long mast which deployed from the shuttle after reaching orbit. This configuration produced single-pass interferometry and during the mission SRTM imaged all of the Earth's land surface between 60 degrees north and 50 degrees south (Carabajal and Harding, 2004). In 2003, the National Aeronautics and Space Administration (NASA) released the Shuttle Radar Topography Mission (SRTM) dataset for some regions, with 3 arc-second resolution for the globe, and 1 arc-second for the United States. The vertical units represent elevation in meters above mean sea level. All elevations are in meters referenced to the WGS84 EGM96 Geoid (Büyüksalih and Jacobsen, 2006) and the horizontally geo-referenced to the WGS84 ellipsoid with the geographic projection of Projection: Geographic Ellipsoid and WGS 84 Datum: WGS 84.

The base map was prepared in compatibility with the LISS-III image and the SRTM data was resampled to LISS-III data. The DEM files have been mosaiced into a seamless global coverage and are available for download as 5° X 5° tiles, in geographic coordinate system-WGS84. These files are available for download in both Arc-Info ASCII format and as GeoTiff for easy use in most GIS and remote sensing software applications. The DEM pertaining to the study area is shown in Fig 5.2.

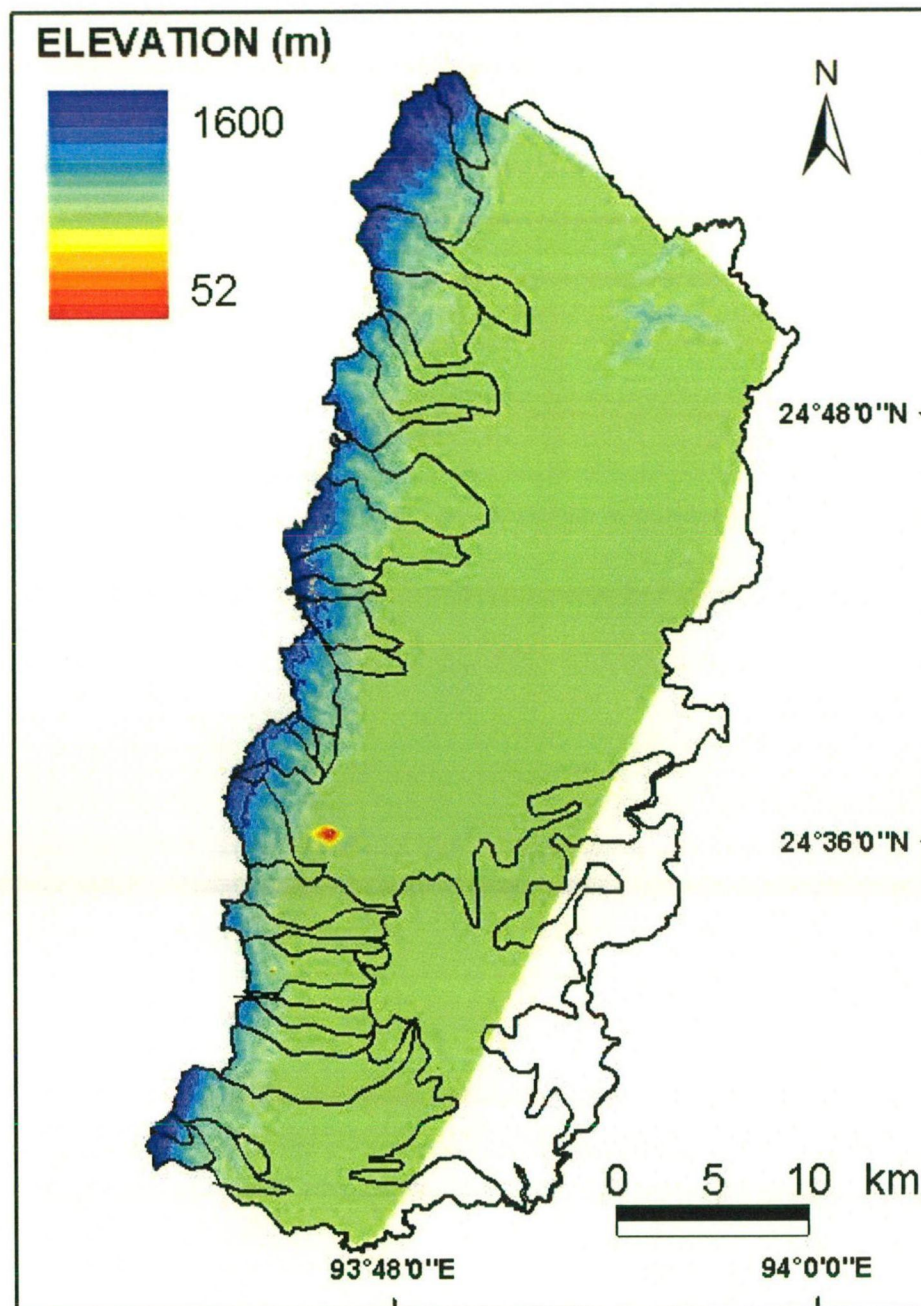


Fig. 5.2: Digital elevation model of the study area

5.1.2 Analysis of Remote Sensing Data

In the processing of remote sensing data, digital analysis of IRS LISS III was carried out for identifying the different land use. The following steps were followed in the analysis:

5.1.2.1 Import and visualization

The data of IRS-LISS III (Path: 113 and Row: 54-55) for the dates-10 April 2000, 21 Nov 2000, 6 Feb 2005 and 19 April 2005 were taken on CD-ROM media. The data were processed and analysed using the ERDAS/IMAGINE 8.5 software. The data can be loaded on the computer from the CD-ROM and it is imported into the ERDAS system. Each scene of LISS-III consists of approximately 2500 rows, 2520 columns and the information in three bands. Initially, a false colour composite (FCC) of 3, 2 and 1 band combination was prepared and visualized (Fig. 5.3 to Fig. 5.6). The base map prepared in ILWIS was also imported in the ERDAS for registration and masking.

5.1.2.2 Geometric registration

While using the temporal satellite data of the same area, it is required to register the images to base map. The images can be registered with this base map. For carrying out the registration, some clearly identifiable ground control points (GCP's) like crossing of the rivers, canals and sharp turns in the rivers etc. were located on both the images. Around ten to fifteen GCP's were sufficient for geo-referencing for the four images. A polynomial transformation of first order was performed and resampling was done using the nearest neighbour interpolation method. Now looking at the statistics, some points, which generate big errors were deleted and replaced by other points so as to obtain the

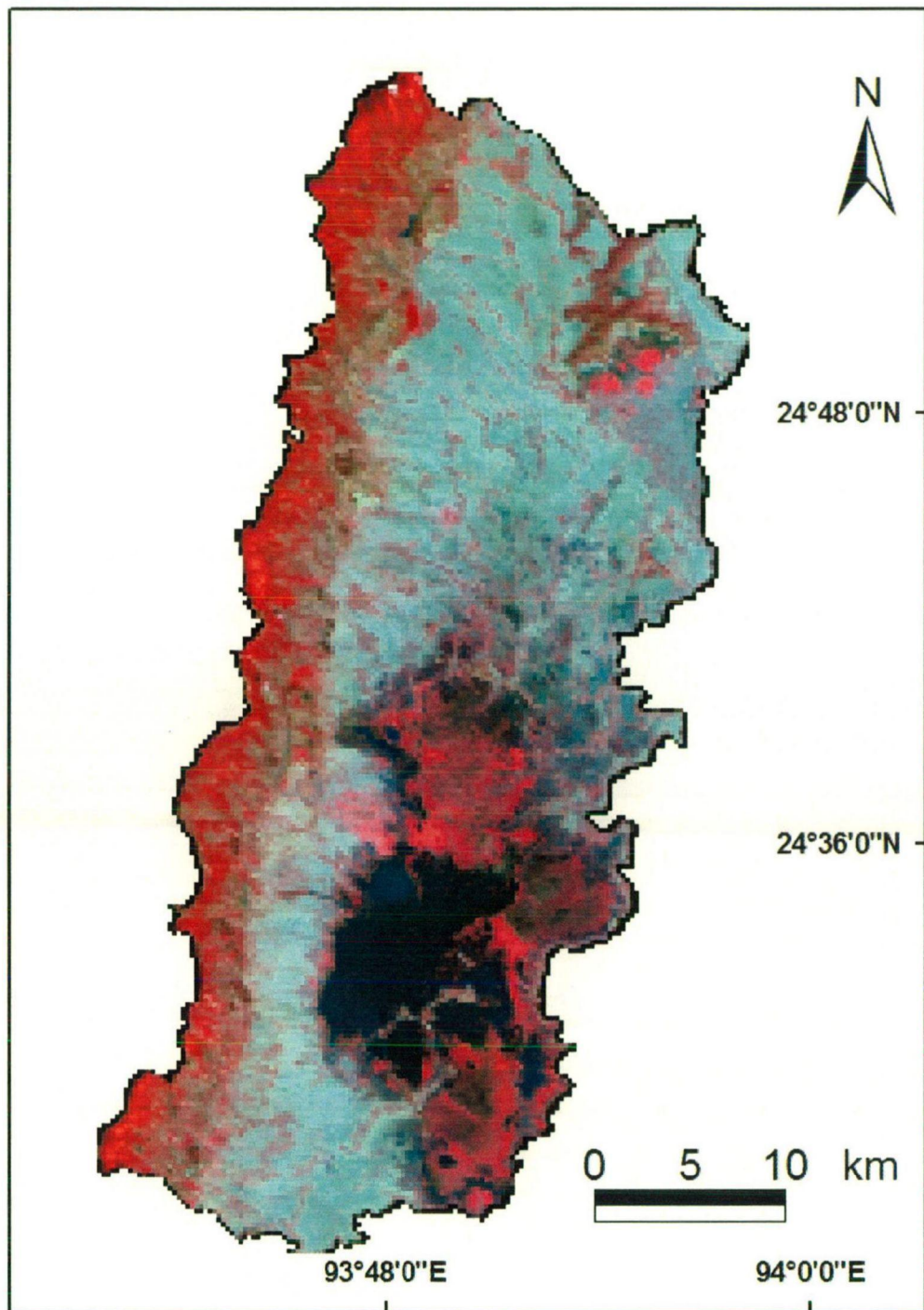


Fig. 5.3: False Colour Composite of 10 April 2000

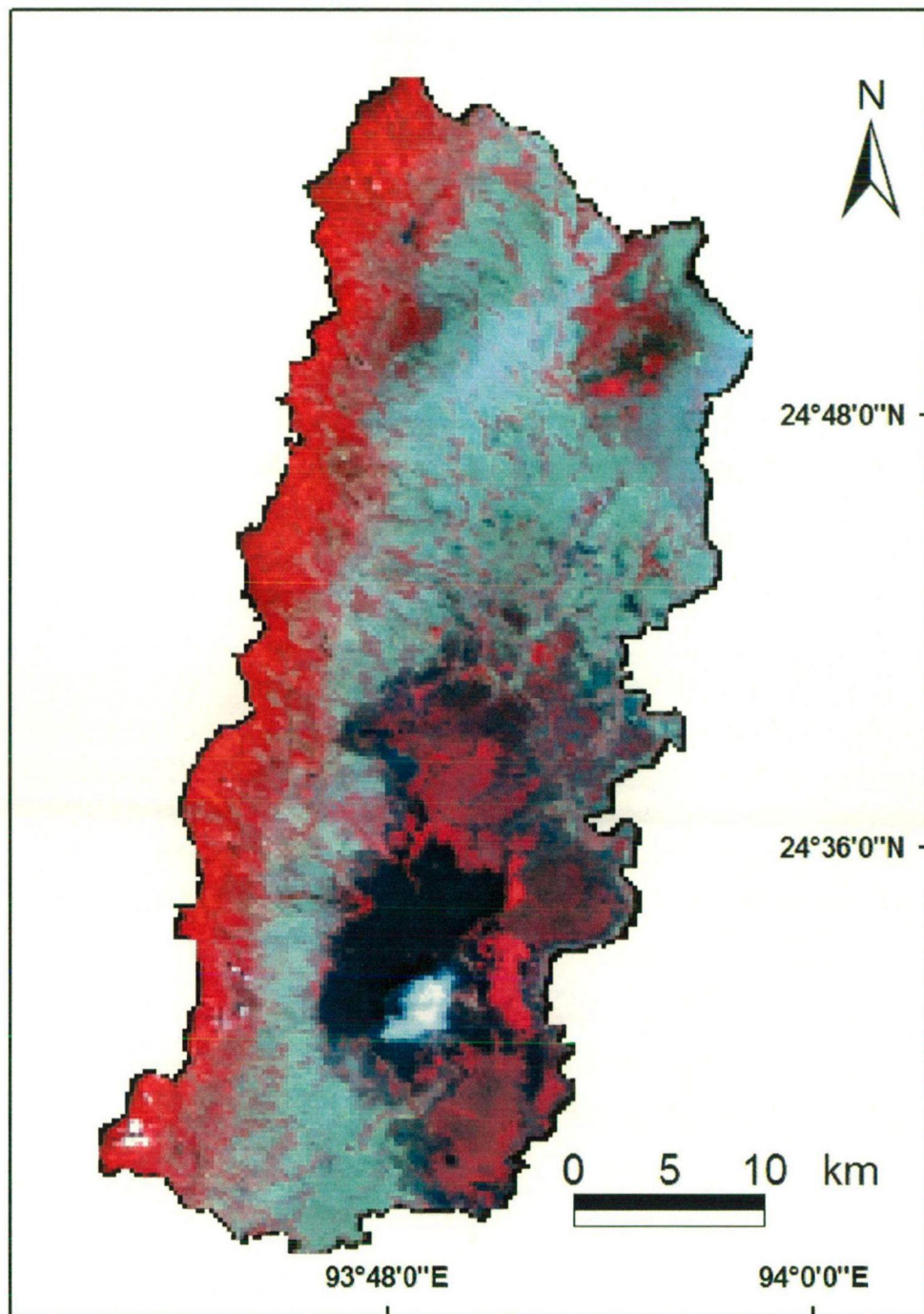


Fig. 5.4: False Colour Composite of 19 April 2005

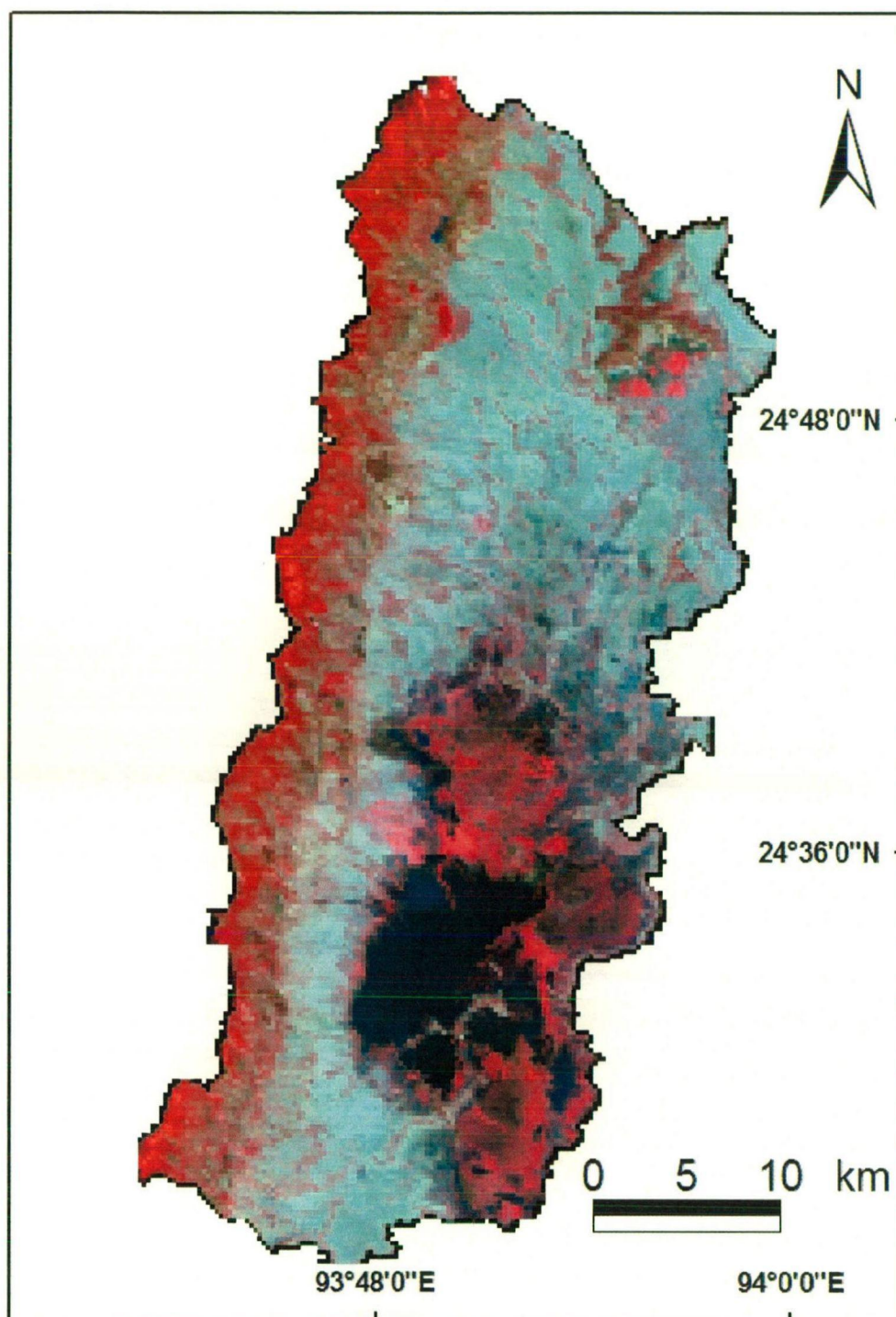


Fig. 5.5: False Colour Composite of 21 November 2000

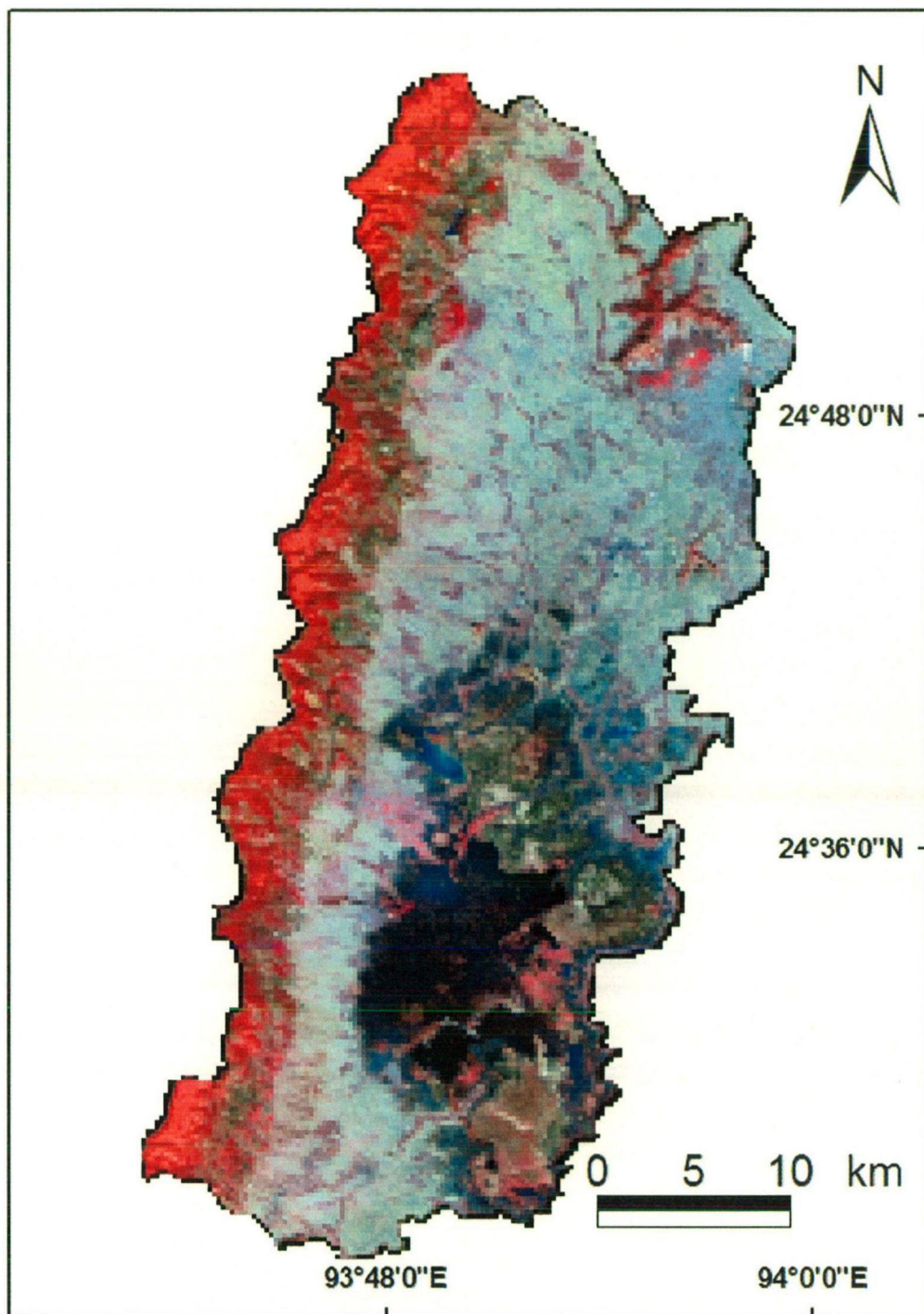


Fig. 5.6: False Colour Composite of 06 February 2005.

satisfactory registration. For any geographic area that uses multi date images, one image may be geo referenced to base map through image to map registration and other date images may be geo-referenced with respect to already rectified images. For rectification of one image, GCP's may be selected spread over the area of interest. The GCP's should be well distributed over the image. These should not be distributed over only one area since many well-defined points can be identified there.

5.1.2.3 Multispectral classification

Since the satellite data are available in digital numbers (DNs), they do not depict directly the normal data e.g. land use. The data are processed to extract information from them. To extract information from the remotely sensed data, multi spectral classification techniques are most often used.

In a multi-spectral classification, DN's in various electromagnetic bands are processed using techniques to obtain information from them. Two approaches namely supervised and unsupervised classification are used. The supervised classification approach is used where location of land use classes e.g. crops, urban, water, wetlands.etc. are known a priori.

5.1.2.4 Supervised classification

In supervised classification, the ground truth data are available priori. Ground truth information may be collected through field visit, collection of scientific reports, revenue statistics etc. Thus, known multi spectral statistics are used to classify the multi-spectral data to thematic classes.

The supervised classification technique requires the following steps:

- i) Collection of ground truth information
- ii) Selection of training samples.

- iii) Computation of multi spectral statistics for the training samples.
- iv) Classification of image pixels into one or other thematic classes.
- v) Evaluation of the classified results for error estimation.

To select training samples, polygons are created over the image. In general 20 or more pixels are taken for each class. The image data area created classified using any of the supervised classification algorithms namely paralleloiped or box, minimum (Euclidean) distance to mean, maximum likelihood etc. Parallelepiped classifier and minimum distance are computationally efficient. Maximum likelihood classifier provides better accuracy.

5.1.2.5 Unsupervised classification

The present catchment has a mixed type of land use and therefore supervised classification could not be applied very effectively. The unsupervised classification was performed and is explained below.

In a multi spectral image, each pixel has a spectral signature determined by the reflectance of that pixel in each of the spectral bands. The details of the classes depend on the spectral and spatial resolution characteristics of the imaging system. Unsupervised classification is a method in which the computer searches for natural groupings of similar pixels called clusters and determines the mean of the classes automatically (Jensen, 1996). The fewer the clusters, the more the pixels within each cluster will vary in terms of spectral signature and vice versa. The determination of the mean of the classes was done using the property of natural groupings of pixels in image space. The classes were assigned a theme based on the signature in the image of the class after the computer classification. Many classes were regrouped to single theme after the classification was done. The steps followed were given below:

- i) The initial mean for classes were supplied.
- ii) The classification i.e. ISODATA (Iterative Self Organizing Data analysis) classifier was used. The image was classified using this algorithm which required multiple iterations.
- iii) The classes were identified based on image signatures. Many classes were given single theme.

For this algorithm, the user inputs the number of cluster desired and a confidence threshold. Since this is an iterative classification algorithm, the computer builds clusters iteratively, in which parameters were given for terminating the iterations in the classification. In this process, with each new iteration, the clusters become more and more refined. These are a number of iterations or maximum percentage of pixels that remain unchanged. If either condition is met, the iterations are terminated. The iterations stop when the confidence level (or a maximum number of iterations specified by the user) is reached (Jensen, 1996).

Other parameters were also used that control the classification algorithm operation within iteration. These are minimum size of cluster, interval after which the cluster merging, mean, maximum clusters, maximum standard deviation for cluster, etc.

After the clusters were built, the land cover classes (Forest, barren land etc.,) were selected and each cluster was assigned to the appropriate class. Once all the clusters were assigned to a class, the image of clusters was recoded into the GIS layer, which displayed each land use cover class with a different colour.

In this study classification using ISODATA algorithm with 20 clusters and a 95% confidence threshold has been applied. The result was an image with 20 groups of pixels each represented by a different colour. Then each cluster was highlighted one at a time and assigned various classes by interpreting the original multispectral image.

The land use maps of the catchment (10 April 2000 and 19 April 2005) are presented in Fig. 5.7 and 5.8.

From the 10 April 2000 image, the land use classes derived were; 399 km² of barren land, 232 km² of dense forest, 172 km² of swampy land, 131 km² of medium forest, 111 km² of built-up land and 78 km² of water body (i.e. the lake).

The land use classes identified from the 19 April 2005 image were; 310 km² of barren land, 284 km² of dense forest, 175 km² of swampy land, 162 km² of medium forest, 116 km² of built-up land and 76 km² of water body. There has been a 2 % decrease in the water spread area in the 5-year span.

In the two watersheds, however, five distinct land use classes were identified namely agriculture, medium forest, dense forest, barren land and built-up land.

5.1.2.6 Accuracy assessment and report

Classifications derived from remotely sensed images are subject to error and uncertainty. In classifying an image, the spectral response of a pixel, representing a fixed area on the ground defined by the resolution of the sensor, is used to assign it to one of a number of classes using various classification techniques.

Accuracy assessment is an important final step of the classification process. Users accuracy gives an idea of what proportion of pixels assigned to a particular class were correctly assigned. Producers accuracy is a measure of how much of the land in each category was classified correctly.

The error matrix can be used to generate various statistics that characterize the accuracy of a classification technique. The goal is to quantitatively determine how effectively pixels were grouped into the correct land cover classes. The

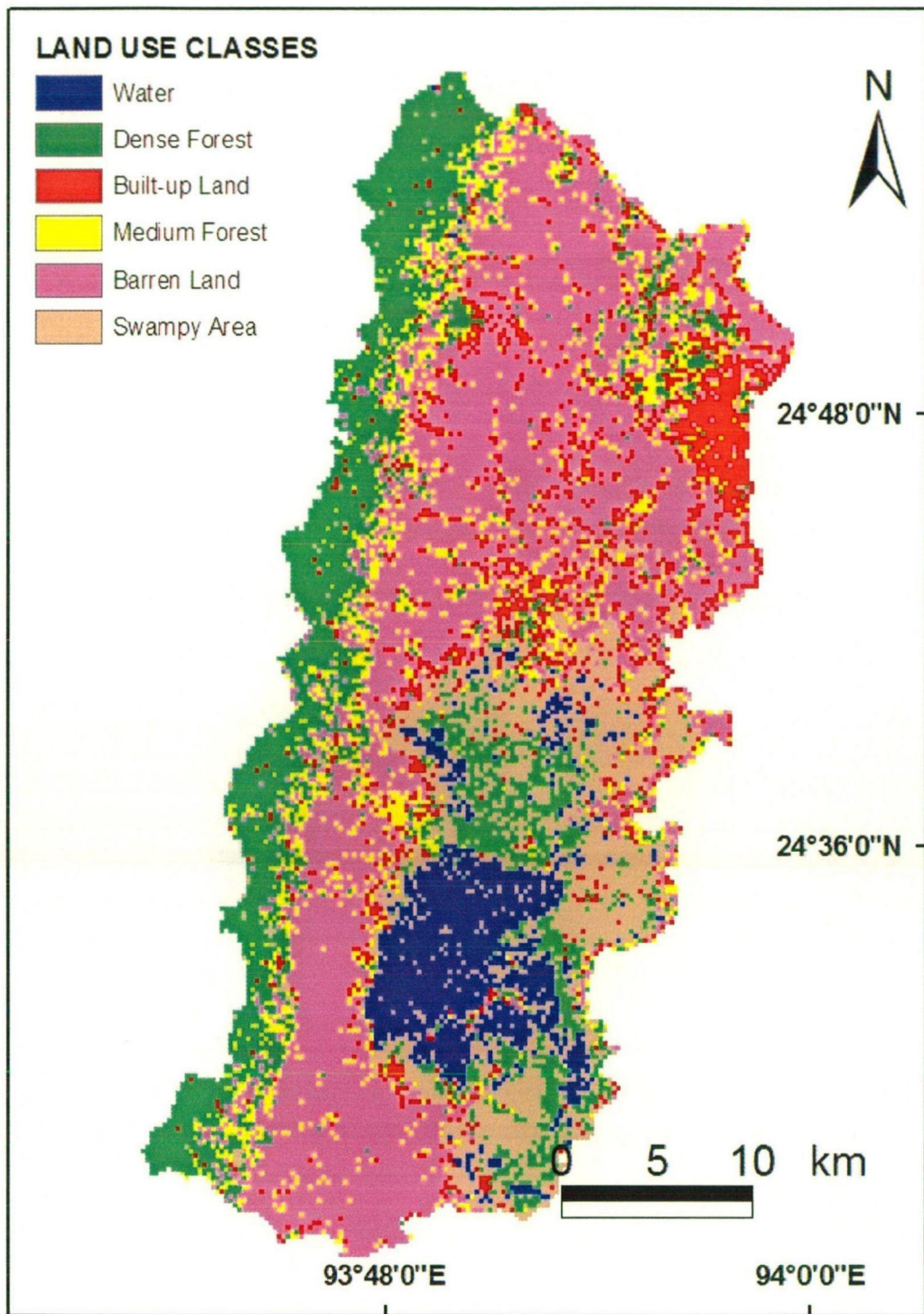


Fig. 5.7: Land use map of the study area (10 April 2009)

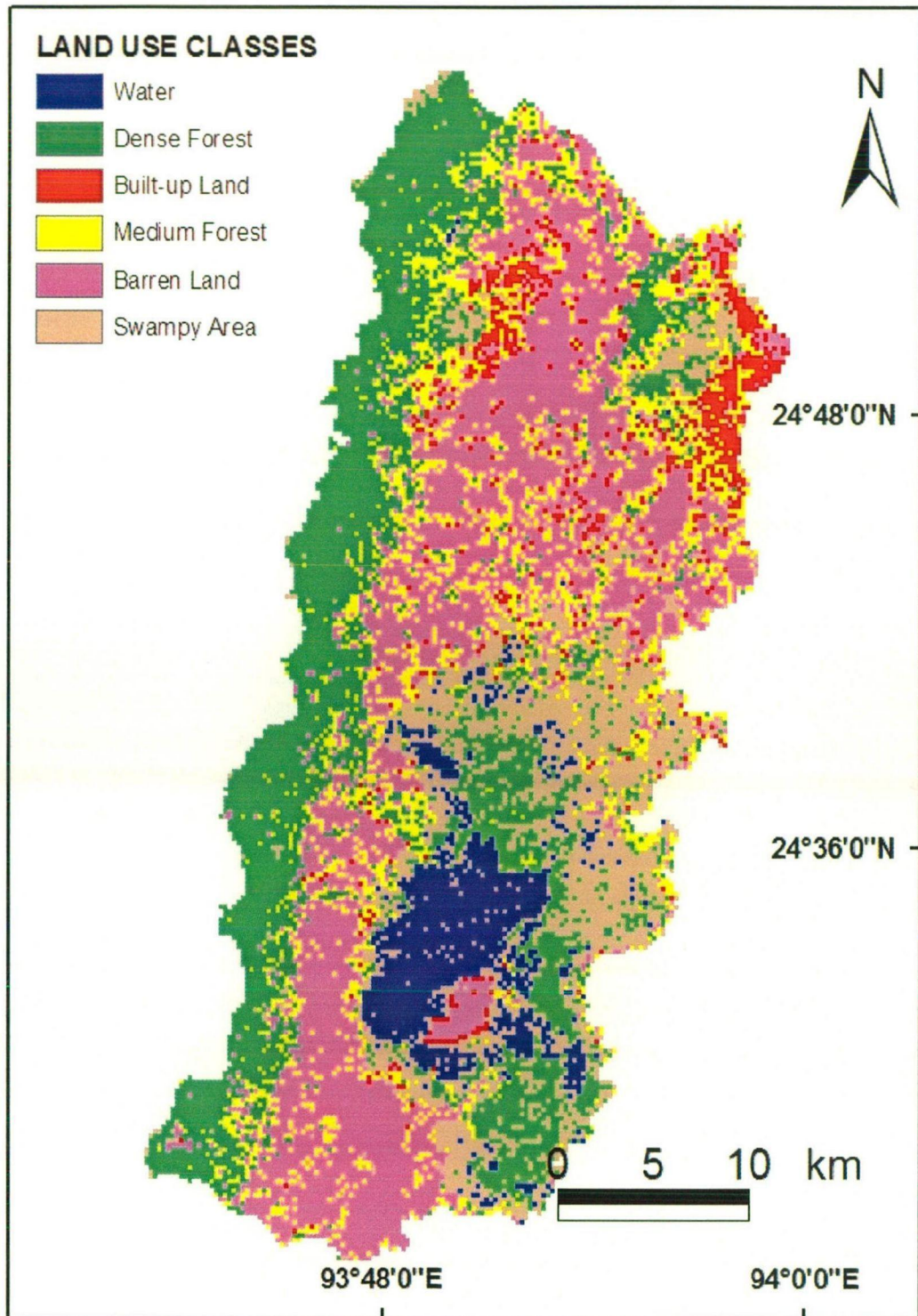


Fig. 5.8: Land use map of the study area (19 April 2005)

procedure is relatively simple. Pixels are randomly selected throughout the image using a specified random distribution method. Then the analyst uses the original image along with ancillary information such as areal photographs or direct field observation to determine the true land cover represented by each random pixel.

This ground truth is compared with classification map. If the ground truth and classification match, then the classification of that pixel is accurate. Given that enough random pixels are checked, the percentage of accurate pixels gives a fairly good estimate of the accuracy of the whole map. A more rigorous and complicated estimate of accuracy is given by the kappa statistics, which are obtained by a statistical formula that utilizes information in an error matrix. An error matrix is simply an array of numbers indicating how many pixels were associated with each class both in terms of the classification and the ground truth (Jensen, 1996). Statistics that can be generated from the error matrix include errors of omission (producer's error) and errors of commission (user's error). These are based on individual classes, dividing the number of pixels that are incorrectly classified by either the column or row totals, respectively.

An accuracy assessment of the classification map was performed in ERDAS, which generated the accuracy report. In the present study, 50 random points were selected.

The accuracy of classification is reported in two manners namely non site-specific and site-specific. In the former, usually high classification accuracy is reported. If the omission is equal to commission in the classification, even 100% accuracy may be reported. Thus another method, namely, error matrix, is a better method to express the accuracy of the classification. In error matrix, a table is prepared in matrix form in which columns represent the reference class and the rows represent the classification result. The diagonal represents the correctly classified pixels. The reference sites were selected through stratified random sampling to produce unbiased classification accuracy. The

reference information were collected at the time of the remotely sensed data acquisition, since the land use is a transient feature.

In this study, the accuracy assessment of classified maps have been performed and results are given in Table 5.1 (10 April 2000) and Table 5.2 (19 April 2005). In Table 5.1, out of the 50 points, 42 were correctly classified yielding a classification accuracy of 84 %. Similarly, in Table 5.2 the correctly classified points were 43 and the overall percentage accuracy was 86%.

5.1.2.7 Soil map

The soil map of the study area at a scale of 1:250,000 are procured from National Bureau of Soil Survey and Land Use Planning (NBSS & LUP) Nagpur. From this map, the boundaries of the study area was extracted. The U.S. Natural Resource Conservation Service (NRCS) classifies soils into four hydrologic groups depending on infiltration characteristics of the soil. NRCS Soil Survey Staff (1996) defines a hydrologic group as a group of soil having similar runoff potential under similar storm and soil cover conditions.

Soil properties which influence runoff potential are those that impact the minimum rate of infiltration for a bare soil after prolonged wetting and when not frozen. These properties are depth to seasonally high water table, saturated hydraulic conductivity and depth to a very slowly permeable layer. Soil may be placed in one of four groups A, B, C, and D, ranging from low runoff potential to high runoff potential groups.

5.2 THE MORGAN, MORGAN AND FINNEY (MMF) MODEL

As given in the earlier chapter, the MMF is an empirical model developed to estimate mean annual soil loss from field-sized areas on hill slopes. The model has been selected for its simplicity and flexibility. The modified MMF model separates the erosion process into a water phase and a sediment phase. The water phase determines the energy

Table 5.1: Classification accuracy assessment report for the FCC of 10th April 2000

Class Name	Reference Totals	Classified Totals	Number Correct	Producers Accuracy (%)	Users Accuracy (%)
Water	7	9	7	100.00	77.78
Dense forest	11	11	9	81.82	81.82
Built-up land	9	8	7	77.77	87.50
Medium forest	13	12	11	84.61	91.67
Barren land	2	3	2	100.00	66.67
Swampy area	8	7	6	75.00	85.71
Totals	50	50	42	-	-

Table 5.2: Classification accuracy assessment report for the FCC of 19th April 2005

Class Name	Reference Totals	Classified Totals	Number Correct	Producers Accuracy (%)	Users Accuracy (%)
Water	6	5	4	66.25	80.00
Dense forest	10	11	9	90.00	81.82
Built-up land	10	9	8	80.00	88.89
Medium forest	13	13	12	92.31	92.31
Barren land	2	3	2	100.00	66.67
Swampy area	9	9	8	88.89	88.89
Totals	50	50	43	-	-

of rainfall and the volume of runoff. The sediment phase computes rates of soil particle detachment by runoff and rainfall, along with the transporting capacity of runoff.

Available input data, DEM (resolution 25 m), a generalised soil map (scale 1:250,000), and satellite images (Landsat, grid resolution 25 m) have been used to obtain land cover information. The model calculates erosion and deposition at the grid level first. Subsequently, the mean erosion rate at subbasin level is obtained by calculating a mean of all grid values within a particular subbasin.

For the estimation of soil loss by Morgan approach, the various factor maps like kinetic energy of rainfall (E), percentage rainfall contributing to permanent interception and stream flow (A), land use have been generated to get final output maps like Rate of soil detachment by raindrop impact, F; Rate of soil detachment by runoff (H), Transport capacity of overland flow (G).

5.2.1 Collection of Input Data

Soil erodibility under various mapping units or landforms has been assessed by a number of simple field tests such as dry crumb test, manipulation test, rainfall acceptance test, pinhole test and shear vane test. From the results of the simple field tests, the availability of erodible material; shear strength of the topsoil; overland flow production and the inter-rill and rill erodibility were assessed. Finally by combining the results of inter rill and rill erodibility a qualitative erodibility class (K factor) was generated to parameterise the model.

The input parameters needed to run the revised version of the model are listed in Table 5.3. details of data input are described in this section.

Table 5.3: Input parameters for the revised MMF model adapted from Morgan, 2001

Factor	Parameter	Definition and remarks
Rainfall	R	Annual or mean annual rainfall (mm).
	R_n	Number of rainy days per year.
	I	Typical value for intensity of erosive rain (mm/h); use 10 for temperate climates, 25 for tropical climates and 30 for strongly seasonal climates (e.g. Mediterranean type and monsoon).
Soil	MS	Soil moisture content at field capacity or 1/3 bar tension (w/w).
	BD	Bulk density of the top soil layer (Mg/m^3).
	EHD	Effective hydrologic depth of soil (m); will depend on vegetation/ crop cover, presence or absence of surface crust, presence of impermeable layer within 0.15m of the surface.
	K	Soil detachability index (g/J) defined as the weight of soil detached from the soil mass per unit of rainfall energy.
	COH	Cohesion of the surface soil (kpa) as measured with a torvane under saturated conditions.
	Landform	S
Land cover	A	Proportion (between 0 and 1) of the rainfall intercepted by the vegetation or crop cover.
	E_t/E_o	Ratio of actual (E_t) to potential (E_o) evapotranspiration.
	C	Crop Cover Management factor; combines the C and P factors of the Universal Soil Loss Equation.
	CC	Percentage canopy cover, expressed as a proportion between 0 and 1.
	GC	Percentage ground cover, expressed as a proportion between 0 and 1.
	PH	Plant height (m), representing the height from which raindrops fall from the crop or vegetation cover to the ground surface.

Rainfall

For assessing soil erosion, rainfall intensity is very important since splash detachment is a function of rainfall energy, soil detachability and rainfall interception by crops. The rainfall energy is directly related to rainfall intensity (Wischmeier & Smith, 1978). Rainfall data, recorded during the last 7 years period (2000 to 2006) were collected from the meteorological station at the watershed (Plate 5.1 and 5.2).

The number of average rainy days in a year was found to be 163 days in the Awang Khujairok watershed and 132 days in the Waikhulok watershed. However, all the rains are not erosive since rain showers of less than 12.5 mm are assumed too small to have practical significance and are not considered erosive (Wischmeier and Smith 1978). Thus, the monthly-recorded rainfall was analysed to get the exact erosive rainy days.

Effective Rainfall (ER)

Effective rainfall also known as excess rainfall is the component of the storm hyetograph which is neither retained on the land surface nor which infiltrates into the soil. The effective rainfall produces overland flow that results in the direct runoff hydrograph from a sub-area of a catchment. The difference between the storm and the effective rainfall hyetographs is termed as the abstractions or rainfall losses. Abstractions are made up of one or more of the following three main components:

- i) interception by vegetation or tree canopy,
- ii) infiltration into the soil,
- iii) storage in surface depressions and hollows.

Rainfall Intensity (I)

The impact of raindrops on the soil surface can break down soil aggregates and



Plate 5.1: Collection of meteorological reading in the study area (Waikhulok waters



Plate 5.2: The meteorological station at the Awang Khujairok watershed

disperse the aggregate material. Lighter aggregate materials such as very fine sand, silt, clay and organic matter can be easily removed by the raindrop splash and runoff water; greater raindrop energy or runoff amounts might be required to move the larger sand and gravel particles.

Soil movement by rainfall (raindrop splash) is usually greatest and most noticeable during short-duration, high-intensity thunderstorms. Although the erosion caused by long-lasting and less-intense storms is not as spectacular or noticeable as that of produced during thunderstorms, the amount of soil loss can be significant, especially when compounded over time (Singh *et al.*, 1981).

In analysing the rainfall data, if the monthly rainfall amount divided by the rainy days exceeds 12.5 mm, then the rainfall was considered erosive and the number of erosive rainy days was considered. Therefore, it was found that the total amount of erosive rainy day and rainfall amount to be 68 days and 800 mm respectively. The rainfall intensity for the study area is taken as 1.38 cm/h. The effective rainfall values are given in Table 5.4.

Table 5.4: Effective rainfall (ER) of various land use patterns in Awang Khujairok watershed

Land use	ER (mm)	
	Awang Khujairok watershed	Waikhulok watershed
Paddy	168	157.5
Medium Forest	240	225
Dense forest	320	300
Barren land	168	168
Built-up	168	168

Abstraction (A)

Gross precipitation is either intercepted by canopy leaves, branches, and trunk or it falls directly to the ground without hitting the tree. This part of the intercepted rainfall is often called abstraction. Intercepted water is stored temporarily on canopy leaf and bark surfaces, eventually drips from leaf surfaces and flows down tree stem surfaces to the ground or it evaporates. Interception accounts for the sum of canopy surface water storage and evaporation. Interception loss accounts for the evaporation of water from canopy surfaces during the rainfall event and the evaporation of retained water on canopy surfaces after both canopy drip and stem flow cease. The total water balance on a canopy surface can be expressed by the following equation:

$$\text{Abstraction} = C + E = P - TH - F - D \quad (5.1)$$

where C is the canopy surface water storage (mm), which includes water storage on leaf and trunk surfaces; E is evaporation from canopy surfaces (mm), which includes evaporation from leaf, branches and trunk surfaces; P is gross precipitation (mm); TH is free throughfall (mm) (precipitation directly passing through the canopy); F is stem flow (mm); and D is water drip from leaves and branches (mm).

Slope (S)

As slope steepness increases, the runoff increases. The runoff then exerts more force on soil particles, breaking their bonds more readily and carrying them farther before deposition. The effect on potential soil loss on increase in slope gradient is magnified by the fact that soil loss is proportional to the square of the sine of the slope angle. Thus, the steeper the slope of a field, the greater the amount of soil loss due to soil erosion by water.

Gravity is the force that pushes both land and water down-hill. Ironically, gravity also keeps soil in its place. The steeper the soil, the more it is pushed down-hill and the faster the water runs.

Crop Cover Management Factor (C)

The cropping management factor (C), is the ratio of soil loss from a field with specified cropping and management to that from the fallow condition on which the factor K is evaluated. The erosion control practice factor (P) is the ratio of soil loss with contouring, strip cropping, or terracing to that with straight-row farming, up-and-down slope.

Canopy Cover (CC)

Canopy is live and dead vegetative cover above the soil surface that intercepts raindrops but is not in contact with the surface runoff. The portion of the above ground plant biomass touching the soil surface is treated as live ground cover.

The canopy intercepts raindrops. Some of the intercepted rainfall reforms as waterdrops that fall from the canopy. The erosivity of these drops is directly related to their impact energy. The impact energy of a waterdrop is one half of the produce of mass, determined by drop diameter, and the square of impact velocity, determined by fall height. In contrast to raindrops that vary over a wide size range, water drops falling from a canopy are all nearly of an equal size (about 3 mm) that is significantly larger than the median raindrop size (about 1.5 mm). Even though the mass of each waterdrop falling from a canopy is greater than the mass of most raindrops, the impact velocity of waterdrops falling from canopy is generally much lower than the impact velocity of raindrops because of the low fall heights from plant canopy.

However, if the bottom of the canopy is greater than about 30 feet (10 meters), the erosivity of water drops falling from canopy is greater than that of raindrops because of the increased mass of the drops falling from the canopy. Some of the rainwater intercepted by the canopy, flows along stems to the soil surface. While this water has no erosivity to detach soil particles by water drop impact, it provides water for runoff, but the delay caused by the water flowing along the stems to the soil surface reduces peak runoff rate, which in turn reduces runoff erosivity. Dense canopies retain a significant amount of water that never reaches the ground because it is evaporated after the storm. While this water is not significant for large storms, it can significantly reduce runoff amounts for small storms. Finally, transpiration, which is related to the leaf area of the canopy, reduces soil moisture, which in turn increases infiltration and reduces runoff.

Senescence

Canopy cover increases during the growth period when plants are accumulating above ground biomass. As plants approach maturity, some vegetation, like soybeans and perennial grasses, lose canopy cover by senescence, and other plants, like cotton, lose canopy cover by being defoliated with chemicals. This loss of canopy cover transfers biomass from standing vegetation to plant residue (litter) on the soil surface. Some plants, like corn, lose canopy cover by leaves drooping without falling to the soil surface,

The other way that canopy is lost is by operations that remove live biomass or remove residue after the vegetation has been killed. Harvest, shredding, mowing, grazing, burning and frost are operations that typically reduce canopy cover.

Ground Cover (GC)

Ground cover, which is material in contact with the soil surface, slows surface runoff and intercepts raindrops and waterdrops falling from the canopy. Ground cover

includes all material that touches the soil surface. Examples are rock fragments, portions of live vegetation including basal area and plant leaves that touch the soil, crypto-gams, crop residue, plant litter and applied materials, including manure, mulch and manufactured erosion control products like blankets.

To be counted as ground cover, the material must remain in place and not be moved downslope by surface runoff during a rainstorm. Also, the material must contact the soil surface sufficiently well that runoff does not flow between the material and the soil to cause erosion. Rock fragments on the soil surface are a special case. Generally, rock fragments must be larger than 5 mm with coarse textured soils in arid and semi-arid regions where runoff is low, and larger than 10 mm in other regions, to be counted as ground cover.

Ground Cover Effect

Ground cover reduces soil loss by protecting the soil surface from direct raindrop impact, which reduces interrill erosion. Ground cover also slows surface runoff and reduces its detachment and transport capacity, which reduces rill erosion. If ground cover is low (less than about 15 percent), and ground cover pieces are long and oriented across slope, ground cover reduces soil loss by causing deposition in numerous small ponds behind ground cover pieces. As ground cover increases, deposition ends and ground cover reduces runoff detachment capacity, which reduces rill erosion. Ground cover reduces rill erosion more than interrill erosion. The net or overall effectiveness of ground cover depends on the relative contributions of rill and interrill erosion. Obviously, ground cover provides the greatest erosion control when it is well anchored and bonded to the soil, which occurs most often on cropland. Conversely, ground cover (mulch) is least effective on construction sites where mulch pieces bridge across soil roughness so that runoff flows under the mulch and where poorly anchored mulch is moved by runoff. These entirely

mechanical effects reduce the forces applied to the soil by waterdrop impact and surface runoff.

Infiltration rate can be very high and runoff low on a freshly tilled soil without a surface seal. If ground cover is placed on the soil before a crust is formed, the ground cover will reduce seal formation and will help maintain high infiltration and low runoff. Thus, ground cover has a lesser effect on reducing soil loss when placed on a soil after it becomes crusted or placed on a soil where internal soil properties, such as a high clay content or high bulk density, control infiltration. A given amount of ground cover reduces soil loss more for cover-management systems, such as no-till cropping, that maintain high soil biomass, improve soil quality, and reduce crusting. Size and shape of ground cover material vary widely from round rock fragments to thin, flat leaves to long slender pieces of unchopped wheat residue to long and bigger diameter unchopped corn stalks to even larger pieces of woody debris left by logging operations. The portion of the soil surface covered is used as a single variable to describe the effect of ground cover on soil loss. For example, above ground residue from a typical agricultural crop includes leaves, pods, hulls, cobs, stems, and stalks and fine and coarse roots for below ground "residue." "Residue" on a disturbed forest range from leaves to broken tree limbs. Furthermore, certain operations, especially harvest operations, frequently reduce size of residue pieces. Ground cover at a specific site can also be composed of several types of residue, such as rock fragments, live ground cover (basal area and plant leaves) and plant litter. Some of the residue types such as plant litter overlap other types such as rock fragments.

How ground cover is added to and removed from the soil surface

Ground cover is added to the soil surface by live vegetation (live ground cover), senescence causing canopy material to fall to the soil surface, natural processes causing standing residue falling over, an operation (e.g., harvest) flattening standing residue, an

operation (e.g., tillage), resurfacing previously buried residue, or an operation applying material (“external residue such as manure, mulch, manufactured erosion control products”) to the soil surface. Ground cover is removed when plant growth stops leaves or other live plant parts from touching the soil surface, an operation (e.g., tillage) buries ground cover, or an operation (e.g., straw baling, burning) removes ground cover. Table 5.5 gives the values of abstraction, crop management factor, canopy cover and ground cover taken for the two watersheds. These values were collected from references (Teklehaimanot, 2003) and also from field surveys.

Table 5.5: Land use cover input values in the two watersheds

Land use	Abstraction	C	Canopy cover	Ground cover
Paddy	0.21	0.300	0	0.30
Medium Forest	0.30	0.030	0.40	0.50
Dense forest	0.40	0.004	0.70	0.80
Barren land	0.08	0.500	0.0	0.07
Built-up	0.10	0.020	0	0.14

The prevailing slopes of the different land use classes as obtained from the DEM in the two watersheds are given in Table 5.6. The average plant height (PH) was taken as 7 m, 5 m and 1 m for the dense forest, medium forest and the paddy field respectively.

Table 5.6: Slope in Awang Khujairok and Waikhulok watersheds.

Land use	Slope (%)	
	Awang Khujairok watershed	Waikhulok watershed
Paddy	18	18
Medium Forest	23	23
Dense forest	35	38
Barren land	18	33
Built-up	18	18

5.2.2 Field Survey

A reconnaissance survey was undertaken to see the accessibility of the study area and to locate suitable investigation sites. After the reconnaissance survey, areas of high erosion risk with respect to topography and land cover were selected. Sites with different characteristics related to erosion risks were selected for studying the soil erodibility and the soil erosion rates. Five land use classes were identified in the study area namely paddy field, medium forest, built-up land, barren land and dense forest (Plates 5.3, 5.4, 5.5 and 5.6). The study was carried out to understand soil and landscape relation. Besides the soil information, other data required to run the erosion model viz. vegetation (land) cover, rainfall and topography were collected for all the sites representing the prevalent five land use classes. Some of the input parameters of land use and vegetation data were retrieved from literature. The values for proportion of the rainfall intercepted by the vegetation or crop cover (A), crop cover management factor (C) and ratio of actual (E_t) to potential (E_o) evapotranspiration (E_t/E_o), were based on literature (Morgan, 1995; Morgan *et al.*, 1984). However, the canopy cover (CC), ground cover (GC), and plant height (PH) were all estimated during actual field surveys.

5.2.3 Application of MMF Model

After all the attribute table and maps of annual rainfall, number of rainy days, typical value for intensity of erosive rain, soil moisture content at field capacity, bulk density, effective hydrological depth of the soil, soil erodibility index from the simple field tests, cohesion of the surface soil (kPa) and the plant parameters (rainfall interception, ratio of actual to potential evapotranspiration, crop cover management factor, percentage canopy cover, percentage ground cover, and plant height) and topography (slope steepness) were generated, the model was applied in a GIS environment using map calculation procedures. One of the results was total annual detachment rate, which was



Plate 5.3: Medium forest land use in the study area



Plate 5.4: Paddy field land use in the study area



Plate 5.5: Dense forest land use in the Waikhulok watershed



Plate 5.6: Barren land use in the Awang Khujairok watershed

estimated by adding the soil particle detachment by raindrop impact and runoff. The second result was the transport capacity of the runoff. The prediction of the total detachment was compared with transport capacity of the runoff and the lesser of the two values was assigned as the annual erosion rate, denoting whether the detachment or transport is the limiting factor. All the results of the analysis are given in the Results and Discussions in chapter six.

Estimation of Rainfall energy

The total kinetic energy of rainfall (KE) for each landform was determined by ILWIS from the total rainfall (R mm) and intensity (I mm/h) of rainfall. In calculating the kinetic energy the way rainfall was partitioned during interception and the energy of rainfall drainage were considered (Shrestha, 1997). Thus, the kinetic energy of the direct through fall [KE (DT); Jm^{-2}] was calculated as function of intensity (I). The kinetic energy of the leaf drainage [KE (LD); J/m^2] is dependent upon the height of the plant canopy (PH). The total kinetic energy of the effective rainfall calculations was obtained by adding KE (DT) and KE (LD). Therefore, after the generation of the attribute table and map of KE (DT) and KE (LD) using map calculation, the total kinetic energy map was also generated in ILWIS for the computation of the soil particle detachment by raindrop impact. The abstraction maps and effective rainfall maps of the Awang Khujairok watershed is given in Fig. 5.9 and 5.10 respectively. The same set of maps for the Waikhulok watershed is given in Fig. 5.11 and 5.12 respectively.

Estimation of runoff

The model performs computation of runoff assuming that runoff generation occurs when the daily rainfall exceeds the soil moisture storage capacity (R_c) and daily rainfall

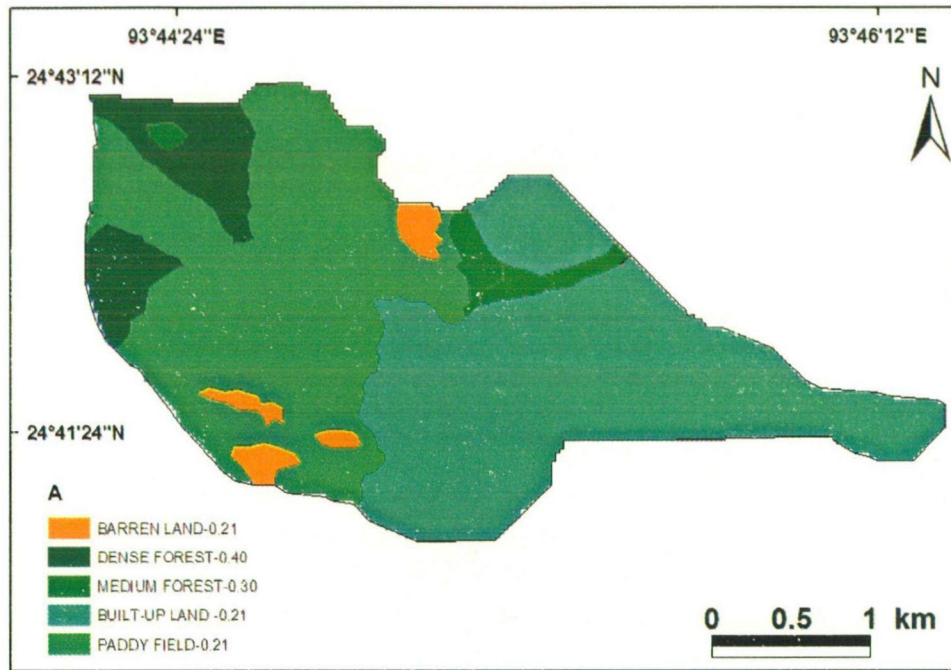


Fig 5.9: Rainfall Interception (A) in Awang Khujairok watershed

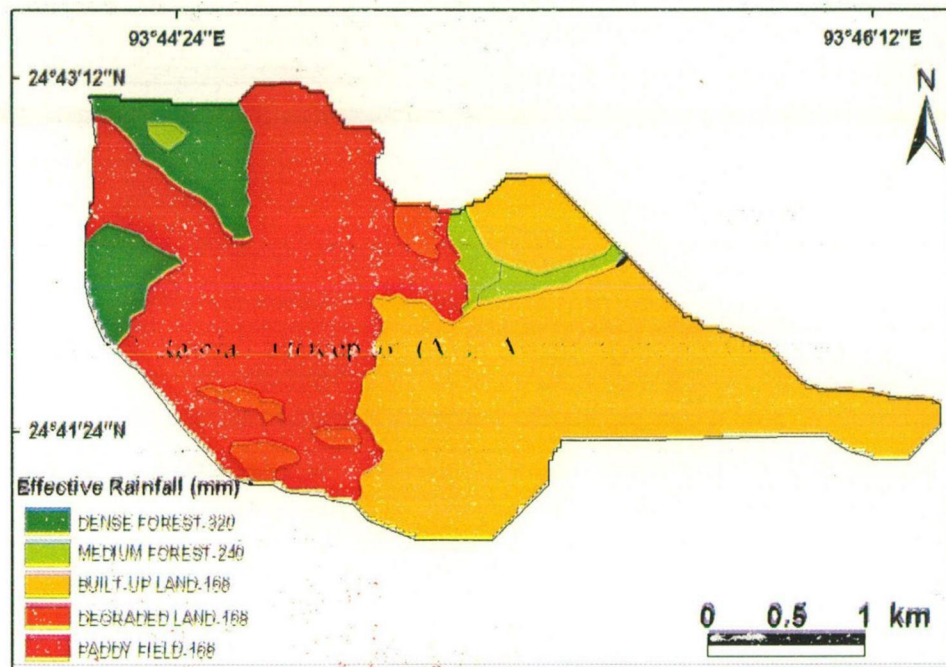


Fig. 5.10: Effective rainfall (mm) in Awang Khujairok watershed

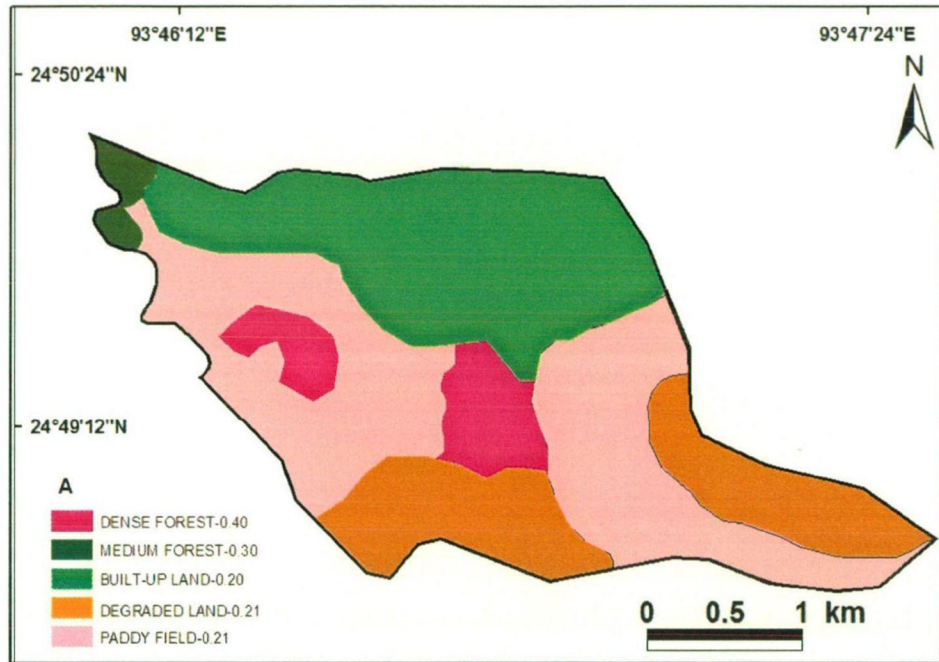


Fig. 5.11: Rainfall interception (A) in Waikhulok watershed

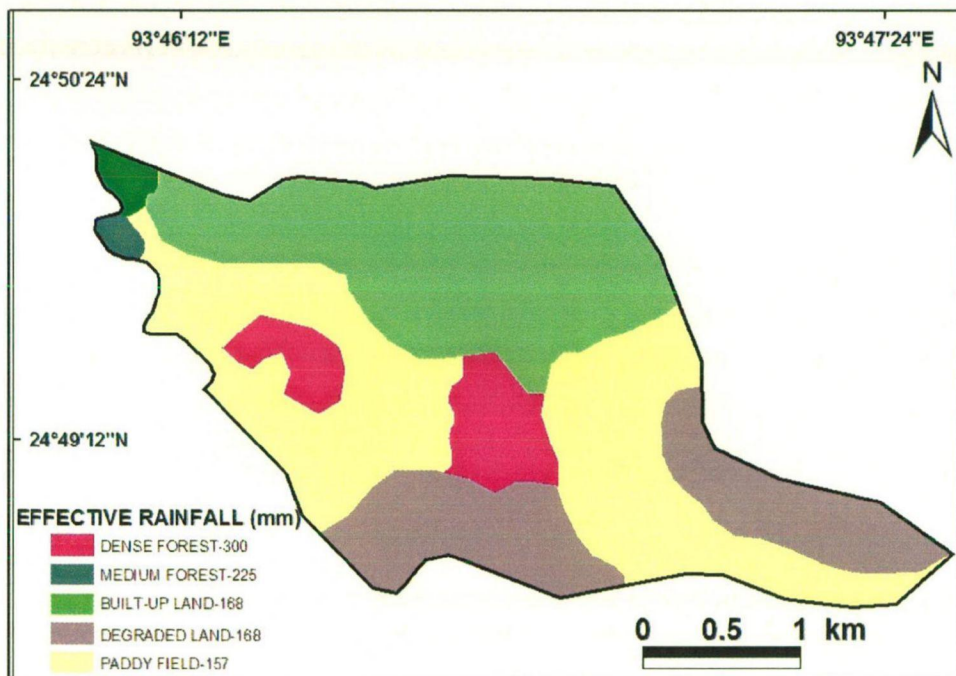


Fig. 5.12: Effective rainfall (mm) in Waikhulok watershed

amount approximate and exponential frequency distribution (Morgan, 2001). The soil moisture content at field capacity (MS) was estimated according to texture of the soil from typical values for soil parameters used (Morgan, 2001). Bulk density (BD) was determined experimentally in the laboratory from the soil samples collected using core sampler method. The effective hydrological depth of soil (m) (EHD) was estimated according to vegetation/crop cover, presence or absence of surface crust, presence of impermeable layer within 0.15 m of the surface. Average values of E_r/E_o ratio were used for each landform to parameterise the model (Teklehaimanot, 2003). Then, runoff volume (Q) was computed using the Equation 4.8. After the generation of the attribute table and map for the soil moisture storage capacity (R_c) using the soil data and land use data and the mean rain per rain day (R_o : mm) from the rainfall data, the volume of runoff map (overland flow) was generated using map calculation procedures in ILWIS. Then, the volume of overland flow generated was used in the calculations of the soil particle detachment by runoff and transport capacity.

Estimation of soil particle detachment

The rate of soil detachment by raindrops impact (splash) depends on the amount of kinetic energy received from rainfall and the erodibility of the topsoil for detachment. In the model, rainfall interception was allowed for the estimation of rainfall energy. For the calculation of detachment rate by raindrop impact, soil erodibility detachment index, mass of detachment per unit tonne energy (g/J) was estimated from the simple field erodibility test undertaken in the field. It was compared with the values given in the guide values for soil parameters (Morgan, 2001). Soil particle detachment rate of the topsoil due to raindrop impact was calculated using the Equation 4.10. The rate of detachment of soil particles by runoff (H : kgm^{-2}) is a function of runoff volume (Q), slope steepness, the resistance of the soil (Z) and percentage of ground cover (GC). The model assumes that soil particle detachment by runoff occurs only where the soil is not protected by ground

cover. In calculating the detachment rate due to runoff the equation 4.11 was used. The resistance of the soil was computed using the cohesion of the surface soil (kPa) as measured with a torvane under saturated condition in the field and GC was also measured in the field. Field measured slope percentage was converted into slope degrees. The slope in degrees was used from the slope degree map generated from the DEM. It was taken in comparison with the slope measured in the field. Finally, the rate of detachment by overland flow ($H: \text{kgm}^{-2}$) was added to the soil particle detachment by raindrop impact to get the total soil particle detachment ($D: \text{kgm}^{-2}$).

Estimation of transport capacity

The transport capacity of overland flow (runoff) depends on the amount of runoff water, slope and crop cover management. The crop cover management was taken from the typical values for plant parameters used (Morgan, 1995). Equation 4.13 was used in calculating the transport capacity of the overland flow (runoff).

Estimation of erosion (soil loss) rate

The total soil particle detachment ($D: \text{kgm}^{-2}$) was compared along with the transport capacity of runoff ($T_c: \text{kgm}^{-2}$). Thus, erosion rate of each land use is equal to the lesser (lower) of the detachment rate or transport capacity of runoff. The calculation methods of the model regarding the various parameters are given in brief in Table 5.7. The various input parameters of the model for the two watersheds are given in Table 5.8 and Table 5.9.

Table 5.7: Calculation of the model parameters

Input parameters	Data source/methods
Rainfall	Collected from the meteorological stations in the watersheds.
MS	(moisture content at field capacity) From literature according to texture class of the top soil.
BD (Bulk density (Mg/m^3))	Determined experimentally in the laboratory from the collected sample.
EHD (Effective hydrological depth of the soil)	From literature according to crop type and conditions considered in the field.
E_v/E_o (ratio of actual to potential evapotranspiration)	From literature according the cover type or crop type.
K Soil Erodibility Index	From simple field erodibility tests.
S° Slope gradient	From DEM in comparison with the field measured.
C Crop Cover management factor	From field measurement and literature according to the type of crop.
CC (Canopy cover)	Measured in the field and literature reference.
PH (Plant height)	Measured in the field and literature reference.
GC (Percentage ground cover)	Measured in the field and determined using FAO guidelines.

Table 5.8: Input values for the MMF model for the Awang Khujairok watershed

Particulars	Land use patterns				
	Paddy	Medium Forest	Dense forest	Barren land	Built-up
Effective rainfall (mm)	168	240	320	168	168
A (proportion between 0 and 1)	0.21	0.30	0.40	0.08	0.10
C	0.3	0.03	0.004	0.500	0.02
I (mm/h)	1.38	1.38	1.38	1.38	1.38
MS (%)	0.25	0.42	0.25	0.25	0.25
PH (m)	1.0	5.0	7.0	0.0	0.00
BD (Mg/m ³)	0.08	0.19	0.08	0.08	0.08
EHD (m)	0.81	0.20	0.81	0.81	0.81
E _t /E _o	0.56	0.95	0.53	0.56	0.56
K (g/J)	1	1	1	1	1
Z	1	1	1	1	1
slope (%)	18	23	35	18	18
GC (proportion between 0 and 1)	0.30	0.50	0.80	0.07	0.14
CC (proportion between 0 and 1)	0	0.40	0.70	0.0	0

Table 5.9: Input values for the MMF model for the Waikhulok watershed

Parameters	Land use patterns				
	Paddy	Forest	Dense forest	Barren land	Built-up
Effective rainfall (mm)	157.5	225	300	168	168
A (proportion between 0 and 1)	0.21	0.30	0.40	0.08	0.10
C	0.3	0.03	0.004	0.500	0.02
I (mm/h)	1.38	1.38	1.38	1.38	1.38
MS (%)	0.25	0.42	0.25	0.25	0.25
PH (m)	1.0	5.0	7.0	0.0	0.0
BD (Mg/m ³)	0.08	0.19	0.08	0.08	0.08
EHD (m)	0.81	0.20	0.81	0.81	0.81
E _t /E _o	0.56	0.95	0.53	0.56	0.56
K (g/J)	1	1	1	1	1
Z	1	1	1	1	1
slope (%)	18	23	38	33	18
GC (proportion between 0 and 1)	0.30	0.50	0.80	0.07	0.14
CC (proportion between 0 and 1)	0	0.40	0.70	0.0	0

The land use patterns in the 27 watersheds in the western catchment are given in Table 5.10. More or less the same pattern of land use classes has been observed in these watersheds. The land use maps of the two watersheds are shown in Fig 5.13 and 5.14 respectively. The percentage composition of the land use classes in these two watersheds are given in Table 5.10.

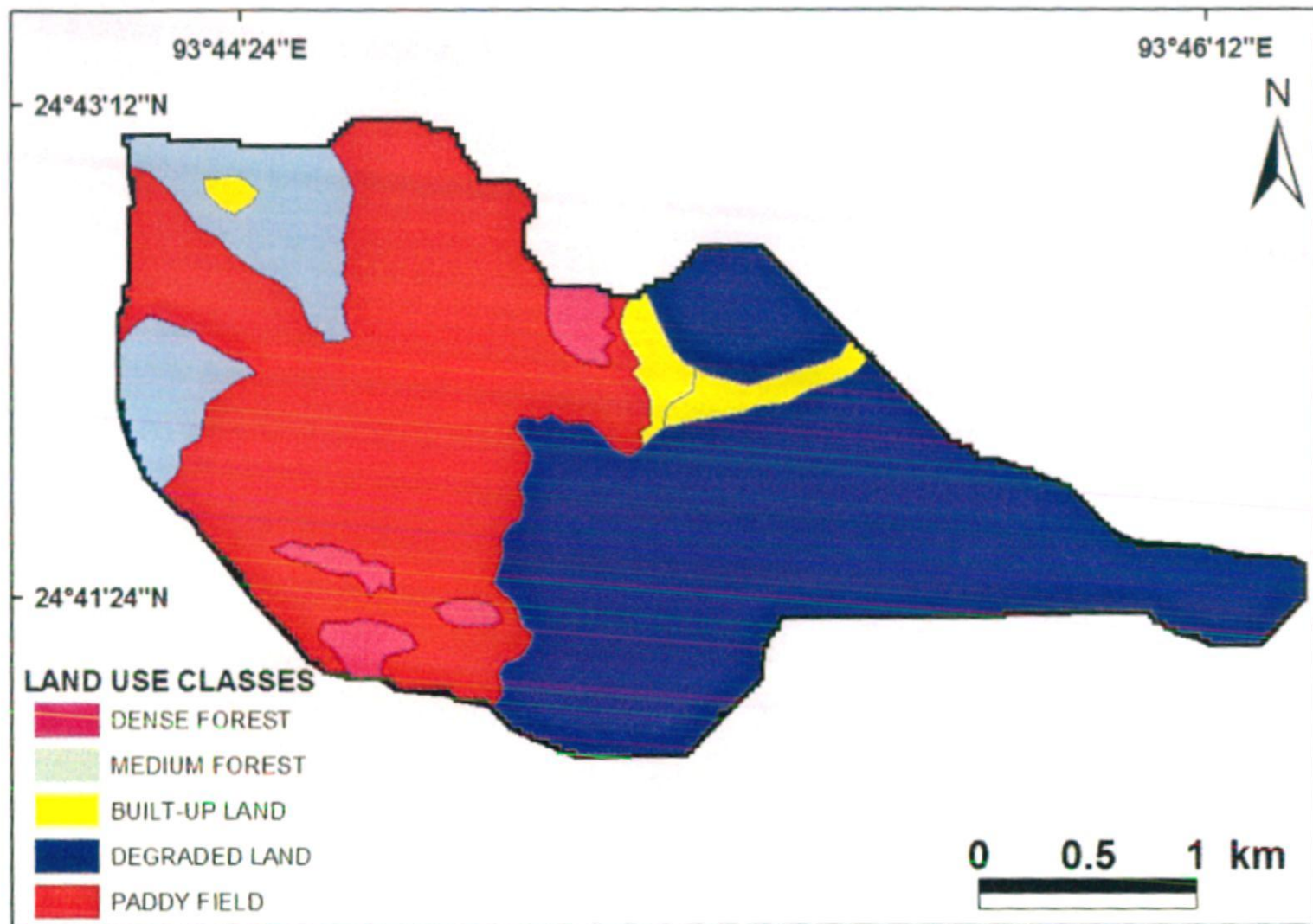


Fig. 5.13: Land use map of Awang Khujairok watershed

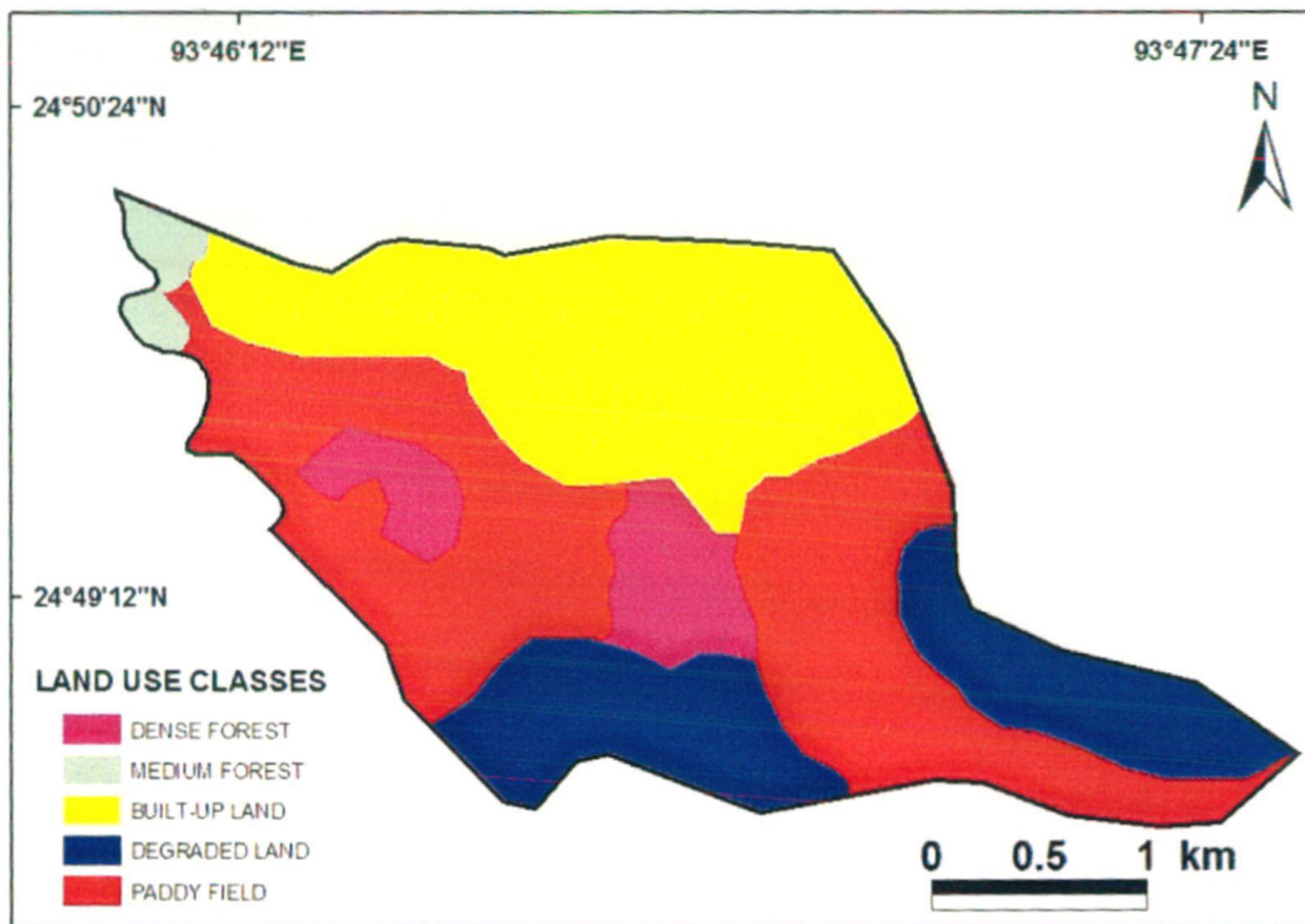


Fig. 5.14: Land use map of Waikhulok watershed

Table 5.10: Land use patterns in the different watersheds of the catchment

Sl. No.	Code	Name	Land use (%)				
			Paddy field	Medium forest	Built-up	Barren land	Dense forest
1	3D2A5a1	Turelu	70	10	10	5	5
2	3D2A5a2	Moirang Turel	80	7	9	0	4
3	3D2A5a3	Mashem (Kwakta)	20	60	8	8	4
4	3D2A5a4	Lajamaril	85	0	5	10	0
5	3D2A5a5	Wangtha	80	10	10	0	0
6	3D2A5a6	Thingin	80	10	10	0	0
7	3D2A5a7	Irum	80	10	10	0	0
8	3D2A5a8	Lenghanbi	80		5	15	0
9	3D2A5a9	Kongdun	50	10	15	25	0
10	3D2A5a10	Ningthoukhong	63	2	25	10	0
11	3D2A5a11	Charoikhui	50	0	10	40	0
12	3D2A5a12	Awang Khujairok	35	15	7	40	3
13	3D2A5a13	Nungshai	80	8	10	2	0
14	3D2A5a14	Keinou	85	0	10	5	0
15	3D2A5a15	Thongjaorok	10	10	0	80	0
16	3D2A5a16	Aigejang	40	10	0	50	0
17	3D2A5a17	Ishinglok	60	0	10	20	10
18	3D2A5a18	Waikhulok	65	5	15	10	5
19	3D2A5a19	Wangjing	40	0	5	50	5
20	3D2A5a20	Sajirok	60	0	2	35	3
21	3D2A5a21	Haibirok	10	0	0	70	20
22	3D2A5a22	Khonga	38	0	2	60	0
23	3D2A5a23	Phayeng	95	0	5		0
24	3D2A5a24	Kangchup	38	0	17	45	0
25	3D2A5a26	Kharamkom	95	0	5		0
26	3D2A5a27	Singda	0	10	12	78	0
27	3D2A5a28	Songtum	60	0	8	32	0

5.3 SOIL EROSION ASSESSMENT USING ^{210}Pb DATING TECHNIQUE OF SEDIMENT

Due to the many limitations associated with the measurement techniques traditionally used to assemble information on rates of soil erosion and sediment redistribution, the use of fallout radionuclides as a basis for estimating erosion and deposition rates would appear to offer considerable potential. Recent studies undertaken in many areas of the world have clearly confirmed the potential of ^{137}Cs measurements for this purpose. Though the radionuclide that has been most widely used for erosion studies is caesium-137 (^{137}Cs) (Zapata, 2002), the use of unsupported or excess lead-210 (^{210}Pb) is also slowly becoming popular. In the foreseeable future, the use of ^{137}Cs measurements is likely to be constrained by the global pattern of bomb fallout inventories and, more particularly, by the measurement problems associated with the resulting low concentrations of ^{137}Cs reported for soil and sediment samples found in some parts of the world, especially equatorial areas (Walling *et al.*, 2003). Lead-210 is different from ^{137}Cs as it is of natural origin, and secondly, its fallout input can be treated as essentially constant over time. Figure 5.15 shows in brief the pathways through which ^{210}Pb reaches into the soil equilibrium and the lake ecosystem.

In the absence of proper observed soil erosion data, ^{210}Pb dating technique of sediment was used for validation of the MMF model.

5.3.1 Field Visit

Three trips to the study area were made during the course of the study. A sediment corer of length around 25 cm and internal diameter approx. 5 cm was used for the sample collection. The corer was inserted smoothly without any jerks into the soil. Care was taken

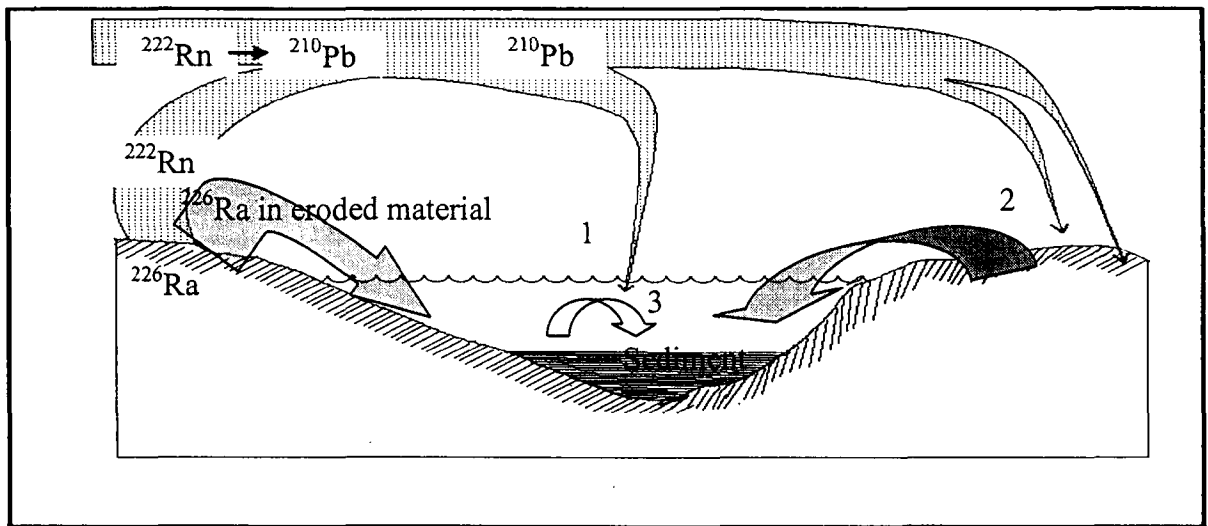


Fig. 5.15: Pathways through which ^{210}Pb reaches lake sediments (Oldfield and Appleby, 1984)

to see that each of the prevalent land use was represented by the soil cores. If the soil surface was found to be hard, it was first sprinkled with water to soften the surface for the ease in the entry of the corer. Extra precaution was taken while removing the corer. It was ensured that the corer came out in one smooth movement and there were no jerks or disturbing movements which might otherwise mix up the different layers of the soil profile, which in turn might give a faulty reading. Altogether 12 soil cores were collected from the watersheds.

Sample preservation, storage and numbering

No special preservation procedures are required for the ^{210}Pb dating technique. The collected cores were placed vertically and a light coloured opaque graduated adhesive tape fixed on the core tube, with markings (in cm) running from top to bottom. The total length of the sediment core was recorded in the sampling information sheet. The sample storage

device (polythene bags/plastic containers) was numbered accordingly. The core was sliced into several sections of the optimum thickness (usually 1 to 2-cm thick) with the aid of a piston (part of the sampling device) and a clean knife and stored in the sample storage devices (polythene bags/wide mouth plastic bottles) sequentially. The numbering system is very important to avoid misinterpretation of results.

Precautions

Cleaning the knife or sample cutting tool after cutting of each sample, with acetone and tissue papers are recommended. Care must be taken in numbering the sample bags/sample containers. It is essential that the piston removes exactly the selected thickness of samples.

Maps and sample records

The locations of the sediment cores collected were recorded in a map. The exactness of markings is very relevant for correct interpretation.

5.3.2 Sample Processing

The samples were then brought into the laboratory for a series of further analysis. Care was taken that each and every sample was kept and stored with proper distinct identification mark.

Bulk density

As soon as the samples were transported to the lab, the samples were emptied in clean and dry stainless containers. The weight of the empty container and the weight of the container plus the sample were recorded properly. Electronic weighing balance with a precision of 0.01 g was used. The bulk density (ρ_b) was calculated as follows:

$$\rho_b = W_w / V \quad (5.2)$$

where, W_w = wet weight of the sample (g)

V = volume of the sample (cc)

Dry density

The SS container was then placed in the temperature controlled oven at a pre-set temperature of 105°C for about 24 hours for the removal of moisture.

The dry density (ρ_d) was determined as

$$\rho_d = W_d/V \quad (5.3)$$

where, W_d = dry weight of the sample (g)

V = volume of the sample (cc)

Moisture content

The moisture content (Q) was determined by

$$Q = (W_w - W_d)/W_w \quad (5.4)$$

where, W_w = wet weight of the sample (g)

W_d = dry weight of the sample (g)

Powdering and sample homogenization

A sediment sample usually contains a considerable proportion of clay fraction. This leads to lumping of samples following the oven drying. For radioactivity measurements these lumps have to be powdered and homogenized. This was carried out manually by using the Agate pestle and mortar that were cleaned with acetone and tissue papers regularly after every sample.

5.3.3 Lead-210 Measurement by Alpha Spectrometry

This method involves digestion of the sample, spontaneous deposition on a silver planchet/copper disc and counting in the Alpha Spectrometer (Silicon surface barrier detector coupled with Multi Channel analyzer). The method uses the granddaughter

product viz. ^{210}Po and a secular equilibrium is presumed for the purpose of ^{210}Pb dating. The steps followed in brief are given below:

Digestion

First of all, 1 g of dried sediment was weighed into a 250 ml Erlenmeyer flask. The sample ID and date were recorded. 1.0 ml of Po-209 standard was poured with help of pipette into flask. The activity of the standard and the date was recorded. 100 ml of 6 N Hydrochloric Acid (1:1) was added to the flask. 2 ml of 30% Hydrogen Peroxide and 2 drops of octanol were then added. The flask was then placed on a hot plate and heated to 90-95°C. The heating was done for 30 min. after which the flask was removed from the hot plate and cooled slightly. Thereafter, two drops of octanol and 2 ml of 30% hydrogen peroxide were added. If the samples foamed vigorously, more octanol was added. The samples were again heated for 30 min. The addition of peroxide was repeated at least two more times. If the samples continued to foam, additional peroxide was added until foaming subsided. The heating process was carried out for a total of four hours. Thereafter, the samples were removed from the hot plate and let to cool down, covered with a watch glass, and let stand over night.

Polished copper disks were labeled at the back with water proof marker and sprayed three light coats of urethane.

Filtration

The sample was filtered through a Whatman No. 42 filter paper into another Erlenmeyer flask. A Buchner funnel attached to vacuum was used for this step. The digestion flask was rinsed three times with small portions of Type 1 water and added to the filter.

Plating

The flask was placed on a hot plate, carefully reducing the volume to approx. 5 ml. Care was taken so that the sample did not get dried. The sample was then cooled. The pH of the sample was then measured and it was maintained between 0.5 and 1.0, using either HCl or NaOH.

0.1 to 0.2 g of Ascorbic acid was added to each sample and dissolved. The ascorbic acid was added to form a complex with ferric iron, thereby preventing its possible interference with the Po-210 plating. The sample was transferred to a 125 ml plastic bottle and the flask was rinsed three times.

The previously labeled disk was polished and rubbed off with a Kimwipe. The disk was put into the sample in the plastic bottle, making sure the polished side was up. The bottle was capped properly. The bottle was then placed in an oven overnight at 95°C (Plate 5.7).

The samples were removed from the oven. For removing the copper disk, the cap on the bottle was tightened and turned upside down, keeping the copper disk in the cap. The bottle is slowly turned over letting the disk remain in the cap. The disk was removed, rinsed first with Type 1 water (Plate 5.8) and then with ethanol, patted dry (without rubbing) and placed in a plastic zip lock bag. The bag was labeled with the sample ID, date digested and the date plated.



Plate 5.7: Bottle containing the sample being kept in the oven

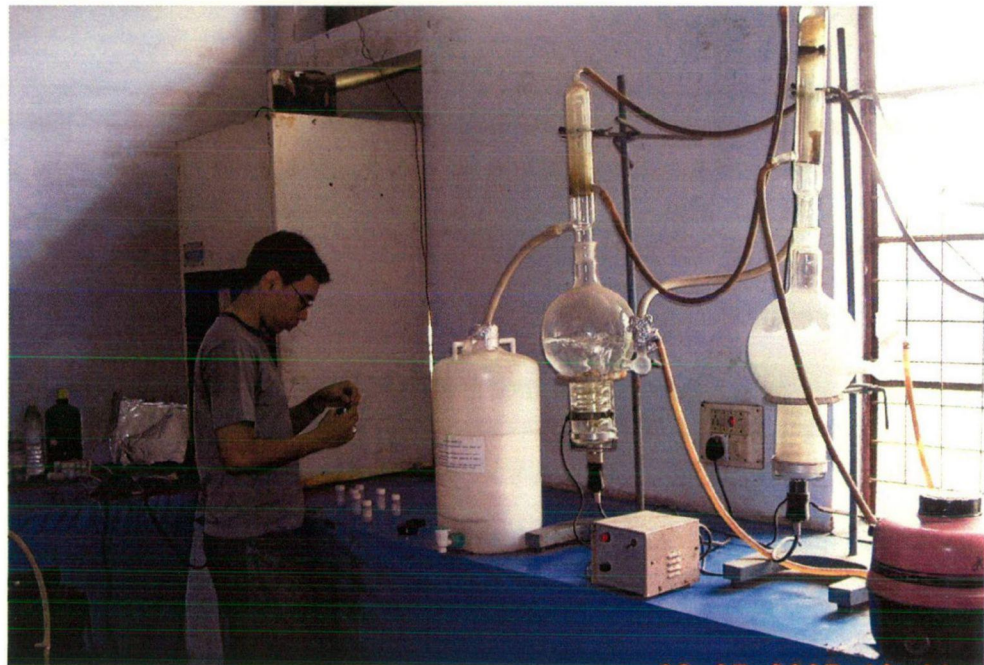


Plate 5.8: Washing of the copper disks with Type 1 water

The ^{210}Po and ^{209}Po activities on each disk were determined by isotope dilution alpha spectrometry (Plate 5.9). The system consisted of a surface barrier detector, preamplifier, amplifier, mixer router, analog to digital converter, multi-channel analyzer, and appropriate computer software. Each radioactive decay of ^{210}Po emits an alpha particle that has energy of 5.3 MeV. The energy of the ^{209}Po alpha particle is about 5.1 MeV. Particles emitted at these two energies can be identified using an alpha spectroscopy system.

The disks were counted in vacuum chambers to enhance the resolution of the ^{210}Po and ^{209}Po alpha peaks as shown in Fig.5.16. The outputs from the silicon detectors were amplified and transmitted through a multiplexer system into a computer based multi-channel analyzer. The activity of ^{210}Po in the sample was determined from the ratio of the total counts of ^{209}Po to ^{210}Po and from the quantities of sediment and ^{209}Po added to the sample. The ^{210}Po and ^{209}Po peaks were displayed on screen across an energy spectrum, separated by cursors and recorded. The relative concentrations were determined from the number of counts within each region of interest and the counting time was typically 14400 sec. Blanks and standards were measured to verify the performance of all aspects of the procedures and the instrumentation. The ^{209}Po standard that was added to each sample also served as an excellent internal standard to monitor the quality of the analysis. The concentration of ^{210}Pb at the time of sediment sampling was calculated from the count rates corrected for counting background, growth and decay, counting efficiency and recovery of the ^{209}Po yield monitor.

The soil erosion rate from the study catchments were estimated using a theoretical mass balance model based on that developed previously at the University of Exeter (Walling and He, 1999), but also incorporating the role of tillage translocation in the redistribution of fallout inputs. The model took into account the essentially continuous

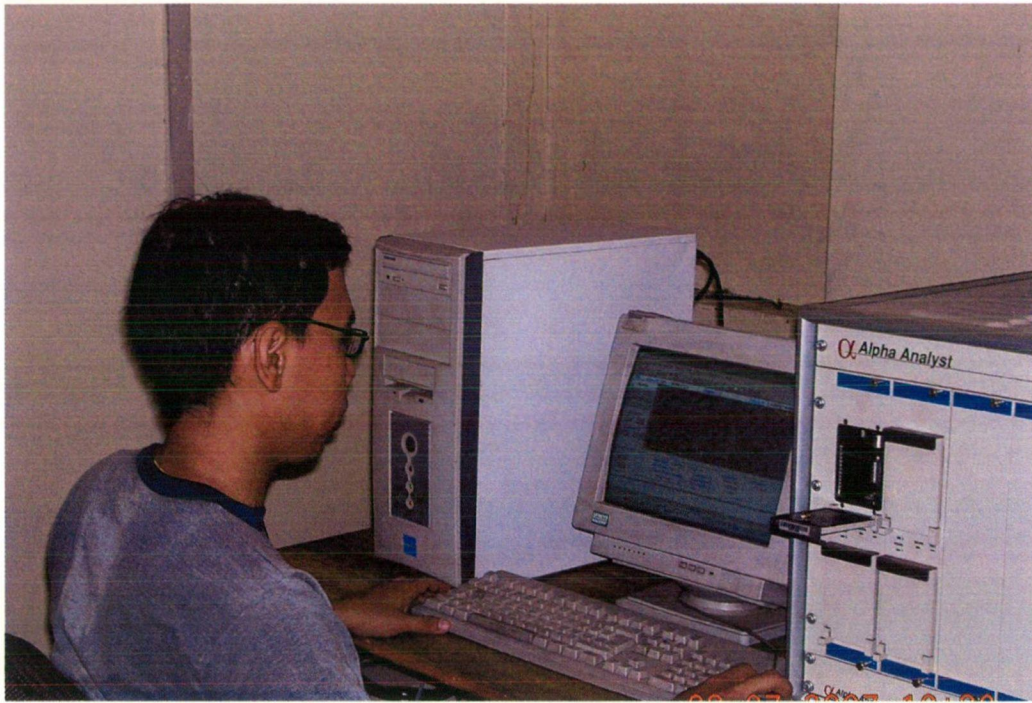


Plate 5.9: Observation of the ^{210}Po counts by the Alpha-spectrometer

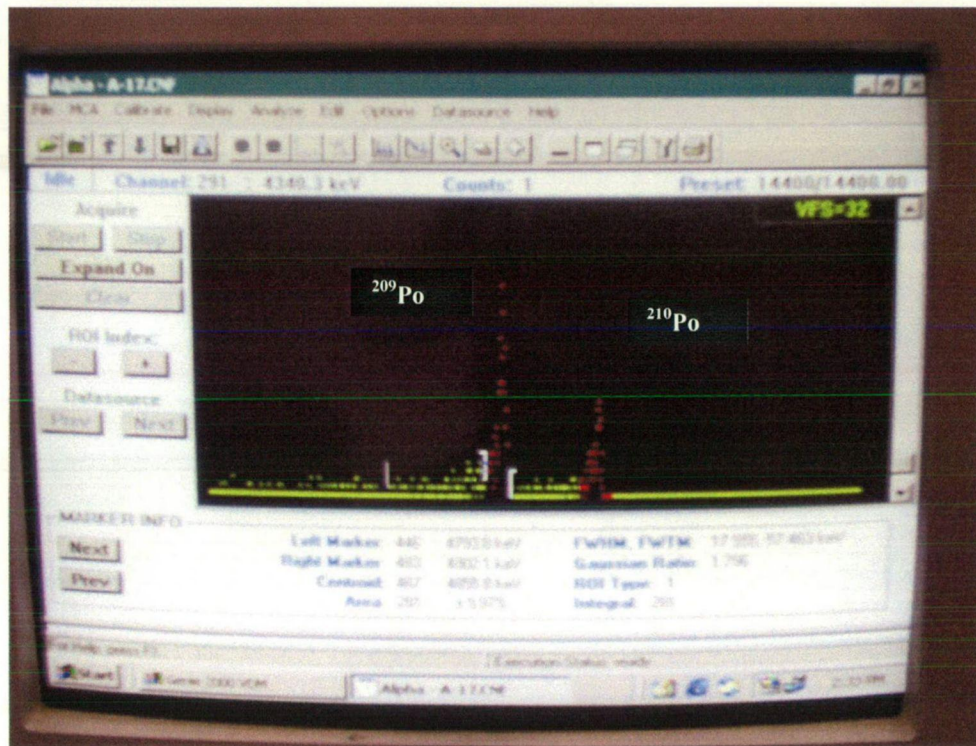


Fig. 5.16: Spectrum of region of interest (ROI) depicting ^{209}Po and ^{210}Po peaks

atmospheric deposition of unsupported ^{210}Pb and its subsequent radioactive decay, as well as its redistribution in association with water-induced erosion or deposition. In addition, the model considered the removal of freshly deposited fallout ^{210}Pb by erosion, before its incorporation into the tillage horizon. The basic form of the model for an eroding site can be expressed as:

$$\frac{dA(t)}{dt} = (1 - \Gamma)I(t) - \left(\lambda + P \frac{R}{d}\right)A(t) \quad (5.5)$$

where, $A(t)$ = cumulative ^{210}Pb inventory (Bq m^{-2}); R = erosion rate ($\text{kg m}^{-2} \text{y}^{-1}$); d = tillage depth (kg m^{-2}); k = ^{210}Pb decay constant (y^{-1}); $I(t)$ = annual fallout ^{210}Pb deposition flux at time t ($\text{Bq m}^{-2} \text{y}^{-1}$); Γ = the proportion of the freshly deposited ^{210}Pb fallout input removed by water erosion before incorporation into the tillage layer and P = a particle size correction factor to take account of differences between the grain size composition of the mobilised sediment and the original soil.

The tillage depth d , expressed as a mass depth, was typically $60\text{--}90 \text{ kg m}^{-2}$ for cultivated areas (Collins *et al.*, 2001). Γ was estimated using experimental data for the initial depth distribution of fallout ^{210}Pb in surface soil (represented by the relaxation mass depth H), and information on the local rainfall regime in relation to the timing of cultivation (represented by a proportion factor C). On the basis of experiments reported by He and Walling (1997), the value of H was assumed to be ca. 4.0 kg m^{-2} . The atmospheric deposition flux of ^{210}Pb at the lake is unknown, therefore the available mean ^{210}Pb atmospheric flux of Mumbai station, India (a value of $0.025 \text{ Bq cm}^{-2} \text{y}^{-1}$ (Joshi *et al.*, 1969) may be assumed to be similar to the Loktak Lake catchment area (the annual rainfall at the study area and at Mumbai is comparable and the difference in latitude is not large). Assuming a continuous input of fallout ^{210}Pb , Equation (5.4) gives,

$$A(t) = A(t_0)e^{-\int_{t_0}^t (PR/d + \lambda) dt} + \int_{t_0}^t [1 - P\gamma \times (1 - e^{-R/H})] I(t') e^{-(PR/d + \lambda)(t-t')} dt' \quad (5.6)$$

where, t_0 = year when cultivation started (taken to be 100 years prior to the sample collection date and assuming negligible erosion before t_0).

The conversion model was used to generate estimates of point soil redistribution rates ($\text{kg m}^{-2} \text{ year}^{-1}$) from the unsupported ^{210}Pb inventories associated with individual soil cores collected along each slope transect. Assuming each transect represented a 1-m wide strip, these point estimates were used to calculate equivalent values of soil loss or deposition (kg year^{-1}) for individual slope segments, extending halfway to the adjacent coring points from the sampling point in each direction. The resulting values for each segment were summed to establish a sediment budget for the overall transect, comprising estimates (~ 100 years) of total erosion, total deposition, net soil loss and the sediment delivery ratio. Finally, the estimates of soil redistribution obtained for the individual transects were averaged to establish the mean sediment budget for each land use (Walling *et al.*, 2003).

The essentially continuous input of ^{210}Pb fallout through time means that the contemporary unsupported ^{210}Pb inventory will reflect redistribution and thus loss and gain of unsupported ^{210}Pb over a longer period. The length of this period is, however, constrained by the half-life of ^{210}Pb (i.e. 22.6 years), because the effect of past changes in the unsupported ^{210}Pb inventory, caused by erosion on the contemporary inventory, will progressively decline as the period of time elapsed increases. Following previous work, it has been assumed that the contemporary unsupported ^{210}Pb inventory will only be sensitive to erosion occurring within a period equivalent to four times the half-life, and thus the past 100 years. Furthermore, the progressive reduction in the effect of past changes in the inventory on the contemporary inventory, as the period of time elapsed since those changes increases is also taken into account when interpreting the impact of the erosional history of a study site on the magnitude of the measured unsupported ^{210}Pb

inventory. The longer-term estimates of soil redistribution rates provided by the unsupported ^{210}Pb measurements can provide useful information on the erosional history of the study area and more particularly of medium- and longer-term changes in rates of soil loss.

RESULTS AND DISCUSSION

6.1 PREAMBLE

This chapter deals with the results of soil erosion assessment using three approaches *viz* the Universal Soil Loss Equation (USLE), the revised MMF model and the nuclear technique. The influence of landforms on soil erodibility is assessed in terms of the relative erosion hazards using the soil properties. The soil erodibility classes derived from the simple field tests are compared and adjusted with quantitative erodibility factor using the guide values for soil parameters given by Morgan (2001). In the section on nuclear techniques, the result obtained using the ^{210}Pb dating technique has been presented. Then the results obtained using both the techniques have been compared. The soil erosion in the remaining watershed has been computed on the basis of land use. An empirical relationship has also been developed between effective rainfall and soil erosion.

6.2 SOIL EROSION USING USLE

The USLE has predicted very less erosion rates for the two watersheds for all the land use classes when compared with observed values as can be seen from the Table 6.1. In fact, the USLE model (Wischmeier and Smith, 1978) was originally developed for gently sloping cropland situations. It gives sheet and rill erosion rates while the study area is hilly.

When using the USLE, the effects of topography on soil erosion were estimated by the slope length (L) and slope steepness (S) constituents of the dimensionless LS factor,

where LS is one of five component factors (R, K, LS, C, and P) that were multiplied together to calculate the average annual soil loss per unit area. The LS factor was calculated as the product of the slope length and steepness constituents converging onto a point of interest (e.g., a farm field or a raster cell on a GIS grid). In mountainous regions, the use of the USLE for GIS-based regional landscape ecology modelling has been hampered by a lack of reliable estimates of the LS factor values. For local conservation planning, the LS factor is usually either estimated or calculated from actual field measurements of length and steepness. Labour-intensive field measurements are obviously not feasible for modelling soil erosion on a regional scale.

Table 6.1: Soil loss estimation by the USLE

Land use class	Erosion (kg/m ² /y)			
	Awang Khujairok watershed		Waikhulok watershed	
	Observed	Estimated	Observed	Estimated
Paddy field	1.54	0.0414	1.21	0.0314
Medium forest	1.96	0.0402	1.96	0.0321
Built-up land	1.23	0.0641	1.32	0.0414
Dense forest	0.01	0.0012	0.21	0.0013
Barren land	4.28	0.4025	2.34	0.4241

Over the years, the USLE has received criticism for its lack of accuracy in predicting annual soil losses (Trieste and Gifford, 1980). It is designed for agricultural field units and tends to yield high estimates when applied to other scenarios (Hart, 1984).

Empirical data that support the equation are from mesic, agricultural landscapes which have three fundamental differences from the present study area.

First, slopes of agricultural landscapes are relatively low (1-18%) and simple (Wischmeier and Smith 1978), whereas slopes of the two watersheds are steeper (upto 38%) and more complex. The model has been tested and verified in the plains and hilly countrysides with 1-20% slopes and excludes young mountains especially with steeper slopes where runoff is a greater source of energy than rain and where there are significant mass movements of earth.

Secondly, the vegetation in the study area is not spatially and taxonomically homogeneous like cropping systems. Although undisturbed rangeland vegetation is relatively stable, there are frequently interspaces of sparse vegetation. A major limitation of the model is that it neglects certain interactions between factors in order to distinguish more easily the individual effect of each. For example, it does not take into account the effect on erosion of slope combined with plant cover or the effect of soil type on the effect of slope.

Third, precipitation that occurs in the present catchment in the form of intense summer rainfall events is different from the more frequent, less intense storms of the regions for which the equation was calibrated. The relations between kinetic energy and rainfall intensity generally used in this model apply only to the American Great Plains and not to the mountainous region.

Also, it has been reported that the USLE over-predicts low annual average erosion and under-predicts high average erosion (Risse *et al.*, 1993; Rapp *et al.*, 2001).

It does not take account of gully erosion and soil loss from stream channels and has been found not applicable in mountainous watersheds since the available plant hydrology data relates mainly to level ground (Calder *et al.*, 1992). Hence, it was decided not to proceed further with this model.

6.3 SOIL EROSION BY THE MMF MODEL

The revised MMF model has been used to estimate the soil loss for each land use in both the watersheds.

6.3.1 Soil Erosion in Awang Khujairok watershed

Detachment rate and Transport Capacity

The rate of soil detachment by raindrops impact (splash) depends on the amount of kinetic energy received from rainfall and the erodibility of the topsoil for detachment. The soil particle detachment by raindrop impact is high in the three land use viz. barren land, built-up land and paddy in case of the Awang Khujairok. This is mainly because of the kinetic energy of the effective rainfall and the erodibility factor (K-value) being high. The low soil particle detachment by raindrop impact is recorded under land use/cover of dense forest (2.33 kg/m^2) in the watershed. This land use has the lowest rainfall kinetic energy of 2333 J/m^2 .

The rate of detachment of soil particles by runoff ($H: \text{kg m}^{-2}$) is a function of runoff volume (Q), slope steepness, the resistance of the soil (Z) and percentage of ground cover (GC). The model assumes that soil particle detachment by runoff occurs only where the soil is not protected by ground cover. The detachment rate, transport capacity and the erosion rates estimated by the model are shown in Table 6.2. The results of the analysis revealed that the highest record of the soil particle detachment by runoff in the case of Awang Khujairok is in the dense forest (1.90 kg/m^2). This is due to the steep slope. The lowest is found in the land use of medium forest (0.29 kg/m^2). The total annual detachment given is the sum of the soil particle detachment by raindrop impact and runoff.

Table 6.2: Soil particle detachment (F and H), transport capacity (TC) and soil loss in the Awang Khujairok watershed

Land use	Area (km ²)	F (kg/m ²)	H (kg/m ²)	(F+H) (kg/m ²)	TC (kg/m ²)	Soil loss (kg/m ² /y)
Paddy field	2.60	4.03	0.73	4.76	1.24	1.24
Medium forest	0.32	3.47	0.29	3.77	1.66	1.66
Built-up land	2.27	4.03	0.73	4.76	1.24	1.24
Barren land	0.32	4.03	1.25	5.28	2.12	2.12
Dense forest	0.97	2.33	1.90	4.23	0.21	0.21
<i>Minimum</i>	0.32	4.03	4.76	5.28	2.12	2.12
<i>Maximum</i>	2.60	2.33	0.29	3.77	0.21	0.21
<i>Mean</i>	1.29	3.58	0.98	4.56	1.29	1.29

F = Soil detachment by raindrop impact (kg/m²).

H = Soil detachment by runoff (kg/m²).

F+H = Total annual detachment (kg/m²).

TC = Transport capacity of the runoff (kg/m²).

The highest total annual detachment is observed in the case of barren land (5.28 kg/m²) and the least in the medium forest (3.77 kg/m²).

The land use of dense forest has negligible amount of transport capacity (0.21 kg/m²) mainly due to the low estimated crop cover management factor (C). The highest record of the transport capacity is in the barren land (2.12 kg/m²) which is highly governed by its sparse ground cover. The model takes the lower values from the estimated detachment rate and transport capacity. Therefore, some of the landforms with high detachment rates show low erosion rates due to low transport capacity. The maps for the detachment rates and transport capacity for the Awang Khujairok watershed are given in Fig. 6.1, Fig. 6.2, Fig. 6.3 and Fig. 6.4. The total kinetic energy map is shown in Fig. 6.5. The erosion map for the watershed is given in Fig. 6.6.

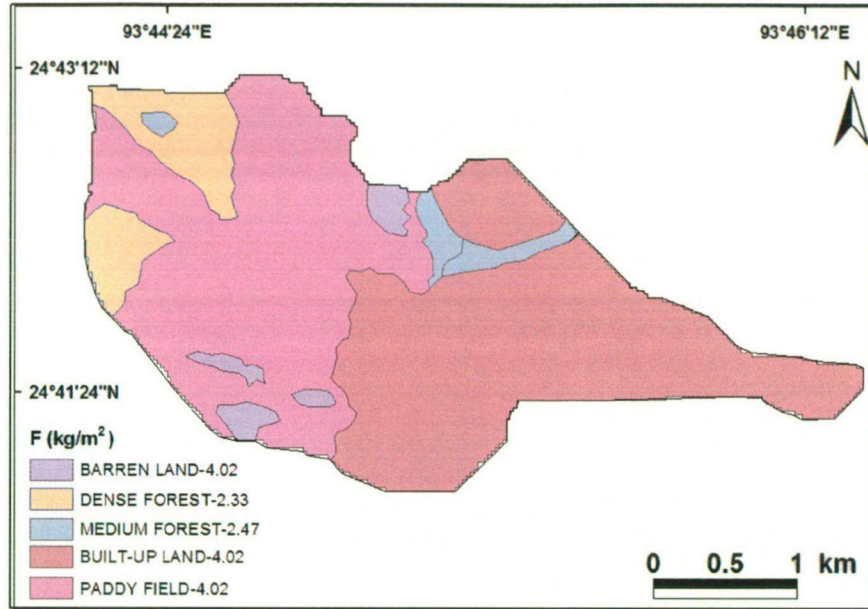


Fig. 6.1: Soil detachment by raindrop impact (F) (kg/m²) in Awang Khujairok watershed

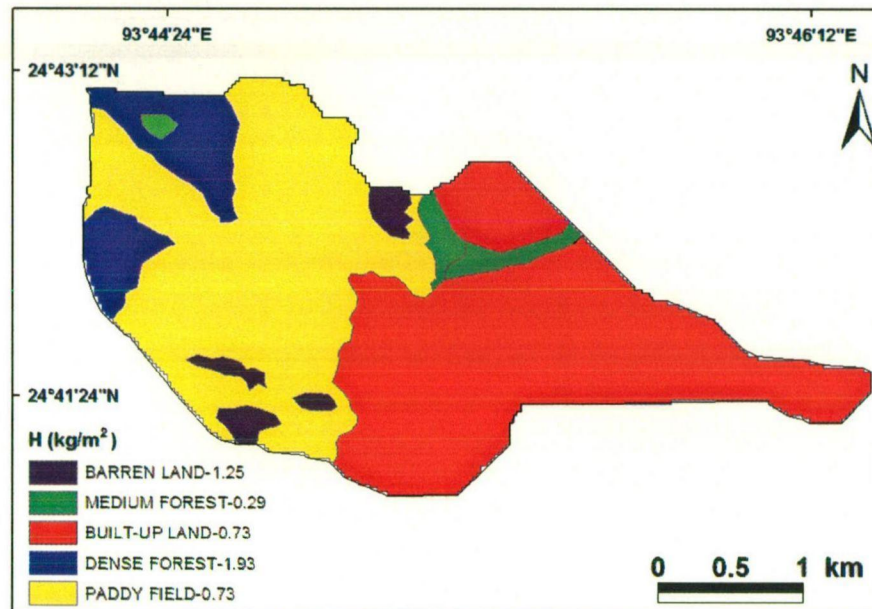


Fig. 6.2: Soil detachment by runoff, H (kg/m²) in Awang Khujairok watershed

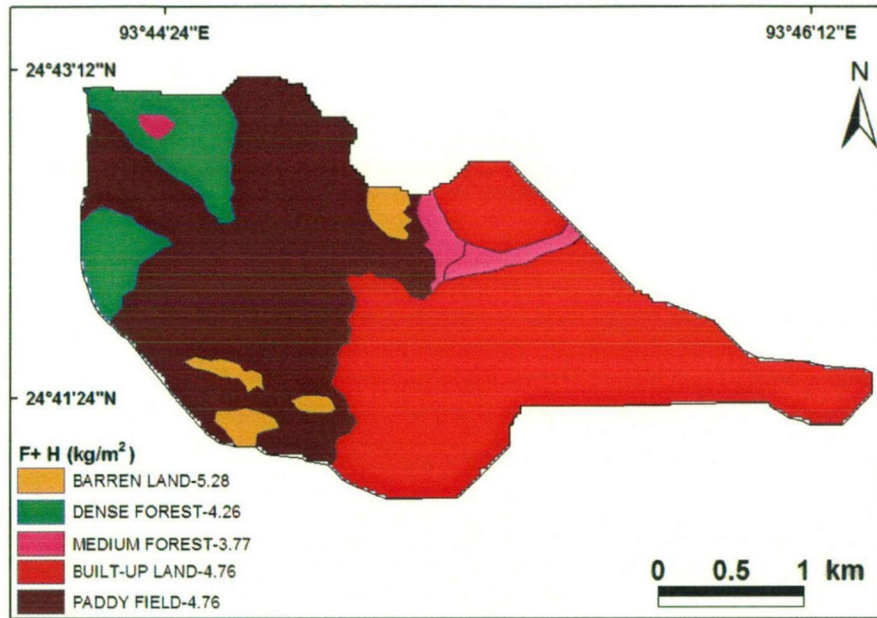


Fig. 6.3: Total annual detachment, F+H (kg/m²) in Awang Khujairok watershed

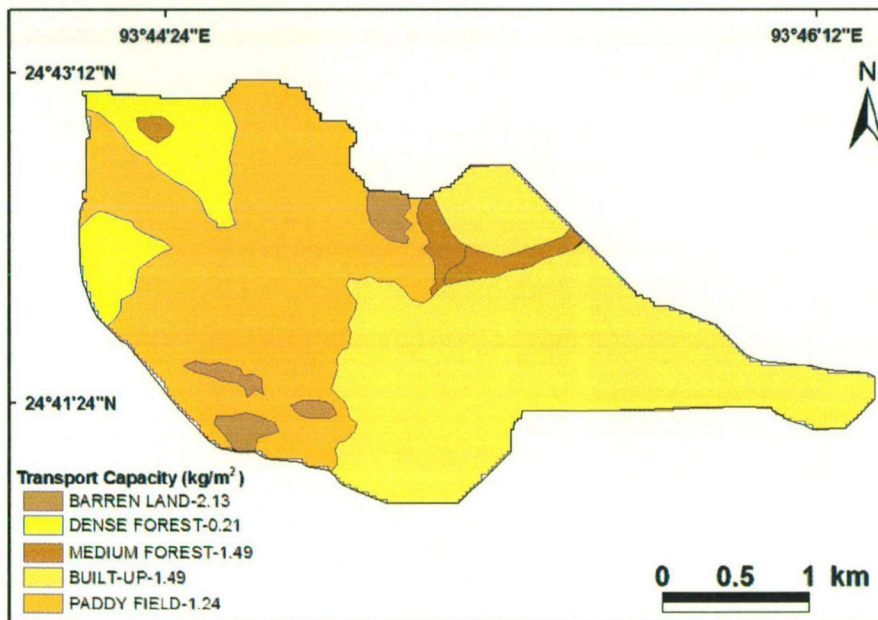


Fig. 6.4: Transport capacity, TC, (kg/m²) in Awang Khujairok watershed

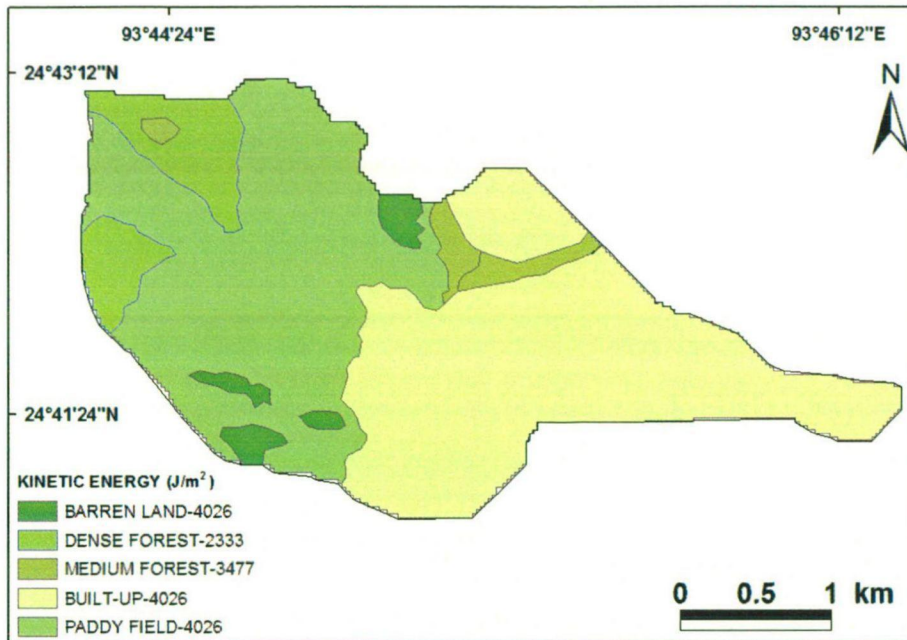


Fig. 6.5: Total Kinetic Energy (J/m^2) in Awang Khujairok watershed

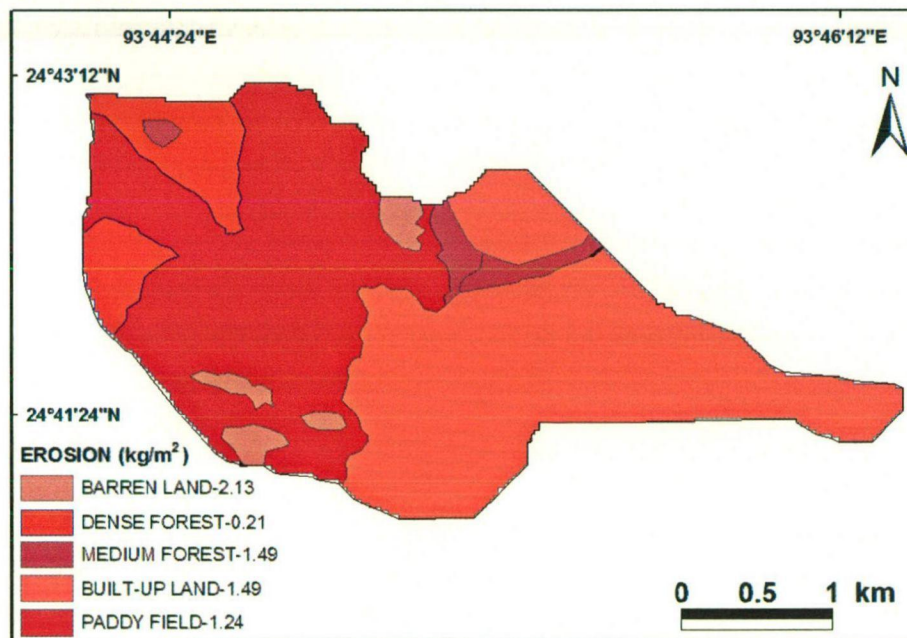


Fig. 6.6: Erosion map of Awang Khujairok watershed

Erosion rate (Soil loss) estimate

The result shows that transport capacity does not exceed the total soil particle detachment rate for all the land use systems. Thus, the estimates of the transport capacity are considered as a final soil loss of the study area. The annual soil loss rates are between 0.21 kg/m^2 to 2.12 kg/m^2 . Therefore, the soil particle transport capacity and the erosion rate are low despite high detachment rate.

6.3.2 Soil Erosion in Waikhulok watershed

In case of the Waikhulok watershed, the soil particle detachment and the soil loss is given in Table 6.3. The soil particle detachment by raindrop impact is found high in the land use of barren land (4.03 kg/m^2) and built-up land (4.02 kg/m^2). Soil particle detachment by runoff was found to be the lowest in the land use of medium forest (0.27 kg/m^2) and the highest in case of dense forest (2.13 kg/m^2). The highest total annual detachment is observed in the case of barren land (5.33 kg/m^2) and the least in the medium forest (3.53 kg/m^2). The transport capacity was highest in case of barren land (2.18 kg/m^2) and quite negligible in the dense forest (0.19 kg/m^2). The soil loss in the watershed is in the range of 0.19 kg/m^2 to 2.18 kg/m^2 . The maps of detachment rates and the transport capacity are given in Fig. 6.7, Fig. 6.8, Fig. 6.9 and Fig 6.10. The kinetic energy map is shown in Fig. 6.11. The erosion map of the watershed is derived and presented in Fig. 6.12.

In this study, the total annual detachment erosion is compared with the transport capacity of the overland flow using the MMF model. The attractiveness of the method besides its simplicity lies in the recognition that erosion can be either transport- or detachment-limited. The detachment map is compared with the transport map and for each pixel in the catchment the smallest value is selected. This minimum value is taken as the

modeled erosion rate. Thus, erosion rates in the defined five land use classes were estimated.

Table 6.3: Soil particle detachment (both F and H), transport capacity (TC) and soil loss in the Waikhulok watershed

Land use	Area (km ²)	F (kg/m ²)	H (kg/m ²)	(F+H) (kg/m ²)	TC (kg/m ²)	Soil loss (kg/m ² /y)
Paddy field	1.52	3.77	0.66	4.44	1.09	1.09
Medium forest	1.33	3.26	0.27	3.53	1.39	1.39
Built-up land	0.304	4.02	0.73	4.76	1.24	1.24
Barren land	0.456	4.03	1.30	5.33	2.18	2.18
Dense forest	0.19	2.19	2.13	4.32	0.19	0.19
<i>Minimum</i>	0.30	2.19	0.27	3.53	0.19	0.19
<i>Maximum</i>	1.52	4.03	2.13	5.33	2.18	2.18
<i>Mean</i>	0.76	3.45	1.02	4.48	1.22	1.22

F = Soil detachment by raindrop impact (kg/m²).

H = Soil detachment by runoff (kg/m²).

F+H = Total annual detachment (kg/m²).

TC = Transport capacity of the runoff (kg/m²).

6.4 SOIL EROSION BY ²¹⁰Pb DATING TECHNIQUE.

In this section the results of ²¹⁰Pb dating technique to estimate the soil erosion rates for areas under different land use in the two small watersheds in Loktak Lake catchment is presented.

Fig. 6.13 shows the depth distributions of unsupported ²¹⁰Pb in the soil cores collected from areas representative of each main land use within the Awang Khujairok watershed. The unsupported ²¹⁰Pb activity was found in the upper 10 cm of the soil profile in the case of dense forest (Fig. 6.13A). In common with depth profiles reported for similar land use class sites in other parts of the world, the unsupported ²¹⁰Pb content of this soil core exhibits peak concentrations at the surface and an approximate exponential decline with depth (He and Walling, 1997).

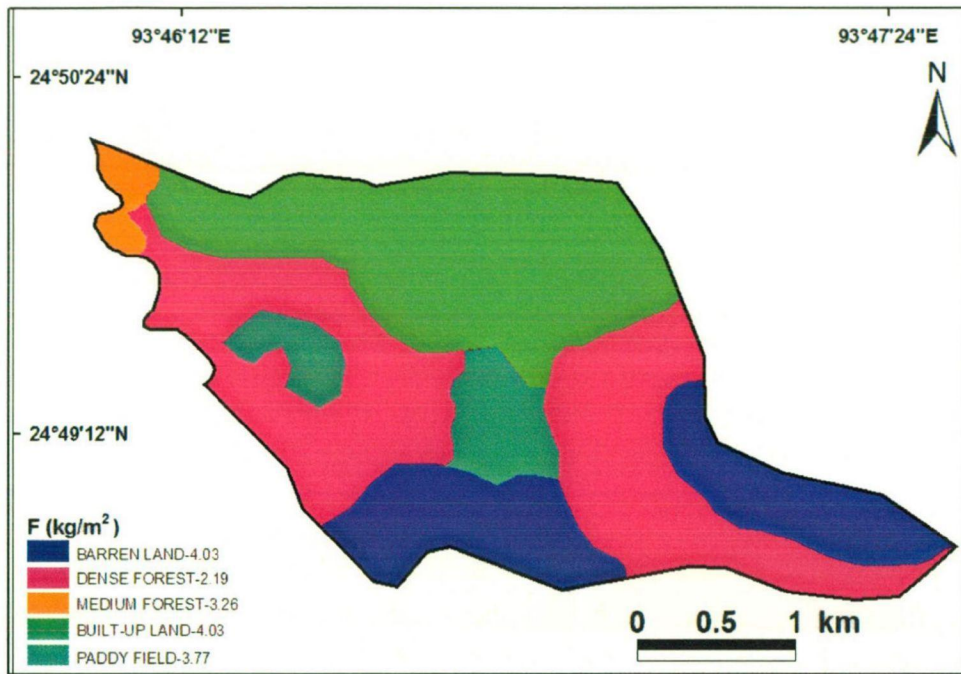


Fig. 6.7: Soil detachment by raindrop impact, F (kg/m²) in Waikhulok watershed

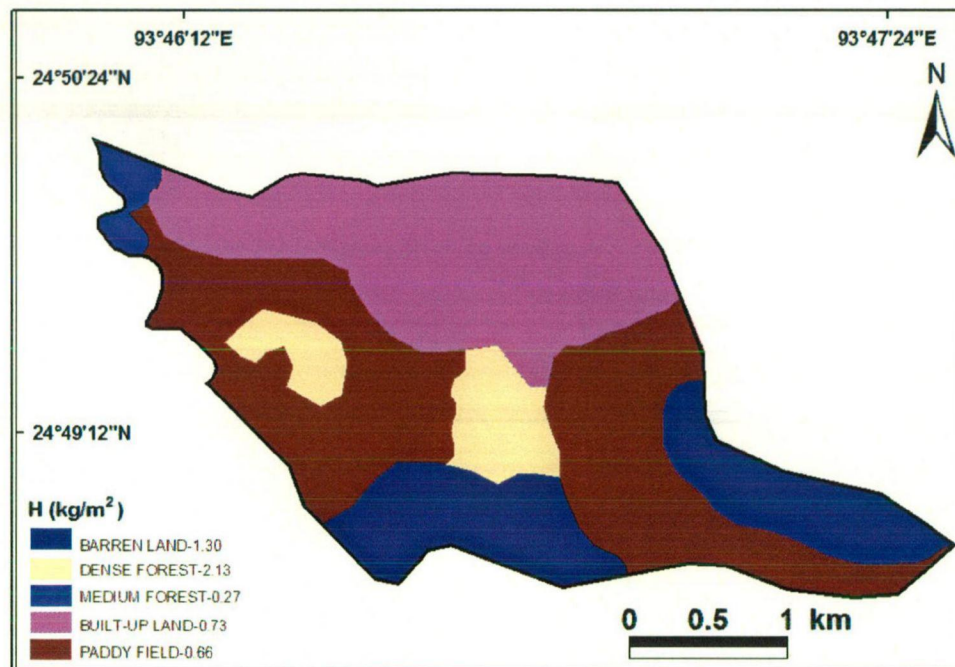


Fig. 6.8: Soil detachment by runoff, H (kg/m²) in Waikhulok watershed

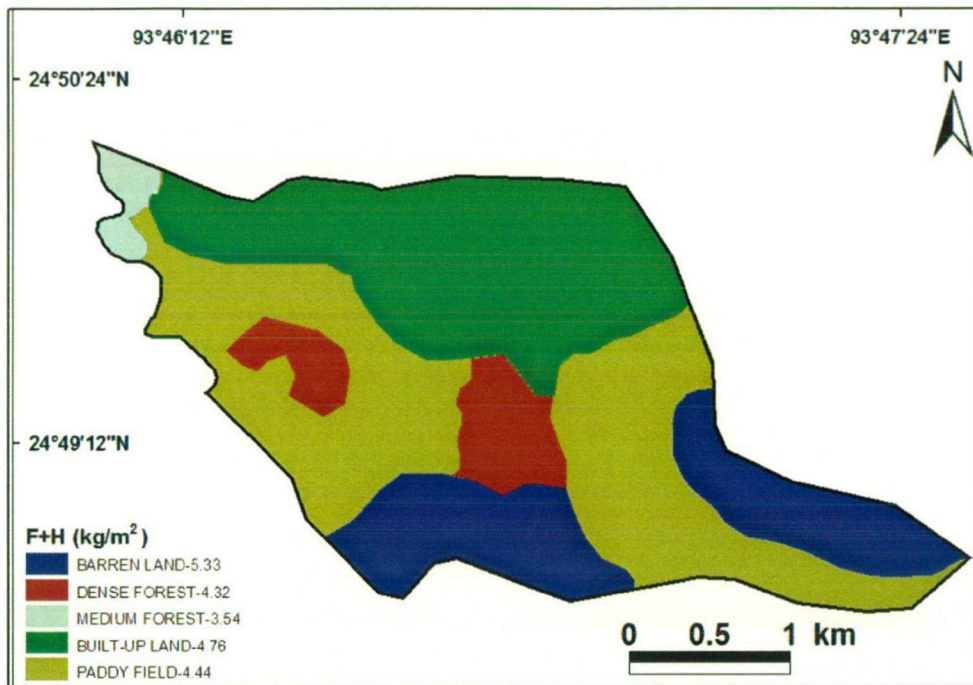


Fig. 6.9: Total annual detachment, F+H (kg/m²) in Waikhulok watershed

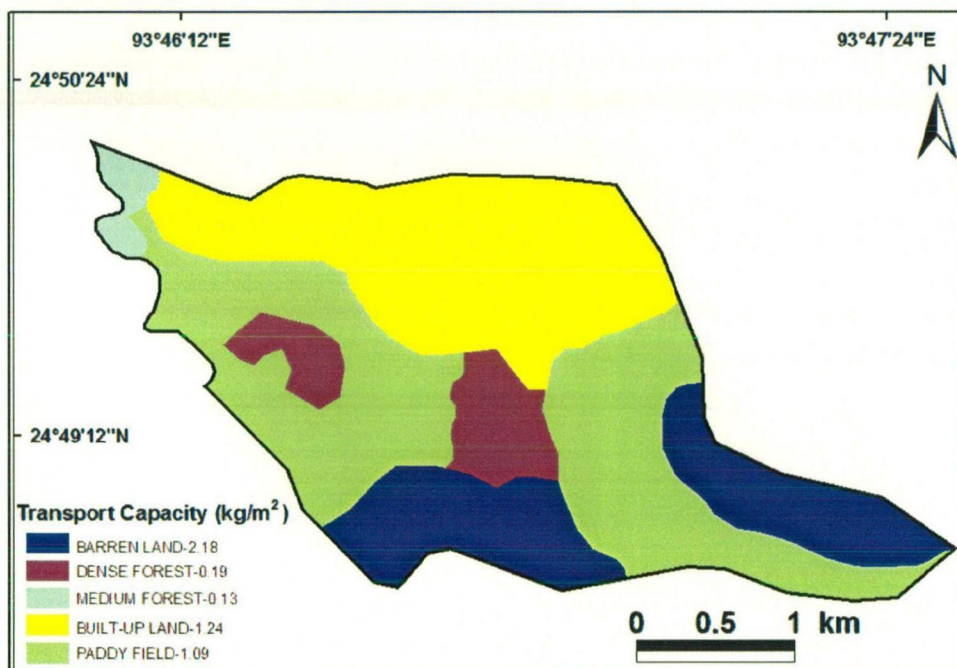


Fig. 6.10: Transport capacity, TC, (kg/m²) in Waikhulok watershed

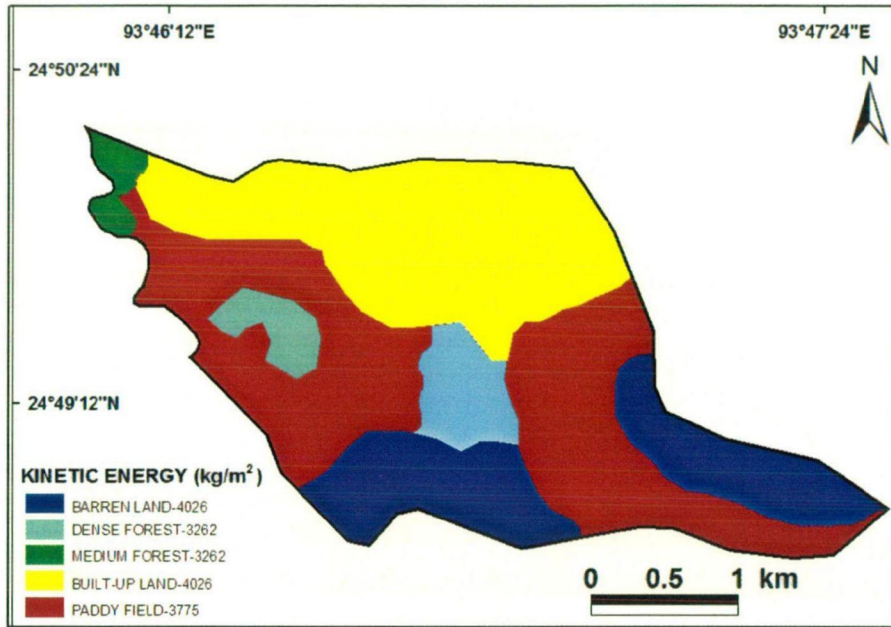


Fig. 6.11: Total kinetic energy (J/m²) in Waikhulok watershed

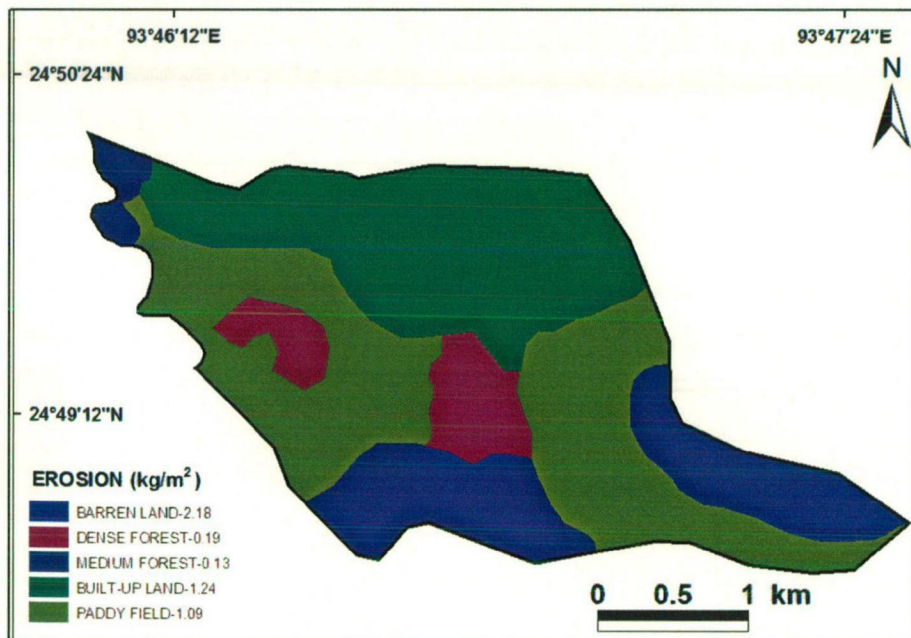


Fig. 6.12: Erosion map of Waikhulok watershed

In contrast, the unsupported ^{210}Pb concentrations associated with cores collected from the medium forest (Fig. 6.13B) depicts a total inventory of 251 mBq/m^2 , which is 23% lower than the dense forest core. The unsupported ^{210}Pb concentrations associated with cores collected from the paddy field (Fig. 6.13C) in the study catchment are essentially uniform throughout the

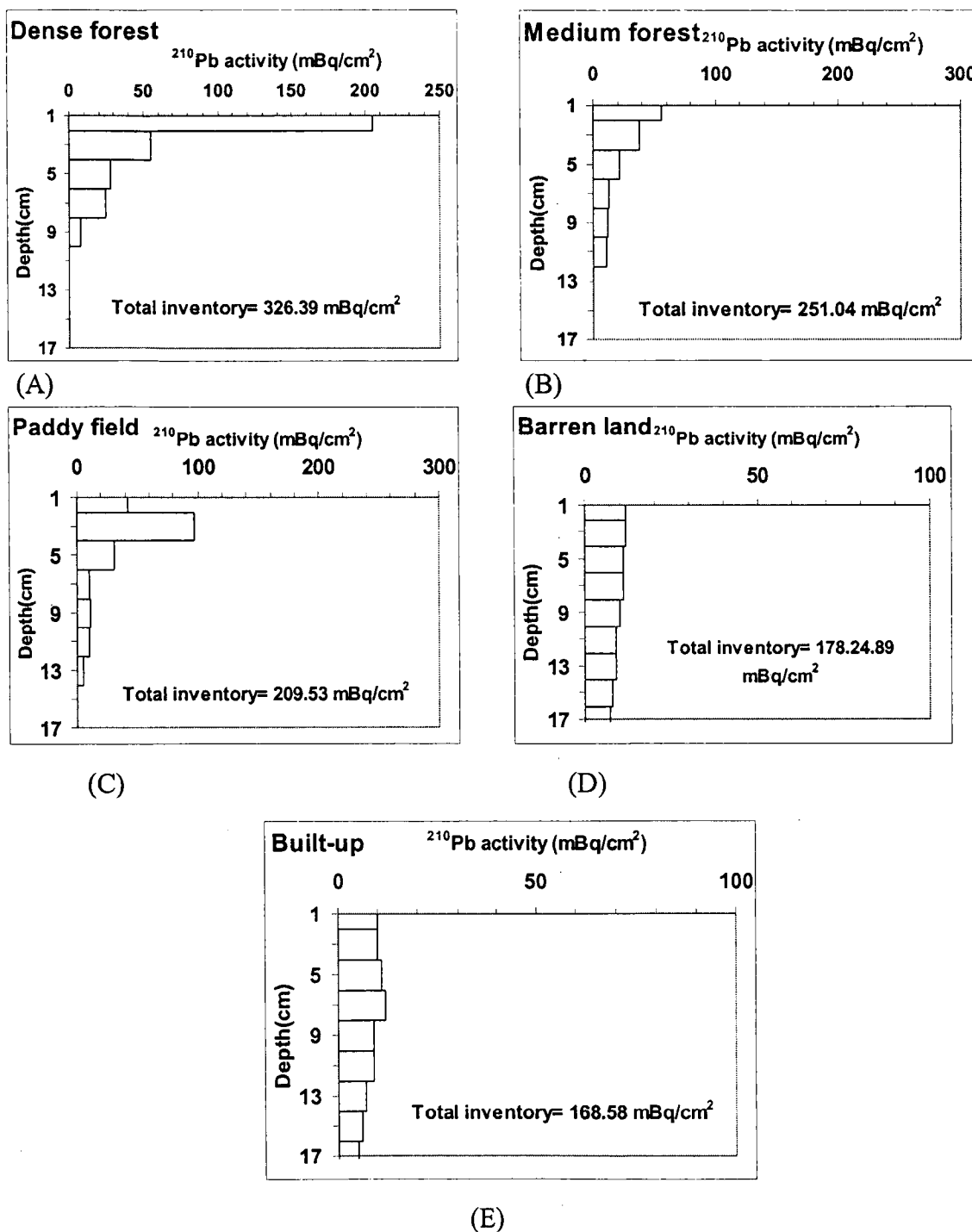


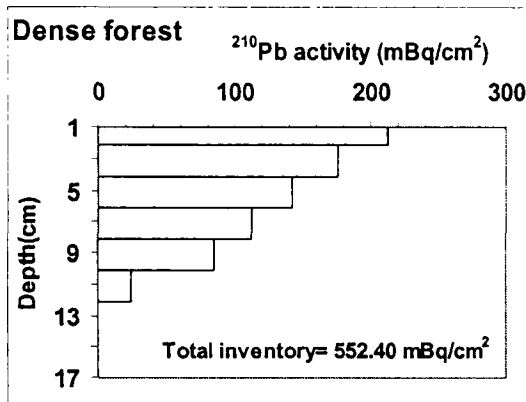
Fig. 6.13: Land use wise ^{210}Pb activity plot in the Awang Khujairok watershed

plough layer, reflecting the mixing caused by tillage. The shape of these profiles conforms to that expected for cultivated soils (He and Walling, 1997). Also, the present profile of this land use is due to the seepage of the ^{210}Pb radionuclide alongwith the infiltrated water in the normally water inundated paddy fields. Unlike observations from other studies conducted elsewhere, greater tillage depths were not observed because modern farming machineries were not in use in the terraced fields. The total inventory of ^{210}Pb for the soil core in paddy field is 36% lower than the inventory measured for the dense forest core (Fig. 6.13A).

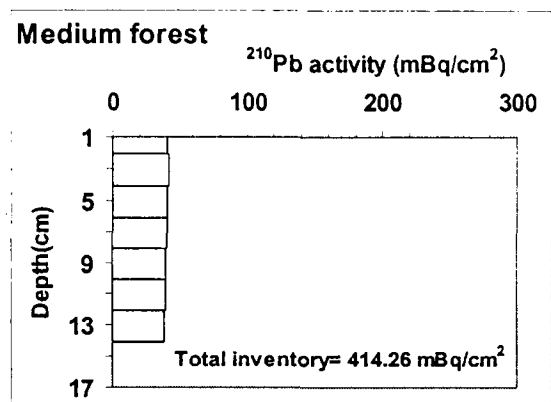
The total inventory in the barren land (Fig. 6.13D) core was 45% lower than the core of the dense forest land use, indicating a huge rate of soil loss. The maximum difference was observed in the case of built-up land (Fig. 6.13E) with 48% difference in the inventory from that of the reference inventory. This indicates that a significant proportion of the fallout input of unsupported ^{210}Pb has been lost from this particular site through erosion.

The results indicate that the longer-term average rates of net soil loss for the principal land use types in the Awang Khujairok catchment can be ranked in the order: built-up land ($1.87 \text{ kg/m}^2/\text{y}$) > barren land ($1.76 \text{ kg/m}^2/\text{y}$) > paddy field ($1.11 \text{ kg/m}^2/\text{y}$) > medium forest ($1.01 \text{ kg/m}^2/\text{y}$) > deep forest ($0.01 \text{ kg/m}^2/\text{y}$).

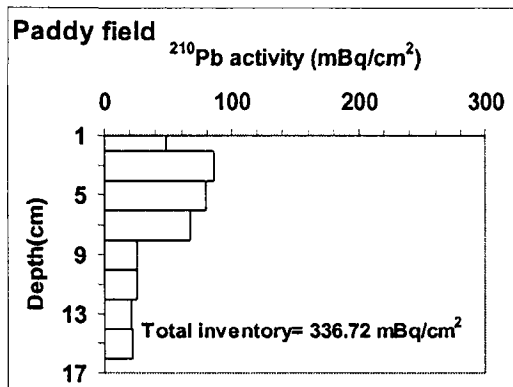
Similarly, in the case of Waikhulok watershed (Fig. 6.14), the highest difference was found in the land use class of barren land (52%) (Fig. 6.14D). This indicates the maximum eroded land use class in this present watershed. The total inventory in case of the paddy filed (Fig. 6.14C) was 336.72 mBq/cm^2 and it was 39% lower than the reference inventory (Fig. 6.14A). The built-up land inventory (292.56 mBq/cm^2) was 47% lesser than the dense forest inventory. The least inventory difference (25%) was observed in case of medium forest (Fig 6.14B) with a total inventory of 414.26 mBq/cm^2 .



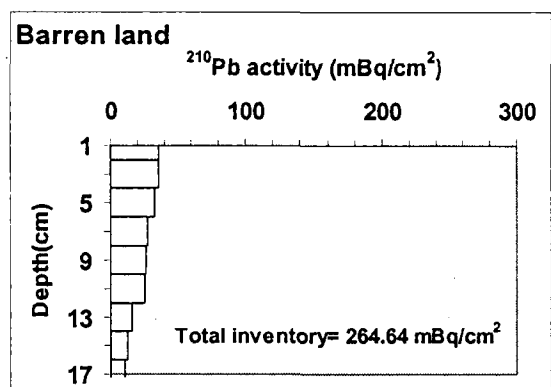
(A)



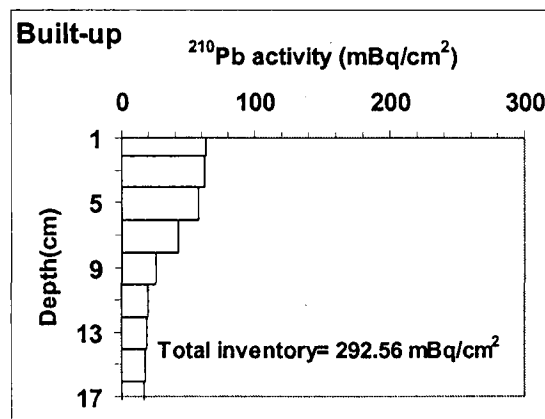
(B)



(C)



(D)



(E)

Fig. 6.14: Land use wise ^{210}Pb activity plot in the Waikhulok watershed

Hence, the longer-term average rates of net soil loss for the principal land use types in the Waikhulok catchment can be ranked in the order: barren land (3.21 kg/m²/y) > built-up (1.98 kg/m²/y) > paddy field (1.24 kg/m²/y) > medium forest (1.12 kg/m²/y) > deep forest (0.18 kg/m²/y).

6.5 COMPARISON OF RESULTS

The soil loss estimated in different types of land use classes by the MMF model in the Awang Khujairok watershed is compared with the observed and estimated values by ²¹⁰Pb dating technique as given in Table 6.4. Except for the barren land, the observed values and those computed using the MMF model are in good agreement. In case of ²¹⁰Pb dating technique, except for the dense forest, the estimated soil loss values are slightly lower than the observed values. This may be because the observed values represent the gross values unlike the values estimated using ²¹⁰Pb dating technique which depict the point values. However the point values may not be always lower as it depends on the location of the experimental site. Therefore, ²¹⁰Pb dating technique, if considered only the erosion aspect (not the depositional aspects) maybe slightly higher or lower, if not estimated at a number of locations and average value considered.

Table 6.4: Land use-wise soil loss in the Awang Khujairok watershed

Land use pattern	Soil loss (kg/m ² /y)		
	Observed value (WAPCOS)	Estimated value (Nuclear technique)	Estimated value (MMF)
Paddy field	1.54	1.11	1.24
Medium forest	1.96	1.01	1.66
Built-up land	1.23	1.87	1.24
Dense Forest	0.01	0.01	0.21
Barren land	4.28	1.76	2.12

The unexpected high value of soil loss in barren land in the Awang Khujairok watershed (4.28 kg/m^2) seem to be erroneous, keeping in view the area of barren land use in the watershed is 2.12 km^2 and 3.39 km^2 in the Waikhulok watershed where the observed value of soil loss is almost half.

The estimated values of soil loss using the MMF model are slightly higher than those determined using the ^{210}Pb dating technique except in case of built up land. This may be because of the specific location of the experimental site in the built up land use where the higher runoff might have resulted in higher soil erosion.

In the case of Waikhulok watershed, the observed trend of variation in the soil loss estimated using ^{210}Pb dating technique, MMF model and those observed experimentally (Table 6.5) is different from the corresponding values in the Awang Khujairok watershed (Table 6.4). The values computed using MMF model are in good agreement with those observed except in case of medium forest that are slightly lower, while the values obtained using the ^{210}Pb dating technique are slightly higher than the observed data in case of built

Table 6.5: Land use-wise soil loss in the Waikhulok watershed

Land use pattern	Soil loss ($\text{kg/m}^2/\text{y}$)		
	Observed value (WAPCOS)	Estimated value (Nuclear technique)	Estimated value (MMF)
Paddy field	1.21	1.24	1.09
Medium forest	1.96	1.12	1.31
Built-up land	1.32	1.98	1.24
Dense Forest	0.21	0.18	0.19
Barren land	2.34	3.21	2.18

up and barren land use classes, slightly lower in case of medium forest and in good agreement in case of paddy field and dense forest.

The comparison of soil loss computed using MMF model and those estimated using ^{210}Pb dating technique are found in good agreement in case of paddy field, medium

forest and dense forest while the model yields slightly lower values in case of built up land and barren land. But as these values are close to the observed data, therefore the validity of the MMF model seems to be satisfactory as the site specific values obtained in case of ^{210}Pb dating techniques may be slightly higher or lower if the numbers of sediment cores representing the different land use classes are limited.

The graphical comparison of the soil erosion estimated by the MMF model with the observed values and also with the values estimated by the ^{210}Pb dating technique for the Awang Khujairok watershed is given in Fig. 6.15 and Fig. 6.16. The coefficient of determination (R^2) for the comparison of MMF result with the observed soil loss is 0.858, showing a good agreement between the two sets of data. The comparison of MMF result with the ^{210}Pb dating technique result gave a R^2 value of 0.787. This slightly lesser value is because of the reason that the MMF results represent the gross values and those from the nuclear technique showed the point values. In case of Waikhulok watershed, the comparison of MMF result with the observed soil loss gave the coefficient of determination as 0.91. The comparison of MMF result with the ^{210}Pb dating technique result exhibited a coefficient of determination of 0.888, which showed a good agreement in this watershed. This investigation therefore confirms the potential for using the MMF model for the present study area and also the use of unsupported ^{210}Pb measurements as a very reliable method to validate the soil erosion estimated by the model.

6.5.1 Error

The root mean square error (RMSE) is a quadratic scoring rule which measures the average magnitude of the error. Expressing the formula in words, the difference between forecast and corresponding observed values are each squared, added up for all the data points and then averaged over the sample by dividing by the number of points. The

squaring is done so that the negative values do not cancel out the positive values. Finally, the square root of the average is taken.

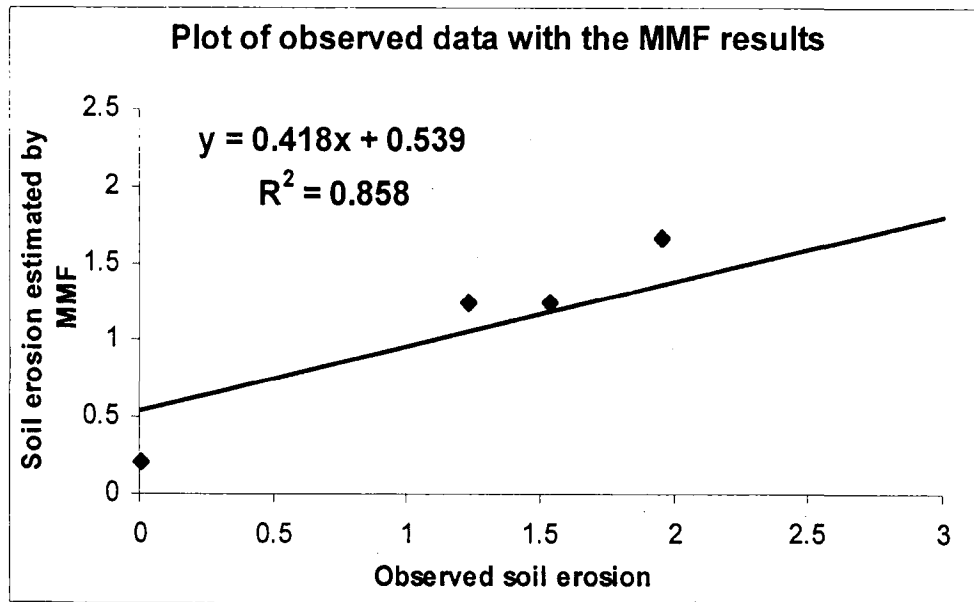


Fig 6.15: Comparison of observed and estimated (MMF) soil erosion for Awang Khujairok watershed

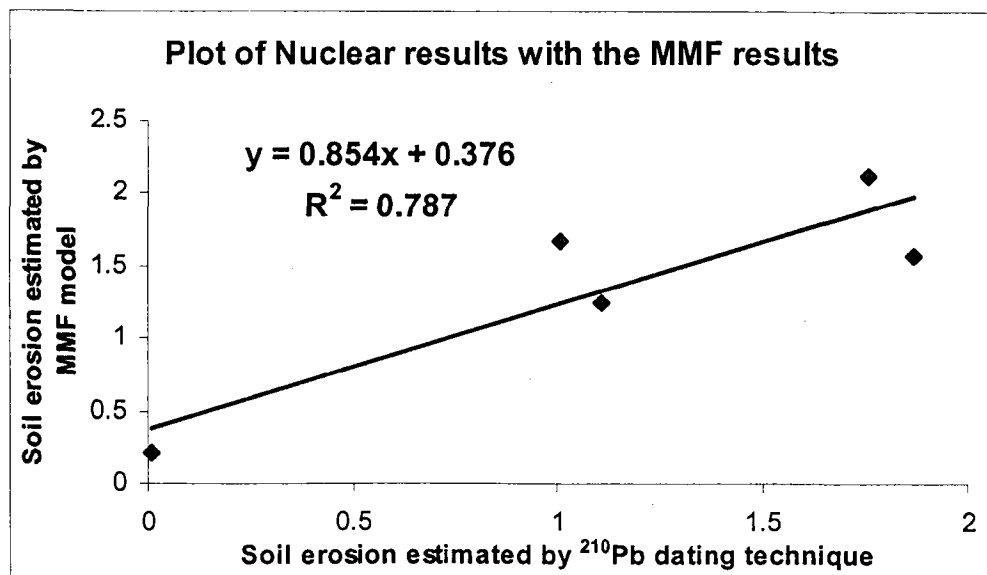


Fig 6.16: Comparison of soil erosion estimated by MMF model and ^{210}Pb dating technique for Awang Khujairok watershed

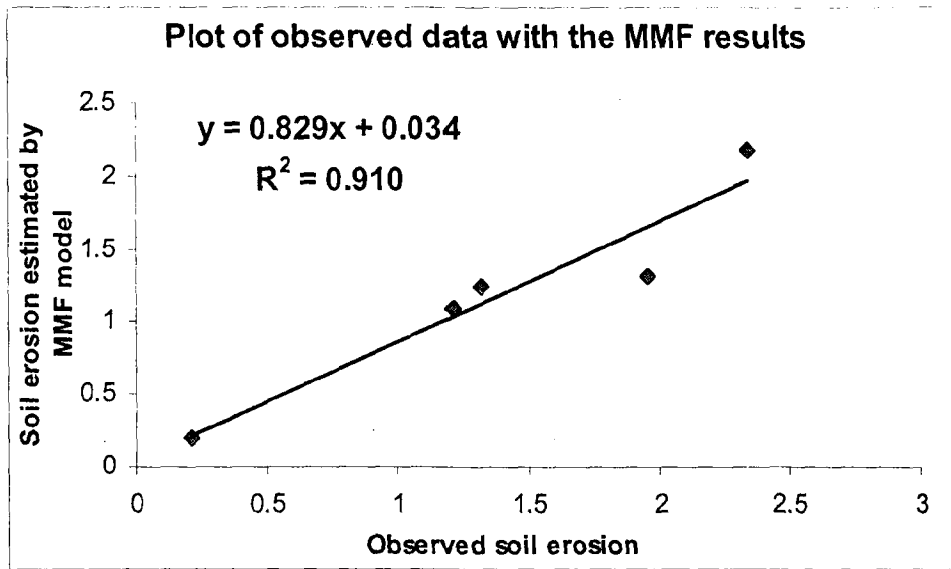


Fig 6.17: Comparison of observed and estimated (MMF) soil erosion for Waikhulok watershed

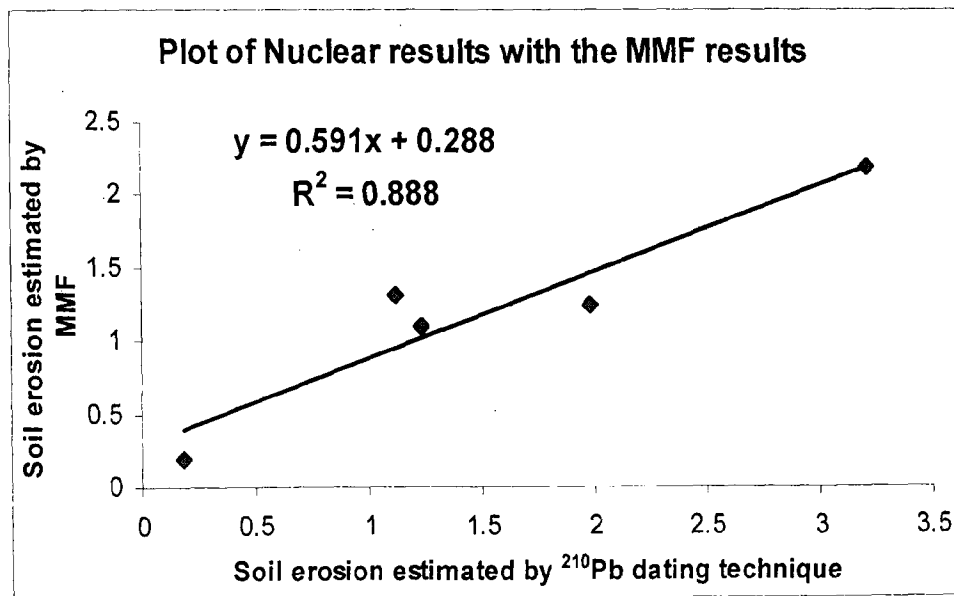


Fig 6.18: Comparison of soil erosion estimated by MMF model and ^{210}Pb dating technique for Waikhulok watershed

Since the errors are squared before they are averaged, the RMSE gives a relatively high weight to large errors. This means the RMSE is most useful when large errors are particularly undesirable. The smaller the Mean Squared Error, the closer the fit is to the data. The MSE has the units squared of whatever is plotted on the vertical axis.

As can be seen from the Table 6.6, the RMSE was lesser in the case of the MMF for both the watersheds considered. The lesser values were seen in the Waikhulok watershed. So this implies that the Morgan Morgan Finney model is more suited to the watersheds.

Table 6.6: Comparison of the RMSE of results obtained from the two techniques

Watersheds	MMF model	Nuclear technique
Awang Khujairok watershed	0.99	1.25
Waikhulok watershed	0.30	0.61

6.6 ESTIMATION OF EROSION RATES IN OTHER WATERSHEDS

The database for all the 27 watersheds have been developed in GIS and land use map for each watershed were also generated. The remaining watersheds are morphologically homogeneous with the two watersheds. On field surveys, it was observed that the pattern of land use classes was almost the same, albeit in different proportion. Hence the erosion rates in the remaining 25 watersheds of the Loktak catchment have been determined (Table 6.7) by using the MMF model for the land use prevalent in those watersheds. The slope is also an important parameter in soil erosion assessment as discussed in the next section. But all the other watersheds represent more or less same type

of topography. Therefore, slope has not been considered for soil erosion estimation in the remaining watersheds.

The highest erosion rates were observed in the barren land class and the least in the dense forest. Thongjaorok and Haibirok watersheds showed an abnormally high rate of erosion in the barren class. The barren land in these two watersheds has very sparse vegetation cover.

6.6.1 Analysis of Effect of Change of Slope on Soil Erosion

In this study, an analysis has been performed to understand the effect of change in slope on soil erosion rate. The change in the slope was considered from ($\pm 1\%$, to $\pm 5\%$) of slope while other parameters were kept constant. The results are reported as the percentage change in the value of soil loss accompanying the percentage changes in slope (Table 6.9). For the paddy field in the Awang Khujairok watershed, the estimated changes in erosion rate are within the range of -0.99% to $+0.77\%$ in case of change of parameter slope from -1% to $+1\%$. A variation of the slope in the range of -5% to $+5\%$ yields a change of -4.86% to $+4.80\%$. For the same watershed, the change of $+1\%$ slope in the medium forest yields the same change as in the paddy field. But a change of $+5\%$ and -5% in slope percentage change was noted as -4.35% and $+4.53\%$. In the dense forest, the percentage

Table 6.7: Erosion rates in the different land use patterns in the watersheds of the catchment

Sl. No.	Code	Name	Erosion rate (kg/m ² /y)				
			Agricultural land	Medium forest	Built-up	Barren land	Dense forest
1	3D2A5a1	Turelu	1.24	0.99	1.77	2.12	0.15
2	3D2A5a2	Moirang Turel	1.42	0.69	1.59		0.12
3	3D2A5a3	Mashem (Kwakta)	0.35	5.94	1.42	3.39	0.12
4	3D2A5a4	Laijamaril	1.50	-	0.88	4.24	-
5	3D2A5a5	Wangtha	1.42	0.99	1.77	-	-
6	3D2A5a6	Thingin	1.42	0.99	1.77	-	-
7	3D2A5a7	Irum	1.42	0.99	1.77	-	-
8	3D2A5a8	Lenghanbi	1.42	-	0.88	6.36	
9	3D2A5a9	Awang Khujairok	1.24	1.48	1.24	2.12	0.09
10	3D2A5a10	Ningthoukhong	1.11	0.19	4.43	4.24	-
11	3D2A5a11	Charoikhui	1.11	-	1.77	16.96	-
12	3D2A5a12	Kongdun	1.11	0.99	2.65	1.06	-
13	3D2A5a13	Nungshai	1.42	0.79	1.77	0.85	-
14	3D2A5a14	Keinou	1.50	-	1.77	2.12	-
15	3D2A5a15	Thongjaorok	1.50	0.99	-	33.92	-
16	3D2A5a16	Aigejang	0.71	0.99	-	21.2	-
17	3D2A5a17	Ishinglok	0.71	-	1.77	8.48	0.29
18	3D2A5a18	Waikhulok	1.24	-	1.77	21.2	0.29
19	3D2A5a19	Wakching	0.71	-	0.88	2.12	0.15
20	3D2A5a20	Sajirok	1.06	-	0.35	14.84	0.09
21	3D2A5a21	Haibirok	0.177	-		29.68	0.59
22	3D2A5a22	Khonga	0.67	-	0.35	25.44	-
23	3D2A5a23	Phayeng	1.68	-	0.88	-	-
24	3D2A5a24	Kangchup	0.67	-	3.01	19.08	-
25	3D2A5a26	Kharamkom	1.68	-	0.88	-	-
26	3D2A5a27	Singda	-	0.99	2.12	33.07	-
27	3D2A5a28	Songtum	1.06	-	1.42	13.56	-

Table 6.8: Effect of change of slope on soil erosion in the Awang Khujairok watershed

Percentage Change in parameter	Paddy		Medium forest		Built-up land		Barren land		Dense forest	
	Simulated soil loss	Percent Change	Simulated soil loss	Percent Change	Simulated soil loss	Percent Change	Simulated soil loss	Percent Change	Simulated soil loss	Percent Change
+1	1.25	+0.77	1.50	+0.77	1.25	+0.96	2.15	+1.11	0.21	+0.87
+2	1.26	+1.91	1.52	+1.79	1.26	+1.90	2.16	+1.86	0.21	+1.61
+3	1.28	+2.87	1.53	+2.81	1.27	+2.87	2.18	+2.85	0.21	+2.62
+4	1.29	+3.85	1.54	+3.55	1.28	+3.84	2.19	+3.59	0.21	+3.47
+5	1.30	+4.80	1.49	+4.70	1.30	+4.80	2.28	+4.53	0.22	+4.04
-1	1.23	-0.99	1.48	-0.54	1.23	-0.99	2.11	-0.77	0.21	-0.87
-2	1.22	-1.96	1.46	-2.08	1.22	-1.96	2.09	-1.72	0.20	-2.28
-3	1.20	-2.93	1.45	-2.82	1.20	-2.93	2.07	-2.47	0.20	-2.58
-4	1.19	-3.89	1.43	-3.84	1.19	-3.89	2.05	-3.46	0.20	-3.49
-5	1.18	-4.86	1.48	-4.74	1.18	-4.86	2.03	-4.35	0.19	-4.58

Table 6.9: Effect of change of slope on soil erosion in the Waikhulok watershed

Percentage Change in parameter	Paddy		Medium forest		Built-up land		Barren land		Dense forest	
	Simulated soil loss	Percent Change	Simulated soil loss	Percent Change	Simulated soil loss	Percent Change	Simulated soil loss	Percent Change	Simulated soil loss	Percent Change
+1	1.10	+0.97	1.32	+0.73	1.25	+0.94	2.20	+0.81	0.19	+0.87
+2	1.11	+1.94	1.33	+1.72	1.26	+1.91	2.22	+1.73	0.20	+1.64
+3	1.12	+2.91	1.35	+2.79	1.28	+2.87	2.24	+2.66	0.21	+2.49
+4	1.13	+3.85	1.36	+3.56	1.29	+3.84	2.26	+3.52	0.20	+3.30
+5	1.14	+4.82	1.31	+4.59	1.30	+4.82	2.28	+4.29	0.20	+4.18
-1	1.08	-1.02	1.29	-1.29	1.23	-0.99	2.17	-0.92	0.19	-0.92
-2	1.07	-2.03	1.28	-2.04	1.22	-1.96	2.15	-1.76	0.19	-1.76
-3	1.06	-2.95	1.27	-2.85	1.20	-2.93	2.13	-2.68	0.19	-2.73
-4	3.85	-3.88	1.26	-3.85	1.19	-3.89	2.11	-3.59	0.19	-3.52
-5	1.04	-4.85	1.30	-4.88	1.18	-4.85	2.09	-5.47	0.18	-4.45

A comparative plot is a graphical comparison of the percent change in objective function and the percentage change in a parameter value. The analysis of effect of slope performed is shown in the form of plots (Fig. 6.19 and 6.20). All the plots shown in the figure shows that the trend of the curve is linear.

The analysis of change of slope on soil erosion rate has revealed slope is sensitive in the MMF model in the determination of soil loss. But since the slope variation in the catchment is not very significant, the variables namely land use and rainfall have been considered for estimation of soil loss in other land use classes. But as similar land use practices are being followed in all the watersheds in the western catchment, albeit, in varying degrees, rainfall was considered as the main variable. Therefore, an empirical relation between the effective rainfall of 6 years (2000-2005) and the soil erosion rate was developed for each land use for both the watersheds. It was observed that the soil loss rate obtained from the relation for the seventh year, i.e. 2006 was in good agreement with the erosion rate obtained for the same year from the MMF model the details of which are described in subsequent section. The details of the empirical relation developed between rainfall and soil erosion rate are discussed in the next section.

6.7 DEVELOPMENT OF EMPIRICAL MODEL FOR SOIL EROSION

The revised MMF model for the estimation of soil erosion in Loktak Lake has been found satisfactory. In the model, the two main parameters-land use and rainfall are considered to arrive at some suitable relationship between the soil erosion and effective rainfall for different land use. Therefore rates of soil erosion have been computed by the MMF model for 6 years out of the seven years for which the rainfall data were available. Then for each land use, the soil erosion rates are plotted against the effective rainfall. The effective rainfall is also plotted against the estimated soil erosion for the individual land

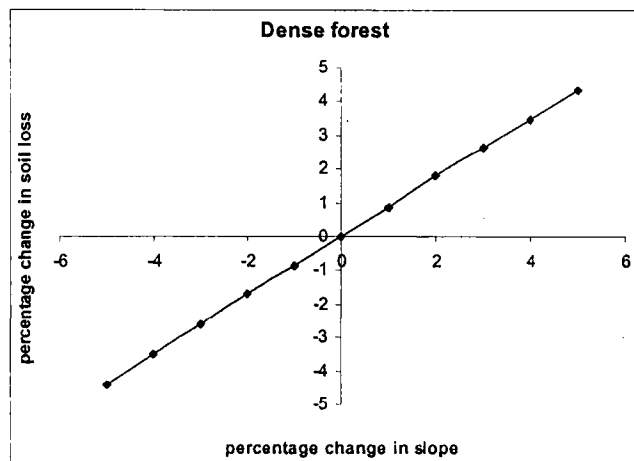
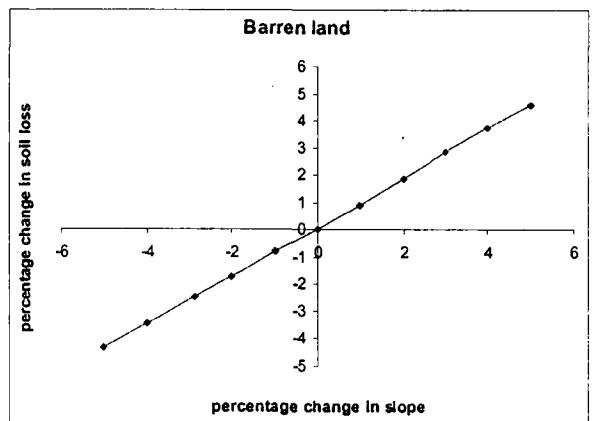
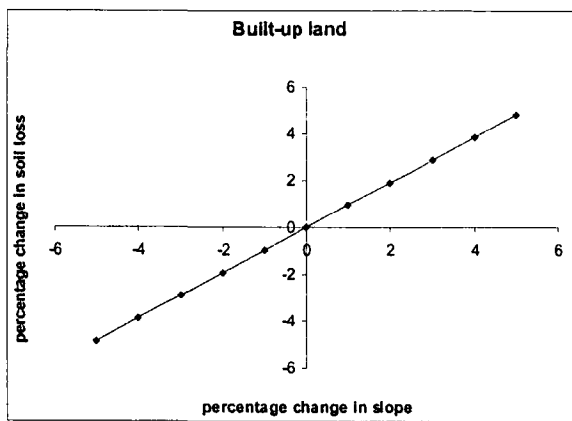
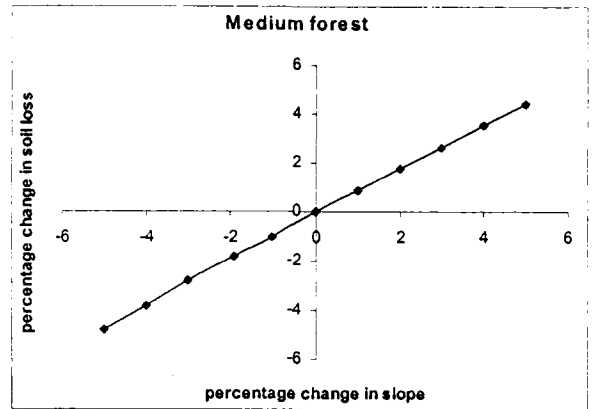
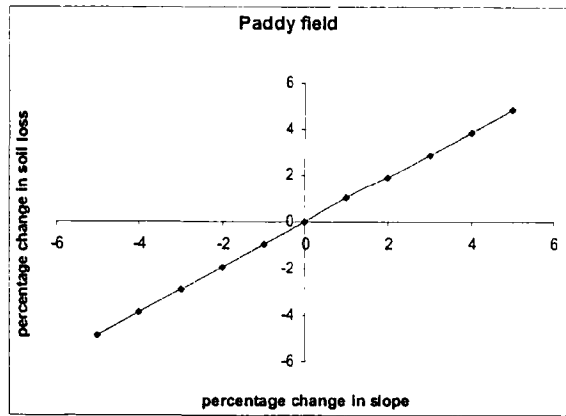


Fig. 6.19: Effect of change of slope on soil erosion for the Awang Khujairok watershed

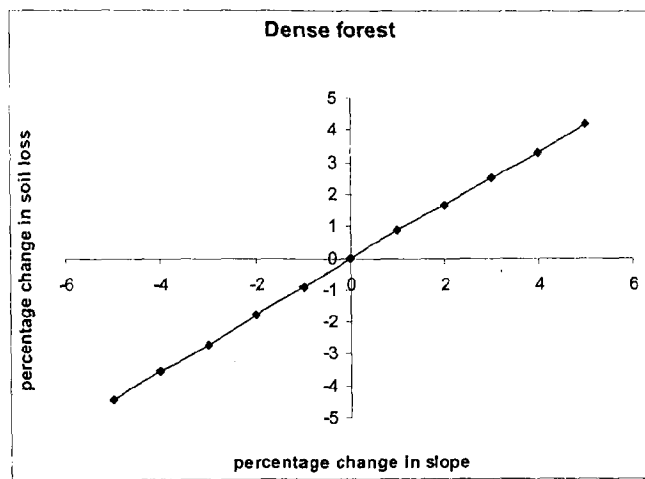
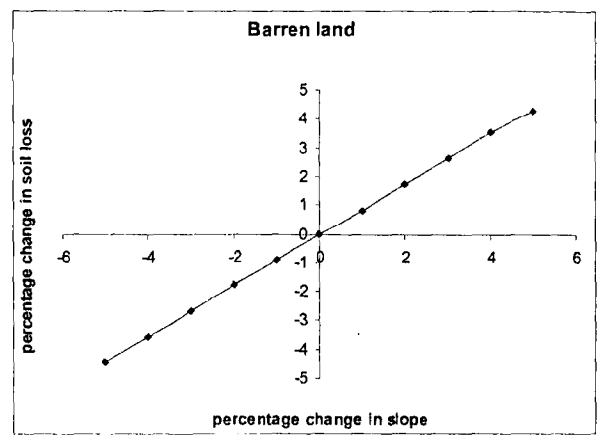
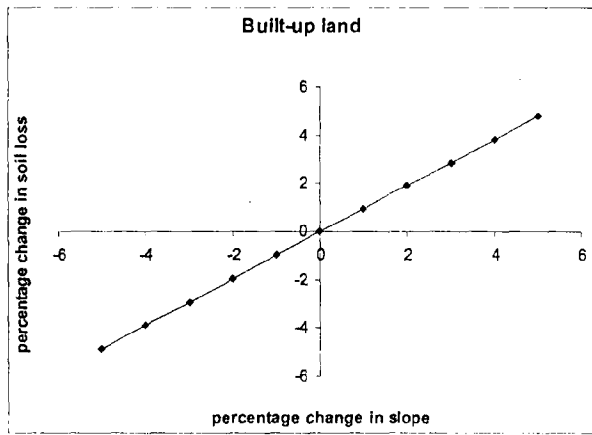
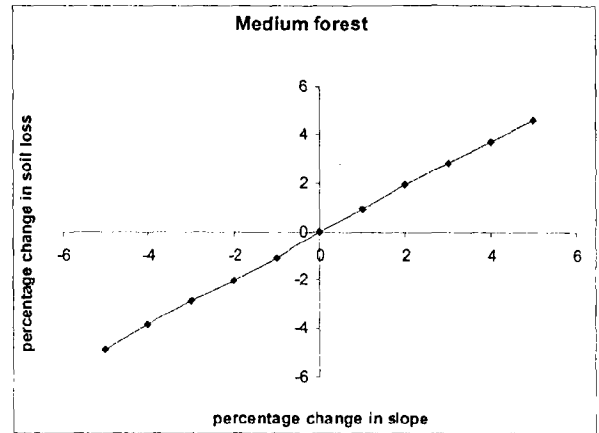
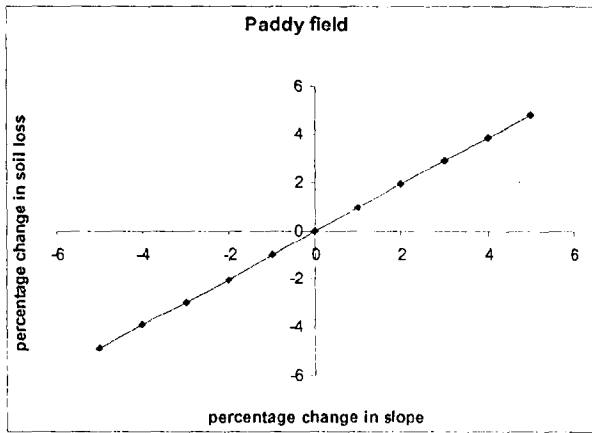


Fig. 6.20: Effect of change of slope on soil erosion for the Waikhulok watershed

use for the Awang Khujairok watershed (Fig. 6.21 to Fig. 6.25) and empirical relation have been developed.

Similarly, the plots were prepared for the Waikhulok watershed and the corresponding empirical relations are developed (Fig. 6.26 to Fig. 6.30).

The watersheds in the western catchment of the lake were morphologically homogeneous with almost the same pattern of land use classes. Also, as can be seen from the Digital Elevation model (Fig 5.2) the slope variation was not much, the empirical relations derived for the two watersheds were combined to have a single empirical equation and the same is used to derive the soil erosion rates for the remaining watersheds in the catchment. Figures 6.31 to 6.35 show the combined plots of effective rainfall and the soil estimated erosion in the two watersheds. Empirical relations between the effective rainfall and the soil erosion rates for each land use are also derived.

Regression analysis is performed on the effective rainfall-soil erosion data set of the two watersheds as well as the combined set of the two watersheds to check the efficacy of the empirical relationships obtained. Correlation, also called correlation coefficient, indicates the strength and direction of a linear relationship between two random variables. In general statistical usage, correlation or co-relation refers to the departure of two variables from independence, although correlation does not imply causation (Rummel, 1970).

In case of the Awang Khujairok watershed, for the data set of rainfall-soil erosion in the paddy field, the coefficient of determination ranged from 0.924 (in medium forest) to 0.999 (in paddy field and dense forest). This indicates a very good correlation between

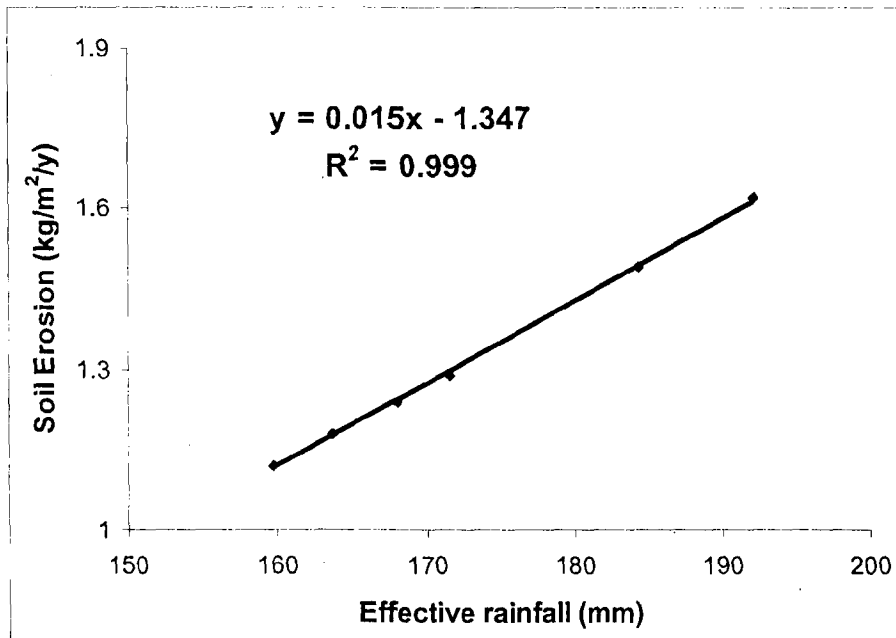


Fig. 6.21: Plot of effective rainfall (mm) & soil erosion rate (kg/m²/y) for the paddy field in the Awang Khujairok watershed

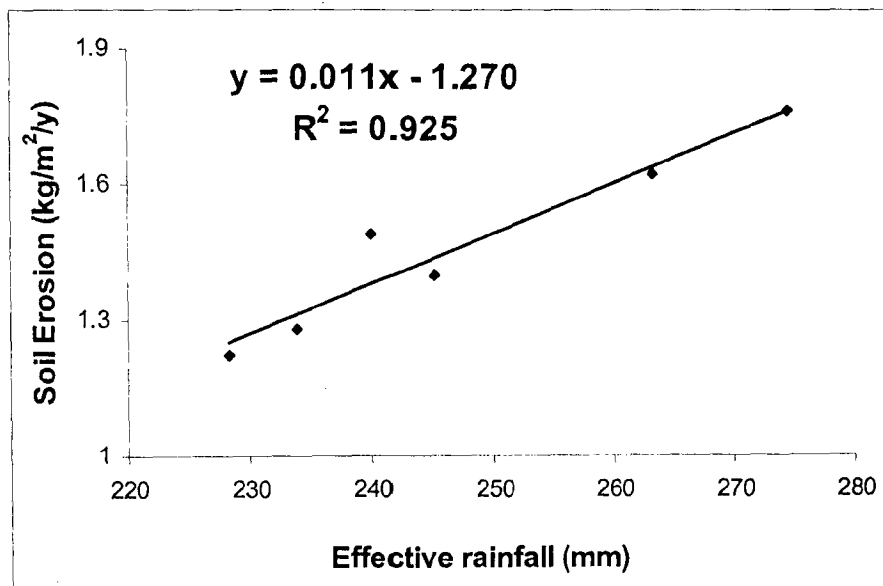


Fig. 6.22: Plot of effective rainfall (mm) & soil erosion rate (kg/m²/y) for the medium forest in the Awang Khujairok watershed

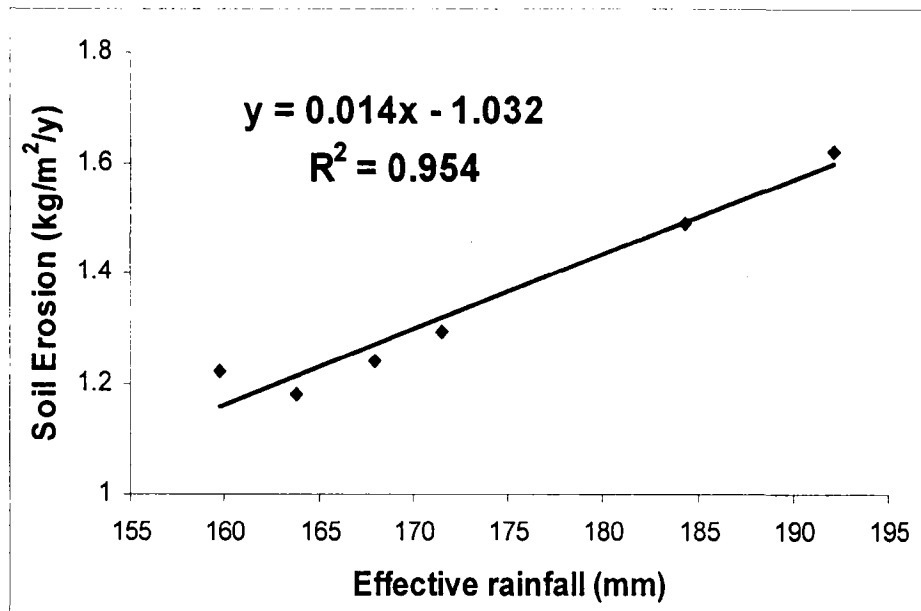


Fig. 6.23: Plot of effective rainfall (mm) & soil erosion rate (kg/m²/y) for the built-up land in the Awang Khujairok watershed

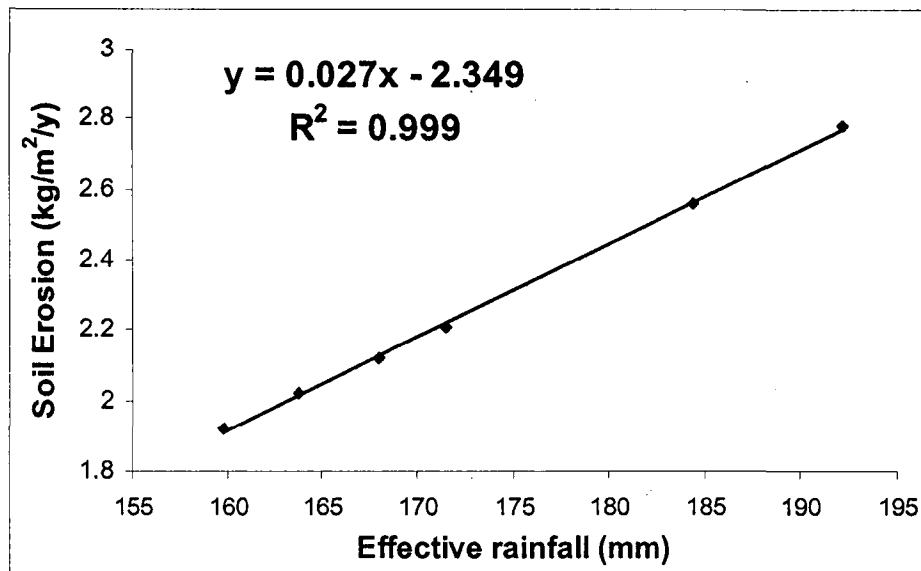


Fig. 6.24: Plot of effective rainfall (mm) & soil erosion rate (kg/m²/y) for the barren land in the Awang Khujairok watershed

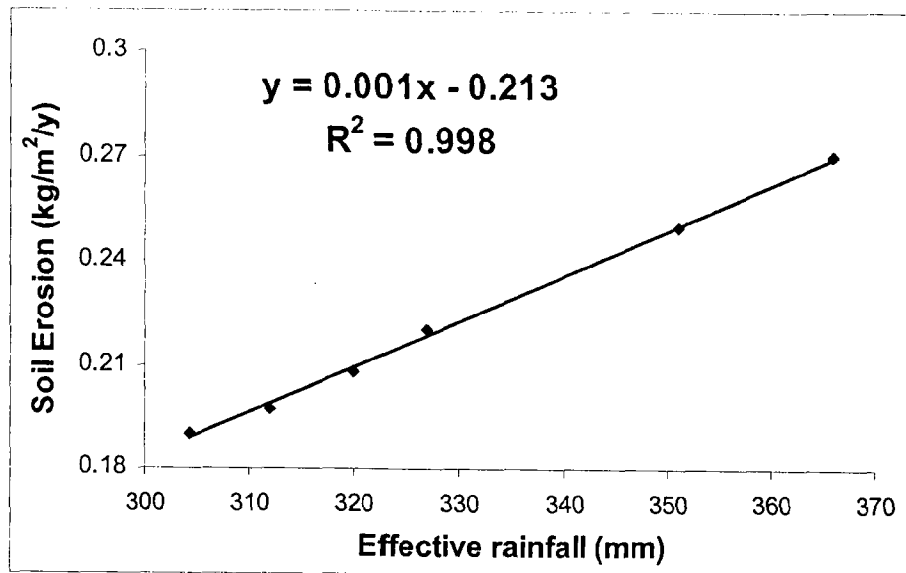


Fig. 6.25: Plot of effective rainfall (mm) & soil erosion rate (kg/m²/y) for the dense forest in the Awang Khujairok watershed

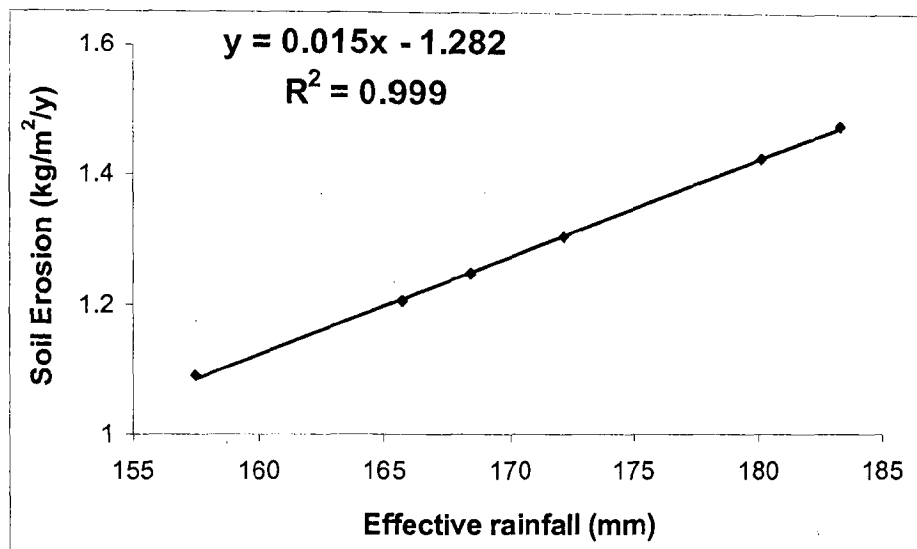


Fig. 6.26: Plot of effective rainfall (mm) & soil erosion rate (kg/m²/y) for the paddy field in the Waikhulok watershed

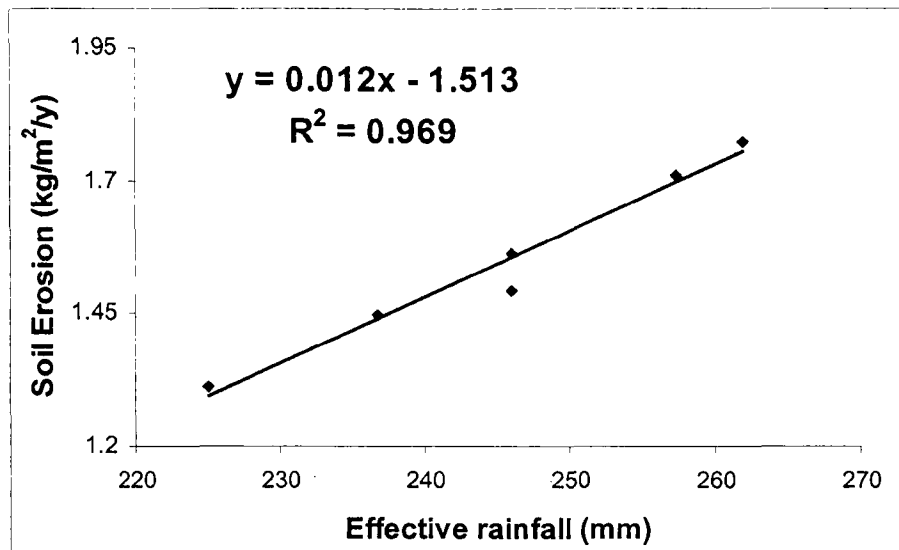


Fig. 6.27: Plot of effective rainfall (mm) & soil erosion rate (kg/m²/y) for the medium forest in the Waikhulok watershed

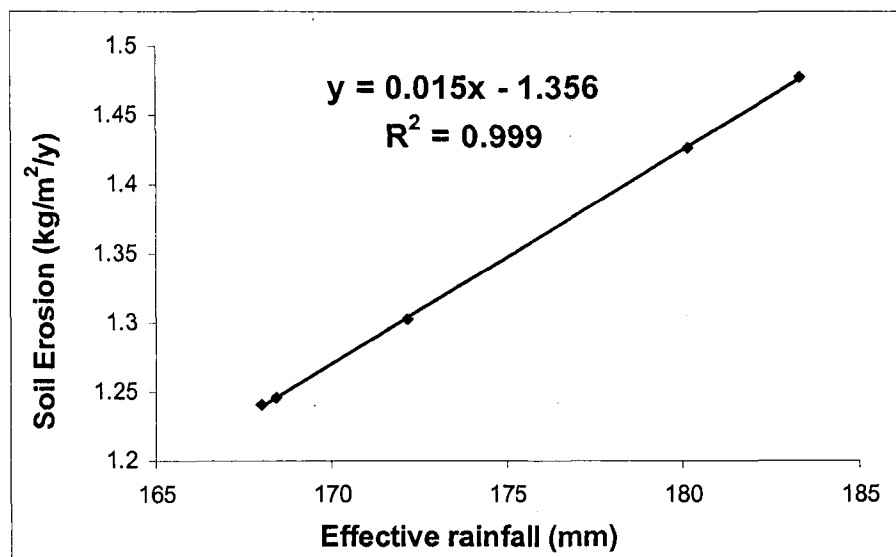


Fig. 6.28: Plot of effective rainfall (mm) & soil erosion rate (kg/m²/y) for the built-up land in the Waikhulok watershed

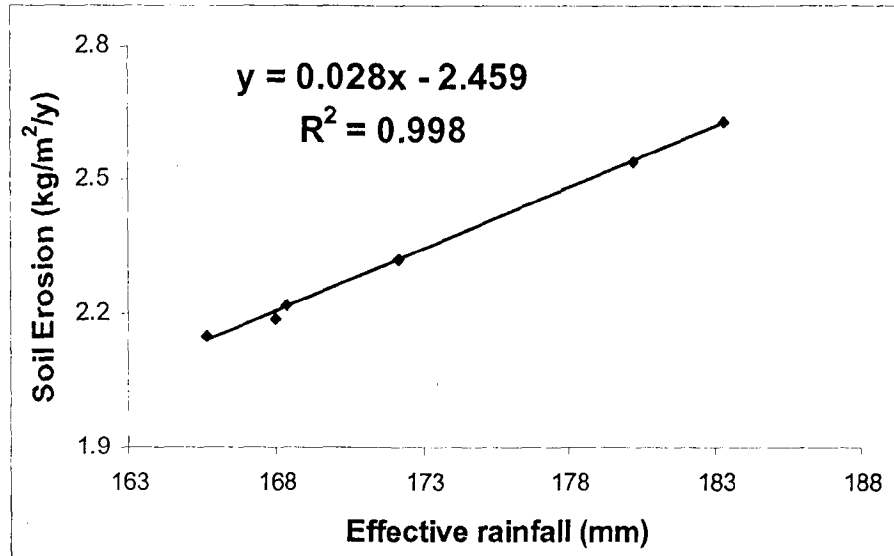


Fig. 6.29: Plot of effective rainfall (mm) & soil erosion rate (kg/m²/y) for the barren land in the Waikhulok watershed

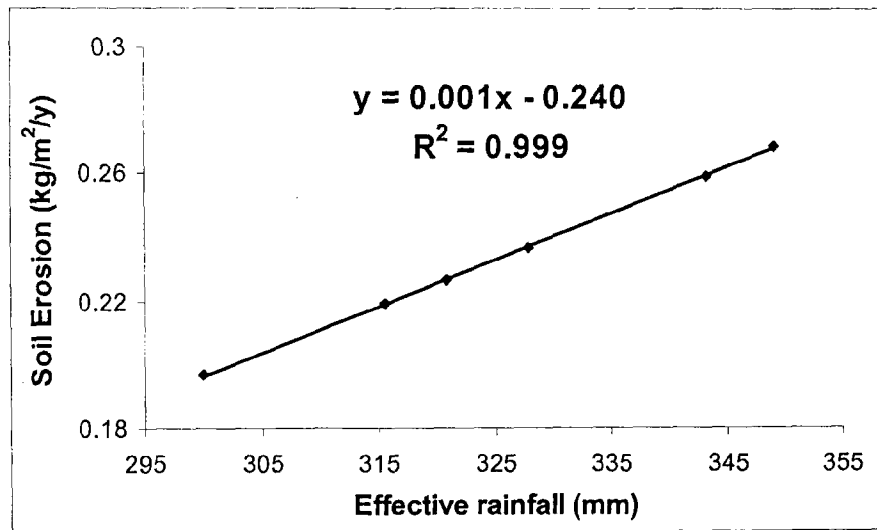


Fig. 6.30: Plot of effective rainfall (mm) & soil erosion rate (kg/m²/y) for the dense forest in the Waikhulok watershed

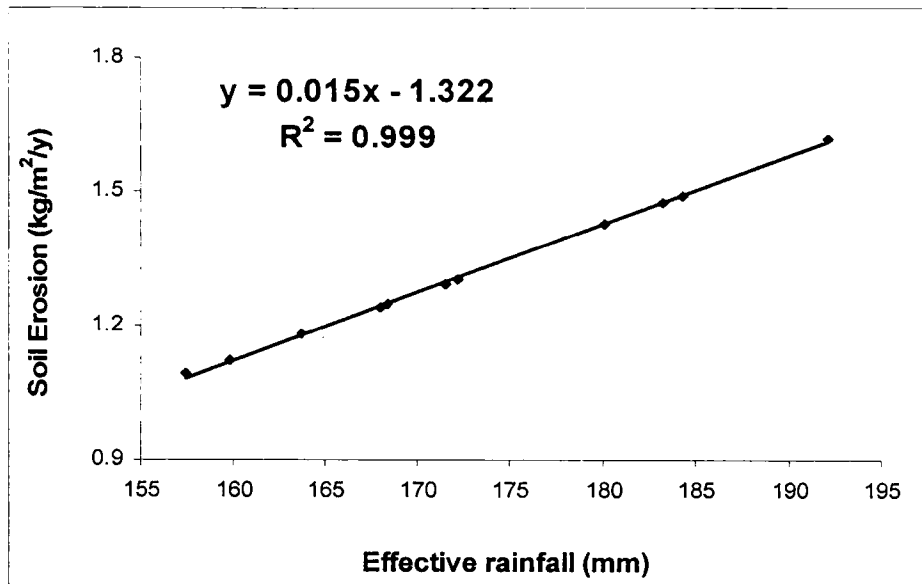


Fig.6.31: Combined plot for the Awang Khujairok and the Waikhulok watersheds for the paddy field

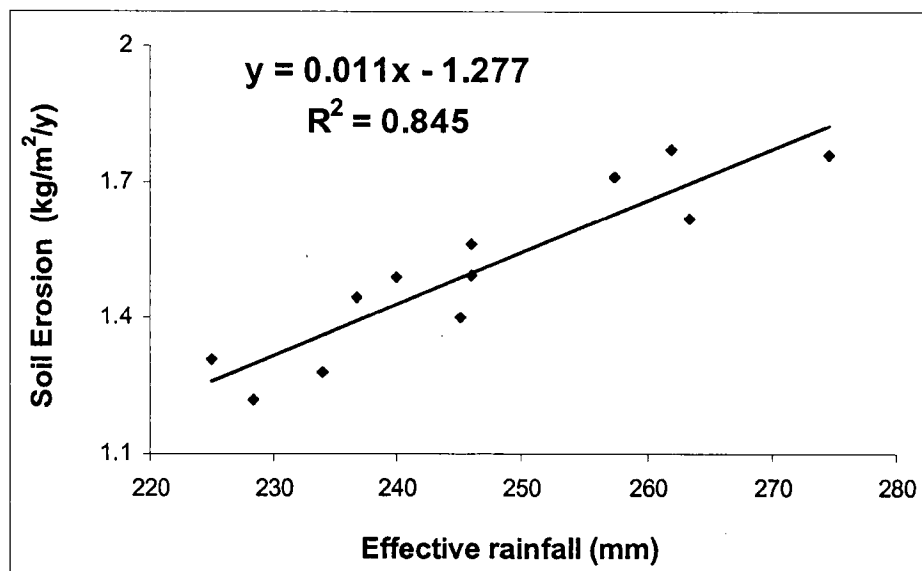


Fig.6.32: Combined plot for the Awang Khujairok and the Waikhulok watersheds for medium forest

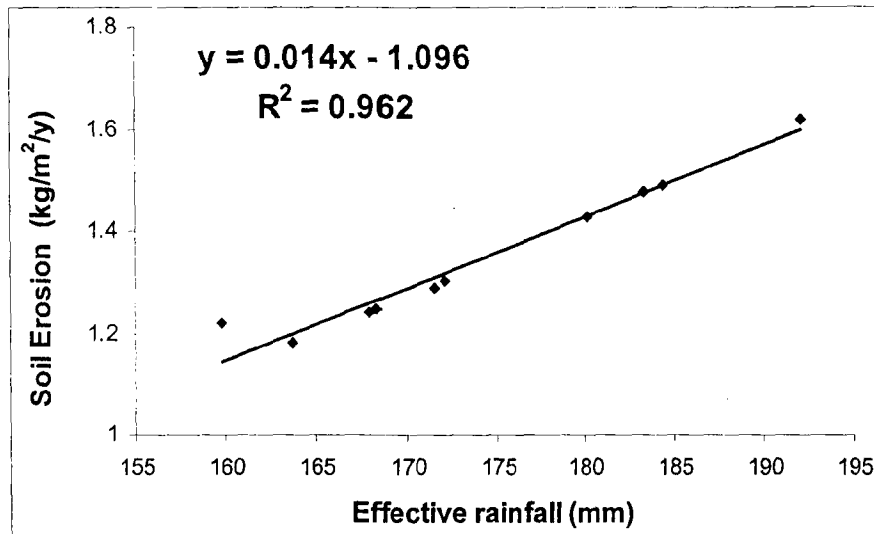


Fig 6.33: Combined plot for the Awang Khujairok and the Waikhulok watersheds for the built-up land

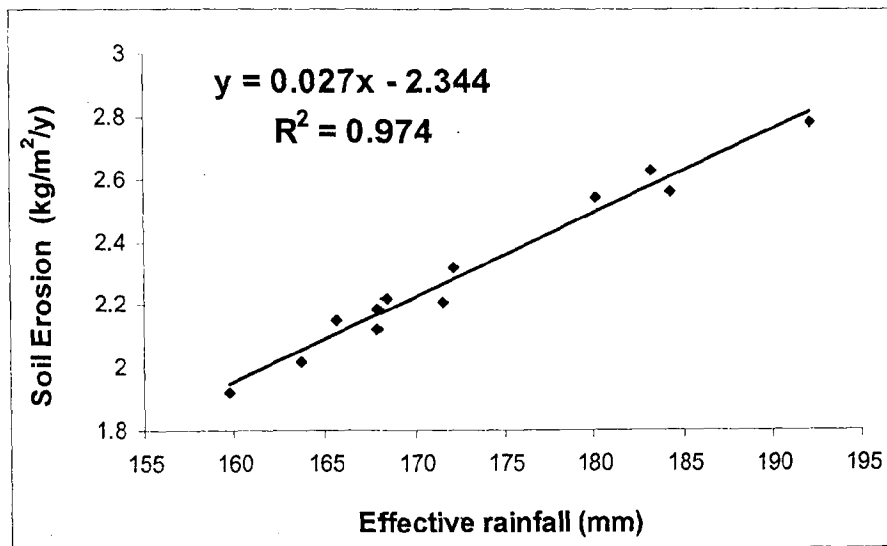


Fig. 6.34: Combined plot for the Awang Khujairok and the Waikhulok watersheds for the barren land

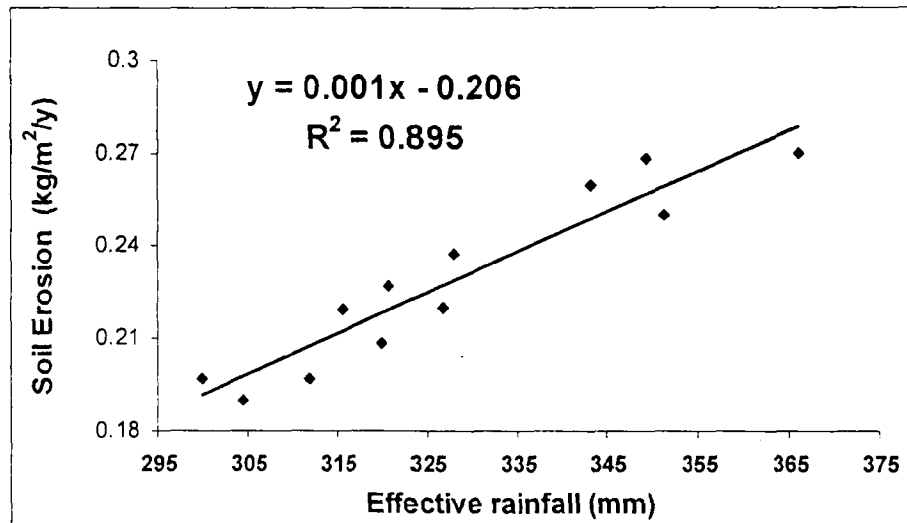


Fig.6.35: Combined plot for the Awang Khujairok and the Waikhulok watersheds for the dense forest

the rainfall and the soil erosion (Table 6.9). In case of the Waikhulok watershed, the coefficient of determination was observed as 0.99 for all the land use classes except for medium forest (0.968).

In case of the combined set of data, the correlation coefficient vary from 0.999 (paddy field) to 0.845 (medium forest) while the standard error ranges from 0.011 (built-up land) to 0.315 (paddy field).

The regression analysis shows clearly that the empirical relations derived are consistent.

Therefore the following models i.e. relationships have developed to estimate the soil loss due to erosion in different land use classes.

Dense forest,

$$y = 0.0013x - 0.206, (x \geq 0.21)$$

Barren land

$$y = 0.0268x - 2.344 (x \geq 0.27)$$

Built-up land

$$y = 0.014x - 1.096 \quad (x \geq 1.1)$$

Medium forest

$$y = 0.0113x - 1.277 \quad (x \geq 1.3)$$

Paddy field

$$y = 0.0113x - 1.277 \quad (x \geq 1.3)$$

where y represents soil loss due to erosion ($\text{kg}/\text{m}^2/\text{y}$) and x is the effective rainfall (mm). These relationships have been applied for the year 2006 and it was found that the results obtained using these relationships and results obtained using the MMF model for this year are in close agreement. Since these relationships have been developed for each land use, therefore they can be applied for estimation of soil erosion by using only rainfall data.

6.8 WATERSHED PRIORITIZATION

The watershed prioritization is the ranking of different areas of a watershed according to the order in which they have to be selected for adopting suitable soil conservation measures (Suresh *et al.*, 2004). The watershed prioritization and formulation of proper watershed management programs for sustainable development require information on watershed soil loss. In most of the cases watershed projects have been predetermined and priorities have not been laid out properly. But looking to the massive investment in watershed development programs, it is not feasible to treat the complete watershed and prioritization has to be carried out so that the most sensitive sub-watershed can be taken up. Hence prioritization will facilitate in addressing the problem areas to arrive at suitable solutions and protective measures can be better planned and implemented.

Depending upon priority levels, the watershed area should be treated with suitable vegetative and structural measures. For effective watershed planning, there must be a close coordination of vegetative and structural control measures and best combination should be decided to tackle the problems of watershed in an integrated manner. Thus, grid based watershed management using MMF, remote sensing and GIS has the potential to alleviate soil erosion in the region and can play significant role in generating parameters from remote areas for watershed management.

On the basis of the Morgan Morgan Finney model, the soil loss in watersheds of western catchment of the Loktak Lake have been estimated and given in Table 6.10. The categorization of these watersheds as per the individual soil loss is done as per details given below.

- **Very high priority category ($>12 \times 10^6 \text{ kg/km}^2$)**

This category covers 5 watersheds (Khonga, Singda, Haibirok, Songtum, and Thongjaorok) extending over an area of 39.6 km^2 . With erosion rate values greater than $12 \times 10^6 \text{ kg/km}^2$, these watersheds are highly prioritized. These watersheds face sheet to rill erosion and moderate to severe gully erosion. Owing to these adverse conditions, these watersheds need higher priority and immediate attention for development and are also ideal for soil and water conservation measures. By adopting suitable watershed treatment practices such as contour bunding, contour cultivation, vegetative bunding and water conservation structures, crop production can be enhanced and will reduce the soil erosion rate.

Table 6.10: Estimation of total soil loss due to erosion in different watersheds of the catchment

Sl. No.	Watersheds	Total soil erosion (10^6 kg/y)
1	Turelu	2.04
2	Moirang Turel	3.22
3	Mashem (Kwakta)	1.26
4	Lajamaril	1.39
5	Wangtha	9.84
6	Thingin	4.80
7	Irum	4.56
8	Lenghanbi	4.20
9	Kongdun	6.47
10	Ningthoukhong	6.81
11	Charoikhui	6.41
12	Awang Khujairok	6.01
13	Nungshai	8.25
14	Keinou	4.97
15	Thongjaorok	12.50
16	Aigejang	3.54
17	Ishinglok	3.94
18	Waikhulok	4.45
19	Wangjing	6.12
20	Sajirok	6.07
21	Haibirok	13.45
22	Khonga	15.62
23	Phayeng	9.19
24	Kangchup	11.01
25	Kharamkom	9.66
26	Singda	15.39
27	Songtum	12.61

- **High priority category ($8-11 \times 10^6$ kg/km²)**

This category covers 5 watersheds (Wangtha, Kharamkom, Phayeng, Nungshai and Kangchup) extending over an area of 38 km². These watersheds also require urgent attention and suitable watershed management practices.

- **Moderate priority category ($4-7 \times 10^6 \text{ kg/km}^2$)**

This covers an area of 50.3 km^2 and comprises of 11 watersheds namely Ningthoukhong, Kongdun, Charoikhui, Wangjing, Sajirok, Awang Khujairok, Keinou, Thingin, Irum, Waikhulok and Lenghanbi. These watersheds have moderately good vegetation cover. Therefore, these watersheds do not suffer from any significant hazards and need no immediate attention. The soil erosion rate is not an alarming rate and these watersheds can be treated at the middle stage of the watershed programme.

- **Low priority category ($1-4 \times 10^6 \text{ kg/km}^2$)**

Low prioritized watersheds have the erosion rate in the range of $1-4 \times 10^6 \text{ kg/km}^2$. Six watersheds namely Ishinglok, Aigejang, Moirang Turel, Turelu, Lajamaril, Mashem (Kwakta) with an area of 11 km^2 were identified under this category. The watersheds of this category have good vegetation cover and do not require immediate soil and water conservation. The topography is dominated by dense and medium forests. However, at present some of these lands are left as barren. These watersheds can be treated at later stages, because of their condition is not deteriorated as that of other watersheds under the above three categories.

6.9 CONCLUDING REMARK

Remote sensing and GIS have been found useful tools in identification and categorization of watersheds on the basis of natural resources and their limitations. A total of 27 watersheds in the Loktak lake catchment have been identified in this watershed prioritization study of which five watersheds were in the very high category, five in the high, eleven in moderate and six watersheds fall under the low priority categories.

The very high priority watersheds have higher erosivity values due to their greater percentage of area under the barren land use class and need immediate attention.

The watersheds under the very high priority category mostly lie in the northern fringe of the catchment. Because of the slope conditions and the moderate to high presence of barren lands, the productivity of cropped lands in these watersheds has been severely limited, therefore, needing high priority.

On the basis of the erosion rates obtained from the watersheds of the catchment (Table 6.12) the erosion rates have been categorized into four classes—very high priority zone, high priority, medium priority and minimum priority zone. The prioritization of the watersheds is shown done in Fig. 6.36.

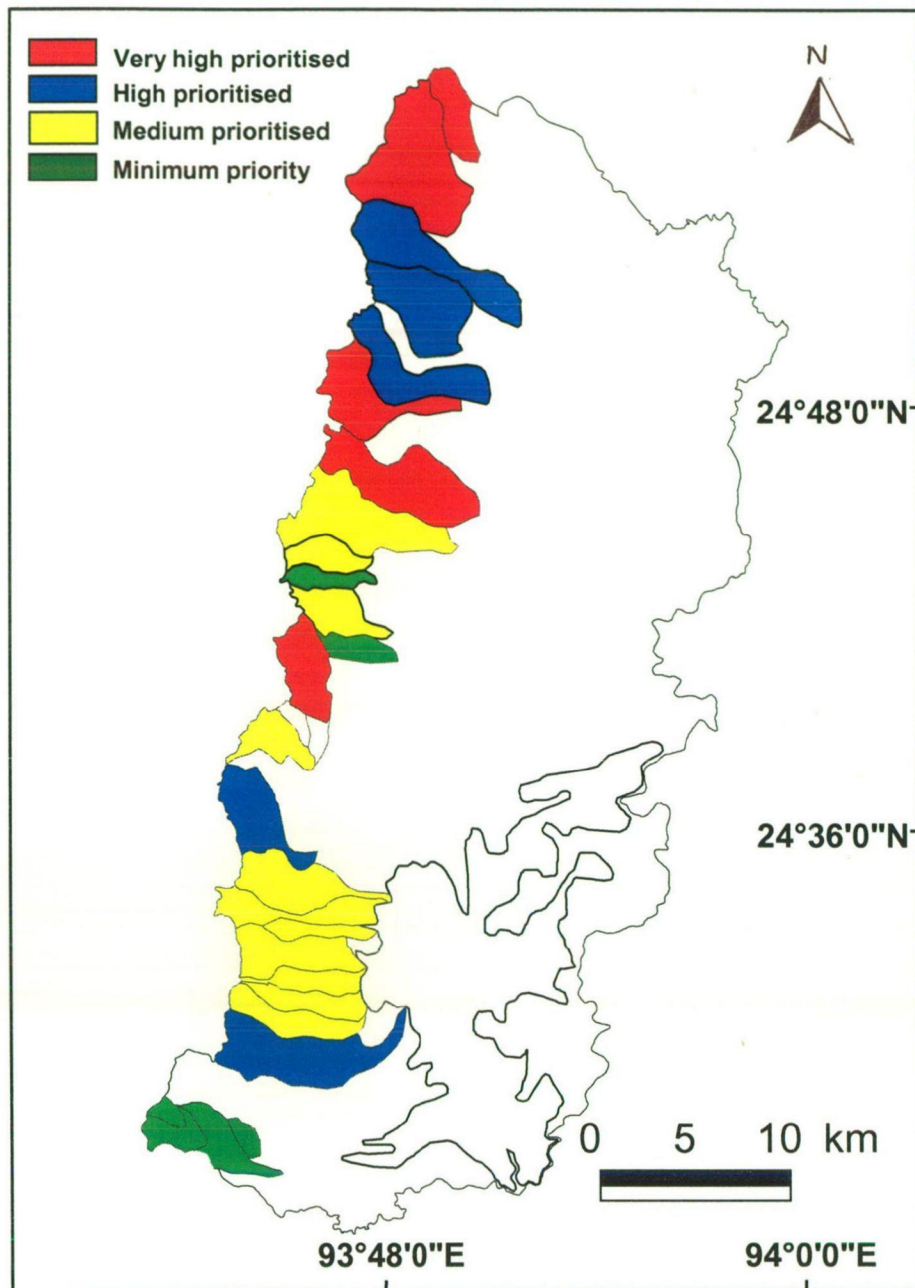


Fig. 6.36: Prioritization of watersheds in the catchment

7.1 CONCLUSIONS

The main objective of the present study was to suggest a simple quantitative soil erosion model for estimating the erosion rates in Loktak Lake catchment. The present study have been therefore, focused on finding a suitable soil erosion model capable of handling conventional inputs as well as inputs from the remote sensing in GIS environment and providing the output in the form of spatial and temporal distribution of soil loss for individual land use patterns. The model adopted herein satisfies these requirements and is also capable of handling distributed information about land use, soil type, land slope etc. and generate soil erosion estimates in spatial and temporal domain.

The spatial data for the study area have been generated using high-resolution remote sensing data and other available information. The study area has been divided into twenty seven watersheds. The spatial data for the two watersheds have been generated in GIS environment. The soil erosion estimates for the remaining twenty five watersheds have been carried out on the basis of land use and rainfall prevailing in these watersheds. Hydrological observations are also made during the course of this study in two small watersheds to collect short interval data on rainfall, soil type and ^{210}Pb in soil cover.

In the present study, soil erosion is estimated using the modified Morgan Morgan Finney model and the results are compared with the estimates obtained from the nuclear technique of sediment and observed data.

The following conclusions have been drawn from the present study:

- (i) The nuclear technique using ^{210}Pb lithogenic radioisotope has been found suitable for the estimation of soil erosion in the study area. This technique has been reported as a potential method for far-flung remote areas where accessibility is difficult and the input data is also not available. Also, frequent trips to the study area are not required in this method.
- (ii) The revised Morgan Morgan Finney model has been found to be suitable model to determine soil erosion in the catchment of the Loktak Lake, as the results obtained by the MMF model have been found in good agreement with the results obtained by the nuclear technique and the observed data.
- (iii) The soil erosion rate estimated by the MMF model varies from $2.12 \text{ kg/m}^2/\text{y}$ for the barren land to $0.21 \text{ kg/m}^2/\text{y}$ for the dense forest in the Awang Khujairok watershed. While the soil erosion rate estimated by the nuclear technique ranges from $1.87 \text{ kg/m}^2/\text{y}$ (built-up land) to $0.01 \text{ kg/m}^2/\text{y}$ (dense forest).
- (iv) For the Waikhulok watershed, the soil erosion rates estimated by the MMF model are found in the range of $2.18 \text{ kg/m}^2/\text{y}$ for the barren land to $0.19 \text{ kg/m}^2/\text{y}$ for the dense forest. Similarly, by the nuclear technique, the maximum soil loss has been computed in the barren land, that comes out to be $3.21 \text{ kg/m}^2/\text{y}$ and the minimum in the dense forest ($0.18 \text{ kg/m}^2/\text{y}$) in the watershed.
- (v) The study also confirms that dense forested area generates less soil loss compared to barren land that produces high soil loss.
- (vi) On the basis of soil erosion estimated by the MMF model in different land use classes in the two watersheds, the soil erosion in other watersheds on the basis of prevailing land use classes have been estimated. The total soil loss in all the watersheds of the study area is in the range of $15.62 \times 10^6 \text{ kg/y}$ in Khonga watershed to $1.26 \times 10^6 \text{ kg/y}$ in Mashem (Kwakta) watershed. This appears to

be justified because of the high percentage of barren land in the former and greater coverage of dense forest in the later.

- (vii) Analysis of the effect of changes in slope on the soil erosion rate reveals that variation of slope by $\pm 1\%$ to $\pm 5\%$ provide the change in soil erosion of the same order. But all the watersheds are topographically similar. Therefore slope has not been considered to compute the soil erosion by MMF model in other watersheds.
- (viii) For the two watersheds, empirical relations between effective rainfall and the erosion rate for different land use classes have been developed on the basis of six years' rainfall data. The relationships have been verified for the seventh year rainfall data. These relationships can be used to compute the soil erosion for any particular land use class if the rainfall is known.
- (ix) Altogether twenty seven watersheds in the Loktak lake catchment have been considered for the watershed prioritization study on the basis of total soil loss due to erosion. The watersheds are grouped into four categories-very high priority ($>12 \times 10^6 \text{ kg/km}^2$), high priority ($8-11 \times 10^6 \text{ kg/km}^2$), moderate priority ($4-7 \times 10^6 \text{ kg/km}^2$) and low priority ($1-4 \times 10^6 \text{ kg/km}^2$). The watersheds namely Khonga, Singda, Haibirok, Songtum and Thongjaorok, extending over an area of 39.6 km^2 fall under very high priority category. The high priority category covers five watersheds (Wangtha, Kharamkom, Phayeng, Nungshai and Kangchup) extending over an area of 38 km^2 . The moderate erosive category covers an area of 50.3 km^2 that comprises of eleven watersheds namely Ningthoukhong, Kongdun, Charoikhui, Wangjing, Sajirok, Awang Khujairok, Keinou, Thingin, Irum, Waikhulok and Lenghanbi. Six watersheds namely Ishinglok, Aigejang, Moirang Turel, Turelu, Laijamaril,

Mashem (Kwakta) with an area of 11 km² have been identified under low erosive category.

- (x) The soil erosion modelling has been successfully done by integrated approach considering the modeling technique i.e. revised MMF model and nuclear technique (²¹⁰Pb technique).

7.2 SCOPE FOR FURTHER STUDIES

In the present study, soil erosion rates from the watersheds of the western catchment of the Loktak Lake have been estimated. Similar studies can be conducted for other catchments in the region using the methodology adopted for this study and the empirical relationships developed can also be used to estimate soil loss in the subsequent years.

The lack of adequate observed data was a hindrance to this study. The incorporation of more detailed data would help in better validation of the model. There is also much scope for extension of this study for assessment of the effect of the total soil erosion in the catchment on the lake bed. Considering the importance of the lake for the state, the sedimentation rate and pattern can be computed using the nuclear technique which in turn would predict the life expectancy of the lake.

On the other hand, suitable watershed treatment practices such as contour bunding, contour cultivation, vegetative bunding etc. need to be adopted in the highly prioritized watersheds in the catchment in order to minimize the soil erosion. The runoff expected need to be properly estimated for proper management and utilization (Parida *et al.*, 2006). Also, appropriate harvesting ponds need to be designed to harness the runoff during the rainy season (Satapathy, 1996; Pandya and Shete, 2006).

REFERENCES

1. Abott, M.B., Bathurst, J.C., Cunge, J.A., O'Connel, P.E. and Rasmussen, J. An introduction to European Hydrological Syatem-systeme Hydrologique European "SHE", part 1 and 2. *J. Hydrology*, 87:61-77. 1986.
2. Abrol, I.P. Caring for our soil resources. Proceedings, International Symposium on Water Erosion, Sedimentation and Resources Conservation, CSWCR&TI, Dehradun, India-I-X. 1990.
3. Adinarayana, J. and Ramakrishna, N. Integration of multi-seasonal remotely sensed images for improved land use classification of a hilly watershed using geographical information systems, *Indian Journal of Remote Sensing*, Vol 17, No. 9, 1679-1688. 1996.
4. Alford, D. Hydrological aspects of the Himalayan region. ICIMOD Occasional Paper No. 18. 1992.
5. Allred, B. and Haan, C. T. SWMHMS - Small Watershed Monthly Hydrologic Modeling System. *Journal of the American Water Resources Association* Vol. 32, No. 3, 541-552. June 1996.
6. Amin-Sichani, S. A Modeling of Phosphorus Transport in Surface Runoff from Agricultural 72 Watersheds. Ph.D. Thesis, Purdue University, W. Lafayette, Indiana, 157. 1982.
7. Anonymous. Development of an index to rioritize riparian buffer restoration efforts in Cooks Creek watershed-Pensylvania, (www.fxbrowne.com-case studies), 2001.
8. Appleby, P.G. and Oldfield, F. In: Ivanovich M, Haiman RS, editors. Application of lead-210 to sedimentation studies. Oxford: Uranium series disequilibrium; Chap. 21. 1992.

9. Arnof, S. Geographic Information System: Adequate management perspective, WDL publications, Ottawa. 1991.
10. Arnold, J.G., Engel, B.A. and Srinivasan, R. Continuous-time grid-cell watershed model. Proc. of the Conf. Spokane, Washington, 267-278. 18-19 June 1993.
11. Ascough, J.C., M.A. Nearing, Flanagan, D.C. and Livingston, S.J. Hydrologic and erosion calculations in the water erosion prediction project (WEPP) watershed model, An ASAE meeting presentation, paper no: 94-2037. 1994.
12. Baban, S.M.J. Modeling soil erosion in tropical environments using remote sensing and geographical information system. Hydrologic Sciences Journal 46(2) 191-197. 2001.
13. Babu, R., Tejwani, K.G., Agrawal, M.C. and Bhushan, L.S. Distribution of erosion index and Iso-erodent map of India. Indian Journal of Soil Conservation, Vol. 6, No. 1, 1-14. 1978.
14. Barg, E. Studies of beryllium geochemistry in soils: feasibility of using $^{10}\text{Be}/^9\text{Be}$ ratios for age determination. Ph.D diss. Univ. California. San Diego. 181. 1992.
15. Barker, D.H. The way ahead - continuing and future developments in vegetative slope engineering or ecoengineering. Proceedings of International Conference on Vegetation and Slopes - Stabilisation, Protection and Ecology, September 1994, Oxford, 238-257. Institution of Civil Engineers, London, UK. 1995.
16. Bartholic, J.F. and Y.T. Kang. Environmental Restoration, Integrated Spatial Analysis System for Planning and Management. In: Proceedings of UCOWR 1994 Annual Meeting: Environmental Restoration. Big Sky, Montana. August 2-5, 1994.
17. Beasley, D.B. and Huggins, L.F. ANSWERS Users Manual. EPA-905/9-82-001, U.S. EPA, Region V. Chicago, IL. 1981.

18. Beasley, D.B., Huggins, L.F. and Monk, E.J. ANSWERS: A model for watershed planning. *Transactions of ASAE*, 23: 938-944. 1980.
19. Benninger, L. K., Lewis, D. M. & Turekian, K. K. The use of natural ^{210}Pb as a heavy metal tracer in the river estuarine system. In: T. M. Church (ed.). *Marine Chemistry in the Coastal Environment*. Am. Chem. Soc. Symp. Ser. 18: 202–210. 1975.
20. Beven, K.J. Changing ideas in hydrology-the case of physically-based models. *J. Hydrology*, 105:157-172. 1989.
21. Blake, W.H., Walling D.E. and He, Q. Fallout beryllium-7 as a tracer in soil erosion investigations. *Applied Radiation and Isotopes* 51: 599-605. 1999.
22. Blake, W.H., Walling, D.E. and He, Q. Using cosmogenic beryllium-7 as a tracer in sediment budget investigations. *Geografiska Annaler: Series A, Physical Geography*, Volume 84, No. 2, 89-102(14). August 2002.
23. Bloesch, J. and Evans, R. D. Lead-210 dating of sediments compared with accumulation rates estimated by natural markers and measured with sediment traps. *Hydrobiologia*. Vol. 91-92, No. 1/July, 1982.
24. Bodoque, J.M., Díez-Herrero, A., Martín-Duque, F.F., Rubiales, F.M., Godfrey, A., Pedraza, J., Carrasco, R.M. and Sanz, M.A. Sheet erosion rates determined by using dendrogeomorphological analysis of exposed tree roots: Two examples from Central Spain. *Catena*. Vol 64: 1, 81-102. 2005.
25. Boughton, W.C. Evaluating partial areas of watershed runoff. *ASCE Journal of Irrigation and Drainage Engineering*, 113, 356-366. 1989.
26. Bouhlassa, S., Moukhchane, M. and Aiachi, A. Estimates of soil erosion and deposition of cultivated soil of Nakhla watershed, Morocco, using ^{137}Cs technique and calibration models. *Acta Geologica Hispanica*, 35, 3-4, 239-249. 2000.

26. Brenner, M., Schelske, C. L. & Keenan, L. W. Historical rates of sediment and nutrient accumulation in marshes of the Upper St. Johns River Basin, Florida, USA. *Journal of Paleolimnology* 26: 241–257, 2001.
27. Brown, L. ^{10}Be : recent applications in earth sciences. *Phil. Trans. R. Soc. (London)* A323:75-86. 1987.
28. Brown, L. Sacks, I.S., Tera, F., Klein, J. and Middleton, R. Beryllium-10 in continental sediments. *Earth Planet. Sci. Lett.* 55: 370-76. 1981.
29. Bryan, R.B., Editor, Rill erosion. Processes and Significance, *Catena Supplement Vol. 8*, Catena Verlag, Cremlingen. 1987.
30. Bryan, R.B. Editor, Soil Erosion. Experiments and Models, *Catena Supplement Vol. 17*, Catena-Verlag Rohdenburg, Cremlingen-Destedt, Federal Republic of Germany. 1990.
31. Bundela, D. S., Singh, R. and Mishra, K. Sediment yield modeling for small watersheds in Barker river valley. *Institution of Engineers (1) Jr.*, Vol. 76, 22-25. 1995.
32. Burch, G.J., Barnes, C.J., Moore, J.D. and Barling, R.D., Mackenzie, D.J., Olley, J.M. Detection and prediction of sediment sources in catchments: use of ^7Be and ^{137}Cs . In: *Proceedings of the Hydrology and Water Resources Symposium*. Aust. Nat'l Univ, Canberra, 146–151. 1988.
33. Burrough, P.A. *Principles of Geographic Information System for land resources assessment*, Clarendon press, Oxford. 1986.
34. Butler, H.J., Hogarth, W.L. and McTainsh, G.H. A source-based model for describing dust concentrations during wind erosion events: an initial study, *Environmental Software* 11:1–3, 45–52. 1996.
35. Büyüksalih G. and Jacobsen, K. Generation and validation of digital elevation models based on Satellite images. www.ipi.uni-hannover.de/html/publikationen/2006.

36. Caillet, S., Arpagaus, P., Monna, F. and Dominik, J. Factors controlling ^7Be and ^{210}Pb atmospheric deposition as revealed by sampling individual rain events in the region of Geneva, Switzerland. *Journal of Environmental Radioactivity* 53, 241–256. 2001.
37. Cairns, M. Consultant's Recommendations to Sustainable Development and Water Resources Management of Loktak Lake. Consultancy Report. Sustainable Development and Water Resource Management of Loktak Lake. 1998.
38. Calder, I.R., Hall, R.L. and Adlard, P.G. Growth and Water Use of Forest Plantations. Wiley, Chichester, England. 1992.
39. Callot, Y., Marticorena, B. and Bergametti, G. Geomorphologic approach for modelling the surface features of arid environments in a model of dust emissions: application to the Sahara desert, *Geodinamica Acta* 13 (2000) (5), 245–270. 2000.
40. Campbell, B.L., Loughran, R. J., Elliott, G. L. and Shelly, D. J. Mapping drainage basin sources caesium-137. *IAHS*, 174, 437-446. 1986.
41. Carabajal, C.C. and Harding, D.J. Validation/calibration of SRTM digital Elevation models using ICESAT data. *Geophysical Research Abstracts*, Vol. 6, 05952. SRef-ID: 1607-7962/gra/EGU04-A-05952. 2004.
42. Carson, B. 1992. The land, the farmer, and the future: A soil fertility management strategy for Nepal. ICIMOD Occasional Paper No. 21. Kathmandu, Nepal. 1992.
43. Central Soil and Water Conservation Research and Training Institute (CS&WC), Evaluation of hydrological data. Indo-German bilateral Project on watershed management, Soil and Water Conservation Division (CS&WI), Ministry of Agriculture, New Delhi, India. 1991.
44. Chakraborty, A.K. Strategies for watershed management planning using remote sensing techniques. *J. Indian Society of Remote Sensing*. Vol. 1(2), 87-89. 1993.

45. Chatterjee, C., Kumar, R., Chakravorty, B., Lohani, A.K. and Kumar, S. Integrating remote sensing and GIS techniques with groundwater flow modeling for assessment of waterlogged areas. *International Journal of Water Resources Management*, 19, 539-554, 2005.
46. Chen, L.D., Fu, B.J., Xu, J.Y. and Gong, J. Location-weighted landscape contrast index: a scale independent approach for landscape pattern evaluation based on "Source-Sink" ecological processes (in Chinese). *Acta Ecol Sinica* 23:2406–2413. 2003.
47. Chillrud, S.N., Shuster, E.L., Chaky, D.A., Walsh, D.C., Choy, C.C., Tolley, L.R., Yarme, A., Bopp, R.F., Simpson, H.J., and Ross, J.M. Twentieth century atmospheric metal fluxes into Central Park Lake, New York City. *Environmental Science and Technology*, v. 33, 657-662. 1999.
48. Clarke, M.L. and Rendell, M. The impact of the farming practice of remodeling hillslope topography on badland morphology and soil erosion process. *Catena* 40:229–250. 2000.
49. Collins, D. N. and Hasnain, S.I. Runoff and sediment transport from the glacierized basins at the Himalayan scale Alpine glacier project working paper 15, University of Manchester, U. K., 14. 1994.
50. Collins, A.L., Walling, D.E., Sickingabula, H.M. and Leeks, G.J.L. Using ¹³⁷Cs measurements to quantify soil erosion and redistribution rates for areas under different land use in the Upper Kaleya River basin, southern Zambia. *Geoderma*. 104, 229– 323. 2001.
51. Coutinho, M.A. and Toma's, P. Characterisation of raindrop size distributions at the Vale Formoso Experimental Erosion Centre. *Catena* 25, 187–197. 1995.

52. Crozaz, G. and Langway, C.C. Dating Greenland firn ice cores with ^{210}Pb . *Earth Planet. Sci. Lett.* 1:194-196. 1966.
53. Crozaz, G., Picciotto E. and Breuck W. De. Antarctic snow chronology with ^{210}Pb . *J. Geophys. Res.* 69, 2597-2604. 1964.
54. Das, B. K. Singh, M. and Borkar, M. D. Sediment accumulation rate in the lakes of Kumaun Himalaya, India using ^{210}Pb and ^{226}Ra . *Environmental Geology*. Vol. 23, No. 2/March, 1994.
55. De Roo, A.P.J., Jetten, J.G., Wesseling, C.G. and Ritsema, C.J. LISEM: A physically-based hydrological and soil erosion model incorporated in a GIS. *Applications of Geographic Information Systems in Hydrology and Water Resources Management HydroGIS 1996*, IAHS Publication No. 235:395-403. 1996.
56. Dhruva Narayana, V.V. and Babu, R. Estimation of soil erosion in India. *Journal of Irrigation and Drainage Engineering*. ASCE, 109 (4), 419-435. 1983.
57. Dissmeyer, G.E. and Foster, G. A. A Guide for Predicting Sheet and Rill Erosion on Forest Land. United States Department of Agriculture Technical Publication SA-TP. 40. 1980.
58. Dos, I.C., Pais-Cuddou, M. and Rawl, N.C. Sedimentation of reservoirs. *J. Irrigation and Drainage Division*, ASCE, 95(IR3): 415-429. 1969.
59. El-Daoushy, F., Olsson, K. and Garcia-Tenorio, R. Accuracies in Po-210 determination for lead-210 dating. *Hydrobiologia*. Vol. 214, No. 1, 1991.
60. Elliot, W.J., G.R. Foster and Elliot, A.V. "Soil erosion: Processes, impacts and prediction." In: *Soil Management for Sustainability*. (Lal, R. and Pierce, R.J., eds.): 25-34. Soil and Water Conservation Society, Ankeny, IA, USA. 1991.
61. Ellison, W.D. Soil erosion studies. Part VI, soil detachment by surface flow, *Agr. Eng.* 28, 402-405. 1947.

62. El-Swaify, S.A. and Dangler, E.W. Erodibilities of selected tropical soils in relation to structural and hydrological parameters. In: Soil Erosion: Prediction and control, Soil Cons. Society of America, Special Publication, 21:105-114. 1976.
63. Erskine, W.D., Mahmoudzadeh, A. and Myer, C. Land use effects on sediment yields and soil loss rates in small basins of Triassic sandstone near Sydney, NSW, Australia. *Catena* 49:271–287. 2002.
64. FAO, Tropical forestry action plan on forest development in the Tropics, FAO, UN, Rome. 1985.
65. Farmer, J. G. Lead concentration profiles in lead-210 dated Lake Ontario sediment cores. *The Science of the Total Environment*, Vol. 10, Issue 2. 117-127. September 1978.
66. Flanagan, D. Erosion. In: R. Lal, Editor, *Encyclopedia of Soil Science*, Marcel Dekker, New York, 395–398. 2002.
67. Flanagan, D.C. and Livingston S.J. USDA-Water Erosion Prediction Project, WEPP user summary conference, August 9-11, Des Moines, Iowa. 1995.
68. Flanagan, D.C., Renschler, C.S. and Cochrane, T.A. Application of the WEPP model with digital geographic information. 4th Int. Conf. on Integration of GIS and Environmental Modelling: Problems, Prospects and Research needs. 2000.
69. Fort, M. Geomorphic and hazards mapping in the dry continental Himalaya: 1:50,000 maps of Mustang District, Nepal. *Mountain Research and Development*, Vol. 7(3), 222-238. 1987.
70. Fortin, J.P., Turcotte, R., Massicote, S. Moussa, R. and Fitzback, J. A distributed watershed model compatible with remote sensing and GIS data, part-1: description of the model. *J. Hydrological engineering, ASCE*, 6(2): 91-99. 2001.
71. Foster, G.R. Understanding ephemeral gully erosion. In: *Committee on Conservation Needs and Opportunities, Board on Agriculture, National Research*

- Council Soil Conservation. (Eds.), *Assessing the National Resources Inventory*, 2. National Academy Press, Washington, 90–125. 1986.
72. Fournier, F. *Climate and Soil Erosion*. Paris: Presses Universitaires de France (cited in Richi, J.C. (2000) *Soil Erosion*. In: Schultz, G.A. and Engman, E.T. (eds.) *Remote Sensing in Hydrology and Water Management*. Springer, New York, 271-286. 1960.
73. Frere, M.H., Ross, J.D. and Lane, L.J. The nutrient submodel. In: *CREAMS: A Field Scale Model for Chemicals, Run-off, and Erosion from Agricultural Management Systems*. Research Report 26, USDA, 65–85. 1980.
74. Froehlich, W. and Walling, D.E. The use of fallout radionuclides in investigations of sediment sources and overbank sedimentation within the Teesta river basin, Sikkim Himalaya and Ganga-Brahmaputra Plain, India. *Proc. International Workshop of IHAS Decade on Prediction in Ungauged Basins-Hydrological Sciences on Mission, IHAS/Univ. of Brasilia*, 1-11. 2002.
75. Fu, B.J., Chen, L.D., Ma, K.M., Zhou, H.F. and Wang, J. The relationships between land use and soil condition in the hilly area of the Loess Plateau in northern Shaanxi, China. *Catena* 39:69–78. 2002a.
76. Fu, B.J., Chen, L.D., Qiu, Y., Wang, J. and Meng, Q. H. Land use structure and ecological process in the hilly and gully area of the Loess Plateau of China (in Chinese). Commercial, Beijing, 5–12. 2002b.
77. Fu, B.J., Qiu, Y., Wang, J. and Chen, L.D. Effects simulations of land use change on the runoff and erosion for a gully catchment of the Loess Plateau, China (in Chinese). *Acta Geogr Sin* 57:717–722. 2002c.
78. Fu, B.J., Meng, Q.H., Qiu, Y., Zhao, W.W. and Zhang, Q.J. Effects of land use on soil erosion and nitrogen loss in the hilly area of the Loess Plateau, China. *Land Degrad Dev* 15:87–96. 2004.

79. Fukuyama, T., Chisato, T. and Onda, Y. ^{137}Cs loss via soil erosion from a mountainous headwater catchment in central Japan. *Science of the Total Environment* 350, 238–247. 2005.
80. Galay, V. J., Okaji, T. and Nkshino, K. 'Erosion from Kulekhani Watershed, Nepal, during the July 1993 rainstorm'. In Schreier, H., P. B. Shah, and S. Brown (Editors), *Challenges in Mountain Resource Management in Nepal, Processes, Trends, and Dynamics in Middle Mountain Watersheds*. ICIMOD/IDRC/UBC. Kathmandu, Nepal. 1995.
81. Garcia-Ruiz, J.M., Lasanta, T., Ortigosa, L., Ruiz-Flano, P., Marti, C. and Gonzalès, C. Sediment yield under different land uses in the Spanish Pyrenees. *Mountain Research and Development* 15: 3, 229–240. 1995.
82. Garde, R. J. and Kothyari, U.C. Sediment yield estimation, *J. Irrig. and Power (India)* Vol. 44(3), 97-123. 1987.
83. Gilman, K. and Newson, M.D. *Soil Pipes and Pipeflows—A Hydrological Study in Upland Wales*, GeoBooks, Norwich. 114. 1980.
84. Golberg, E.D. Geochronology with ^{210}Pb . In: *Radioactive Dating*, I.A.E.A, Vienna: 121-131. 1963.
85. Golosov, V.N., Walling, D.E. and Panin, A.V. Post-fallout redistribution of Chernobyl-derived caesium-137 in small catchments within the Lokna River basin. *International Association of Hydrological Sciences Publication No. 263*:49-57. 2000.
86. Golosov, V., Litvin L., Walling D. E. and Horowitz A. J. The sediment budgets of cultivated slopes and slope catchments: an evaluation of the influence of slope morphology. *International symposium on sediment budgets, Foz do Iguação, Bresil (03/04/2005)* 20051973, vol. 291, 3-10. 2005.
87. Goswami, M., O'Connor, K.M. and Bhattarai, K.P. Development of regionalisation procedures using a multi-model approach for flow simulation in an ungauged catchment. *Journal of Hydrology*. 333, 517–531. 2007.

88. Goyal, R. Surface water resource mapping using multi-date remote sensing data. Symposium on Prediction in Ungauged Basins for Sustainable Water Resources Planning and Management, PUBSWRPM, Pilani, India. 30 Oct, 2004.
89. Gray, D.H. Influence of vegetation on the stability of slopes. Proceedings of International Conference on Vegetation and Slopes - Stabilisation, Protection and Ecology, September 1994, Oxford, 2-25. Institution of Civil Engineers, London, UK. 1995.
90. Grayson, R., Moore, I.D. and McMahon, T.A. Physically based hydrologic modelling, I.A. terrain based model for investigative purposes. *Water Resources Research*, 28(10): 2639-2658. 1992.
91. Guo, X.D., Chen, L.D. and Fu, B.J. Effects of land use/land cover changes on regional ecological environment (in Chinese). *Adv Environ Sci* 7:66–75. 1999.
92. Hacıyakupoglu, S., Ertek, S.A., Walling, D.E., Ozturk, Z. F., Karahan, G., Erginal, A.E. and Celebi, N. Using caesium-137 measurements to investigate soil erosion rates in western Istanbul (NW Turkey). *Catena*. Vol.64, Issues 2-3, 222-231. 2005.
93. Hadley, R.F., Lal, R., Onstad, C.A., Walling, D.E. and Yair, A. Recent Developments in Erosion and Sediment Yield studies. UNESCO, (IHP) Publication, Paris: 127. 1985.
94. Hammond, D. E. and Fuller, C. The use of radon-222 to estimate benthic exchange and atmospheric exchange rates in San Francisco Bay, 213-229. *In San Francisco Bay: The urbanized estuary. Symp. Pac. Div. Am. Assoc. Adv. Sci.* 1979.
95. Hart, G.E. Erosion from simulated rainfall on mountain rangeland in Utah. *J. Soil Water Conserv.* 39:330-334. 1984.
96. Hawley, N., Robbins, J.A. and Eadie, B.J. The partitioning of 7-beryllium in fresh water. *Geochim. Cosmochim. Acta* 50:1127–1131. 1986.
97. He, Q. and Owens, P. Determination of suspended sediment provenance using caesium-137, unsupported lead-210 and radium-226: a numerical mixing model

- approach. In: Foster, I.D.L., Gurnell, A.M., Webb, B.W. (Eds.), *Sediment and Water Quality in River Catchments*. Wiley, New York, 207–227. 1995.
98. He, Q. and Walling, D.E. The distribution of fallout ^{137}Cs and ^{210}Pb in undisturbed and cultivated soils. *Appl. Radiat. Isotopes* 48, 677– 690. 1997.
 99. He, Q. and Walling, D.E. Rates of overbank sedimentation on the floodplains of British lowland rivers documented using fallout ^{137}Cs . *Geografiska Annaler* 78A: 223-234. 1996.
 100. Hotchkiss, R.H. and Huang, X. Hydrosuction sediment-removal system (HSRS): principles and field test. *J. Hydraulic Engineering*. 1995.
 101. Hudson, N. *Soil Conservation*. B.T. Batsford Ltd, London, UK. 1981.
 102. Hudson, N.W. The influence of rainfall on the mechanics of soil erosion with particular reference to Southern Rhodesia, MSc Thesis, University of Cape Town. 1965.
 103. Huh, C. A., Chu, K.S., Wei, C.L. and Liew, P.M. Pb-210 and plutonium fallout in Taiwan as recorded at a subalpine lake. *Journal of Southeast Asian Earth Science*, 14(5), 373-376. 1996.
 104. Indian Council for Agricultural Research (ICAR). *Guidelines and Status of Hydraulic and Sediment Management of Watersheds in selected River Valley Catchments*. Water and Soil Conservation division, Ministry of Agriculture, New Delhi, India. 1984.
 105. Irlweck, K. and Danielopol, D. L. Caesium-137 and lead-210 dating of recent sediments from Mondsee (Austria). *Hydrobiologia*. Vol. 128, September, 1985
 106. Ives, J. D. and Messerli, B. *The Himalayan Dilemma: Reconciling Development and Conservation*. United Nations University and Routledge, London. 1989.
 107. Jackson, A. *Glossary of Geology*, American Geological Institute, Alexandria. 1997.
 108. Jain, S. K. and Dolezal, F. Modeling soil erosion using EPIC supported by GIS, Bohemia, Czech Republic. 8: 1-11, 2000.

109. Jain, S.K., Kumar, S. and Varghese. J. Estimation of Soil Erosion for a Himalayan Watershed using GIS Technique. *Journal of Water Resources Management* 15:41-54, 2001.
110. Jensen, J.R. *Introductory Digital Image Processing: A Remote Sensing Perspective*. 2nd ed. Prentice-Hall, Inc, Upper Saddle River, NJ. 316. 1996.
111. Joglekar, D. V. *Irrigation research in India*. Central Board of Irrigation and Power Publ. India, No. 78. 1965.
112. Jones, J.A.A. and Bryan, R.B., Editors. *Piping Erosion Spec. Iss. Geomorphol.* 20 3-4, 319. 1997.
113. Joshi, L.V., Rangarajan, C. and Gopalakrishnan, S. Measurement of ^{210}Pb in surface, air and precipitation. *Tellus* 21, 107-112. 1969.
114. Joshi, S. R., McCrea, R. C., Shukla, B. S. and Roy, J.C. Partitioning and transport of lead-210 in the Ottawa River watershed. *Water, Air, & Soil Pollution*. Vol. 59, Numbers 3-4/October, 1991.
115. Joshi, S.R. Nondestructive determination of lead-210 and radium-226 in sediments by direct photon analysis. *Journal of Radioanalytical and Nuclear Chemistry*. Vol. 116, Number 1/November, 1987.
116. Joshi, V. and Negi G.C. Garwhal Himalaya mein vibhinn bhumi upyog wale do Jalagamo mein jal utpadan udhyayan, Jalvigyan evam Jal Sansadhan par Rasthriya Sangosthi, 303-307, National Institute of Hydrology, Roorkee. 1995.
117. Julian, P.Y., Saghafian, B. and Ogden, F.L. Raster based hydrological modelling of spatially-varied surface runoff. *Water Resources Bulletin*, 31(3): 523-536. 1995.
118. Jurgen, G., Fred, O.L., Paul, A.D. and Devid, R.M. GIS and distributed watershed models I-data coverages and resources. *J. Hydrologic Engineering*. Vol. 6. No. 6. 506-508. 2001.

119. Khan, M.A., Gupta, K. and Mohranna. Cazri Jodhpur, Watershed prioritization using remote sensing and GIS-A case study of Guhiya, *Journal of Arid Environments*, Volume 49, Issue 3, Pages-465-475. 2001.
120. Khare, D., Singh, K. S., Dhore, K.A. and Bhatnagar, T. Watershed prioritization considering soil erosion status: a case study of India. *Proc. of Watershed Management-to meet water quality standards and TMDL*. San Antonio, Texas. 10-14 March 2007.
121. Kirkby, M.J. Hydrological slope models: the influence of climate. In: *Derbyshire, Geomorphology and Climate*. Wiley, London, 247–267. 1976.
122. Kothyari, U. C. Erosion and sedimentation problems in India. In: *Proceedings of International Symposium on Erosion and Sediment Yield*. Exeter, U. K. IAHS Publication No. 236, 531-539. 1996.
123. Kothyari, U. C., Tewari, A.K. and Singh, R. Prediction of sediment yield. *J. Irrig. Drain Eng.*, ASCE Vol. 20(6), 1122-1131. 1994.
124. Krause, A.K., Loughran, R.J. and Kalma, J.D. The use of Caesium-137 to Assess Surface Soil Erosion Status in a Water-Supply Catchment in the Hunter Valley, New South Wales, Australia. *Australian Geographical Studies*, Vol 41, No 1, 73-84(12). March 2003.
125. Krishnaswamy, S. & Lal, D. Radionuclide Limnology. In: Lerman, A. (Ed.). *Lakes, Chemistry, Geology & Physics*. Springer Verlag, N.Y.: 153–177. 1978.
126. Krishnaswamy, S., Lal, D., Martin, J.M. & Meybeck, M. Geochronology of lake sediments. *Earth Planet. Sci.Lett.* 11:407-414. 1971.
127. Kumar, B., Rai, S. P., Nachiappan, Rm. P., Saravana, K. U., Singh, S. and Diwedi, V. K. Sedimentation rate in North Indian lakes estimated using ¹³⁷Cs and ²¹⁰Pb dating techniques. *Current Science*, Vol. 92, No. 10, 1416-1420. 2007.
128. Kumar, U. S., Navada, S.V., Rao, S.M., Nachiappan, R.P., Kumar, B., Krishnamoorthy, T.M., Jha , S.K. and Shukla, V.K. Determination of recent

- sedimentation rates and pattern in Lake Naini, India by ^{210}Pb and ^{137}Cs dating techniques. *Applied Radiation and Isotopes*, Vol 51, Issue 1, Pages 97-105. July 1999.
129. Lal, R. (ed) *Soil erosion*. Ankeny, IA, Soil and Water Conservation Society. 1994.
130. Lal, R. 2001. Soil degradation by erosion. *Land Degradation & Development*, 12: 519 – 539. 2001.
131. Lillisand, T.M. & Keifer, R.W. *Remote Sensing and Image Interpretation*, Jon Willey and Sons, New York. 1987.
132. Liu, B.Y., Xie, Y. and Zhang, K.L. Soil loss prediction model (in Chinese). *China Science and Technology*, Beijing, 114–118. 2001.
133. Loughran, R. J., Campbell, B.L., Shelly, D.J. and Elliott, G.L. Developing a sediment budget for a small drainage basin Australia. *Hydrological Processes* 6: 145-158. 1992.
134. Loughran, R.J. The measurement of soil erosion. *Progress in Physical Geography* 13:216-233. 1989.
135. Loughran, R.J., Elliott, G.L. McFarlane, D.J. and Campbell, B.L. A Survey of Soil Erosion in Australia using Caesium-137. *Australian Geographical Studies*, Vol 42, No 2, 221-233(13). July 2004.
136. Lu, H. and Shao, Y.P. Toward quantitative prediction of dust storms: an integrated wind erosion modelling system and its applications, *Environmental Modelling and Software* 16 (2001) (3), 233–249. 2001.
137. Lu, X. and Matsumoto, E. Recent sedimentation rates derived from ^{210}Pb and ^{137}Cs methods in Ise Bay, Japan. *Estuarine, Coastal and Shelf Science*, Vol. 65, Issues 1-2, 83-93. October 2005.
138. Ludwig, B. Boiffin, J. Chadoeuf, J. and Auzet, A.V. Hydrological structure and erosion damage caused by concentrated flow in cultivated catchments. *Catena* 25:227–252. 1995.

139. Maji, A. K., Nayak, D. C., Krishna, N. D. R., Srinivas, C. V., Kamble, K., Reddy, G. P. O. and Velayutham, M. Soil information system of Arunachal Pradesh in a GIS environment for land use planning. *International Journal of Applied Earth Observation and Geoinformation*, Volume 3, Issue 1, 69-77. 2001.
140. Manju, G., Chowdary, V.M., Srivastava, Y.K., Selvamani, S. Jeyaram, A. and Adiga, S. Mapping and Characterization of inland wetlands using Remote Sensing and GIS. *J. of Indian Society of Remote Sensing*. Vol 33, No. 1, 2005.
141. Matisoff, G., Bonniwell, E.C., Whiting, P.J. Soil erosion and sediment sources in an Ohio watershed using beryllium-7, cesium-137, and lead-210. *Journal of Environmental Quality* 31, 54-61. 2002.
142. McCaig, M. Contributions to storm quickflow in a small headwater catchment: the role of natural pipes and soil macropores. *Earth Surf. Process. Landf.* 8, 239–252. 1983.
143. Meybeck, M. Total mineral dissolved transport by world major rivers, *Hydrological Science Bulletin*, Vol. 21, 265-284. 1976.
144. Meyer, L.D. and Wischmeier, W.H. Mathematical simulation of the process of soil erosion by water. *Transactions of the American Society of Agricultural Engineers* 12, 754–758 and 762. 1969.
145. Milliman, J. D. and Meade, R.H. Worldwide delivery of river sediments to the Oceans, *Journal of Geology*, Vol. 91, 1-19. 1993.
146. Mishra, N. and Satyanarayan, T. A new approach to predict sediment yield from small ungauged watersheds, *Journal of Institution of Engineers (India) Agriculture Engg. Div.*, Vol. 73, 30-36. 1991.
147. Mitchell, J.K., Engel B.A., Srinivasan R., and Wang S.S.Y. ‘Validation of AGNPS for small watersheds using an integrated AGNPS/GIS system. *Water Resources Bulletin*, 29, No. 5. 1993.

148. Mizugaki, S., Nakamura, F. and Araya, T. Using dendrogeomorphology and ^{137}Cs and ^{210}Pb radiochronology to estimate recent changes in sedimentation rates in Kushiro Mire, Northern Japan, resulting from land use change and river channelization. *CATENA*, Vol. 68, Issue 1, 25-40. 15 December 2006.
149. Monaghan, M.C. Krishnaswami, S. and Turekian, K.K. The global average-production rate of ^{10}Be . *Earth Planet. Sci. Lett.* 76:179-187. 1985.
150. Mongkosawat, C., Thurangoon, P. and Sriwongsa. Soil erosion mapping with USLE and GIS. *Proc. Asian Conf. Rem. Sens., C-1-1 to C-1-6.* 1994.
151. Moore, I.D. and Gallant, J.C. Overview of hydrologic and Water quality modelling. 1-8 in Moore, I.D., ed., *Modelling the fate of Chemicals in the Environment.* Canberra: Centre for Resource and Environmental studies, Australian National University. 1991.
152. Moore, I.D., Turner, A.K., Wilson, J.P., Jensen, S.K. and Band, L.E. GIS and land surface-subsurface process modeling. In *GIS and Environmental Modeling*, edited by Goodchild, M.F., Parks, B., Steyaert, L.T., Oxford University Press, New York, 196-203. 1993.
153. Morgan, R.P.C. *Soil erosion.* Longman Group limited, London. Published in the United States of America by Longman Inc., New York. 1979.
154. Morgan, R.P.C. *Soil erosion and Conservation.* Longman Scientific & Technical, Longman Group UK limited Essex CM20 2JE, England and associated Companies throughout the world. Copublished in the United States with John Wiley & Sons, Inc., 605 Third Avenue, New York, NY 10158. 1986.
155. Morgan, R.P.C. *Soil Erosion and Conservation.* Longman, Harlow. 1995.
156. Morgan, R.P.C. A simple approach to soil loss prediction: a revised Morgan–Morgan–Finney model. *Catena* 44. 2001. 305–322. 2001.

157. Morgan, R.P.C., Morgan, D.D.V. and Finney, H.J. A predictive model for the assessment of erosion risk. *J. Agricultural Engineering Research* 30: 245 – 253. 1984.
158. Moser, R. N. A comparison of methods for the determination of the dating-nuclides ^{210}Pb and ^{226}Ra . *Journal of Radioanalytical and Nuclear Chemistry*. Vol.173, No.2/ October, 1993.
159. Narayana, Y., Shetty, P. K. and Siddappa, K. Behavior of ^{210}Po and ^{210}Pb in high background areas of coastal Kerala on the south west coast of India. *Applied Radiation and Isotopes*, Vol. 64, Issue 3, 396-401. March 2006.
160. National Resources Data Management System. Project Report. An Integrated Sustainable Management of Two Microwatersheds in Manipur. Ref. No. ES/11/347/98. 2005.
161. Natural Resources Conservation Service. National Soil Survey Handbook.1996.
162. Ni, J.R. and Li, Y.K. Dynamic assessment for soil erosion based on land-use structure change (in Chinese). *Acta Geogr Sin* 56:611– 621. 2001.
163. O'Farrell, C. R., Heimsath, A. M. and Kaste, J. M. Quantifying hillslope erosion rates and processes for a coastal California landscape over varying timescales. *Earth Surface Processes and Landforms*. *Earth Surf. Process. Landforms*. 32, 544–560. 2007.
164. Odermerho, F.O. Variation in erosion-slope relationship on cut slopes along a tropical highway. *Singapore Journal of Tropical Geography*, 7, 2, 98-107. 1986.
165. Oldeman, L.R. The global extent of soil degradation. In: D.J. Greenland and I. Szabolcs, Editors, *Soil Resilience and Sustainable Land Use*, CAB International (1994), pp. 99–118 Chapter 7.1994.

166. Oldfield, F. and Appleby, P.G. Empirical Testing of ^{210}Pb dating models for lake sediments. In: *Lake Sediments and Environmental History* (eds. E. Y. Haworth and J. W. G. Lund). Leicester University Press, 93-114. 1984.
167. Oldfield, F. and Appleby, P.G. The Role of ^{210}Pb Dating in Sediment Based Erosion Studies in Drainage Basin Erosion and Sedimentation Conference Papers: A conference on erosion, transportation and sedimentation. in *Australian drainage basins*. Loughran R. (ed) University of Newcastle, NSW. 175-182. 14-17 May, 1984.
168. Olley, J.M. and Deere, D. 2003. Targeting rectification action in the Wingcarribee Catchment. CSIRO Land and Water Technical Report 47/03.
169. Ologe, K.O. Gullies in the Zaria area. A preliminary study of headscarp recession, *Savanna* 1, 55-66. 1972.
170. Onaga, K., Shirai, K., Yoshinaga, A. Rainfall erosion and how to control its effects on farmland in Okinawa. In: Rimwanich, S. (Ed.), *Land Conservation for Future Generations*. Department of Land Development, Bangkok, 627–639. 1988.
171. Onstad, C.A. Modelling of sediment yields. In: Hadley, R.F., and Walling, D.E. (Eds) *Erosion and sediment yields: some methods of measurements and modelling*. Norwich, Geobooks. 1984.
172. Oost, K.V., Govers, G. and Desmet, P. Evaluating the effects of changes in landscape structure on soil erosion by water and tillage. *Landscape Ecol* 15:577–589. 2000.
173. Orlandini, S., Mancini, M., Paniconi, C. and Rosso, R. Local contributions to infiltration excess runoff for a conceptual catchment model. *Water Resources research*, 32(7): 2003-2012. 1996.
174. Owens, P. N., Walling, D. E., He, Q., Shanahan, J. and Foster, I. D. The use of Caesium-137 measurements to establish a sediment budget for the Start catchment, Devon, UK. *Hydrological Sciences Journal*. 42: 405-423. 1997.

175. Pande, L.M., Prasad, J., Saha, S.K. and Subramanyam, C. Review of Remote Sensing applications to soils and agriculture. Proc. Silver Jubilee Seminar, IIRS, Dehra Dun. 1992.
176. Pandey, V.K., Panda, S.N., Sudhakar, S. and Raghuwanshi, N.S. Prioritization of sub watersheds using Remote Sensing and physically based hydrological model. Hydrology and Watershed Management: Proceedings of International Conference: With a Focal Theme on Water Quality and Conservation for Sustainable Development. December 18-20, 2002.
177. Pandya, U. H. and Shete, D. T. Efficacy of Rainwater Harvesting Structure in Vallabhipur Village in Vallabhipur Taluka of Bhavnagar District. National Seminar on Rainwater Harvesting and Water Management, Nagpur 11-12 Nov. 2006.
178. Panuska, J.C. and Moore, I.D. Water quality modeling: Terrain analysis and the agricultural nonpoint source pollution (AGNPS) model. Minnesota Water Resources Research Center, Tech Report No. 132, 30.1991.
179. Parida, B. P., Moalafh, D.B., and Kenabatho, P.K. Forecasting runoff coefficients using ANN for water resources management: The case of Notwane catchment in Eastern Botswana. *Physics and Chemistry of the Earth* 31: 928–934. 2006.
180. Partap, T. and H. R. Watson. Sloping Agricultural Land Technology (SALT): A Regenerative Option for Sustainable Mountain Farming. ICIMOD Occasional paper No. 23. 1994. Kathmandu, Nepal. 1994.
181. Picciotto, E., G. Crozaz, W. Ambach & H. Eisner. Lead-210 and Strontium-90 in an alpine glacier. *Earth Planet. Sci.Lett.* 3:237-242. 1967.
182. Ponce, V.M. *Engineering Hydrology: Principles and practice.* Prentice Hall, Englewood Cliffs, New Jersey, USA. 1989.
183. Porto, P., Walling, D.E., Callegari, G, and Catona, F. Using Fallout Lead-210 Measurements to Estimate Soil Erosion in Three Small Catchments in Southern

- Italy. *The Interactions between Sediments and Water*. Publisher: Springer Netherlands. 10.1007/978-1-4020-5478-5. 2007
184. Prasad B., Honda, K. and Murai, S. Sub watershed prioritization for watershed management using remote sensing and GIS. *Asian Conference on Remote Sensing*. 1997.
185. Prospero, J.M., Ginoux, P., Torres, O., Nicholson, V. and Gill, T.E. Environmental characterization of global sources of atmospheric soil dust identified with the Nimbus 7 Total Ozone Mapping Spectrometer (TOMS) absorbing aerosol product, *Reviews in Geophysics* 40 (2002) (1), 1–26. 2002.
186. Qiu, Y., Fu, B.J. and Wang, Y. Spatiotemporal variation in soil erosion and its relation to environmental factors (in Chinese). *J Soil Water Conserv* 16:108–111. 2002.
187. Quine, T. A., Navas, A., Walling, D. E. & Machin, J. Soil erosion and redistribution on cultivated and uncultivated land near Las Bardenas in the central Ebro river basin, Spain, *Land Degradation and Rehabilitation*: 5, 41-55. 1994.
188. Rao, S. V. N., Ramasastri K.S. and Singh R.N.P. A simple monthly model for snow dominated catchments in Western Himalayas. *Nordic Hydrology*, Vol. 27(4), 255-274. 1996.
189. Rao, S. V. N., Rao, M. V., Ramasastri, K.S. and Singh, R.N.P. A study of Sedimentation in Chenab Basin in Western Himalayas. *Nordic Hydrology*, Vol. 28, 201-206. 1997.
190. Rapp, J.F., Lopes, V.L. and Renard, K.G. Comparing soil erosion estimates from RUSLE and USLE on natural runoff plots. *Proc. International Symposium Soil Erosion Research for the 21st Century*, Jan. 3-5, Honolulu, HI. J.C. Aschough II and D.C. Flanagan (eds.), 24-27. American Society Agricultural Engineers, St. Joseph, MI. 2001.

191. Ravishanker, H.M. Watershed prioritization through the USLE using digital satellite data and an integrated approach. *Asian-Pacific Remote Sensing Journal*, Vol. 6(2), 101-108. 1994.
192. Rawat, J. S. and Rawat, M.S. Accelerated erosion and denudation in the Nana Kosi watershed, Central Himalaya, India, Part I: sediment load. *Journal of Mountain Research and Development*, Vol. 14(1), 25-38. 1994.
193. Raymo, M. E. and Ruddiman, W.F. Tectonic forcing of Late Cenozoic climate. *Nature*, Vol. 359, 117-122. 1992.
194. Renard, K.G., Foster, G.R., Lane, I.J. and Laflen, J.M. Soil loss estimation. In *Soil Erosion, Conservation and Rehabilitation*; Agassi, M. (ed.). Marcel Dekkar, New York, 169-202. 1996.
195. Renard, K.G., Foster, G.R., Weesies, G.A., Mc Cool, D.K. and Yoder, D.C. Predicting soil erosion by water: A guide to conservation planning with the revised USLE. USDA Hand Book No. 703, USDA, Washington, D.C. 1997.
196. Risse, L.M., Nearing, M.A., Nicks, A. D. and Laflen, J.M. Error assessment in the Universal Soil Loss Equation. *Soil Science Society of America Journal*. 57, 825-833. 1993.
197. Ritchie, J.C., McHenry. J. R. and Gill, A.C. Fallout ^{137}Cs in the soils and sediments of three small watersheds. *Ecology* 55: 887-890. 1974.
198. Ritchie, J.C. and Ritchie, C.A. Bibliography of publications of cesium-137 studies related to erosion and sediment deposition. Available from: <http://hydrolab.arsusda.gov/cesium/Cesium137/bib2005i.html>. 2005.
199. Robbins, J. A. Geochemical and geophysical applications of radioactive lead. In (Nriagu, J. O. editor) *Biogeochemistry of lead in the environment*. Elsevier, Holland. 285-393. 1978.
200. Rosewell, C.J. Rainfall kinetic energy in eastern Australia. *Journal of Climate and Applied Meteorology* 25, 1695–1701. 1986.

201. Rummel, R. J., Applied Factor Analysis. Evanston, Ill.: Northwestern University Press, 1970.
202. Sa' nchez, L.A., Ataroff, M. and Lo' pez, R. Soil erosion under different vegetation covers in the Venezuelan Andes. *Environmentalist* 22:161–172. 2002.
203. Sah, B. P. and Shimizu, E. Land Use Planning to Avert the Migration Oriented Watershed Degradation. *Proceedings of Asian Conference on Remote Sensing*. 1998.
204. Saha, S.K. and Pande, L.M. 1993. Integrated approach towards soil erosion inventory for environmental conservation using satellite and agro-meteorological data. *Asia-Pacific Rem. Sens. J.*, 5(2): 21-28. 1993.
205. Saha, S.K., Kudrat, M. and Bhan, S.K. Erosional soil loss prediction using digital satellite data and USLE, 369-372. In *Applications of Remote Sensing in Asia and Oceania – environmental change monitoring* (Shunji Murai ed.). Asian Association of Remote Sensing. 1991.
206. Satapathy, K.K. Hydrological aspects of Water Harvesting tanks in Hills. ICAR Research Bulletin No. 42, ICAR, Meghalaya. 12-14. 1996.
207. Saxena, R.K., Verma, K.S., Chary, G.R., Shrivastava, R. and Barthwal, A.K. IRS-1C application in watershed characterization and management. *J. of Remote Sensing*, 21 (17), 3197-3208. 2000.
208. Schroeder, S.A. Reliability of SCS curve number method on semiarid reclaimed minelands. *International Journal of Surface Mining, Reclamation and Environment*, 8, 41-45. 1994.
209. Schuller, P., Iroume, A., Walling, D. E., Mancilla, H. B., Castillo, A. and Trumper, R. E. Use of beryllium-7 to document soil redistribution following forest harvest operations. *Journal of Environmental Quality*. Vol. 35, 1756-1763. 2006.

210. Schumann, A.H., Funke, R. and Schultz G.A. Application of geographical information system for conceptual rainfall runoff modeling. *J. of Hydrology*, 240 (2000), 45-61. 2000.
211. Semmens, D., Goodrich, D., Unkrich, C., Smith, R., Woolhiser, D. and Miller, S. Distributed modelling–KINEROS. International G-WADI Modelling Workshop, Roorkee, India. 28 Feb- 5th Mar, 2005.
212. Shangle, A.K. Sedimentation in Indian reservoirs, Paper presented at the International symposium on special problems of Alluvial rivers including those of international rivers, held at Seoul, Korea, Sept., 1991.
213. Shao, Y., Raupach, M. and Short, D. Preliminary assessment of wind erosion patterns in the Murray–Darling Basin, *Australian Journal of Soil and Water Conservation* 7 (1994) (3), 46–51. 1994.
214. Shrestha, S.S., Honda, K. and Murai, S. Watershed prioritization for soil conservation planning with MOS-I Messr data, GIS application and socio economic information: A case study of Tinau watershed, Nepal, ACRS. 1997.
215. Singh, G., Chandra, S. and Babu, R. Soil loss and prediction research in India. Central and Water Conservation Research Training Institute, Bulletin No. T-12/D9.
216. Singh, P., Ramashastri, K.S. and Kumar, N. Topographical influence on precipitation distribution in different ranges of western Himalayas. *Nordic Hydrology*, 26, 259-284. 1995.
217. Singh, R.K., Aggarwal, S.P., Turdukulov, U. and Prasad, V. H. Prioritization of Bata River Basin using Remote Sensing and GIS Technique. *Indian Journal of Soil Cons.*, 30(3): 200-205, 2002.
218. Slattery, M.C. and Burt, T.P. Particle size characteristics of suspended sediment in hillslope runoff and stream flow. *Earth Surf Proc Landforms* 22:705–719. 1997.
219. Smith, R.E. A kinematic model for surface mine sediment yield, *Transactions of the ASAE*, 1508–1514. 1981.

220. Smith, T., Appleby, P.G., Hilton, J. and Richardson, N. Inventories and fluxes of ^{210}Pb , ^{137}Cs and ^{241}Am determined from the soils of three small catchments in Cumbria, UK *Journal of Environmental Radioactivity*. Vol 37, Number 2, 127-142(16). 1997.
221. So, H.B. and Yatapanage, K.G. *Minerosion 3: a user friendly integrated package for monitoring and Prediction of potential erosion from steep minesites*. ISCO 2004 - 13th International Soil Conservation Organisation Conference – Brisbane. *Conserving Soil and Water for Society: Sharing Solutions*. July 2004
222. Soil Conservation Service (SCS) of NSW: *Land Degradation Survey*. New South Wales 1987-1988. SCS of NSW, Sydney. Department of Land and Water Conservation library, 10 Valentine Avenue, Parramatta, NSW 2150. 1989.
223. Sombrock, W. *Soil degradation and contamination: A global perspective*. *Soil and environment*, 5:3-13. 1995.
224. Spanner, M.A., Strahler, A.H. and Estes, J.E. *Proc. Int. Symp. Rem. Sens. Environ.*, Michigan, USA. 1982.
225. Srinivasan, R., and Arnold, J. G. 1993. Basin scale water quality modeling using GIS. In *Proceedings of Application of Advanced Information Technologies for the Management of Natural Resources*. ASAE. Spokane, WA. pp. 475-484. June 17-19, 1993.
226. Srinivasan, R., and Engel, B. A. Effect of slope prediction methods on slope and erosion estimates. *Journal of Applied Engineering in Agriculture*. Vol.7 (6): November 1991.
227. Sthapit, K. M. Sedimentation of lakes and reservoirs with special reference to the Kulehkani Reservoir. In Schreier, H., P. B. Shah, and S. Brown (Editors), *Challenges in Mountain Resource Management in Nepal, Processes, Trends, and Dynamics in Middle Mountain Watersheds*. ICIMOD/IDRC/UBC. Kathmandu, Nepal. 1995.

228. Suresh, M., Sudhakar, S., Tiwari, K.N. and Chowdary V.M. Prioritization of watersheds using morphometric parameters and assessment of surface water potential using remote sensing. *J. Indian Society of Remote Sensing*, Vol. 32, No. 3, 2004.
229. Takken, I. Beuselinck, L., Nachtergaele, J. Govers, G. Poesen, J. and Degraer, G. Spatial evaluation of a physically based distributed erosion model (LISEM). *Catena* 37:431–437. 1999.
230. Teklehaimanot, G. Master of Science thesis submitted to the International Institute for Geo-information Science and Earth Observation, Enschede, The Netherlands. 2003.
231. Toy, T.J., Foster, G.R. and Renard, K.G. *Soil Erosion: Processes, Prediction, Measurement, and Control*, Wiley, New York. 2002.
232. Trieste, D.J. and Gifford, G.F. Application of the universal soil loss equation to rangeland on a per-storm basis. *J. Range Manage.* 33:66-70. 1980.
233. Tripathi, K.P. Identification of watershed project formulation and implementation, National workshop on watershed area development: Challenges & solutions, Lucknow. 2001.
234. Trisal, C.L. and Manihar, Th. *Loktak-the atlas of Loktak Lake*. Loktak Development Authority and Wetlands International - South Asia, 2004.
235. U.S. Army Construction Engineering Research Laboratory. Geographic resource analysis support system (GRASS)-users and programmers manual. USA-CERL ADP Report N-87/22, Environmental Division, U.S. Army Construction Engineering Research Laboratory, Champaign, Illinois. 1988.
236. Valdiya, K.S. Accelerated erosion and landslide-prone zones in the central Himalayan region. (In: Singh, J H, ed., *Environmental Regeneration in the Himalaya: Concepts and Strategies*, Proceedings of the Kathmandu Symposium,

- November 1992. 12-38. The Central Himalayan Environmental Association: Nainital, India.). 1985.
237. Valenzuela, C. R. ILWIS overview. *ITC Journal* 1: 4–14. 1988.
238. Van Hoof, P.I. and Andren, A.W. Partitioning and transport of ^{210}Pb in Lake Michigan. *J. Great Lakes Res.* 15, 498–509. 1989.
239. Vandaele, K. and Poesen, J. Spatial and temporal patterns soil erosion rates in an agricultural catchment, central Belgium. *Catena* 25:213–226. 1995.
240. Varshney, R. S. Text of Engineering Hydrology. Nemchand Brothers publication, Roorkee, India, 24. 1975.
241. Verma, B., Tejwani K.G., Kale M.V. and Patel A.P. Evaluation of different cropping patterns for runoff and soil loss in Ravine lands. *Journal of the Indian Society of Agronomy*, Vol. 13, 262-270. 1968.
242. Vieux, B.E. and Gaur, N. Finite Element modelling of storm water runoff using GRASS GIS. *Microcomputers I Civil Engineering*, 9(4): 263-270. 1994.
243. Vittorini, S. The effects of soil erosion in an experimental station in the Pliocene clay of the Pliocene clay of the Val d’Era (Tuscany) and its influence on the evolution of the slopes, *Acta Geographica Debrecina* 10, 71-81. 1972.
244. Wallbrink, P. J. and Croke, J. A combined rainfall simulator and tracer approach to assess the role of Best Management practices in minimising sediment redistribution and loss in forests after harvesting. *Forest Ecology and Management* 170: 217-232. 2002.
245. Wallbrink, P.J. and Murray, A.S. Use of fallout radionuclides as indicators of erosion processes. *J. Hyd. Proc.* 7, 297–304. 1993.
246. Wallbrink, P.J. and Murray, A.S. Determining soil loss using the inventory ratio of excess lead-210 to cesium-137. *Soil Science Society of America Journal* 60, 1201-1208. 1996.

247. Wallbrink, P.J. and Murray, A.S. Distribution and variability of ^7Be in soils under different surface cover conditions and its potential for describing soil redistribution processes. *Water Resources Research* 32: 467-476. 1996.
248. Wallbrink, P.J., Murray, A.S. and Olley, J.M. Relating suspended sediment to its original soil depth using fallout radionuclides. *Soil Science Society of America Journal* 63: 369-378. 1999.
249. Wallbrink, P. J. Olley, J. M. and Hancock, G. Tracer assessment of catchment sediment contributions to Western Port, Victoria. CSIRO Land and Water Technical Report 8/03. 2003.
250. Wallbrink, P.J., Roddy, B.P. and Olley, J.M., 2002. A tracer budget quantifying soil redistribution on hillslopes after forest harvesting. *Catena* 47: 179-201.
251. Walling, D.E. The sediment delivery problem. *J. Hydrology*, 65:209-237. 1983.
252. Walling, D.E. Rainfall, runoff and soil erosion of the land: a global review, In: Gregory, K.J. (ed.) *Energetics of the Physical Environment*, Chichester, England, John Wiley and sons, Ltd: 89-117. 1987.
253. Walling, D.E. Erosion and sediment yield research-some recent perspectives. *J. Hydrology*, 100:113-141. 1988.
254. Walling, D.E. "Recent advances in the use of environmental radionuclides in soil erosion investigations." In: *Nuclear techniques in integrated plant nutrient, water and soil management*", Proc. FAO/IAEA Int. Symp. Vienna, October 2000. (IAEA, ed.): 279-301. IAEA C&S Papers Series 11P, Vienna: IAEA Publications. 2001.
255. Walling, D. E. and Bradley, S. B. Some applications of caesium-137 measurements in the study of fluvial erosion, transport and deposition. In: *Erosion, Transport and Deposition Processes* (ed. by D. E. Walling, A. Yair and S. Berkowicz) (Proc. Jerusalem Workshop, April 1987), IAHS Publ. No. 189, 179-203. 1990.

256. Walling, D. E., Bradley, S. B. and Wilkson, C. J. A Caesium-137 budget approach to the investigation of sediment delivery from a small agricultural drainage basin in Devon, UK. *Drainage Basin Sediment Delivery*. Hadley, R.F. (ed) Proceedings of the Albuquerque Symposium, August 1986. IAHS Publication No. 159. 1986.
257. Walling, D. E., Collins, A. L. and Sichingabula, H. M. Using unsupported lead-210 measurements to investigate soil erosion and sediment delivery in a small Zambian catchment. *Geomorphology*, Vol 52, Issues 3-4, 193-213. 16 June 2003.
258. Walling, D.E. and He, Q. Using fallout lead-210 measurements to estimate soil erosion on cultivated land. *Soil Science Society of America Journal* 63, 1404-1412. 1999.
259. Walling, D.E., He, Q. and Blake, W. Use of ^7Be and ^{137}Cs measurements to document short- and medium-term rates of water-induced soil erosion on agricultural land. *Water Resources Research* 35 (12), 3865-3874. 2000.
260. Walling, D. E. and Quine, T. A. The use of caesium-137 measurements to provide quantitative erosion rate data. *Land Degradation and Rehabilitation* 2, 161-175. 1991.
261. Walling, D. E. and Quine, T. A. The use of caesium-137 in soil erosion surveys. In: *Erosion and Sediment Transport Monitoring Programmes in River Basins* (ed. By J. Bogen), 1992.
262. Walling, D.E. and Woodward, J.C. Use the radiometric fingerprints to derive information on suspended sediment source. In: *Erosion and Sediment Transport Monitoring Programmes in River Basins* (ed. by J. Bogen, D.E. Walling and T. Day) (Proc. Oslo Symp., August 1992), IAHS Publ. No. 210, 153-164. 1992.
263. Wang, M. and Hjelmfelt, A.T. DEM based overland flow routing model. *J. Hydrologic Engineering*, ASCE, 3(1):1-8. 1998.
264. Williams, J.R. Sediment-yield prediction with universal equation using runoff energy factor. p. 244–252. *In Present and prospective technology for predicting*

- sediment yield and sources. ARS.S-40, U.S. Gov. Print. Office, Washington, DC. 1975.
265. Williams, J.R., Jones, C.A. and Dyke, P.T. 1984. A modeling approach to determining the relationship between erosion and soil productivity. *Trans. ASAE* 27:129-144. 1984.
266. Wilson, C.G., Matisoff, G. and Whiting, P.J. Short-term erosion rates from a ^7Be inventory balance. *Earth Surface Processes and Landforms* 28(9):967-977. 2003.
267. Wischmeier, W.H. and Smith, D.D. Predicting rainfall erosion losses – A guide to conservation planning. US Department of Agriculture, Handbook No. 537. National Technical Information Service, Springfield, Virginia, USA. Boughton. 1948.
268. Wischmeier, W.H., and Smith, D.D. Predicting Rainfall Erosion Losses - A Guide to Conservation Planning. Agriculture Handbook. 537. U.S. Department of Agriculture Science and Education Administration, Washington, District of Columbia. USA. 1978.
269. Woodruff, N.P. and Siddoway, F.H. A wind erosion equation. *Soil Sci. Soc. Am. Proc.*, 29: 602-608. 1965.
270. Woods, P. and Epp, G. Kentucky watershed management and framework- Approach to Prioritize Watershed within the Licking and Kentucky River basins, Kentucky Water Resources Annual Symposium Proceedings. 2001.
271. Woolhiser, D.A. Unsteady free surface problems in mathematical models of surface water Hydrology. In: Criani, T.A., Marison, V., and Wallis, J. R. (eds) *A Wiley Intersciences Publication*; 195-213. 1977.
272. Xinbao, Z., Walling, D. E., Mingyi, F. and Anbang, W. 2003. *Chinese Science Bulletin*. Vol.48 No.8, 813-818. 2003.

273. Young, R.A., Onstad, C.A., Bosch, D.D. and Anderson, W.P. AGNPS – Agriculture- Non-Point Source Pollution Model: A watershed analysis tool. Conservation Res. Report 35, USDA, ARS, Morris, MN, USA. 1989.
274. Yu, Q.G. Research on the relationship between land use and soil & water loss in the loess hilly area using remote sensing (in Chinese). *J Soil Erosion Soil Water Conserv* 2:24–31. 1996.
275. Zanchi, C. and Torri, D. Evaluation of rainfall energy in central Italy. In: De Boodt, M., Gabriels, D. (Eds.), *Assessment of Erosion*. Wiley, London, 133–142. 1980.
276. Zapata, F. and García-Agudo, E. Report of the Second Research Co-ordination Meeting of the Co-ordinated Research Projects on "Assessment of soil erosion through the use of the Cs-137 and related techniques as a basis for soil conservation, sustainable agricultural production and environmental protection" and "Sediment assessment studies by environmental radionuclides and their application to soil conservation measures", May 1998, Bucharest. IAEA, Vienna, Austria. 1998.
277. Zapata, F. ed. *Handbook for the Assessment of Soil Erosion and Sedimentation Using Environmental Radionuclides*. Kluwer, Dordrecht. 2002.
278. Zapata, F. The use of environmental radionuclides as tracers in soil erosion and sedimentation investigations: recent advances and future developments. *Soil & Tillage Research* 69, 3-13. 2003.
279. Zhao, W.W., Fu, B. J., Meng, Q.H., Zhang, Q. J. and Zhang, Y. H. Effects of land-use pattern on rainfall-runoff and runoff-sediment relations: a case study in Zichang watershed of the Loess Plateau of China. *J Environ Sci* 16:436–442. 2004b.
280. Zhao, W.W., Fu, B.J., Chen, L.D., Lu", Y.H. and Liu, Y.Q. Effects of land-use pattern change on soil and water loss at the catchment scale in the hilly and gully area of the loess plateau of China (in Chinese). *Acta Ecol Sin* 24:1358–1364. 2004a.

281. Zhu, L.Q., Xu, S.M. and Chen, P.Y. Effects of land use / land cover change on soil erosion in mountain area (in Chinese). *Geogr Res* 22:432–428. 2003.
282. Zhu, T.X., Luk, S.H. and Cai, Q.G. Tunnel erosion and sediment production in the hilly loess region, North China. *Journal of Hydrology*. Vol 257: 1-4, 78-90. 2002.

Websites

- 1 <http://www.necouncil.nic.in> (accessed on 4/3/2007).
- 2 <http://www.yosemite.epa.gov> (accessed on 10/2/2007).